BEAMFORMING FOR ENERGY HARVESTING AND MULTI-USER COMMUNICATIONS

A THESIS SUBMITTED TO
THE GRADUATE SCHOOL OF NATURAL AND APPLIED SCIENCES
OF
MIDDLE EAST TECHNICAL UNIVERSITY

BY

ÖZLEM TUĞFE DEMİR

IN PARTIAL FULFILLMENT OF THE REQUIREMENTS
FOR
THE DEGREE OF DOCTOR OF PHILOSOPHY
IN
ELECTRICAL AND ELECTRONICS ENGINEERING

NOVEMBER 2018

Approval of the thesis:

BEAMFORMING FOR ENERGY HARVESTING AND MULTI-USER COMMUNICATIONS

submitted by **ÖZLEM TUĞFE DEMİR** in partial fulfillment of the requirements for the degree of **Doctor of Philosophy in Electrical and Electronics Engineering Department, Middle East Technical University** by,

Prof. Dr. Halil Kalıpçılar
Dean, Graduate School of **Natural and Applied Sciences**

Prof. Dr. Tolga Çiloğlu
Head of Department, **Electrical and Electronics Engineering**

Prof. Dr. T. Engin Tuncer
Supervisor, **Electrical and Electronics Eng. Dep., METU**

Examining Committee Members:

Prof. Dr. Çağatay Candan
Electrical and Electronics Engineering Dept., METU

Prof. Dr. T. Engin Tuncer
Electrical and Electronics Engineering Dept., METU

Prof. Dr. Emre Aktaş
Electrical and Electronics Engineering Dept., Hacettepe Univ.

Prof. Dr. Elif Uysal Bıyıkoğlu
Electrical and Electronics Engineering Dept., METU

Assoc. Prof. Dr. Cenk Toker
Electrical and Electronics Engineering Dept., Hacettepe Univ.

Date: 02.11.2018

I hereby declare that all information in this document has been obtained and presented in accordance with academic rules and ethical conduct. I also declare that, as required by these rules and conduct, I have fully cited and referenced all material and results that are not original to this work.

Name, Last Name: Özlem Tuğfe Demir

Signature   :

ABSTRACT

BEAMFORMING FOR ENERGY HARVESTING AND MULTI-USER COMMUNICATIONS

Demir, Özlem Tuğfe

Ph.D., Department of Electrical and Electronics Engineering

Supervisor   : Prof. Dr. T. Engin Tuncer

November 2018, 233 pages

In this thesis, several optimization problems are considered related to beamforming for energy harvesting and multi-user communications. In multi-user communications scenarios, physical layer multi-group multicasting systems are considered where there are multiple groups of users who are interested in common information signals. In energy harvesting related scenarios, different protocols are investigated, namely power splitting and self-energy recycling, respectively. In power splitting mode, the mobile device has a power splitting device and some portion of the received radio frequency power is used for energy harvesting while the remaining part is used for information decoding. In self-energy recycling protocol, a separate receive antenna on the relay uses the transmitted signal as an energy source. The contributions of this thesis can be outlined as follows. First, efficient algorithms are proposed for antenna selection and hybrid beamforming in multi-group multicasting systems. The users have a power splitting device and the joint optimization of transmit beamformers and power splitting ratios is considered. Multi-group multicasting is also used for OFDM systems where users harvest energy from some portion of the received signal. The difficult combinatorial problem for the joint optimization of resource allocation and power splitting ratios is solved effectively. In addition, several fast algorithms are proposed

for full digital beamforming and two different hybrid beamforming structures with per-antenna power constraints. Apart from multi-group multicasting, relay assisted single user communications is also studied in this thesis. Several scenarios are investigated for energy harvesting relays which use power splitting and self-energy recycling protocols. Both amplify-and-forward and decode-and-forward relaying protocols are considered. For most of the problems, optimum solutions are obtained while for the others, efficient near-optimum solutions are presented.

ÖZ

ENERJİ HASATLI VE ÇOK KULLANICILI İLETİŞİM İÇİN HÜZME ŞEKİLLENDİRME

Demir, Özlem Tuğfe

Doktora, Elektrik ve Elektronik Mühendisliği Bölümü

Tez Yöneticisi   : Prof. Dr. T. Engin Tuncer

Kasım 2018 , 233 sayfa

Bu tezde, enerji hasatlı ve çok kullanıcılı iletişim için hüzme şekillendirmeye ilişkin birçok optimizasyon problemi ele alınmaktadır. Çok kullanıcılı iletişim senaryolarında, ortak bilgi sinyallerine ilgili çoklu kullanıcı gruplarının olduğu fiziksel katman çok gruplu çoğa gönderim sistemleri ele alınmaktadır. Enerji hasadına ilişkin senaryolarda, sırasıyla güç bölme ve öz-enerji geridöngüsü olarak adlandırılan farklı protokoller incelenmektedir. Güç bölme modunda, mobil cihaz bir güç bölücü cihazına sahiptir ve alınan radyo frekans gücünün bir kısmı enerji hasadı için kullanılırken, geri kalanı bilgi çözme için kullanılmaktadır. Öz-enerji geridöngüsü protokolünde, röledeki ayrı bir alıcı anten iletilen sinyali enerji kaynağı olarak kullanmaktadır. Bu tezdeki katkılar aşağıda belirtildiği şekilde özetlenebilir. Öncelikle, çok gruplu çoğa gönderim sistemlerinde anten seçimi ve melez hüzme şekillendirme için verimli algoritmalar önerilmektedir. Kullanıcılar bir güç bölme cihazına sahiptir ve verici hüzme şekillendiricileri ve güç bölme oranlarının ortak optimizasyonu ele alınmaktadır. Çok gruplu çoğa gönderim, kullanıcıların alınan sinyalin bir kısmından enerji hasadı yaptıkları OFDM sistemleri için de kullanılmaktadır. Kaynak paylaştırması ve güç bölme oranlarının ortak optimizasyonu için zor kombinasyonal problem etkili bir şekilde çözülmektedir. Ek olarak, anten başına güç kısıtları ile tam dijital ve iki farklı melez

hüzme şekillendirme yapıları için birçok hızlı algoritma önerilmektedir. Çok gruplu çoğa gönderimden ayrı olarak, bu tezde ayrıca röle destekli tek kullanıcılı iletişim çalışılmaktadır. Güç bölme ve öz-enerji geridöngüsü protokollerini kullanan enerji hasatlı röleler için birçok senaryo incelenmektedir. Hem yükselt-ve-ilet hem de çöz-ve-ilet aktarma prokolleri ele alınmaktadır. Problemlerin çoğu için optimum çözümler elde edilirken diğerleri için verimli optimuma yakın çözümler sunulmaktadır.

Anahtar Kelimeler: Çok Gruplu Çoğa Gönderim Hüzme Şekillendirme, Anten Seçimi, Melez Hüzme Şekillendirme, Kaynak Paylaştırması, Öz-Enerji Geridöngüsü, Eşzamanlı Kablosuz Bilgi ve Güç İletimi, Kablosuz Güçlendirilmiş Aktarma, Güç Bölme, Enerji Hasadı, Çok Antenli Aktarma

To my dear parents and advisor...

ACKNOWLEDGMENTS

TABLE OF CONTENTS

xiii

LIST OF TABLES

TABLES

LIST OF FIGURES

FIGURES

xviii

CHAPTER 1

INTRODUCTION

The material in this thesis consists of several papers which are published or submitted for publication. Each chapter of the thesis is a separate research work in the context of beamforming for energy harvesting and multi-user communications. The following is a list of the publications related to Chapter 2-8:

- **Chapter 2:** O. T. Demir and T. E. Tuncer, "Antenna selection and hybrid beamforming for simultaneous wireless information and power transfer in multi-group multicasting systems," IEEE Transactions on Wireless Communications, vol. 15, pp. 6948–6962, Oct 2016.

- **Chapter 3:** O. T. Demir and T. E. Tuncer, "Max–min fair resource allocation for SWIPT in multi-group multicast OFDM systems," IEEE Communications Letters, vol. 21, pp. 2508–2511, Nov 2017.

- **Chapter 4:** O. T. Demir and T. E. Tuncer, "Optimum QoS-aware beamformer design for full-duplex relay with self-energy recycling," IEEE Wireless Communications Letters, vol. 7, pp. 122–125, Feb 2018.

- **Chapter 5:** O. T. Demir and T. E. Tuncer, "Optimum closed-form beamformers for self-energy recycling full-duplex relay with a new power splitting protocol." Manuscript to be submitted for publication, 2018.

- **Chapter 6:** O. T. Demir and T. E. Tuncer, "Joint source power allocation and relay beamformer design for wireless-powered relaying with self-energy recycling." Manuscript to be submitted for publication, 2018.

- **Chapter 7:** O. T. Demir and T. E. Tuncer, "Optimum and near-optimum beam-formers for decode-and-forward full-duplex multi-antenna relay with self-energy recycling." Manuscript submitted for publication, 2018.

- **Chapter 8:** O. T. Demir and T. E. Tuncer, "Improved admm-based algorithms for multi-group multicasting in large-scale antenna systems with extension to hybrid beamforming." Manuscript to be submitted for publication, 2018.

In modern wireless communications systems, energy consumption is high to satisfy the demand for high data rates and ubiquitous services [1]. Usually, mobile devices use a battery with a limited lifetime [2]. Replacing batteries manually or recharging them is costly and sometimes impractical [2], [3], [4]. Recently energy harvesting has attracted great interest from the research community as a solution to limited battery problem as well as a green communication approach [1], [2], [3], [4], [5], [6], [7]. One promising solution is the wireless power transfer (WPT) technology in this context to have battery independent mobile devices as well as relays in communication systems [3], [6], [7]. Up to now, several WPT methods have been developed such as inductive and magnetic resonance coupling, RF energy transfer [3], etc. Among these, radiative WPT which is based on RF energy transfer is the most suitable technique for wireless networks by providing longer transmission range and more flexible deployment for powering large number of devices [3], [7]. Hence, RF energy harvesting is expected to be one of the key components in next generation wireless communications systems including Internet of Things/Everything (IoT/IoE) [3], [6].

One of the application areas of WPT is the recently developed paradigm, simultaneous wireless information and power transfer (SWIPT) [5], [6]. SWIPT has become a promising research area to improve the energy efficiency and battery duration [2], [8], [9], [10]. In SWIPT, information carrying radio frequency (RF) signals are not only used for information decoding (ID) but also for energy harvesting (EH) at the receiver side. The idea of SWIPT was first introduced in [11] and initially considered for point-to-point single antenna systems [11], [12]. Multiple antennas at the transmitter and/or receiver can be employed for increasing both power transfer efficiency and channel capacity [2]. In particular, SWIPT is also considered for multi-user multi-input single-output (MISO) systems in [8], [13], and [14]. SWIPT has also

2

been considered for OFDM systems in several recent works [1], [15], [16], [17], [18]. SWIPT has attracted significant interest and been considered for a variety of scenarios including multiple input multiple output (MIMO) broadcasting [2], multi-group multicast beamforming [10], relaying protocols [19], [20], [21], secure beamforming [22], non-orthogonal multiple access (NOMA) [23].

Two main practical receiver structures, namely time switching (TS) and power splitting (PS), are proposed in [2] for SWIPT. In the TS scheme, users either decode information or harvest energy from the received RF signal in a prescribed time slot. On the other hand, the received signal is split into two streams with different powers, one for decoding information and the other for harvesting energy in PS scheme. PS architecture has higher degrees of freedom due to the fact that TS is a special form of PS with binary PS values [8]. In some of the problems in this thesis, PS based SWIPT is considered.

An important application area of SWIPT is multicasting where common information is sent to multiple users simultaneously [24], [25]. The mobile data traffic has been growing in a rapid manner due to the widespread use of smartphones, tablets and data hungry applications. A significant amount of this data is of simultaneous interest to groups of users [26], [27], [28], [29], [30]. Live broadcast of sporting events, mobile TV, news headlines, regular system updates, infotainment systems in airplanes, trains and V2X are a few examples for common interest data applications. For an efficient delivery of such data, group-oriented services such as multicasting and broadcasting should be incorporated in future generation wireless systems [31]. In fact, the 3rd Generation Partnership Project (3GPP) included the multimedia broadcast/multicast service (MBMS) in the third and fourth generations of cellular networks [26], [32], [33]. When there is a single group of users which are interested in a common data stream, we call this data transmission mode single-group multicasting or broadcasting [24]. When there are multiple groups of users where the desired data flow is different for each group, this is known as multi-group multicasting [25]. In Chapter 2 and 3, we consider SWIPT in multi-group multicasting systems. A base station transmits more than one information signal to the single-antenna users equipped with a PS device. In Chapter 2, we propose two low-cost alternatives to full digital beamforming, which are antenna selection and hybrid beamforming, respectively

to reduce the hardware complexity. The joint optimization problem is converted to a quadratically constrained quadratic programming (QCQP) problem by introducing new variables for PS ratios. This enables us to adapt the state-of-the-art techniques in the literature, namely alternating minimization (AM) [14], and feasible point pursuit-successive convex approximation (FPP-SCA) [34].

As the antenna technology and fabrication techniques develop, antennas become cheaper and antenna selection strategy is shown to be a good low-cost alternative to increase spatial diversity [35], [36]. In antenna selection, only the selected antennas become active and use the corresponding RF chains with the help of RF switches. Hence, fewer RF chains are required in comparison to the number of antennas. Antenna subset selection is shown to be more power efficient compared to the fixed antenna structures for the same number of RF chains [35], [36], [37]. In Chapter 2, we formulate the joint SWIPT and multi-group multicast beamforming problem in antenna selection scheme and propose an effective algorithm for the solution. **To the best of our knowledge, this is the first work which considers SWIPT and antenna selection in a joint manner for multi-group multicasting.**

Another low-cost alternative to the full digital beamforming is the hybrid structures composed of analog and digital beamformers. Hybrid beamformers decrease hardware cost while maintaining comparable performance to the full digital beamformer [38], [39]. In Chapter 2, we propose the hybrid beamforming structure in Fig. 2.2. Furthermore, two different algorithms are proposed for continuous-phase hybrid beamformers while the problem is investigated in depth for a variety of scenarios. **To the best of our knowledge, this is the first work which considers hybrid beamforming in the context of multi-group multicasting.** In this hybrid structure, there is a smaller number of RF chains than antennas dedicated to each multicast stream. Each RF chain is followed by several RF phase shifters. The existing hybrid beamformers in the literature usually consider continuous-phase analog beamformer where phase shifters have infinite-resolution [40], [41]. In Chapter 2, we design two algorithms for continuous-phase hybrid beamformer where the phase shifts satisfy only the equal gain constraint.

While ideal continuous-phase beamformers have better performance, most practical RF phase shifters have finite resolution and supply only discrete phase changes [39], [42]. In Chapter 2, we propose a discrete-phase hybrid beamformer which uses two-bit RF phase shifters for efficient, effective and low-cost implementation. The special structure of the two-bit hybrid beamformer problem is exploited to convert the combinatorial problem into a continuous formulation by introducing equivalent linear constraints. In the simulations, it is shown that it performs much better than the quantized two-bit beamformer and has moderate degradation in comparison to the continuous-phase hybrid beamformer.

In Chapter 3, we consider resource allocation for SWIPT in multi-group multicasting OFDM systems where a subcarrier assigned to a multicast group serves all the users in that group. In resource allocation, it is possible to have some users with relatively poor channel conditions that may not be assigned with sufficient subcarriers. Hence, enforcing fairness among the users is an important problem that should be addressed [43], [44], [45]. Different from the conventional approach which considers the sum-rate fairness, we maximize the minimum SNR for each subcarrier using the same motivation in [46], [47]. In addition to per-subcarrier fairness, subcarrier need for each multicast group is considered in the proposed design.

The joint optimization of resource allocation and PS ratios for multi-group multicasting has not been considered in the literature before and it is a difficult combinatorial problem. In Chapter 3, a novel approach based on maximizing the minimum SNR among all subcarriers considering the request of each multicast group is proposed. An effective solution is obtained by dividing the problem in two parts. In the first part, subcarriers are assigned to each group based on the user requests. A fairness based near-optimal algorithm is proposed for the solution. The problem for the power allocation and PS ratios is cast as a convex optimization problem given the subcarrier assignments. Hence, optimum solution is guaranteed for the second stage. The proposed approach is shown to perform very close to the joint optimum solution obtained with exhaustive search (ES) while the computational complexity is decreased significantly.

In Chapter 4, 5, 6, and 7 wireless-powered relaying is investigated. Cooperative communication involving wireless relays improves the system throughput, reliability and network coverage [48], [49]. Hence, it is an important technology for the fifth generation (5G) of wireless networks [49]. Mobile and remote relays usually have limited battery lifetime. Hence, SWIPT also has been an appealing research topic in the context of wireless-powered relaying (WPR) in order to improve the lifetime of the relaying system. The works in [5], [20], [50] studied PS based SWIPT for wireless relaying whereas TS protocol is considered in [20], [51]. All of these works are based on half-duplex (HD) relaying, where in the first phase, information and energy carrying RF signal is received and in the second phase, information signal is forwarded to the destination. Although HD relaying does not suffer from self-interference cancellation, it is inefficient in terms of spectral utilization compared to full-duplex (FD) relaying [22], [52]. FD relaying has gained great popularity in the context of SWIPT by using TS [53], [54], [55] and PS [23], [49], [52], [56], [57], [58] protocols.

In the above studies on FD, self-interference is the main design challenge which is handled by several analog, digital, and analog/digital self-interference cancellation techniques [59], [60]. One interesting approach different from TS and PS protocols is to take advantage of self-interference in self-energy recycling [59]. In [19], a two-phase self-energy recycling protocol is proposed for FD WPR. In the first phase, the source node transmits information signal to the relay. Then, the relay forwards the amplified signal to the destination in the second phase. At the same time, source transmits an energy-bearing signal to the relay and relay harvests energy from this dedicated signal as well as its self-interference loop channel which is the channel between the transmitting and receive antennas of the relay. Since information transmission and energy reception occur during the same slot, this scheme is referred to as FD. In this protocol, there are multiple-transmit antennas and a single receiving antenna at the relay. The problem is to design the relay transmit beamformer such that its transmission power does not exceed the harvested power. Later, this idea is used in several works including [4], [21], [22], [61], [62]. In particular, signal-to-noise ratio (SNR) maximization problem for this protocol is considered for a more general case in which multiple receiving antennas are employed at the relay [4].

6

In Chapter 4, we consider the two-phase amplify-and-forward (AF) protocol in [19] as shown in Fig. 4.1. In the first phase, information signal is transmitted from the source (**S**) to the relay (**R**). Then, **R** forwards its received signal to the destination (**D**) and harvests energy by using both the dedicated energy signal sent from **S** and self-recycling. Since information reception and forwarding occur in different slots, no self-interference cancellation is required in this scheme. Note that in [19], only one antenna is used at **R** for information reception while the remaining antennas are not in use in the first phase. In Chapter 4, we modify the system such that all the antennas of **R** are employed for better performance. In addition, we propose quality of service (QoS)-aware design approach different from [19] which considers signal-to-noise ratio (SNR) maximization. The design problem is cast to satisfy the SNR requirement of the destination using the minimum amount of power from the relay's battery with the help of harvested energy.

In Chapter 4, the closed-form optimum solution is derived for the QoS-aware beam-former design problem. In addition to finding the closed-form optimum solution, we derive feasibility conditions for the source power and the relay's maximum power limit. Simulation results show that energy harvesting assists the relay by reducing the dependency on the external power supply. For most of the scenarios, transmission power is greater than the harvested power showing the strictness of the constraint in [19] and the importance of the proposed approach.

In Chapter 5, three SWIPT protocols are investigated. While the first two of these protocols are known in the literature, the third protocol is proposed in the said chapter in order to improve the energy efficiency and the SNR at the destination. It is shown that this new protocol achieves up to 3 dB SNR gain in comparison to the previous protocols. A major contribution of Chapter 5 is the derivation of the closed-form expressions for the optimum relay transmit beamformers. In addition, optimum power splitting ratio is derived for the PS based protocols. While the optimum closed-form solutions are presented for real-valued PS ratios, discrete optimum solutions are also provided. Furthermore, the beamformer design problem is also considered for the optimized energy-bearing signal for multiple-receive antenna relay by presenting the closed-form solutions.

In all the above works related to the self-energy recycling and similar ones in [4], [22], [59], [62], it is assumed that equal power is used for information and energy transfer at the source side. As a more power efficient approach, power allocation optimization can be realized [55], [63], [64] in addition to relay transmit beamformer. In [63], power allocation between information and energy transfer phases is considered for self-energy recycling assisted full-duplex relaying. In this work, beamforming optimization is not taken into account since there is only one transmitting antenna at the relay. Furthermore, only SNR maximization is considered. In Chapter 6, we jointly optimize the relay transmit beamformer and power division parameter for both SNR maximization and QoS-aware design problem. The problem formulations for both of the problems are simplified in an equivalent manner in order to obtain the optimum solution. Karush Kuhn Tucker (KKT) conditions are obtained to better analyze the problems via several lemmas. For the SNR maximization problem, the joint optimum solution is derived. For the QoS-aware problem, an approximation is needed for some of the KKT conditions and a near-optimum joint solution is found. Simulation results verify the effectiveness of the proposed methods compared to equal power allocation scheme. The proposed method achieves 3 dB SNR improvement for the SNR maximization problem. For the QoS-aware problem, the required power input from the relay's own battery is reduced to half. Furthermore, additional power savings are achieved.

In [65], PS-based SWIPT with decode-and-forward FD relaying is considered for single transmit and single receive antenna relay. Then in [49], this scenario is generalized by employing multiple transmit antennas at the relay. A sub-optimum solution is presented for signal-to-interference-plus-noise ratio (SINR) maximization problem.

Unlike SINR maximization, the QoS-aware design problem is not considered in the literature for the above mentioned system to the best of our knowledge. In Chapter 7, we first study the QoS-aware design optimization and present the optimum solution. In this problem, the aim is to minimize the transmission power used by the relay's own battery such that the effective SINR of the system is above a certain threshold. The optimization variables are the relay transmit beamformer and power splitting ratio. The joint optimum solution is found by reformulating the original problem to obtain and equivalent but simple form. In the following part of Chapter 7, we revisit

the SINR maximization problem whose sub-optimum solution is given in [49]. Using bisection search over SINR threshold for QoS-aware problem, we obtain the optimum solution for the SINR maximization as well. Simulation results indicate that the gap between the optimum and sub-optimum solution in [49] can sometimes be large.

In the above problems, it is assumed that there are multiple transmit antennas whereas there is a single receive antenna at the relay. There are several works in the literature which prove the efficiency of multiple receive antennas in energy harvesting systems [66], [67]. In Chapter 7, we further study QoS-aware and SINR maximization problems for the multiple-receive antenna case. Since the joint optimum solution is difficult to obtain, we follow an alternating optimization approach for the design of transmit and receive beamformers together with the power splitting factor. Then, using a bisection search similar to the single antenna case, we present a near-optimum solution for the SINR maximization problem. Several simulations are performed and it is shown that using multiple receive antennas increases the SINR and energy performance of the system. As the number of antennas increases, the improvement becomes more significant.

Chapter 8 considers per-antenna power constrained multi-group multicast beamforming for large-scale antenna systems. Apart from SWIPT, multicast beamforming is extensively studied in the literature. In [68], a consensus alternating directions method of multipliers (ADMM) algorithm is presented for efficient and fast solution of general QCQP problems. Since, multi-group multicast beamforming can be formulated as a QCQP problem, this algorithm is applicable for it. Later in [69], a more efficient ADMM method is developed for multi-group multicast beamforming by reducing the number of dual variables in the algorithm. This work is the current state of the art algorithm for single base station multi-group multicast beamforming problem and we will take it as our benchmark in Chapter 8.

The increasing mobile data traffic necessitates reducing the resulting severe interference in modern cellular systems. Using massive number of antennas at the base station is a promising solution to mitigate the intracell interference and to provide high energy, spectral efficiency and reliability [32], [70], [71], [72]. In large scale antenna concept, massive MIMO technology is seen as one of the key technologies

for the 5G cellular networks [26], [29], [32], [71]. Multicast beamforming is also considered for large scale antenna systems for a more efficient system design [28], [29], [32], [71], [72].

In Chapter 8, we consider multi-group multicast beamforming for large-scale antenna systems. We adopt QoS-aware design approach also by including per-antenna power constraints to the problem to be more practical as in the works [69], [73], and [74]. In the first part of the chapter, we consider full digital beamforming where each antenna is connected to a separate RF chain. Full digital beamforming achieves higher performance compared to analog and hybrid beamforming. This comes from the fact that the elements of each beamformer weight vector can be chosen an arbitrary complex number without any restriction except the per-antenna power constraints. For full digital beamforming, we decompose each beamformer weight vector into two orthogonal subspaces. In this case, the SINR constraints becomes dependent only one of the subspaces. When the number of antennas is very high compared to the rank of overall channel matrix, which is a practical scenario for large-scale antenna systems, the dimension of this subspace becomes significantly small compared to that of the orthogonal subspace. Then, we present the optimum updates for the ADMM framework and arrange the algorithm for a more memory efficient implementation. This together with the proposed decomposition brings us a computational advantage compared to the algorithm in [69] which uses the original problem formulation. Secondly, we deal with the nonconvex original problem directly instead of applying two-layer optimization as in [69]. The motivation behind this is the efficient use of ADMM for nonconvex problems [75], [76], [77], [78], [79]. Since, we use one-layer iteration sequence, our proposed algorithm shows better convergence and requires less time to converge. In the second part of Chapter 8, we focus on two hybrid beamforming systems and several extensive simulations are carried out to show the performance of the proposed algorithms.

One of the important application areas of large scale antenna systems is millimeter wave communications which is among the keystones of 5G systems. Millimeter wave communications is a promising technique in order to increase capacity of future generation cellular systems by using the vast spectrum available in millimeter wave bands [38], [80], [81], [82], [83], [84]. In comparison to current communications

systems, millimeter wave communications suffers from higher propagation loss [80], [81], [83], [84], [85], [86], [87]. However decreased bandwidth at these frequencies enables packing a larger number of antenna elements into small physical size. Hence, narrower and more directive beams can be constructed by compensating high path loss [38], [80], [81], [83], [84], [85], [86], [87], [88], [89]. In conventional cellular frequency band, multiple antenna systems are realized by employing full digital beamforming. In this scheme, each antenna is connected to a separate RF chain including digital-to-analog / analog-to-digital converter, up/downconverter. In millimeter wave frequencies, a large portion of the total energy consumption is due to the RF chains. Furthermore, large number of RF chains is highly costly [85], [86], [87], [89]. Hence, implementing beamforming at the analog side, i.e. analog beamforming, is one of the solutions for reducing power loss and cost. This can be done using cost efficient phase-shifters following a single RF-chain. However, hybrid analog/digital beamforming systems are more efficient by taking advantage of digital beamformer also. In these systems, there is more than one RF chain and each RF chain is followed by multiple phase-shifters [38], [81], [82], [83], [84]. There are mainly two types of structures, i.e. fully-connected and partially-connected. Although better performance is expected for fully-connected structure, the hardware complexity is rather high in this case [38], [81]. In Chapter 8, we will consider partially-connected structure for hybrid beamforming due to its reduced complexity as in Chapter 2.

Hybrid beamforming design is considered for several scenarios including point-to-point MIMO and multi-user MIMO systems [85], [86], [87], [89]. In our previous work [10], a new partially-connected hybrid beamforming structure is proposed for multi-group multicasting systems. In [10], semidefinite relaxation (SDR) and successive convex approximation (SCA) based algorithms are proposed for the considered system. In Chapter 8, we propose an efficient ADMM based algorithm and solve each subproblem of it optimally by adopting this system. In [81], an alternating minimization algorithm based on ADMM is realized over two different optimization problems each of which requires solving a two-layer optimization problem for a partially-connected hybrid structure with vector modulators. Vector modulators are used in place of the phase shifter and power amplifier. In Chapter 8, we formulate this problem according to our proposed efficient ADMM form and tackle the nonconvex

problem directly instead of a three-layer optimization framework as in [81]. Simulation results show that our proposed algorithm performs significantly better in terms of both base station transmission power and computational complexity.

CHAPTER 2

ANTENNA SELECTION AND HYBRID BEAMFORMING FOR SIMULTANEOUS WIRELESS INFORMATION AND POWER TRANSFER IN MULTI-GROUP MULTICASTING SYSTEMS

In this chapter, low-cost alternatives to full digital beamforming, namely antenna selection and hybrid beamforming, are proposed for simultaneous wireless information and power transfer (SWIPT) in a multi-group multicasting scenario. Power splitting (PS) based SWIPT is considered. The joint problem can be outlined as the design of beamformer weight vectors and PS ratios in order to satisfy both signal-to-interference-plus-noise-ratio (SINR) and harvested power constraints at each user with minimum transmission power. An efficient algorithm is developed for antenna selection by converting the original mixed integer programming problem into a continuous one and adapting feasible point pursuit-successive convex approximation (FPP-SCA). Secondly, a new hybrid beamforming structure is presented for multi-group multicasting. Both continuous and discrete-phase hybrid beamformers are considered in this content. Two algorithms for continuous-phase case are developed by employing two competing techniques. In addition, a special two-bit discrete-phase hybrid beamformer design is considered for practical systems. The integer constraints are converted into linear equality and inequalities for this specific structure and an efficient algorithm is designed. The proposed algorithms are compared for different scenarios revealing some interesting characteristics of each technique.

2.1 Related Works and Contributions

In [13], the joint design of beamformer weight vector and user PS ratios is studied for single-group multicasting scenario. Unfortunately, the optimum solution is not guaranteed unless the number of users is less than or equal to 4. In fact, optimum multicast beamforming problem even without SWIPT is NP-hard [25]. The joint multi-group multicast beamforming and SWIPT is considered in [14] for the first time in the literature. In [14], digital beamforming is utilized similar to the previous works [8], [13], [25]. Although the best performance can be achieved with digital beamforming, it may not be the best choice regarding the hardware cost and complexity. Since digital beamforming is performed at the baseband, a separate RF chain for each antenna is required, which results high power consumption [38]. In this chapter, we propose two low-cost alternatives, which are antenna selection and hybrid beamforming, respectively to reduce the hardware complexity. The joint optimization problem is converted to a quadratically constrained quadratic programming (QCQP) problem by introducing new variables for PS ratios. This enables to adapt the state-of-the-art techniques in the literature, namely alternating minimization (AM) [14], and feasible point pursuit-successive convex approximation (FPP-SCA) [34].

Antenna selection is introduced in [35] for multi-group multicast beamforming. The performance of this scheme is improved for the same scenario in [36]. In this chapter, we formulate the joint SWIPT and multi-group multicast beamforming problem in antenna selection scheme and propose an effective algorithm for the solution. To the best of our knowledge, this is the first work which considers SWIPT and antenna selection in a joint manner for multi-group multicasting. The resulting optimization problem has a mixed binary nonlinear programming structure. In order to solve the problem effectively, the idea in [36] is used to convert the binary constraints to quadratic and linear constraints of continuous variables. Furthermore, the nonconvex quadratic constraint is moved to the objective using absolute exact penalty function. Different from [36], we design a new algorithm using FPP-SCA approach proposed recently for QCQP problems [34]. This new algorithm has lower worst-case computational complexity than the one in [36] and simulation results show that it performs much better than the random antenna selection scheme.

Another low-cost alternative to the full digital beamforming is the hybrid structures composed of analog and digital beamformers. Hybrid beamformers decrease hardware cost while maintaining comparable performance to the full digital beamformer [38], [39]. In [90], two-bit hybrid beamforming is considered for single group multicasting where analog phase shifters supply only four phase shift values. In this chapter, we extend the problem for multi-group multicasting and propose the hybrid beamforming structure in Fig. 2.2. Furthermore, two different algorithms are proposed for continuous-phase hybrid beamformers while the problem is investigated in depth for a variety of scenarios. To the best of our knowledge, this is the first work which considers hybrid beamforming in the context of multi-group multicasting. In this hybrid structure, there are less number of RF chains than antennas dedicated to each multicast stream. Each RF chain is followed by several RF phase shifters. The existing hybrid beamformers in the literature usually consider continuous-phase analog beamformer where phase shifters have infinite-resolution [40], [41]. In this chapter, we design two algorithms for continuous-phase hybrid beamformer where the phase shifts satisfy only the equal gain constraint. The first algorithm is developed using the AM technique in [36]. As a second approach, the problem is modified using some conversions and exact penalty function for the application of FPP-SCA. While FPP-SCA has lower worst-case computational complexity, the problem formulation for the proposed hybrid beamforming is more suitable for the AM technique resulting better performance in certain cases. These two powerful techniques are compared in multi-group multicasting with SWIPT showing the potential benefits of each technique in certain scenarios.

While ideal continuous-phase beamformers have better performance, most practical RF phase shifters have finite-resolution and supply only discrete phase changes [39], [42]. In this chapter, we propose a discrete-phase hybrid beamformer which uses two-bit RF phase shifters for efficient, effective and low-cost implementation. The special structure of the two-bit hybrid beamformer problem is exploited to convert the combinatorial problem into a continuous formulation by introducing equivalent linear constraints. This conversion is possible only when AM technique is adapted. Hence, a two-bit hybrid beamformer algorithm with AM is developed. In the simulations, it is shown that it performs much better than the quantized two-bit beamformer and has

moderate degradation in comparison to the continuous-phase hybrid beamformer.

2.2 System Model

Consider a wireless downlink comprising a base station equipped with M transmit antennas and N users as shown in Fig. 2.1. Each user has a single antenna. Assume that there are G multicast groups, $\{\mathcal{G}_1, ..., \mathcal{G}_G\}$, where $\mathcal{G}_k$ denotes the kth multicast group of users. Each user listens to a single multicast, i.e., $\mathcal{G}_k \cap \mathcal{G}_l = \emptyset$ for $k \neq l$. A narrowband block-fading channel model is adopted. The signal transmitted from the antenna array is $\mathbf{x} = \sum_{k=1}^{G} \mathbf{w}_k s_k$ where s_k is the information signal for the users in $\mathcal{G}_k$ and $\mathbf{w}_k$ is the related $M \times 1$ complex beamformer weight vector. It is assumed that the information signals $\{s_k\}_{k=1}^{G}$ are mutually uncorrelated each with zero mean and unit variance, $\sigma_{s_k}^2 = 1$. In this case, the total transmitted power is $P_{tot} = \sum_{k=1}^{G} \mathbf{w}_k^H \mathbf{w}_k$. The received signal at the ith user is given as,

$$y_i = \mathbf{h}_i^H \mathbf{x} + n_{A,i}, \quad i = 1, ..., N \tag{2.1}$$

where $\mathbf{h}_i^H$ is the $1 \times M$ complex channel vector for the ith user and $n_{A,i}$ is the additive zero mean Gaussian noise at the ith user's antenna with variance $\sigma_{A,i}^2$. $n_{A,i}$ is uncorrelated with the information signals.

As illustrated in Fig. 2.1, each user has the energy harvesting capability. The received signal at the ith user is split to the energy harvester (EH) and the information decoder (ID) with the aid of a PS device. PS is assumed to be ideal and does not induce any noise. A portion of the signal power denoted by $0 < \rho_i < 1$ is transferred to the ID while the remaining $1 - \rho_i$ portion is fed into the EH. The received signal at the ID of the ith user can be expressed as,

$$y_{I,i} = \sqrt{\rho_i}(\mathbf{h}_i^H \mathbf{x} + n_{A,i}) + n_{I,i}, \ i = 1, ..., N \tag{2.2}$$

where $n_{I,i}$ is the additional zero-mean Gaussian noise introduced by the ID of the ith user. The variance of $n_{I,i}$ is $\sigma_{I,i}^2$ and it is independent of the information signals and $n_{A,i}$. Assuming that the ith user is in the kth multicast group, $\mathcal{G}_k$, SINR for the ith user is,

$$SINR_i = \frac{\rho_i |\mathbf{w}_k^H \mathbf{h}_i|^2}{\rho_i(\sum_{l \neq k} |\mathbf{w}_l^H \mathbf{h}_i|^2 + \sigma_{A,i}^2) + \sigma_{I,i}^2}. \tag{2.3}$$

16
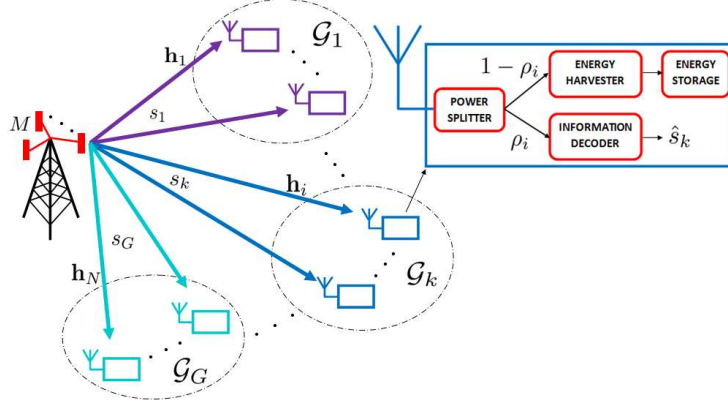
Figure 2.1: SWIPT Multi-Group Multicasting System.

The signal fed into the EH of the ith user can be expressed as,

$$y_{E,i} = \sqrt{1 - \rho_i}(\mathbf{h}_i^H \mathbf{x} + n_{A,i}), \ i = 1, ..., N. \tag{2.4}$$

Then, the power harvested by the EH of the ith user is given as,

$$P_i = \xi_i(1 - \rho_i)(\sum_{k=1}^{G} |\mathbf{w}_k^H \mathbf{h}_i|^2 + \sigma_{A,i}^2) \tag{2.5}$$

where $0 < \xi_i \leq 1$ is the energy conversion efficiency at the ith user.

In this chapter, quality of service (QoS) together with energy harvesting for the users are considered. QoS-aware joint SWIPT and multi-group multicast beamforming problem is to minimize the total transmitted power subject to receive-SINR and harvested power constraints for each user, i.e.,

$$\min_{\{\mathbf{w}_k\}_{k=1}^{G}, \{\rho_i\}_{i=1}^{N}} \sum_{k=1}^{G} \mathbf{w}_k^H \mathbf{w}_k \tag{2.6a}$$

$$s.t. \quad \frac{\rho_i \mathbf{w}_k^H \mathbf{R}_i \mathbf{w}_k}{\rho_i(\sum_{l \neq k} \mathbf{w}_l^H \mathbf{R}_i \mathbf{w}_l + \sigma_{A,i}^2) + \sigma_{I,i}^2} \geq \gamma_i \tag{2.6b}$$

$$\xi_i(1 - \rho_i)(\sum_{k=1}^{G} \mathbf{w}_k^H \mathbf{R}_i \mathbf{w}_k + \sigma_{A,i}^2) \geq \mu_i \tag{2.6c}$$

$$0 < \rho_i < 1, \quad \forall \, i \in \mathcal{G}_k, \forall \, k, l \in \{1, ..., G\} \tag{2.6d}$$

$$\sum_{k=1}^{G} \mathbf{w}_k^H \mathbf{w}_k \leq P_{max} \tag{2.6e}$$

where γ_i and μ_i are the SINR and harvested power thresholds respectively for the ith user and $\mathbf{R}_i = \mathbf{h}_i \mathbf{h}_i^H$. P_{max} is the maximum allowable power at the base station.

17

The problem in (2.6) is not convex and hence should be handled appropriately for an effective solution.

Let us express (2.6) in a simpler way by decoupling $\mathbf{w}_k$'s and ρ_i's as follows,

$$\min_{\{\mathbf{w}_k\}_{k=1}^{G}, \{\rho_i\}_{i=1}^{N}} \quad \sum_{k=1}^{G} \mathbf{w}_k^H \mathbf{w}_k \tag{2.7a}$$

$$s.t. \quad \mathbf{w}_k^H \mathbf{R}_i \mathbf{w}_k - \gamma_i \sum_{l \neq k} \mathbf{w}_l^H \mathbf{R}_i \mathbf{w}_l \geq \frac{\gamma_i \sigma_{I,i}^2}{\rho_i} + \gamma_i \sigma_{A,i}^2 \tag{2.7b}$$

$$\sum_{k=1}^{G} \mathbf{w}_k^H \mathbf{R}_i \mathbf{w}_k \geq \frac{\mu_i}{\xi_i(1 - \rho_i)} - \sigma_{A,i}^2 \tag{2.7c}$$

$$\text{(2.6d-e)} . \tag{2.7d}$$

Although $\frac{1}{\rho_i}$ and $\frac{1}{1-\rho_i}$ are convex functions of ρ_i for $0 < \rho_i < 1$ [8], the problem in (2.7) is still not convex since $\mathbf{R}_i$ is positive semidefinite, $i = 1, ..., N$. Note that the problem in (2.7) is not always feasible due to both SINR constraints coupled by all the multicast beamforming weight vectors and maximum power constraint in (2.6e). It is not easy to analyze feasibility of such a problem even if we discard energy harvesting constraints in (2.7c) except some special cases. In [8], a necessary and sufficient condition is stated for the feasibility of a similar transmit power minimization with QoS and energy harvesting constraints without maximum power limit as follows,

$$\sum_{i=1}^{N} \frac{\gamma_i}{1 + \gamma_i} \leq rank(\mathbf{H}) \tag{2.8}$$

where $\mathbf{H} = [\ \mathbf{h}_1\ \mathbf{h}_2\ ...\ \mathbf{h}_N\ ]$. Note that the condition in (2.8) is valid in downlink beamforming scenario where a separate stream is transmitted to each user. In multicasting scenario, (2.8) is only a necessary condition since groups of users share the same beamforming weight vector, hence the feasibility rate of (2.7) is obviously less than that of downlink beamforming.

Another special case is single group multicast beamforming. In this scenario, there is no interference on the users and power of a given beamforming weight vector can be increased such that all the constraints are satisfied if there is no maximum power constraint. Hence, if we discard (2.6e), the problem in (2.7) is always feasible for single group multicasting.

The problem in (2.7) can be solved using two approaches, namely AM [36], and

FPP-SCA [34], respectively. In the following parts of this chapter, these two methods will be elaborated further. While FPP-SCA is an efficient iterative method for QCQP problems, it cannot be applied directly for (2.7). In order to apply FPP-SCA, the following theorem is presented to express (2.7b) and (2.7c) as quadratic constraints.

Theorem 2.1:: Let $\{\{\mathbf{w}_{k_{opt}}\}_{k=1}^{G}, \{v_{i_{opt}}, \kappa_{i_{opt}}\}_{i=1}^{N}\}$ be an optimum solution of (2.9). Then $\{\{\mathbf{w}_{k_{opt}}\}_{k=1}^{G}, \{\rho_{i_{opt}}\}_{i=1}^{N}\}$ is an optimum solution of (2.7) where $\rho_{i_{opt}} = \frac{\kappa_{i_{opt}}}{v_{i_{opt}} + \kappa_{i_{opt}}}$.

$$\min_{\{\mathbf{w}_k\}_{k=1}^{G}, \{v_i, \kappa_i\}_{i=1}^{N}} \sum_{k=1}^{G} \mathbf{w}_k^H \mathbf{w}_k \qquad (2.9a)$$

$$s.t.\ \mathbf{w}_k^H \mathbf{R}_i \mathbf{w}_k - \gamma_i \sum_{l \neq k} \mathbf{w}_l^H \mathbf{R}_i \mathbf{w}_l \geq \gamma_i \sigma_{I,i}^2 v_i + \gamma_i \sigma_{A,i}^2 \qquad (2.9b)$$

$$\sum_{k=1}^{G} \mathbf{w}_k^H \mathbf{R}_i \mathbf{w}_k \geq \frac{\mu_i}{\xi_i} \kappa_i - \sigma_{A,i}^2 \qquad (2.9c)$$

$$\left\|\begin{matrix} v_i - \kappa_i \\ 2 \end{matrix}\right\|_2 \leq v_i + \kappa_i - 2, \quad \forall i \in \mathcal{G}_k, \forall\ k, l \in \{1, ..., G\} \qquad (2.9d)$$

$$\sum_{k=1}^{G} \mathbf{w}_k^H \mathbf{w}_k \leq P_{max}. \qquad (2.9e)$$

Proof: In (2.9), $\frac{1}{\rho_i}$ and $\frac{1}{1-\rho_i}$ are represented by v_i and κ_i, respectively. The condition in (2.9d) implies the following inequality,

$$v_i + \kappa_i \leq v_i \kappa_i. \qquad (2.10)$$

Note that $v_i + \kappa_i \geq 2$ from (2.9d). This and (2.10) imply $v_i \kappa_i \geq 0$. If we divide (2.10) by $v_i \kappa_i$, we obtain the following inequality,

$$\frac{1}{v_i} + \frac{1}{\kappa_i} \leq 1. \qquad (2.11)$$

Let $\{\{\mathbf{w}_{k_{opt}}\}_{k=1}^{G}, \{v_{i_{opt}}, \kappa_{i_{opt}}\}_{i=1}^{N}\}$ be a global optimum solution of (2.9) resulting minimum objective value among all the others. If (2.11) is satisfied with equality for all pairs $\{v_{i_{opt}}, \kappa_{i_{opt}}\}$, then $\{\{\mathbf{w}_{k_{opt}}\}_{k=1}^{G}, \{\rho_{i_{opt}}\}_{i=1}^{N}\}$ ($\rho_{i_{opt}} = \frac{\kappa_{i_{opt}}}{v_{i_{opt}} + \kappa_{i_{opt}}}$) is a global optimum solution for (2.7) since the same problem is solved with a change of variables. Otherwise, assume that (2.11) is not satisfied with equality for at least one of the pairs $\{v_{i_{opt}}, \kappa_{i_{opt}}\}$. Then, we can scale $\{v_{i_{opt}}, \kappa_{i_{opt}}\}$ by $(\frac{1}{v_{i_{opt}}} + \frac{1}{\kappa_{i_{opt}}})$ such that (2.11) is satisfied with equality without violating SINR and harvested power constraints since scale

factor is less than 1. Furthermore, we have the same objective value as before scaling since the objective is only a function of $\{\mathbf{w}_k\}_{k=1}^G$. Hence, $\{\{\mathbf{w}_{k_{opt}}\}_{k=1}^G, \{\hat{\upsilon}_{i_{opt}}, \hat{\kappa}_{i_{opt}}\}_{i=1}^N\}$ is another global optimum solution of (2.9) where $\frac{1}{\hat{\upsilon}_{i_{opt}}} + \frac{1}{\hat{\kappa}_{i_{opt}}} = 1$. By the change of variables, it is easily seen that $\rho_{i_{opt}} = \frac{1}{\hat{\upsilon}_{i_{opt}}}$ is an optimum PS ratio for the ith user. Hence, the theorem is proved. ∎

The equivalent problem in (2.9) is now suitable for the application of FPP-SCA.

2.3 FPP-SCA Approach

The problem in (2.9) is convex except the quadratic constraints in (2.9b) and (2.9c). The terms that destroy convexity are $\mathbf{w}_k^H \mathbf{R}_i \mathbf{w}_k$ and $\sum_{k=1}^G \mathbf{w}_k^H \mathbf{R}_i \mathbf{w}_k$ in (2.9b) and (2.9c), respectively. In conventional successive convex approximation (SCA), linear approximation of these terms is used in the neighborhood of the solution found in the previous iteration [91]. For any $\{\mathbf{z}_k\}_{k=1}^G$ where $\mathbf{z}_k \in \mathbb{C}^M$, $k = 1, ..., G$, $(\mathbf{w}_k - \mathbf{z}_k)^H \mathbf{R}_i (\mathbf{w}_k - \mathbf{z}_k) \geq 0$. Expanding the left-hand side of the inequality, we obtain, $\mathbf{w}_k^H \mathbf{R}_i \mathbf{w}_k \geq 2 \operatorname{Re}\{\mathbf{z}_k^H \mathbf{R}_i \mathbf{w}_k\} - \mathbf{z}_k^H \mathbf{R}_i \mathbf{z}_k$. SCA solves the problem in (2.9) iteratively by approximating (2.9b-c) using this linear restriction around the previous iterant, i.e., $\{\mathbf{z}_k\}_{k=1}^G$. In this case, (2.9b-c) is replaced by the following constraints in the iterative scheme, i.e.,

$$2 \operatorname{Re}\{\mathbf{z}_k^H \mathbf{R}_i \mathbf{w}_k\} - \mathbf{z}_k^H \mathbf{R}_i \mathbf{z}_k - \gamma_i \sum_{l \neq k} \mathbf{w}_l^H \mathbf{R}_i \mathbf{w}_l \geq \gamma_i \sigma_{I,i}^2 \upsilon_i + \gamma_i \sigma_{A,i}^2 \tag{2.12a}$$

$$\sum_{k=1}^G (2 \operatorname{Re}\{\mathbf{z}_k^H \mathbf{R}_i \mathbf{w}_k\} - \mathbf{z}_k^H \mathbf{R}_i \mathbf{z}_k) \geq \frac{\mu_i}{\xi_i} \kappa_i - \sigma_{A,i}^2. \tag{2.12b}$$

A sequence of feasible points is obtained with decreasing objective values by solving (2.9) iteratively [91]. Note that if (2.12a) and (2.12b) are satisfied at some iteration, then (2.9b) and (2.9c) are also satisfied by the bound $\mathbf{w}_k^H \mathbf{R}_i \mathbf{w}_k \geq 2 \operatorname{Re}\{\mathbf{z}_k^H \mathbf{R}_i \mathbf{w}_k\} - \mathbf{z}_k^H \mathbf{R}_i \mathbf{z}_k$. The drawback of this method is that it requires an initial feasible point. In [34], the infeasibility problem is solved by adding slack variables and a slack penalty

to the original problem as follows,

$$\min_{\{\mathbf{w}_k\}_{k=1}^{G}, \{v_i,\kappa_i,s_i,r_i\}_{i=1}^{N}} \sum_{k=1}^{G} \mathbf{w}_k^H \mathbf{w}_k + \alpha \sum_{i=1}^{N} (s_i + r_i) \tag{2.13a}$$

$$s.t. \ 2\operatorname{Re}\{\mathbf{z}_k{}^H \mathbf{R}_i \mathbf{w}_k\} - \mathbf{z}_k{}^H \mathbf{R}_i \mathbf{z}_k - \gamma_i \sum_{l \neq k} \mathbf{w}_l^H \mathbf{R}_i \mathbf{w}_l \geq \gamma_i \sigma_{I,i}^2 v_i + \gamma_i \sigma_{A,i}^2 - s_i \tag{2.13b}$$

$$\sum_{k=1}^{G} (2\operatorname{Re}\{\mathbf{z}_k{}^H \mathbf{R}_i \mathbf{w}_k\} - \mathbf{z}_k{}^H \mathbf{R}_i \mathbf{z}_k) \geq \frac{\mu_i}{\xi_i} \kappa_i - \sigma_{A,i}^2 - r_i \tag{2.13c}$$

$$s_i \geq 0, \ r_i \geq 0 \tag{2.13d}$$

$$(2.9\text{d-e}). \tag{2.13e}$$

The problem in (2.13) is always feasible at every iteration due to nonnegative slack variables $\{s_i, r_i\}_{i=1}^{N}$. However, these slack variables should be zero in order to obtain a feasible solution to the original problem (2.9). If we choose $\alpha \gg 1$ and the original problem is feasible, the slack variables $\{s_i, r_i\}_{i=1}^{N}$ tend to go to zero. Note that [34] optimizes slack variables to reach a compromise, where the achieved solution minimizes the constraint violations even if the problem is infeasible. However, we use the slack variables only to find a feasible starting point for the proposed algorithms assuming that the original problem is feasible. In the following part, the details of the FPP-SCA based algorithm will be presented within the context of antenna selection scheme.

2.4 Multicasting Problem with Antenna Selection for SWIPT

While digital beamforming has the highest capacity, its hardware cost and complexity necessitate alternative approaches for efficient system design. Antenna selection scheme is a lower-cost and effective alternative to the full digital beamforming. In this part, FPP-SCA will be used to solve the problem of multicast beamforming with antenna selection. It is also possible to use AM approach for antenna selection [36]. It turns out that both of these techniques return similar performances. However, FPP-SCA is known to be computationally more efficient and hence it is selected for the implementation of antenna selection scheme.

Assume that L RF transmission chains are available, while there are $M \geq L$ antennas. The problem is to select the best L out of M antennas and find the corresponding

beamforming weight vectors and PS ratios to minimize the total transmitted power. Let us define a $M \times 1$ vector, $\mathbf{b}$, whose elements are either 0 or 1. The mth element of $\mathbf{b}$, b_m, is the antenna selection coefficient for the mth antenna. Hence, $b_m = 1$ if the mth antenna is selected, and it is zero otherwise. We can use big-M approach to formulate the antenna selection problem with the aid of binary variables, b_m [92]. If there is an upper bound $\mathcal{M}$ on antenna power, then the constraint $\sum_{k=1}^{G} |w_{k_m}|^2 \leq \mathcal{M} b_m$ links b_m's and antennas. Here, $\sum_{k=1}^{G} |w_{k_m}|^2$ is the power transmitted from the mth antenna. If $b_m = 0$, then the power of the mth antenna should be zero indicating that the mth antenna is not selected. Otherwise, since $\mathcal{M}$ is an upper bound, the antenna's power is not restricted. This approach is known as big-M in the literature [92]. The upper bound $\mathcal{M}$ can be selected as the power limit of the base station, i.e., $\mathcal{M} = P_{max}$. In this case the joint problem can be written as,

$$\min_{\{\mathbf{w}_k\}_{k=1}^{G}, \mathbf{b}, \{v_i, \kappa_i\}_{i=1}^{N}} \quad \sum_{k=1}^{G} \mathbf{w}_k^H \mathbf{w}_k \tag{2.14a}$$

$$s.t. \quad \sum_{k=1}^{G} |w_{k_m}|^2 \leq P_{max} b_m, \quad m = 1, ..., M \tag{2.14b}$$

$$\sum_{m=1}^{M} b_m = L \tag{2.14c}$$

$$b_m \in \{0, 1\}, \quad m = 1, ..., M \tag{2.14d}$$

$$\mathbf{w}_k^H \mathbf{R}_i \mathbf{w}_k - \gamma_i \sum_{l \neq k} \mathbf{w}_l^H \mathbf{R}_i \mathbf{w}_l \geq \gamma_i \sigma_{I,i}^2 v_i + \gamma_i \sigma_{A,i}^2 \tag{2.14e}$$

$$\sum_{k=1}^{G} \mathbf{w}_k^H \mathbf{R}_i \mathbf{w}_k \geq \frac{\mu_i}{\xi_i} \kappa_i - \sigma_{A,i}^2 \tag{2.14f}$$

$$\left\| \begin{matrix} v_i - \kappa_i \\ 2 \end{matrix} \right\|_2 \leq v_i + \kappa_i - 2, \quad \forall i \in \mathcal{G}_k, \forall k, l \in \{1, ..., G\} \tag{2.14g}$$

$$\sum_{k=1}^{G} \mathbf{w}_k^H \mathbf{w}_k \leq P_{max}. \tag{2.14h}$$

In the above problem, (2.14d-f) are the only nonconvex constraints. A linear approximation in the neighborhood of the previous iterate can be used for (2.14e-f) in order to express them as convex constraints as explained in the previous section. The problem in (2.14) is a mixed integer nonlinear programming problem due to the binary vector, $\mathbf{b}$. In the following lemma, binary constraints are expressed in terms of continuous variables. Hence, the computational complexity of (2.14) is decreased significantly.

22

Lemma 2.1: (2.15a-b) with (2.14c) in terms of continuous variables, b_m, are equivalent to the binary constraints in (2.14d), i.e.,

$$\sum_{m=1}^{M} b_m^2 = L \tag{2.15a}$$

$$0 \le b_m \le 1, \quad m = 1, ..., M. \tag{2.15b}$$

Proof: Consider the difference of (2.15a) and (2.14c), i.e.,

$$\sum_{m=1}^{M} b_m^2 - \sum_{m=1}^{M} b_m = \sum_{m=1}^{M} b_m(b_m - 1) = 0. \tag{2.16}$$

Each term in the summation in (2.16) is nonpositive from (2.15b). (2.16) implies that all the terms in the summation are equal to zero, i.e., $b_m \in \{0, 1\}$. Hence, (2.14d) can be replaced by (2.15a) and (2.15b). ■

The constraint in (2.15a) is not convex. We can use exact penalty function to move the constraint in (2.15a) to the objective function [93]. Exact penalty functions allow us to transform a constrained optimization problem into an unconstrained one with finite penalty parameters. The following lemma presents an equivalent problem by moving only the nonconvex constraint in (2.15a) to the objective function.

Lemma 2.2: If an optimum solution of (2.14) where (2.14d) is replaced by (2.15a-b), satisfies Karush-Kuhn-Tucker conditions, then it is also an optimum solution of the following problem in (2.17) for $\zeta > \zeta_0$ with $\zeta_0 > 0$ being a finite value.

$$\min_{\{\mathbf{w}_k\}_{k=1}^{G}, \mathbf{b}, \{v_i, \kappa_i\}_{i=1}^{N}} \sum_{k=1}^{G} \mathbf{w}_k^H \mathbf{w}_k + \zeta |L - \mathbf{b}^T \mathbf{b}| \tag{2.17a}$$

$$s.t. \quad (2.14\text{b-c}), (2.14\text{e-h}), (2.15\text{b}). \tag{2.17b}$$

Proof: Please refer to Appendix A.1. ■

Note that absolute exact penalty term $\zeta |L - \mathbf{b}^T \mathbf{b}|$ is equal to $\zeta(L - \mathbf{b}^T \mathbf{b})$ since $\mathbf{b}^T \mathbf{b} = \sum_{m=1}^{M} b_m^2 \le \sum_{m=1}^{M} b_m = L$. Now, we can solve (2.17) using FPP-SCA and alternating $\mathbf{b}$ at each iteration. Random initial points can be generated for the algorithm. However, it is observed that semidefinite relaxation provides good initialization points in accordance with [34]. For a starting point, let us define $\mathbf{W}_k = \mathbf{w}_k \mathbf{w}_k^H$, $k = 1, ..., G$. The problem in (2.14) where (2.14d) is replaced by (2.15a-b), can be expressed in

terms of $\{\mathbf{W}_k\}_{k=1}^{G}$ as follows,

$$\min_{\{\mathbf{W}_k\}_{k=1}^{G}, \mathbf{b}, \{v_i, \kappa_i\}_{i=1}^{N}} \sum_{k=1}^{G} Tr\{\mathbf{W}_k\} \tag{2.18a}$$

$$s.t. \sum_{k=1}^{G} W_k(m, m) \leq P_{max} b_m, \quad m = 1, ..., M \tag{2.18b}$$

$$Tr\{\mathbf{R}_i \mathbf{W}_k\} - \gamma_i \sum_{l \neq k} Tr\{\mathbf{R}_i \mathbf{W}_l\} \geq \gamma_i \sigma_{I,i}^2 v_i + \gamma_i \sigma_{A,i}^2 \tag{2.18c}$$

$$\sum_{k=1}^{G} Tr\{\mathbf{R}_i \mathbf{W}_k\} \geq \frac{\mu_i}{\xi_i} \kappa_i - \sigma_{A,i}^2 \tag{2.18d}$$

$$\left\| \begin{matrix} v_i - \kappa_i \\ 2 \end{matrix} \right\|_2 \leq v_i + \kappa_i - 2, \quad \forall i \in \mathcal{G}_k, \forall k, l \in \{1, ..., G\} \tag{2.18e}$$

$$\sum_{k=1}^{G} Tr\{\mathbf{W}_k\} \leq P_{max} \tag{2.18f}$$

$$\mathbf{W}_k \succeq 0 \tag{2.18g}$$

$$rank(\mathbf{W}_k) = 1, \quad k = 1, ..., G \tag{2.18h}$$

$$(2.14c), (2.15a\text{-}b). \tag{2.18i}$$

The problem in (2.18) is not convex and it can be solved using semidefinite relaxation (SDR) by dropping the rank constraint in (2.18h) [25] and (2.15a). In this case, we obtain a convex problem whose solution gives a good starting point.

The steps of the proposed algorithm for the problem in (2.17) are given as follows.

Algorithm 2.1: Antenna Selection for SWIPT in Multi-Group Multicasting Systems Using FPP-SCA (AS-FPP)

Let $\lambda_1(\mathbf{W})$ and $\mathbf{u}_1(\mathbf{W})$ denote the maximum eigenvalue and the corresponding eigenvector of the Hermitian symmetric matrix $\mathbf{W}$, respectively.

Initialization: $q = 0$,

Set proper $\zeta > 0$. Let $\{\{\mathbf{W}_k^{(0)}\}_{k=1}^{G}, \mathbf{b}^{(0)}, \{v_i^{(0)}, \kappa_i^{(0)}\}_{i=1}^{N}\}$ denote the solution obtained by SDR. Take the initial points as $\mathbf{w}_k^{(0)} = \sqrt{\lambda_1(\mathbf{W}_k^{(0)})} \mathbf{u}_1(\mathbf{W}_k^{(0)})$, $k = 1, ..., G$.

Phase 1: Iterations ($q \rightarrow q + 1$)

1) Solve the following problem in (2.19) and denote the optimum solution as
$\{\{\mathbf{w}_k^{(q)}\}_{k=1}^G, \mathbf{b}^{(q)}, \{\upsilon_i^{(q)}, \kappa_i^{(q)}\}_{i=1}^N\}$.

$$\min_{\{\mathbf{w}_k\}_{k=1}^G, \mathbf{b}, \{\upsilon_i, \kappa_i, s_i, r_i\}_{i=1}^N} \sum_{k=1}^G \mathbf{w}_k^H \mathbf{w}_k - \zeta \mathbf{b}^{(q-1)^T} \mathbf{b} + \alpha \sum_{i=1}^N (s_i + r_i) \quad (2.19a)$$

$$s.t. \ 2\operatorname{Re}\{\mathbf{w}_k^{(q-1)^H} \mathbf{R}_i \mathbf{w}_k\} - \mathbf{w}_k^{(q-1)^H} \mathbf{R}_i \mathbf{w}_k^{(q-1)}$$
$$- \gamma_i \sum_{l \neq k} \mathbf{w}_l^H \mathbf{R}_i \mathbf{w}_l \geq \gamma_i \sigma_{I,i}^2 \upsilon_i + \gamma_i \sigma_{A,i}^2 - s_i \quad (2.19b)$$

$$\sum_{k=1}^G (2\operatorname{Re}\{\mathbf{w}_k^{(q-1)^H} \mathbf{R}_i \mathbf{w}_k\} - \mathbf{w}_k^{(q-1)^H} \mathbf{R}_i \mathbf{w}_k^{(q-1)}) \geq \frac{\mu_i}{\xi_i} \kappa_i - \sigma_{A,i}^2 - r_i \quad (2.19c)$$

$$s_i \geq 0, \ r_i \geq 0, \quad \forall i \in \mathcal{G}_k, \forall k, l \in \{1, ..., G\} \quad (2.19d)$$

$$(2.14b\text{-}c), (2.14g\text{-}h), (2.15b) . \quad (2.19e)$$

2) If $\mathbf{b}^{(q)^T} \mathbf{b}^{(q)} = L$ or $\mathbf{b}^{(q)^T} \mathbf{b}^{(q)} \geq \beta \mathbf{b}^{(q-1)^T} \mathbf{b}^{(q-1)}$, (improved solution), where $\beta > 1$ is a proper value (Ex: 1.2), keep the value of ζ same. Otherwise, increase ζ (Ex: $\zeta \rightarrow 2\zeta$).

3) If the maximum iteration number for Phase 1 is reached, $q = q_{1,max}$, or $|| \sum_{k=1}^G (\mathbf{w}_k^{(q)} - \mathbf{w}_k^{(q-1)})||_2 \leq \epsilon$ for sufficiently small $\epsilon > 0$, go to Phase 2.

Phase 2:

4) Select the antennas corresponding to the indices of the largest L values of $\mathbf{b}^{(q)}$. Repeat Phase 1 for the reduced-size problem with the selected antennas. In this case, replace $\mathbf{R}_i$ and $\mathbf{w}_k$ in (2.19) by $\tilde{\mathbf{R}}_i = \tilde{\mathbf{h}}_i \tilde{\mathbf{h}}_i^H$ and $\tilde{\mathbf{w}}_k$ where $\tilde{\mathbf{h}}_i^H$ is the $1 \times L$ reduced-size channel vector related to the selected antennas and $\tilde{\mathbf{w}}_k \in \mathbb{C}^L$ is the corresponding reduced-size beamformer weight vector. Furthermore, the modified problem does not include $\mathbf{b}$.

5) Terminate if the maximum iteration number for Phase 2, $q_{2,max}$, is reached or the algorithm converges. Take the candidate beamforming weight vectors as $\{\tilde{\mathbf{w}}_k'\}_{k=1}^G$ and PS ratios as $\rho_i' = \frac{\kappa_i'}{\upsilon_i' + \kappa_i'}$, $i = 1, ..., N$, where $\{\{\tilde{\mathbf{w}}_k'\}_{k=1}^G, \{\upsilon_i', \kappa_i'\}_{i=1}^N\}$ is the obtained solution at the end of the iterations.

If the algorithm stops by reaching the maximum number of iterations, the candidate beamforming weight vectors $\{\tilde{\mathbf{w}}_k'\}_{k=1}^G$ may not satisfy the SINR and harvested power

constraints in (2.14e) and (2.14f), respectively. In order to generate a feasible solution, an additional linear programming problem is solved for finding the appropriate scale factors, $\sqrt{c_k}$, $k = 1, ..., G$, for the candidate beamforming weight vectors similar to [25]. Let us define $a_{k,i} = |\tilde{\mathbf{w}}_k'^H \tilde{\mathbf{h}}_i|^2$ and $\pi_k = ||\tilde{\mathbf{w}}_k'||_2^2$. The following linear programming problem is solved to generate a feasible solution from $\{\tilde{\mathbf{w}}_k'\}_{k=1}^G$:

$$\min_{\{c_k\}_{k=1}^G} \sum_{k=1}^G \pi_k c_k \tag{2.20a}$$

$$s.t. \ \rho_i' a_{k,i} c_k - \gamma_i \rho_i' \sum_{l \neq k} a_{l,i} c_l - \gamma_i \rho_i' \sigma_{A,i}^2 - \gamma_i \sigma_{I,i}^2 \geq 0 \tag{2.20b}$$

$$\xi_i(1 - \rho_i')(\sum_{k=1}^G a_{k,i} c_k + \sigma_{A,i}^2) - \mu_i \geq 0, \quad \forall i \in \mathcal{G}_k, \ \forall k, l \in \{1, ..., G\} \tag{2.20c}$$

$$\sum_{k=1}^G \pi_k c_k \leq P_{max}, \ c_k \geq 0 \ \ \forall k \in \{1, ..., G\}. \tag{2.20d}$$

After solving (2.20), we obtain the reduced-size beamforming weight vectors as $\sqrt{c_{k_{opt}}} \tilde{\mathbf{w}}_k'$. Note that the remaining beamformer weights are zero since the corresponding antennas are not used.

Selecting a good initial value for the penalty parameter ζ is not an easy task since it is problem dependent. When the initial value of ζ is selected large, the solution is forced to the feasible region in a fast manner. It may result high transmitted power due to fast convergence. If the initial value of ζ is too small, then the required number of iterations can increase. A reasonable value for the initial value of ζ can be one in order to give equal weight to each term in the objective function.

The computational complexity of the proposed algorithm, AS-FPP, can be easily expressed by formulating the QCQP problem in (2.19) as a second order cone programming form. The worst-case complexity of solving (2.19) is $O([GM + M + 4N]^{3.5})$ (the number of variables is $GM + M + 4N$) while it is $O([GL + 4N]^{3.5})$ for Phase 2 of AS-FPP [34]. The worst case complexity of the linear programming problem in (2.20) is $O(\sqrt{G} log(1/\varepsilon))$ iterations where ε is the accuracy of the solution at termination, each requiring at most $O(G^3 + (2N + 1)G)$ arithmetic operations using interior point methods [25].

26
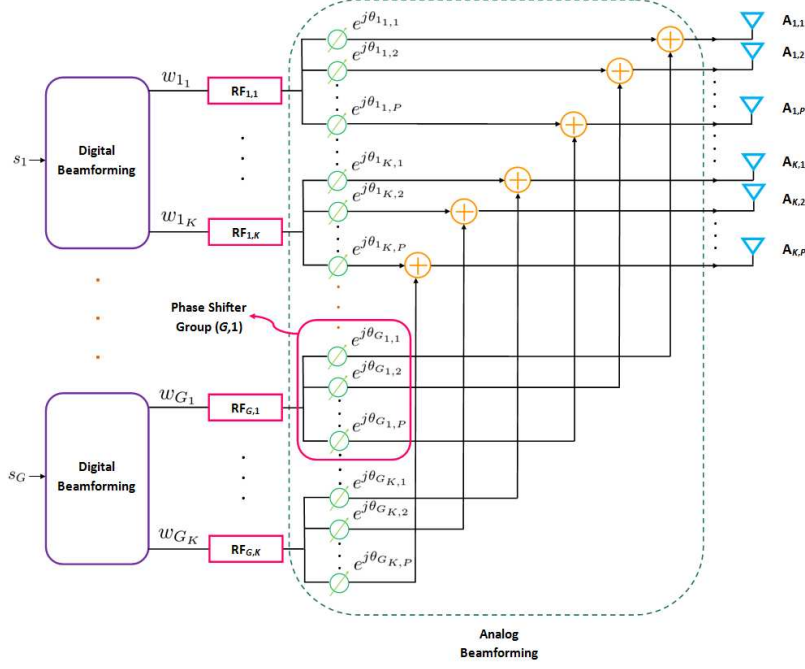
Figure 2.2: Hybrid Multi-Group Multicast Beamforming System.

2.5 Hybrid Beamforming

While antenna selection is an effective and low-cost approach, hybrid beamforming presents new opportunities for better performance in certain cases. In this chapter, hybrid beamformer structure as shown in Fig. 2.2 is considered for multi-group multicasting scenario. This hybrid structure consists of two stages, namely digital and analog beamformer which should be jointly designed for effective power utilization. This structure presents a trade-off between performance and the number of RF chains. When the number of RF chains for each multicast stream is the same as the number of antennas (full digital beamformer), the best performance is achieved. If it is less than the number of antennas (i.e., hybrid beamformer), the system cost is decreased while there is a certain performance loss. In Fig. 2.2, there are GK RF chains. Each RF chain is followed by P RF phase shifters. The analog signals coming from phase shifters of each multicast group are added up and the summed signal is fed into an antenna. As can be seen in Fig. 2.2, the total number of antennas is KP.

The beamforming weight vector for the kth multicast group is $KP \times 1$ complex vector $\mathbf{w}_k = [\, w_{k_{1,1}} \; w_{k_{1,2}} \; ... \; w_{k_{1,P}} \; w_{k_{2,1}} \; ... \; w_{k_{2,P}} \; ... \; w_{k_{K,1}} \; ... \; w_{k_{K,P}} \,]^T$ where $w_{k_{n,p}} = w_{k_n} e^{j\theta_{k_{n,p}}}$.

w_{k_n} is the digital beamformer coefficient corresponding to the nth RF chain for the kth multicast stream. $\theta_{k_{n,p}}$ is the phase shift introduced by the pth phase shifter following the nth RF chain of the kth digital beamformer block. Hence, the elements of the beamforming weight vectors, $\{\mathbf{w}_k\}_{k=1}^G$, are the phase shifted versions of the digital weights $\{w_{k_1}, w_{k_2}, ..., w_{k_K}\}_{k=1}^G$. As a result, the amplitude of the complex weights inside each phase shifter group should be the same, i.e., $|w_{k_n}| = |w_{k_{n,p}}|$ for $p = 1, ..., P$, $n = 1, ..., K$ and $k = 1, ..., G$ where the phase shifters following $\text{RF}_{k,n}$ constitute the phase shifter group (k, n). The first weight of the phase shifter group (k, n), $w_{k_{n,1}}$, can be chosen as w_{k_n}, i.e., $w_{k_{n,1}} = w_{k_n}$ for $k = 1, ..., G$ and $n = 1, ..., K$ without loss of generality.

In this chapter, three different hybrid beamformer designs are considered. The first two of these beamformers are continuous-phase. The third beamformer employs two-bit discrete phase shifters while the weights of the beamformer are computed without resorting to combinatorial optimization. This special beamformer is especially valuable for practical implementations and its performance is close to its continuous counterparts.

The continuous-phase beamformers are constructed using two competing schemes namely AM and FPP-SCA, respectively. While FPP-SCA is theoretically more computationally efficient, it is found that AM can perform better than FPP-SCA in certain cases. This is due to the fact that the problem structure is more suitable for semidefinite programming resulting from matrix lifting ($\mathbf{W}_k = \mathbf{w}_k \mathbf{w}_k^H$). These points will be further elaborated in Section 2.6.

In the following parts, these three beamformers are introduced in order.

2.5.1 Hybrid Beamforming with Continuous Phase Shifters

Phase shifts $\theta_{k_{n,p}}$ can be continuous or discrete leading to continuous-phase and discrete-phase beamformers, respectively. In this part, the hybrid beamformer design problem is first constructed in its general form, namely in continuous form.

The QoS-aware SWIPT optimization problem for the hybrid structure with continu-

ous phase shifters can be expressed as,

$$\min_{\{\mathbf{w}_k\}_{k=1}^{G}, \{\upsilon_i, \kappa_i\}_{i=1}^{N}} \sum_{k=1}^{G} \mathbf{w}_k^H \mathbf{w}_k \tag{2.21a}$$

$$s.t. \quad |w_{k_{n,p}}| = |w_{k_{n,1}}|, \quad p = 2, ..., P, \ n = 1, ..., K, \ k = 1, ..., G \tag{2.21b}$$

$$\mathbf{w}_k^H \mathbf{R}_i \mathbf{w}_k - \gamma_i \sum_{l \neq k} \mathbf{w}_l^H \mathbf{R}_i \mathbf{w}_l \geq \gamma_i \sigma_{I,i}^2 \upsilon_i + \gamma_i \sigma_{A,i}^2 \tag{2.21c}$$

$$\sum_{k=1}^{G} \mathbf{w}_k^H \mathbf{R}_i \mathbf{w}_k \geq \frac{\mu_i}{\xi_i} \kappa_i - \sigma_{A,i}^2 \tag{2.21d}$$

$$\left\| \begin{matrix} \upsilon_i - \kappa_i \\ 2 \end{matrix} \right\|_2 \leq \upsilon_i + \kappa_i - 2, \quad \forall \, i \in \mathcal{G}_k, \forall \, k, l \in \{1, ..., G\} \tag{2.21e}$$

$$\sum_{k=1}^{G} \mathbf{w}_k^H \mathbf{w}_k \leq P_{max}. \tag{2.21f}$$

The above problem is not convex. By introducing $\mathbf{W}_k = \mathbf{w}_k \mathbf{w}_k^H$ this problem can be written as,

$$\min_{\{\mathbf{W}_k\}_{k=1}^{G}, \{\upsilon_i, \kappa_i\}_{i=1}^{N}} \sum_{k=1}^{G} Tr\{\mathbf{W}_k\} \tag{2.22a}$$

$$s.t. \quad W_{k_{n,n}}(p, p) = W_{k_{n,n}}(1, 1), \quad p = 2, ..., P, \ n = 1, ..., K, \ k = 1, ..., G \tag{2.22b}$$

$$Tr\{\mathbf{R}_i \mathbf{W}_k\} - \gamma_i \sum_{l \neq k} Tr\{\mathbf{R}_i \mathbf{W}_l\} \geq \gamma_i \sigma_{I,i}^2 \upsilon_i + \gamma_i \sigma_{A,i}^2 \tag{2.22c}$$

$$\sum_{k=1}^{G} Tr\{\mathbf{R}_i \mathbf{W}_k\} \geq \frac{\mu_i}{\xi_i} \kappa_i - \sigma_{A,i}^2 \tag{2.22d}$$

$$\left\| \begin{matrix} \upsilon_i - \kappa_i \\ 2 \end{matrix} \right\|_2 \leq \upsilon_i + \kappa_i - 2, \quad \forall \, i \in \mathcal{G}_k, \forall \, k, l \in \{1, ..., G\} \tag{2.22e}$$

$$\sum_{k=1}^{G} Tr\{\mathbf{W}_k\} \leq P_{max} \tag{2.22f}$$

$$\mathbf{W}_k \succeq 0 \tag{2.22g}$$

$$rank(\mathbf{W}_k) = 1, \quad k = 1, ..., G \tag{2.22h}$$

where $W_{k_{n_1, n_2}}(p_1, p_2)$ denotes the (p_1, p_2)-th entry of the (n_1, n_2)-th $P \times P$ submatrix of $\mathbf{W}_k$. The optimization problem in (2.22) is still nonconvex due to the rank constraints in (2.22h). The following theorem is used to express the rank constraint in a more suitable way.

Theorem 2.2: For a $M \times M$ Hermitian symmetric, positive semidefinite matrix $\mathbf{W}$, $Tr\{\mathbf{W}^2\}$ is upper bounded by $(Tr\{\mathbf{W}\})^2$, i.e. $Tr\{\mathbf{W}^2\} \leq (Tr\{\mathbf{W}\})^2$. This upper bound is reached if and only if $rank(\mathbf{W}) = 1$.

Proof: The proof of this theorem can be found in [94]. ∎

Corollary 2.1: For a Hermitian symmetric, positive semidefinite matrix $\mathbf{W}$, the condition $(Tr\{\mathbf{W}\})^2 - Tr\{\mathbf{W}^2\} \leq 0$ implies that $\mathbf{W}$ has rank one.

We can use the condition given in Corollary 2.1 in place of the rank constraints in (2.22h). This condition is nonconvex but quadratic, hence we can use absolute exact penalty function to move it to the objective.

Lemma 2.3: If an optimum solution of (2.22) satisfies Karush-Kuhn-Tucker conditions, then it is also an optimum solution of the following problem in (2.23) for $\zeta_1, ..., \zeta_G > \zeta_0$ with $\zeta_0 > 0$ being a finite value.

$$\min_{\{\mathbf{W}_k\}_{k=1}^{G}, \{v_i, \kappa_i\}_{i=1}^{N}} \sum_{k=1}^{G} Tr\{\mathbf{W}_k\} + \sum_{k=1}^{G} \zeta_k \max\{0, (Tr\{\mathbf{W}_k\})^2 - Tr\{\mathbf{W}_k^2\}\} \quad (2.23a)$$

$$s.t. \quad (2.22b\text{-}g) \quad (2.23b)$$

Proof: Please refer to Appendix A.2. ∎

Note that $\max\{0, (Tr\{\mathbf{W}_k\})^2 - Tr\{\mathbf{W}_k{}^2\}\} = (Tr\{\mathbf{W}_k\})^2 - Tr\{\mathbf{W}_k{}^2\}$ from Theorem 2.2. Hence, AM can be used to solve (2.23) with convex optimization at each step [36]. Furthermore, the second order cone constraints in (2.22e) can be expressed as positive semidefinite cone constraints as follows,

$$\begin{bmatrix} v_i - 1 & 1 \\ 1 & \kappa_i - 1 \end{bmatrix} \geq 0, \quad i = 1, ..., N. \quad (2.24)$$

The condition in (2.24) implies the following inequalities from the determinant of the matrix in (2.24) and the positivity of its diagonal elements,

$$v_i \geq 1, \ \kappa_i \geq 1 \quad (2.25a)$$

$$v_i \kappa_i - v_i - \kappa_i \geq 0. \quad (2.25b)$$

Hence, (2.24) can be used in place of (2.22e) and a semidefinite programming prob-

lem is solved at the qth iteration of AM, i.e.,

$$\min_{\{\mathbf{W}_k\}_{k=1}^{G}, \{v_i, \kappa_i\}_{i=1}^{N}} \sum_{k=1}^{G} Tr\{\mathbf{W}_k\} + \sum_{k=1}^{G} \zeta_k(Tr\{\mathbf{W}_k^{(q-1)}\}Tr\{\mathbf{W}_k\} - Tr\{\mathbf{W}_k^{(q-1)}\mathbf{W}_k\})$$

(2.26a)

$$s.t. \quad (2.22\text{b-d}), (2.22\text{f-g}), (2.24) .$$

(2.26b)

Since the objective function in (2.26a) is lower bounded and a convex programming problem is solved at each iteration, the objective function improves at each iteration and the iterative approach is guaranteed to converge [95].

The steps of the proposed AM approach for the solution of (2.26) are given below.

Algorithm 2.2: Hybrid Beamforming for SWIPT in Multi-Group Multicasting Systems with Continuous Phase Shifters Using AM (HB-CPS-AM)

Let $\lambda_1(\mathbf{W})$ and $\mathbf{u}_1(\mathbf{W})$ denote the maximum eigenvalue and the corresponding eigenvector of the Hermitian symmetric matrix $\mathbf{W}$, respectively.

Initialization: $q = 0$,

Set $\zeta_1, ..., \zeta_G > 0$ and $\{\mathbf{W}_k^{(0)}\}_{k=1}^{G}$ to zero.

Iterations: $(q \to q + 1)$

1) Solve (2.26) for $\{\{\mathbf{W}_k^{(q)}\}_{k=1}^{G}, \{v_i^{(q)}, \kappa_i^{(q)}\}_{i=1}^{N}\}$ while fixing $\{\mathbf{W}_k^{(q-1)}\}_{k=1}^{G}$.

2) *for* $k = 1 : G$

If $rank(\mathbf{W}_k^{(q)}) = 1$ or $\frac{\lambda_1(\mathbf{W}_k^{(q)})}{Tr\{\mathbf{W}_k^{(q)}\}} \geq \beta_k \frac{\lambda_1(\mathbf{W}_k^{(q-1)})}{Tr\{\mathbf{W}_k^{(q-1)}\}}$ (improved solution),where $\beta_k > 1$ is a proper value (Ex: $\beta_k = 1.2$), keep the value of ζ_k same. Otherwise, increase ζ_k (Ex: $\zeta_k \to 2\zeta_k$).

3) Terminate if the maximum iteration number is reached, $q = q_{max}$, or $\sum_{k=1}^{G}(Tr\{\mathbf{W}_k^{(q)}\})^2 - Tr\{\mathbf{W}_k^{(q)^2}\} \leq \epsilon$ for sufficiently small $\epsilon > 0$.

End:

4) *for* $k = 1 : G$

If $rank(\mathbf{W}_k^{(q)}) = 1$, take the candidate beamformer weight vector for the kth multicast group, $\mathbf{w}'_k$, as $\sqrt{\lambda_1(\mathbf{W}_k^{(q)})}\mathbf{u}_1(\mathbf{W}_k^{(q)})$. Otherwise, select the elements of the candidate

beamformer weight vector as,

$$w'_{k_{n,p}} = \sqrt{W^{(q)}_{k_{n,n}}(1,1)} e^{j\angle u_1(\mathbf{W}^{(q)}_k)_{P(n-1)+p}}, \ p = 1, ..., P, \ n = 1, ..., K \qquad (2.27)$$

where $u_1(\mathbf{W}^{(q)}_k)_{P(n-1)+p}$ denotes the $(P(n-1)+p)^{th}$ element of $\mathbf{u}_1(\mathbf{W}^{(q)}_k)$.

5) Take the PS ratios as $\rho'_i = \frac{\kappa^{(q)}_i}{v^{(q)}_i + \kappa^{(q)}_i}, \ i = 1, ..., N$.

6) Define $a_{k,i} = |\mathbf{w}'^H_k \mathbf{h}_i|^2$ and $\pi_k = ||\mathbf{w}'_k||^2_2$. Solve (2.20) and obtain the beamforming weight vectors as $\sqrt{c_{k_{opt}}} \mathbf{w}'_k$.

The worst case complexity of HB-CPS-AM at each iteration using interior point methods is $O(\sqrt{GKP + 2N} log(1/\varepsilon))$ iterations where ε is the accuracy of the solution at termination. Each iteration requires at most $O((GK^2P^2 + 2N)^3 + (GK^2P^2 + 2N)(2N + 1 + GK(P-1)))$ arithmetic operations [25].

FPP-SCA Approach with Lower Complexity

While HB-CPS-AM algorithm is more suitable for hybrid beamforming problem, FPP-SCA presents a computationally efficient alternative. Hence, FPP-SCA is also implemented for the hybrid beamforming in order to characterize the advantages of both techniques. Some nontrivial modifications for FPP-SCA can be easily implemented to adapt this approach for the hybrid beamforming structure.

The hybrid beamforming problem in (2.21) can be expressed equivalently as follows,

$$\min_{\{\mathbf{w}_k, \mathbf{t}_k\}^G_{k=1}, \{v_i, \kappa_i\}^N_{i=1}} P \sum_{k=1}^{G} \mathbf{t}^T_k \mathbf{t}_k \qquad (2.28a)$$

$$s.t. \ |w_{k_{n,p}}| = t_{k_n} \ p = 1, ..., P, \ n = 1, ..., K, \ k = 1, ..., G \qquad (2.28b)$$

$$(2.21\text{c-f}) \qquad (2.28c)$$

where $\mathbf{t}_k$ is a $K \times 1$ real positive vector whose elements are the magnitudes of the digital weights for the kth multicast beamforming weight vector. t_{k_n} denotes the nth

element of $\mathbf{t}_k$. It is possible to express (2.28) in an alternative form, i.e.,

$$\min_{\{\mathbf{w}_k, \mathbf{t}_k\}_{k=1}^G, \{\upsilon_i, \kappa_i\}_{i=1}^N} \quad P \sum_{k=1}^G \mathbf{t}_k^T \mathbf{t}_k \tag{2.29a}$$

$$s.t. \; |w_{k_{n,p}}| \le t_{k_n} \tag{2.29b}$$

$$|w_{k_{n,p}}| \ge t_{k_n}, \; p = 1, ..., P, \; n = 1, ..., K, \; k = 1, ..., G \tag{2.29c}$$

$$(2.21c\text{-}f) \; . \tag{2.29d}$$

The constraints in (2.29c) are not convex. We can express the constraints in (2.29c) as $t_{k_n}^2 - |w_{k_{n,p}}|^2 \le 0$ and use absolute exact penalty function to move them to the objective function. Similar to Lemma 2.3, the following problem for a finite $\zeta > 0$ is equivalent to (2.29) in the sense that their optimum solutions are the same, i.e.,

$$\min_{\{\mathbf{w}_k, \mathbf{t}_k\}_{k=1}^G, \{\upsilon_i, \kappa_i\}_{i=1}^N} \quad P \sum_{k=1}^G \mathbf{t}_k^T \mathbf{t}_k + \zeta \sum_{k=1}^G \sum_{n=1}^K \sum_{p=1}^P \max\{0, t_{k_n}^2 - |w_{k_{n,p}}|^2\} \tag{2.30a}$$

$$s.t. \; (2.21c\text{-}f), (2.29b) \; . \tag{2.30b}$$

Note that the terms in exact penalty function satisfy $\max\{0, t_{k_n}^2 - |w_{k_{n,p}}|^2\} = t_{k_n}^2 - |w_{k_{n,p}}|^2$ by (2.29b) and exact penalty function can be written as $\zeta \sum_{k=1}^G (P\mathbf{t}_k^T \mathbf{t}_k - \mathbf{w}_k^H \mathbf{w}_k)$. In this case, the objective function is not convex due to $-\mathbf{w}_k^H \mathbf{w}_k$ term. In the following FPP-SCA based algorithm, we replace the nonconvex $\zeta \sum_{k=1}^G (P\mathbf{t}_k^T \mathbf{t}_k - \mathbf{w}_k^H \mathbf{w}_k)$ term by $\zeta \sum_{k=1}^G (P\mathbf{t}_k^T \mathbf{t}_k - \mathrm{Re}(\mathbf{w}_k^{(q-1)H} \mathbf{w}_k))$ at the qth iteration where $\mathbf{w}_k^{(q-1)}$ is the previous iterant. The steps of the proposed algorithm are given as follows.

Algorithm 2.3: Hybrid Beamforming for SWIPT in Multi-Group Multicasting Systems with Continuous Phase Shifters Using FPP-SCA (HB-CPS-FPP)

Let $\lambda_1(\mathbf{W})$ and $\mathbf{u}_1(\mathbf{W})$ denote the maximum eigenvalue and the corresponding eigenvector of the Hermitian symmetric matrix $\mathbf{W}$, respectively.

Initialization: $q = 0$,

Set $\zeta > 0$ and solve (2.22) by dropping (2.22h). Let $\{\{\mathbf{W}_k^{(0)}\}_{k=1}^G, \{\upsilon_i^{(0)}, \kappa_i^{(0)}\}_{i=1}^N\}$ denote the solution of (2.22). Take the initial point as $\mathbf{w}_k^{(0)} = \sqrt{\lambda_1(\mathbf{W}_k^{(0)})}\mathbf{u}_1(\mathbf{W}_k^{(0)})$,

$k = 1, ..., G$. Set the elements of $\mathbf{t}_k^{(0)}$ as $t_{k_n}^{(0)} = \max_p |w_{k_{n,p}}^{(0)}|$, $n = 1, ..., K$, $k = 1, ..., G$.

Iterations: $(q \to q + 1)$

1) Solve the following problem in (2.31) and denote the optimum solution as $\{\{\mathbf{w}_k^{(q)}, \mathbf{t}_k^{(q)}\}_{k=1}^G, \{v_i^{(q)}, \kappa_i^{(q)}\}_{i=1}^N\}$.

$$\min_{\{\mathbf{w}_k, \mathbf{t}_k\}_{k=1}^G, \{v_i, \kappa_i, s_i, r_i\}_{i=1}^N} P \sum_{k=1}^G \mathbf{t}_k^T \mathbf{t}_k + \zeta \sum_{k=1}^G (P\mathbf{t}_k^T \mathbf{t}_k - \mathrm{Re}(\mathbf{w}_k^{(q-1)H} \mathbf{w}_k)) + \alpha \sum_{i=1}^N (s_i + r_i)$$

$$(2.31a)$$

$$s.t. \ 2\,\mathrm{Re}\{\mathbf{w}_k^{(q-1)H} \mathbf{R}_i \mathbf{w}_k\} - \mathbf{w}_k^{(q-1)H} \mathbf{R}_i \mathbf{w}_k^{(q-1)}$$
$$- \gamma_i \sum_{l \neq k} \mathbf{w}_l^H \mathbf{R}_i \mathbf{w}_l \geq \gamma_i \sigma_{I,i}^2 v_i + \gamma_i \sigma_{A,i}^2 - s_i \qquad (2.31b)$$

$$\sum_{k=1}^G (2\,\mathrm{Re}\{\mathbf{w}_k^{(q-1)H} \mathbf{R}_i \mathbf{w}_k\} - \mathbf{w}_k^{(q-1)H} \mathbf{R}_i \mathbf{w}_k^{(q-1)}) \geq \frac{\mu_i}{\xi_i} \kappa_i - \sigma_{A,i}^2 - r_i \qquad (2.31c)$$

$$s_i \geq 0, \ r_i \geq 0, \quad \forall i \in \mathcal{G}_k, \forall k, l \in \{1, ..., G\} \qquad (2.31d)$$

(2.21e-f), (2.29b). $\qquad (2.31e)$

2) If $\sum_{k=1}^G (P\mathbf{t}_k^{(q)T} \mathbf{t}_k^{(q)} - \mathbf{w}_k^{(q)H} \mathbf{w}_k^{(q)}) = 0$ or $\sum_{k=1}^G (P\mathbf{t}_k^{(q)T} \mathbf{t}_k^{(q)} - \mathbf{w}_k^{(q)H} \mathbf{w}_k^{(q)}) \leq \beta \sum_{k=1}^G (P\mathbf{t}_k^{(q-1)T} \mathbf{t}_k^{(q-1)} - \mathbf{w}_k^{(q-1)H} \mathbf{w}_k^{(q-1)})$, (improved solution), where $\beta < 1$ is a proper value (Ex: 0.7), keep the value of ζ same. Otherwise, increase ζ (Ex: $\zeta \to 2\zeta$).

3) Terminate if the maximum iteration number is reached, $q = q_{max}$, or $|| \sum_{k=1}^G (\mathbf{w}_k^{(q)} - \mathbf{w}_k^{(q-1)})||_2 \leq \epsilon$ for sufficiently small $\epsilon > 0$.

End:

4) *for $k = 1 : G$*

Select the elements of the candidate beamformer weight vector $\mathbf{w}_k'$ as follows,

$$w_{k_{n,p}}' = t_{k_n}^{(q)} e^{j \angle w_{k_{n,p}}^{(q)}}, \ p = 1, ..., P, \ n = 1, ..., K. \qquad (2.32)$$

5) Take the PS ratios as $\rho_i' = \frac{\kappa_i^{(q)}}{v_i^{(q)} + \kappa_i^{(q)}}$, $i = 1, ..., N$.

6) Define $a_{k,i} = |\mathbf{w}_k'^H \mathbf{h}_i|^2$ and $\pi_k = ||\mathbf{w}_k'||_2^2$. Solve (2.20) and obtain the beamforming weight vectors as $\sqrt{c_{k_{opt}}} \mathbf{w}_k'$.

The worst-case complexity of solving (2.31) in second-order cone form is $O([GKP + GK + 4N]^{3.5})$ [34]. Note that it is less than the worst-case complexity of the HB-CPS-AM algorithm.

2.5.2 Hybrid Beamforming with Two-Bit Phase Shifters

Practical RF phase shifters usually have discrete set of phase angles. Using small number of bit values for the phase shifters is advantageous in terms of cost, hardware complexity and accuracy. It turns out that the beamformer design has an important simplification when two-bit RF phase shifters are used. This is due to the fact that for two-bit case, the discrete constraints can be written in terms of continuous linear equality and inequalities. This is unique to the two-bit case and may not be extended to higher bits easily.

In two-bit phase system, there are four possible discrete phase angles for $w_{k_{n,p}}/w_{k_{n,1}}$, $p = 2, ..., P$, $n = 1, ..., K$, $k = 1, ...G$, i.e., $\{1, j, -1, -j\}$.

The QoS-aware SWIPT optimization problem for this hybrid structure can be expressed as,

$$\min_{\{\mathbf{w}_k\}_{k=1}^{G}, \{\upsilon_i, \kappa_i\}_{i=1}^{N}} \quad \sum_{k=1}^{G} \mathbf{w}_k^H \mathbf{w}_k \tag{2.33a}$$

$$s.t. \quad \frac{w_{k_{n,p}}}{w_{k_{n,1}}} \in \{1, j, -1, -j\}, \quad p = 2, ..., P, \ n = 1, ..., K, \ k = 1, ..., G \tag{2.33b}$$

$$(2.21\text{c-f}) . \tag{2.33c}$$

The above problem is not convex. Furthermore, it has a combinatorial nature. By

introducing $\mathbf{W}_k = \mathbf{w}_k \mathbf{w}_k^H$, it can be written as,

$$\min_{\{\mathbf{W}_k\}_{k=1}^{G}, \{v_i, \kappa_i\}_{i=1}^{N}} \sum_{k=1}^{G} Tr\{\mathbf{W}_k\} \tag{2.34a}$$

$$s.t. \quad \frac{W_{k_{n,n}}(p, 1)}{W_{k_{n,n}}(1, 1)} \in \{1, j, -1, -j\}, \quad p = 2, ..., P, \ n = 1, ..., K, \ k = 1, ..., G \tag{2.34b}$$

$$Tr\{\mathbf{R}_i \mathbf{W}_k\} - \gamma_i \sum_{l \neq k} Tr\{\mathbf{R}_i \mathbf{W}_l\} \geq \gamma_i \sigma_{I,i}^2 v_i + \gamma_i \sigma_{A,i}^2 \tag{2.34c}$$

$$\sum_{k=1}^{G} Tr\{\mathbf{R}_i \mathbf{W}_k\} \geq \frac{\mu_i}{\xi_i} \kappa_i - \sigma_{A,i}^2 \tag{2.34d}$$

$$\begin{bmatrix} v_i - 1 & 1 \\ 1 & \kappa_i - 1 \end{bmatrix} \geq 0, \quad \forall i \in \mathcal{G}_k, \forall k, l \in \{1, ..., G\} \tag{2.34e}$$

$$\sum_{k=1}^{G} Tr\{\mathbf{W}_k\} \leq P_{max} \tag{2.34f}$$

$$\mathbf{W}_k \geq 0 \tag{2.34g}$$

$$rank(\mathbf{W}_k) = 1, \quad k = 1, ..., G. \tag{2.34h}$$

The optimization problem in (2.34) is still nonconvex due to (2.34b) and (2.34h).

Lemma 2.4: The constraints in (2.34b) can be expressed as linear equality and inequalities as follows,

$$\frac{-W_{k_{n,n}}(1, 1)}{\sqrt{2}} \leq \text{Re}(W_{k_{n,n}}(p, 1)e^{j\pi/4}) \leq \frac{W_{k_{n,n}}(1, 1)}{\sqrt{2}} \tag{2.35a}$$

$$\frac{-W_{k_{n,n}}(1, 1)}{\sqrt{2}} \leq \text{Im}(W_{k_{n,n}}(p, 1)e^{j\pi/4}) \leq \frac{W_{k_{n,n}}(1, 1)}{\sqrt{2}} \tag{2.35b}$$

$$W_{k_{n,n}}(p, p) = W_{k_{n,n}}(1, 1), \quad p = 2, ..., P, \ n = 1, ..., K, \ k = 1, ..., G. \tag{2.35c}$$

Proof: $|W_{k_{n,n}}(p, 1)| = W_{k_{n,n}}(p, p) = W_{k_{n,n}}(1, 1)$ from the rank constraints in (2.34h) and (2.35c). Hence, $(\text{Re}(W_{k_{n,n}}(p, 1)e^{j\pi/4}))^2 + (\text{Im}(W_{k_{n,n}}(p, 1)e^{j\pi/4}))^2 = W_{k_{n,n}}(1, 1)^2$. In addition, $(\text{Re}(W_{k_{n,n}}(p, 1)e^{j\pi/4}))^2 \leq W_{k_{n,n}}(1, 1)^2/2$ and $(\text{Im}(W_{k_{n,n}}(p, 1)e^{j\pi/4}))^2 \leq W_{k_{n,n}}(1, 1)^2/2$ by (2.35a-b). It turns out that (2.35a-c) imply that $\text{Re}(W_{k_{n,n}}(p, 1)e^{j\pi/4}) = \pm W_{k_{n,n}}(1, 1)/\sqrt{2}$ and $\text{Im}(W_{k_{n,n}}(p, 1)e^{j\pi/4}) = \pm W_{k_{n,n}}(1, 1)/\sqrt{2}$. As a result, $W_{k_{n,n}}(p, 1)/W_{k_{n,n}}(1, 1) \in \{1, j, -1, -j\}$ which is the condition in (2.34b). ∎

When (2.34b) is replaced by (2.35a-c), the problem in (2.34) can be solved by iterative semidefinite programming using the same approach in the previous section. Hence,

AM algorithm is used for the two-bit hybrid beamformer design. At the qth iteration, the following semidefinite programming problem is solved,

$$\min_{\{\mathbf{W}_k\}_{k=1}^{G},\{\upsilon_i,\kappa_i\}_{i=1}^{N}} \sum_{k=1}^{G} Tr\{\mathbf{W}_k\} + \sum_{k=1}^{G} \zeta_k (Tr\{\mathbf{W}_k^{(q-1)}\}Tr\{\mathbf{W}_k\} - Tr\{\mathbf{W}_k^{(q-1)}\mathbf{W}_k\})$$

(2.36a)

$$s.t. \quad (2.34c\text{-}g), (2.35a\text{-}c) .$$

(2.36b)

The steps for the proposed two-bit hybrid beamformer algorithm can be presented as follows.

Algorithm 2.4: Hybrid Beamforming for SWIPT in Multi-Group Multicasting Systems with Two-Bit Phase Shifters (HB-TBPS)

Let $\lambda_1(\mathbf{W})$ and $\mathbf{u}_1(\mathbf{W})$ denote the maximum eigenvalue and the corresponding eigenvector of the Hermitian symmetric matrix $\mathbf{W}$, respectively.

Initialization: $q = 0$,

Set $\zeta_1, ..., \zeta_G > 0$ and $\{\mathbf{W}_k^{(0)}\}_{k=1}^{G}$ to zero.

Iterations: $(q \rightarrow q + 1)$

1) Solve (2.36) for $\{\{\mathbf{W}_k^{(q)}\}_{k=1}^{G}, \{\upsilon_i^{(q)}, \kappa_i^{(q)}\}_{i=1}^{N}\}$ while fixing $\{\mathbf{W}_k^{(q-1)}\}_{k=1}^{G}$.

2) *for* $k = 1 : G$

If $rank(\mathbf{W}_k^{(q)}) = 1$ or $\frac{\lambda_1(\mathbf{W}_k^{(q)})}{Tr\{\mathbf{W}_k^{(q)}\}} \geq \beta_k \frac{\lambda_1(\mathbf{W}_k^{(q-1)})}{Tr\{\mathbf{W}_k^{(q-1)}\}}$ (improved solution), where $\beta_k > 1$ is a proper value (Ex: $\beta_k = 1.2$), keep the value of ζ_k same. Otherwise, increase ζ_k (Ex: $\zeta_k \rightarrow 2\zeta_k$).

3) Terminate if the maximum iteration number is reached, $q = q_{max}$, or $\sum_{k=1}^{G}(Tr\{\mathbf{W}_k^{(q)}\})^2 - Tr\{\mathbf{W}_k^{(q)2}\} \leq \epsilon$ for sufficiently small $\epsilon > 0$.

End:

4) *for* $k = 1 : G$

If $rank(\mathbf{W}_k^{(q)}) = 1$, take the candidate beamformer weight vector for the kth multicast group, $\mathbf{w}'_k$, as $\sqrt{\lambda_1(\mathbf{W}_k^{(q)})}\mathbf{u}_1(\mathbf{W}_k^{(q)})$. Otherwise, select the elements of the candidate

beamformer weight vector as,

$$w'_{k_n,1} = \sqrt{W^{(q)}_{k_{n,n}}(1,1)}e^{j\angle(W^{(q)}_{k_n,1}(1,1)/W^{(q)}_{k_{1,1}}(1,1))} \tag{2.37a}$$

$$w'_{k_n,p} = w'_{k_n,1}e^{j\hat{\theta}(W^{(q)}_{k_{n,n}}(p,1)/W^{(q)}_{k_{n,n}}(1,1))}, \quad p = 2, ..., P, \quad n = 1, ..., K \tag{2.37b}$$

where $\hat{\theta}(W^{(q)}_{k_{n,n}}(p,1)/W^{(q)}_{k_{n,n}}(1,1))$ is the quantized angle such that
$\hat{\theta}(W^{(q)}_{k_{n,n}}(p,1)/W^{(q)}_{k_{n,n}}(1,1)) \in \{0, \pi/2, \pi, 3\pi/2\}$.

5) Take the PS ratios as $\rho'_i = \frac{\kappa^{(q)}_i}{\upsilon^{(q)}_i + \kappa^{(q)}_i}, i = 1, ..., N$.

6) Define $a_{k,i} = |\mathbf{w}'_k{}^H\mathbf{h}_i|^2$ and $\pi_k = ||\mathbf{w}'_k||^2_2$. Solve (2.20) and obtain the beamforming weight vectors as $\sqrt{c_{k_{opt}}}\mathbf{w}'_k$.

In the worst case, (2.36) requires $O(\sqrt{GKP + 2N}log(1/\varepsilon))$ iterations using interior point methods where ε is the accuracy of the solution at termination. Each iteration requires at most $O((GK^2P^2 + 2N)^3 + (GK^2P^2 + 2N)(2N + 1 + 5GK(P-1)))$ arithmetic operations [25].

2.6 Simulation Results

The proposed algorithms for antenna selection (AS-FPP) and hybrid beamforming (HB-CPS-AM, HB-CPS-FPP, HB-TBPS) are implemented using convex programming solver CVX [96]. In addition, full digital beamformer (FDB) which uses a separate RF chain for each antenna is presented as a baseline scheme. Algorithm 2.1 without antenna selection is implemented to obtain FDB. The algorithms are tested for different channel models and the results are obtained by averaging 100 feasible random channel realizations. The maximum allowable power at the base station is $P_{max} = 3$ W. Antenna and ID noise variances for each user are equal, i.e., $\sigma^2_A = \sigma^2_I = -40$ dBm. The signal attenuation from the base station to all users is 60 dB. The energy conversion efficiency at the EH of all users are selected as $\xi = 1$. SINR and harvested power thresholds for each user are set to be the same, i.e., $\gamma_i = \gamma$ and $\mu_i = \mu$ for $i = 1, ..., N$ for simplicity.

The parameters of the proposed algorithms are selected as follows. Maximum iteration number, q_{max} for each algorithm is taken as 30, where $q_{1,max} = q_{2,max} = 15$ for

AS-FPP. Initial exact penalty coefficients, ζ, $\{\zeta_k\}_{k=1}^{G}$ are set to 1. Penalty coefficient for the slack variables, α, in FPP-SCA based algorithms (AS-FPP, HB-CPS-FPP) is selected as 10 in accordance with [34].

2.6.1 Comparison of AS-FPP with Exhaustive Search and Random Antenna Selection

In the first experiment, there are $G = 2$ multicast groups with two users in each group, i.e., $N = 4$. The number of transmit antennas is $M = 10$. The SINR and harvested power thresholds are $\gamma = 0$ dB and $\mu = -30$ dBm, respectively. Rayleigh fading channel model is assumed. Fig. 2.3 shows the transmitted power for AS-FPP, FDB, exhaustive search (ES) which tries all antenna subset selections and random antenna selection (RAS) for different number of selected antennas. In RAS method, L antennas are randomly selected out of $M = 10$ antennas and Phase 2 of the AS-FPP algorithm is implemented with the selected antennas. As it is seen in Fig. 2.3, the search procedure introduced by the antenna selection coefficients, b_m, in Phase 1 of AS-FPP is more effective in comparison to RAS. In fact, the proposed AS-FPP introduces approximately 2 dBW power gain for $L = 4$. As the number of selected antennas, L, increases, the performance gap decreases since the likelihood of having good channels for random selection increases. In addition, the performance loss in comparison to exhaustive search is less than 0.8 dB for all points.
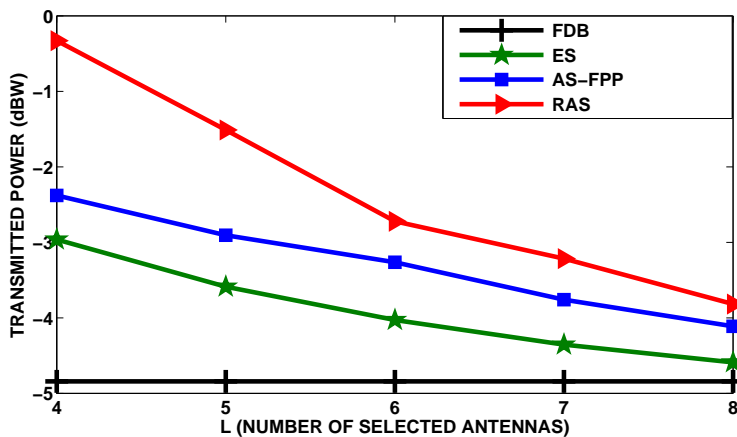
Figure 2.3: Transmitted power for FDB, AS-FPP, ES and RAS in two-group multi-casting scenario.
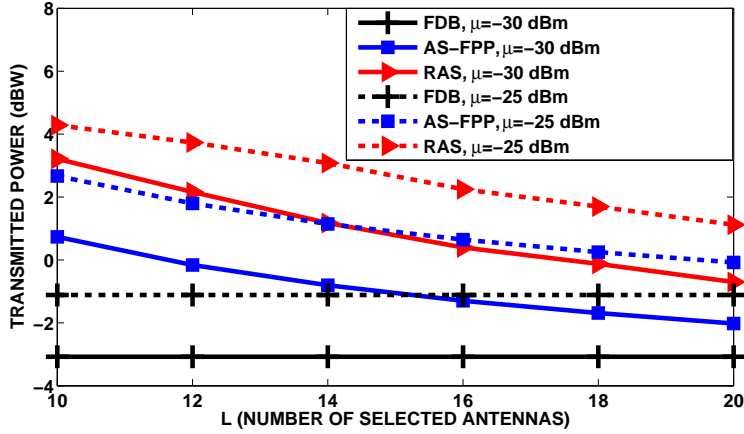
Figure 2.4: Transmitted power for FDB, AS-FPP and RAS in three-group multicasting scenario.

In Fig. 2.4, there are $M = 32$ antennas for three-group multicasting scenario ($G = 3$) with two users in each group, namely $N = 6$. Similar to Fig. 2.3, AS-FPP performs much better than RAS. The required power for $\mu = -25$ dBm is larger than that of $\mu = -30$ dBm as expected.

2.6.2 Comparison of Antenna Selection with the Hybrid Beamformers

In this part, the proposed beamforming methods, namely AS-FPP, HB-CPS-AM, HB-CPS-FPP, HB-TBPS, and FDB are compared. The first three beamformers are continuous-phase whereas HB-TBPS is a two-bit discrete-phase beamformer. Several experiments are performed and some interesting characteristics of these methods are presented in the following part.

Two-Group Multicasting Scenario: Two-group multicasting scenario, $G = 2$, is considered and there are two users in each multicast group, i.e., $N = 4$. The number of RF chains per each multicast stream is set to $K = 2$ for hybrid beamformers. Hence, the total number of RF chains is $GK = 4$. The same number of RF chains and antennas are used for both antenna selection and hybrid beamforming schemes for a fair comparison. In this case, the number of selected antennas is $L = GK = 4$ whereas the total number of antennas is $M = KP = 2P$. Note that the total number of antennas is the same for FDB.

In Fig. 2.5, all the proposed algorithms are compared in terms of the transmitted power for different number phase shifters per RF chain, P. The channel is assumed to be Rayleigh fading. The SINR and harvested power thresholds of the users are kept constant at $\gamma = 10$ dB and $\mu = -30$ dBm. Except $P = 4$, the required transmitted power for AS-FPP is the largest among the proposed schemes. As P increases, the performance gap between AS-FPP and hybrid beamformer algorithms increases. This is due to the fact that AS-FPP uses only $GK = 4$ antennas out of $M = 2P$ antennas whereas hybrid beamformers employ all the antennas. Specifically, continuous-phase hybrid beamformers require approximately 6.5 dBW less power while the gap between two-bit hybrid beamformer and antenna selection is approximately 5 dBW for $P = 16$.

Note that both HB-CPS-AM and HB-CPS-FPP perform almost the same and require approximately 1 dBW additional transmitted power compared to FDB. Although the order of worst-case computational complexity of HB-CPS-FPP is less than that of HB-CPS-AM, it is observed that the required time is higher for some scenarios.

As shown Fig. 2.5, the power difference between continuous and two-bit discrete-phase hybrid beamformers does not exceed 1.6 dBW for all P values showing the effectiveness of the two-bit phase shifters in hybrid beamformers. In this part, the proposed two-bit discrete-phase hybrid beamformer, HB-TBPS, is also compared with the beamformer obtained from continuous-phase hybrid beamformer through quantization (QHB). The beamformer weight vector is obtained by HP-CPP-AM algorithm and then the phase terms are quantized by two bits as in (2.37a-b). Note that the maximum power of the quantized beamformer is taken as $P_{max} = 100$ to prevent any feasibility problem. As it is seen in Fig. 2.5, the trivial quantization method performs worse than HB-TBPS showing the necessity of a separate design for discrete-phase beamformers.

In Fig. 2.6, the same experiment in Fig. 2.5 is repeated for mmWave channel with limited multipath components. The geometric channel model in [97] is adopted with $N_p = 15$ paths for a uniform linear array (ULA), i.e.,

$$\mathbf{h}_i^H = \sqrt{\frac{M}{P_L N_p}} \sum_{n_p=1}^{N_p} \alpha_{n_p}^i \mathbf{a}^H(\phi_{n_p}^i) \tag{2.38}$$

41
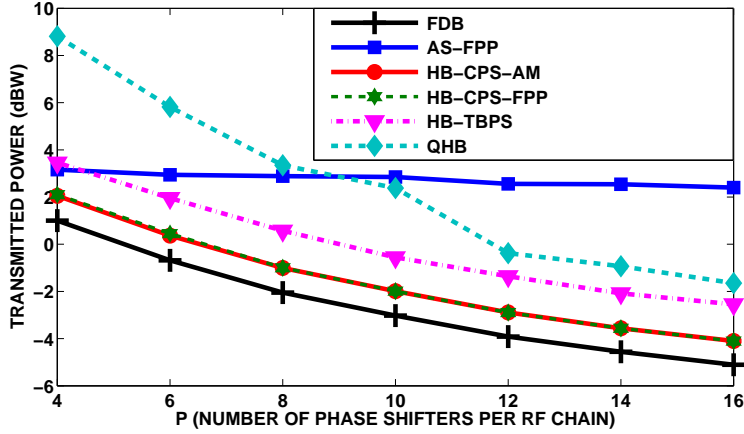
Figure 2.5: Comparison of antenna selection and hybrid beamformers for Rayleigh fading channel with $G = 2$.

where P_L and $\alpha_{n_p}^i$ denote the path loss and the strength associated with the n_p^{th} path seen by the ith user, respectively. $\alpha_{n_p}^i$ is selected from complex circularly symmetric Gaussian distribution with unit variance. $\mathbf{a}(\phi_{n_p}^i)$ is the array response vector for ULA, i.e., $\mathbf{a}(\phi) = 1/\sqrt{M}[\ 1\ e^{\frac{2\pi}{\lambda}dsin(\phi)}\ \dots\ e^{\frac{2\pi}{\lambda}(M-1)dsin(\phi)}]^T$ where ϕ is the azimuth angle. d is the antenna spacing and it is taken as $\lambda/2$. $\phi_{n_p}^i$ is selected independently from a uniform distribution over $[0, 2\pi]$. As shown in Fig. 2.6, a similar characteristics is observed as in Fig. 2.5.

Three-Group Multicasting Scenario: In this part, there are $G = 3$ multicast groups and 2 users in each group ($N = 6$). The number of RF chains per each multicast stream is selected as $K = 3$ for hybrid beamformers resulting $GK = 9$ RF chains. The number of selected antennas is $L = GK = 9$ for antenna selection. The number of antennas available at the base station is $M = KP = 3P$ for all methods.

In Fig. 2.7, we consider the same experiment in Fig. 2.5 for P between 4 and 12. Similar to Fig. 2.5, as P increases, the performance of AS-FPP gets worse relative to other algorithms. Different from Fig. 2.5, it performs better than HB-TBPS for $P = 4$ and $P = 6$. Hence, the difference between AS-FPP and HB-TBPS gets smaller as G increases since the number of digital weights that can be adjusted is GK in the proposed hybrid beamformer structure while it is G^2K in antenna selection system. One advantage of AS-FPP is that there is no direct link between the number of RF chains and multicast groups. On the contrary, hybrid beamformers require RF chains
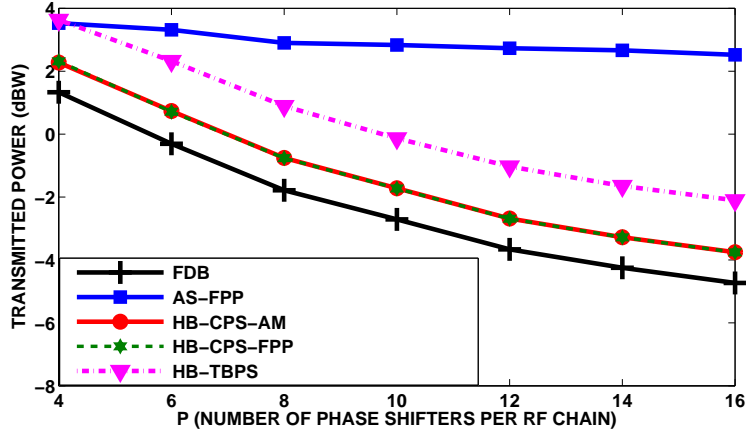
Figure 2.6: Comparison of antenna selection and hybrid beamformers for mmWave channel with $G = 2$.

as an integer multiple of the number of multicast groups.

In Fig. 2.8, the mmWave channel model in (2.38) is used. A very similar performance is obtained for all the algorithms. Furthermore, the power gap between FDB and hybrid beamformers which use continuous phase shifters is approximately 1 dBW as in Fig. 2.5 and 2.6.

Feasibility Rate: Table 2.1 shows the number of feasible instances in 100 Rayleigh fading random channel trials for different scenarios. The SINR threshold is $\gamma = 10$ dB. In all cases, as harvested power threshold increases, feasibility rate decreases. As it can be seen from Table 2.1, feasibility becomes an important issue for small number of phase shifters per RF chain, P. An important observation is that the feasibility rate of HB-CPS-AM is higher than HB-CPS-FPP for small values of P. Note that, as it is pointed previously the problem structure for continuous-phase hybrid beamformer is inherently more suitable for HB-CPS-AM. The constraints in (2.22b) are linear and hence do not require any modification for HB-CPS-AM. However, the corresponding constraints in (2.28b) are approximated in the neighborhood of the previous iterant in HB-CPS-FPP algorithm (2.31a).
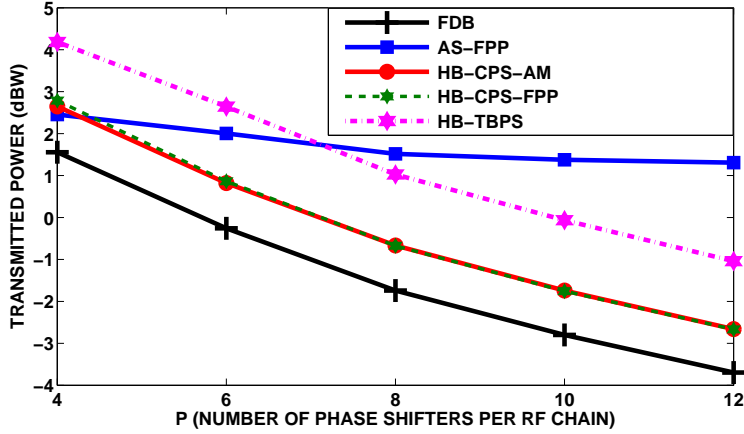
Figure 2.7: Comparison of antenna selection and hybrid beamformers for Rayleigh fading channel with $G = 3$.

Table 2.1: Number of Feasible Instances in 100 Random Trials

		$G = 2, N = 4, K = 2$					$G = 3, N = 6, K = 3$				
		$P = 4$	$P = 6$	$P = 8$	$P = 10$	$P = 12$	$P = 4$	$P = 6$	$P = 8$	$P = 10$	$P = 12$
FDB	$\mu = -30$ dBm	99	100	100	100	100	100	100	100	100	100
	$\mu = -25$ dBm	83	100	100	100	100	77	100	100	100	100
AS-FPP	$\mu = -30$ dBm	73	83	88	89	90	97	100	100	100	100
	$\mu = -25$ dBm	15	43	54	56	57	50	87	95	99	100
HB-CPS-AM	$\mu = -30$ dBm	93	100	100	100	100	92	100	100	100	100
	$\mu = -25$ dBm	46	100	100	100	100	28	99	100	100	100
HB-CPS-FPP	$\mu = -30$ dBm	88	100	100	100	100	72	97	100	100	100
	$\mu = -25$ dBm	45	99	100	100	100	26	99	100	100	100
HB-TBPS	$\mu = -30$ dBm	63	98	100	100	100	51	100	100	100	100
	$\mu = -25$ dBm	15	93	99	100	100	2	86	97	100	100

2.7 Conclusion

In this chapter, antenna selection and hybrid beamforming based transmitter structures are proposed for the joint problem of SWIPT and multi-group multicast beamforming. Several algorithms are developed using efficient QCQP techniques. First, an efficient algorithm for antenna selection is presented by expressing binary constraints in terms of continuous variables. Absolute exact penalty function and FPP-SCA are used to deal with the nonconvex constraints. It is shown that the proposed algorithm performs very well in comparison to the random antenna selection scheme. A novel

44
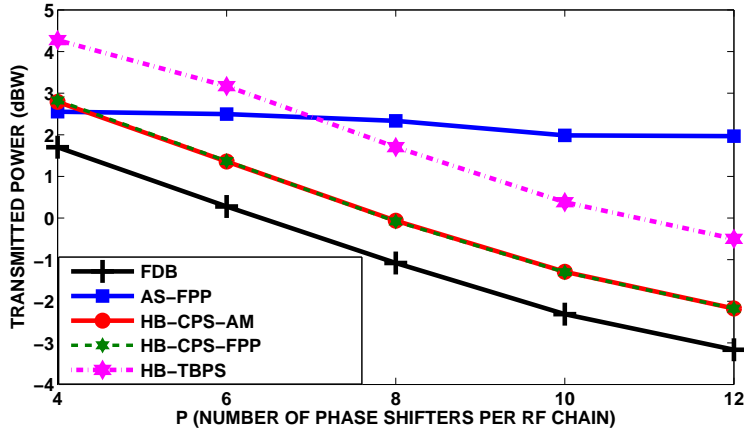
Figure 2.8: Comparison of antenna selection and hybrid beamformers for mmWave channel with $G = 3$.

hybrid beamforming method is proposed as an alternative to the antenna selection. Two new continuous-phase beamformers are presented. In this respect, the formulation of the problem is adapted for AM and FPP-SCA techniques, respectively. Although both methods are shown to perform similarly, the hybrid beamformer which uses the AM has better feasibility rate. A special two-bit discrete-phase hybrid beamformer is designed by converting the integer constraints into simple linear equality and inequalities. This formulation is possible if semidefinite programming with AM is used. This two-bit beamformer performs much better than the quantized form of the continuous-phase beamformer. Furthermore, it results only moderate amount of power loss compared to its continuous-phase counterpart.

The comparison of two competing techniques, namely antenna selection and hybrid beamforming, revealed some interesting results. For small number of phase-shifter per RF chain, P, antenna selection performs better than two-bit hybrid beamforming. As the number of antennas increases, hybrid beamformer performs better since it employs all the antennas.

CHAPTER 3

MAX-MIN FAIR RESOURCE ALLOCATION FOR SWIPT IN MULTI-GROUP MULTICAST OFDM SYSTEMS

Simultaneous wireless information and power transfer (SWIPT) is considered for multi-group multicasting OFDM systems. Each user has the energy harvesting capability through a power splitter (PS). The power and subcarrier allocation at the base station is done such that the minimum signal-to-noise ratio (SNR) among the users for each subcarrier is maximized while user needs for harvested power are satisfied. The optimization of PS ratios in addition to resource allocation is realized in a joint manner. It is shown that the problem can be cast in a convex optimization form for the given subcarrier sets. In order to determine the subcarrier sets, an efficient subcarrier allocation algorithm is proposed. It is shown that the proposed method performs very close to the exhaustive search which gives the optimum solution.

3.1 Related Works and Contributions

In this chapter, resource allocation for multi-group multicasting OFDM systems is considered where a subcarrier assigned to a multicast group serves all the users in that group. In resource allocation, it is possible to have some users with relatively poor channel conditions that may not be assigned with sufficient subcarriers. Hence, enforcing fairness among the users is an important problem that should be addressed [43], [44], [45]. Different from the conventional approach which considers the sum-rate fairness, we maximize the minimum SNR for each subcarrier using the same motivation in [46], [47]. Unsatisfactory SNR values for some subcarriers degrade the system efficiency [46] indicating the importance of balanced subcarrier SNRs.

Per-subcarrier SNR fairness leads to a reliable communication with improved quality of service (QoS). In addition to per-subcarrier fairness, subcarrier need for each multicast group is considered in the proposed design.

SWIPT has been considered for OFDM systems in several recent works [1], [15], [16], [17], [18]. In this chapter, PS technique is considered where each user splits the received OFDM signal into two, one for information decoding (ID) and the other for energy harvesting (EH). This scheme has the advantage that all the subcarriers can be used for EH [16]. For ID, only assigned subcarriers for each group are used.

The joint optimization of resource allocation and PS ratios for multi-group multicasting is not considered in the literature before and it is a difficult combinatorial problem. In this chapter, a novel approach based on maximizing the minimum SNR among all subcarriers considering the request of each multicast group is proposed. An effective solution is obtained by dividing the problem in two parts. In the first part, subcarriers are assigned to each group based on the user requests. A fairness based near-optimal algorithm is proposed for the solution. The problem for the power allocation and PS ratios is cast as a convex optimization problem given the subcarrier assignments. Hence, optimum solution is guaranteed for the second stage. The proposed approach is shown to perform very close to the joint optimum solution obtained with exhaustive search (ES) while the computational complexity is decreased significantly.

3.2 System Model and Problem Formulation

We consider a multi-group multicasting OFDM-based system with a base station (BS) and K users. The BS and the users are equipped with a single antenna. Assume that there are G multicast groups, $\{\mathcal{G}_1, ..., \mathcal{G}_G\}$, where $\mathcal{G}_g$ denotes the gth multicast group of users. The users in each group are interested in the same data stream and each user listens to a single multicast, i.e., $\mathcal{G}_g \cap \mathcal{G}_{g'} = \emptyset$ for $g \neq g'$. The total bandwidth of the system is equally divided into N subcarriers and the set of all subcarriers is denoted by $\mathcal{N} = \{1, ..., N\}$. The power allocated to the nth subcarrier is denoted by p_n, $n = 1, ..., N$ and the total transmission power is limited by P_{max}, i.e., $\sum_{n=1}^{N} p_n \leq P_{max}$.

Each user has the energy harvesting capability. The received signal at the kth user

is split into the energy harvester (EH) and the information decoder (ID) with the aid of a PS device. A portion of the signal power denoted by $0 < \rho_k < 1$ is transferred to the ID while the remaining $1 - \rho_k$ portion is fed into the EH. Each subcarrier can be allocated to only one multicast group of users and the users in each multicast group can decode information only on its assigned subcarriers. On the other hand, all the subcarriers can be used for energy harvesting at each user. Let $h_{k,n}$ denote the channel power gain of the kth user on the nth subcarrier. The received signal on the nth subcarrier for the kth user is thus given by,

$$y_{k,n} = \sqrt{h_{k,n}p_n}s_n + n_{k,n}^A, \quad k = 1, ..., K, \quad n = 1, ..., N \tag{3.1}$$

where s_n is the information signal transmitted on the nth subcarrier and $n_{k,n}^A$ is the additive complex zero mean Gaussian noise on the nth subcarrier at the kth user's antenna. It is assumed that all information signals $\{s_n\}_{n=1}^N$ have unit variance. The variance of $n_{k,n}^A$ is denoted by $\sigma_{k,n}^2$. The received signal at the ID of the kth user on the nth subcarrier can be expressed as,

$$y_{k,n}^I = \sqrt{\rho_k}(\sqrt{h_{k,n}p_n}s_n + n_{k,n}^A) + n_{k,n}^I \tag{3.2}$$

where $n_{k,n}^I$ is the additive complex zero mean Gaussian noise introduced by the ID of the kth user on the nth subcarrier. Its variance is $\delta_{k,n}^2$ and it is independent of $n_{k,n}^A$ and s_n. The SNR of the kth user on the nth subcarrier is given by,

$$SNR_{k,n} = \frac{\rho_k h_{k,n} p_n}{\rho_k \sigma_{k,n}^2 + \delta_{k,n}^2}. \tag{3.3}$$

The signal fed into the EH of the kth user on the nth subcarrier can be expressed as,

$$y_{k,n}^E = \sqrt{1 - \rho_k}(\sqrt{h_{k,n}p_n}s_n + n_{k,n}^A) \tag{3.4}$$

Then, the power harvested at the kth user is given as $P_k = \xi_k(1 - \rho_k) \sum_{n=1}^N (h_{k,n}p_n + \sigma_{k,n}^2)$, where $0 < \xi_k \leq 1$ is the energy conversion efficiency at the kth user. In this chapter, the joint max-min fair resource allocation and PS problem is considered. Hence, our aim is to find the best subcarrier assignment and power allocation scheme together with PS ratios of the users in order to maximize the minimum SNR among all users on each assigned subcarrier. In addition, each user has a minimum power

requirement, denoted by μ_k, $k = 1, ..., K$, for EH. Let $\mathcal{N}_g$ denote the set of subcarriers assigned to the gth multicast group. Thus, the joint optimization problem can be stated as

$$\max_{\{p_n\}_{n=1}^N, \{\rho_k\}_{k=1}^K, \{\mathcal{N}_g\}_{g=1}^G, t} \quad t \tag{3.5a}$$

$$s.t. \quad \frac{\rho_k h_{k,n} p_n}{\rho_k \sigma_{k,n}^2 + \delta_{k,n}^2} \geq t, \; \forall k \in \mathcal{G}_g, \forall n \in \mathcal{N}_g, \forall g \tag{3.5b}$$

$$\xi_k(1 - \rho_k) \sum_{n=1}^N (h_{k,n} p_n + \sigma_{k,n}^2) \geq \mu_k, \;\; \forall k \tag{3.5c}$$

$$0 < \rho_k < 1, \;\; \forall k \tag{3.5d}$$

$$|\mathcal{N}_g| \geq L_g, \;\; \forall g \tag{3.5e}$$

$$p_n \geq 0, \;\; \forall n, \;\; \sum_{n=1}^N p_n \leq P_{max} \tag{3.5f}$$

where $|\mathcal{N}_g|$ shows the cardinality of the set $\mathcal{N}_g$ and L_g is the minimum number of subcarriers for the gth multicast group of users. The constraints in (3.5e) guarantee that subcarriers are allocated in a fair way according to the need of each multicast group. Therefore, (3.5e) prevents some multicast groups with relatively poor channel conditions from being ignored.

Finding the optimum solution of the problem in (3.5) is not an easy task due to the combinatorial nature of the problem. The trivial approach is computationally very expensive and requires brute-force search for the assignment of subcarriers to the multicast groups. In this chapter, we propose a two-step approach for an efficient solution. In the following section, it will be shown that the joint power allocation and PS problem can be cast as a second order cone programming (SOCP) problem given the subcarrier sets $\{\mathcal{N}_g\}_{g=1}^G$. Hence, optimum solution is guaranteed for the predetermined subcarrier sets. In Section 3.4, a suboptimal simple algorithm is presented for subcarrier assignment.

3.3 Optimum Solution for the Given Subcarrier Assignment

If we assume that the subcarrier sets, $\{\mathcal{N}_g\}_{g=1}^G$, are determined by some method or given as a priori information, the problem in (3.5) reduces to the following optimiza-

tion problem for power allocation and PS, i.e.,

$$\max_{\{p_n\}_{n=1}^N, \{\rho_k\}_{k=1}^K, t} \quad t \tag{3.6a}$$

$$s.t. \quad (3.5\text{b-d}), (3.5\text{f}) \tag{3.6b}$$

where $\{\mathcal{N}_g\}_{g=1}^G$ are no more variables and (3.5e) is removed. (3.6) is not a convex optimization problem in its current form. We will transform (3.6) into an equivalent problem in the sense that the optimum solutions of both problems are the same. This new SOCP formulation will be obtained by defining additional variables and some transformations.

Note that (3.5b) is the only nonconvex constraint in (3.6). (3.5c) is a hyperbolic constraint and it can be expressed in second order cone form which is convex as follows [98],

$$\left\| \begin{array}{c} 1 - \rho_k \\ \sum_{n=1}^N (h_{k,n} p_n + \sigma_{k,n}^2) \\ \sqrt{\frac{2\mu_k}{\xi_k}} \end{array} \right\|_2 \leq 1 - \rho_k + \sum_{n=1}^N (h_{k,n} p_n + \sigma_{k,n}^2). \tag{3.7}$$

For (3.5b), consider the equivalent reformulation of (3.6) where (3.5b) is expressed as a convex constraint in (3.8b), i.e.,

$$\min_{\{p_n\}_{n=1}^N, \{\rho_k, \upsilon_k\}_{k=1}^K, \bar{t}} \quad \bar{t} \tag{3.8a}$$

$$s.t. \quad h_{k,n} p_n \bar{t} \geq \sigma_{k,n}^2 + \delta_{k,n}^2 \upsilon_k^2, \ \forall k \in \mathcal{G}_g, \forall n \in \mathcal{N}_g, \forall g \tag{3.8b}$$

$$(3.5\text{d}), (3.5\text{f}), (3.7) \tag{3.8c}$$

$$\upsilon_k = \frac{1}{\sqrt{\rho_k}}, \quad \forall k \tag{3.8d}$$

where $\bar{t}$ corresponds to t^{-1} in (3.6). In the above problem, (3.8b) can be written as a SOCP constraint as follows [98],

$$\left\| \left[\begin{array}{cccc} p_n & \bar{t} & \sqrt{\frac{2\delta_{k,n}^2}{h_{k,n}}} \upsilon_k & \sqrt{\frac{2\sigma_{k,n}^2}{h_{k,n}}} \end{array} \right]^T \right\|_2 \leq p_n + \bar{t}. \tag{3.9}$$

(3.8d) destroys the convexity of the problem in (3.8) and Theorem 3.1 shows a way for casting (3.8) as a SOCP problem in an equivalent manner by defining new variables $\{\omega_k\}_{k=1}^K$.

Theorem 3.1: Let $\{\{p_{n_{opt}}^{(10)}\}_{n=1}^N, \{\rho_{k_{opt}}^{(10)}, \upsilon_{k_{opt}}^{(10)}, \omega_{k_{opt}}^{(10)}\}_{k=1}^K, \bar{t}_{opt}^{(10)}\}$ be the optimum solution of (3.10). Then $\{\{p_{n_{opt}}^{(8)}\}_{n=1}^N, \{\rho_{k_{opt}}^{(8)}, \upsilon_{k_{opt}}^{(8)}\}_{k=1}^K, \bar{t}_{opt}^{(8)}\}$ is an optimum solution of (3.8) where $p_{n_{opt}}^{(8)} = p_{n_{opt}}^{(10)}, n = 1, ..., N, \rho_{k_{opt}}^{(8)} = \rho_{k_{opt}}^{(10)}, k = 1, ..., K$, and $\bar{t}_{opt}^{(8)} = \bar{t}_{opt}^{(10)}$.

$$\min_{\{p_n\}_{n=1}^N, \{\rho_k, \upsilon_k, \omega_k\}_{k=1}^K, \bar{t}} \quad \bar{t} \tag{3.10a}$$

$$s.t. \quad (3.9), (3.5d), (3.5f), (3.7), \tag{3.10b}$$

$$\upsilon_k \omega_k \geq 1, \quad \forall k \tag{3.10c}$$

$$\omega_k^2 \leq \rho_k, \quad \forall k. \tag{3.10d}$$

Proof: By (3.10c) and (3.10d), the optimum solution of (3.10) satisfies $(\upsilon_{k_{opt}}^{(10)})^2 \geq 1 / (\omega_{k_{opt}}^{(10)})^2 \geq 1 / \rho_{k_{opt}}^{(10)}$. By this bound, all the constraints of (3.8) are satisfied by $\{\{p_{n_{opt}}^{(10)}\}_{n=1}^N, \{\rho_{k_{opt}}^{(10)}\}_{k=1}^K, \bar{t}_{opt}^{(10)}\}$ where υ_k in (3.8) is set as $\upsilon_k = 1/\sqrt{\rho_{k_{opt}}^{(10)}}$. Suppose that the optimum objective value of (3.8) is smaller than that of (3.10), i.e., $\bar{t}_{opt}^{(10)}$. In this case, this objective value can also be attained by (3.10) where all the constraints in (3.10c) and (3.10d) are satisfied with equality, which corresponds to (3.8d). Hence $\{\{p_{n_{opt}}^{(10)}\}_{n=1}^N, \{\rho_{k_{opt}}^{(10)}\}_{k=1}^K, \bar{t}_{opt}^{(10)}\}$ is also an optimum solution of (3.8). ∎

Note that the constraints in (3.10c-d) are convex and they can be written as second order cone constraints similar to (3.7) and (3.9). In this case, (3.10) can be solved to find the optimum solution of (3.8) and hence (3.6). The worst-case computational complexity of solving (3.10) in SOCP form is $\mathcal{O}\big((\sqrt{\sum_{g=1}^G |\mathcal{G}_g||\mathcal{N}_g| + 5K + N + 1})(N + 3K + 1)^2(5\sum_{g=1}^G |\mathcal{G}_g||\mathcal{N}_g| + 14K + N + 1)\big)$ [98].

3.4 Subcarrier Assignment

In this section, an algorithm based on max-min fairness among the multicast groups is proposed for subcarrier assignments as shown in Algorithm 3.1. This algorithm assigns subcarriers to the groups according to channel gains in order to maximize the minimum SNR per subcarrier while the subcarrier need of each group is considered. Similar to the previous works in [99], [100], the minimum channel gain among the users of each multicast group is considered as in line 1. This is due to the fact that the user with minimum channel gain in each multicast group determines the minimum SNR for each subcarrier assigned to that group. In the initialization of Algorithm

3.1, a request set for subcarriers, $\{\mathcal{J}'_g\}_{g=1}^G$ is constructed in line 3 by taking the first L_g subcarrier indices corresponding to the largest channel gains. In the procedure between the lines 5-26, each subcarrier is checked whether it is assigned to a group which has no more than L_g subcarriers. If this is the case, then nothing is done since the group cannot lend any subcarrier. Otherwise, the set $\mathcal{F}_n$ is constructed for that subcarrier, whose elements are the groups which still need subcarrier allocation and includes that subcarrier in their request set (line 7). If $\mathcal{F}_n$ is empty (Part A of the algorithm), then the set $\mathcal{D}$ is constructed with groups whose needs cannot be realized. If this set is not empty, the subcarrier n is allocated to the group with the maximum channel gain in $\mathcal{D}$ (line 11 and 24). Otherwise, the channels of all the groups are considered (line 13 and 24). If there is only one group in $\mathcal{F}_n$, then the subcarrier n is allocated to this group (line 16 and 24). If there are more than one group (Part B of the algorithm), then the set $\mathcal{T}_g$ is constructed using the channel gains for the subcarriers other than n. Its elements correspond to the subcarriers which are either idle or assigned to a group whose requirements are satisfied more than necessary (line 18). The worst case channel conditions are checked for each group using the elements in $\mathcal{T}_g$ set in the event that the subcarrier n is not allocated to that group (line 19). The subcarrier n is allocated to the group with the worst case condition (line 20 and 24). For the other groups, the required number of subcarriers to satisfy (3.5e) are included to their request sets (line 21). The procedure between the lines 5-26 are repeated until (3.5e) is satisfied for each group. Note that Algorithm 3.1 is designed to obtain a feasible solution by satisfying (3.5e) (lines 9-11).

The solution of (3.5) can be found in two steps. First, the subcarrier sets $\{\mathcal{N}_g\}_{g=1}^G$ are found by implementing Algorithm 3.1. Then, the convex optimization problem in (3.10) is solved for $\{\{p_n\}_{n=1}^N, \{\rho_k\}_{k=1}^K\}$.

Sorting operation determines the worst case computational complexity in Algorithm 3.1. In the simulations, it is observed that only a few iterations for line 4-27 are needed for the algorithm to terminate due to enforced fairness to satisfy (3.5e). Since sorting in line 19 is realized for N times, the worst case computational complexity of Algorithm 3.1 is given approximately as $\mathcal{O}(GN^2 \log N)$ [101].

3.5 Simulation Results

The second step of the proposed method (PM) is implemented using convex programming solver CVX [96]. The PM is tested for randomly generated Rayleigh fading channels with -40 dB path loss. The maximum power at the base station is $P_{max} = 1$ W. Antenna and ID noise variances for each user and subcarrier are set at -80 dB. The energy conversion efficiency at the EH of all users is selected as $\xi = 0.9$. The harvested power threshold for each user is set to be the same, i.e., $\mu_i = \mu$ for $i = 1, ..., N$ for simplicity.

In the first experiment, the PM is compared with the exhaustive search (ES) and random selection (RS). In Table 3.1, minimum SNRs for small scale scenarios are presented for single random realization due to the extremely high complexity of ES. In ES, the convex optimization problem (3.10) for all possible combinations of subcarrier allocations is solved and the minimum SNR for the best case is noted. Hence, ES gives the optimum solution of the problem in (3.5), but its complexity is very high. Since solving (3.10) dominates the computational complexity of PM, the complexity of ES is given at least $\prod_{g=1}^{G} \binom{N - \sum_{j=0}^{g-1} L_j}{L_g}$ (where $L_0 = 0$) times the order of PM. In RS approach, the subcarriers are randomly assigned and (3.10) is solved for each random selection. The best result of 10 random allocations where (3.5e) is satisfied are given in Table 3.1. Hence, the computational complexity of RS is approximately 10 times greater than PM. As shown in Table 3.1, PM performs very close to the ES due to the effectiveness of the fairness based Algorithm 3.1. At some scenarios, PM gives the optimum solution of (3.5). Moreover, PM always performs better than RS and the gap between them increases as the problem size increases.

In the second experiment, the number of subcarriers is taken as $N = 36$ and the minimum number of subcarriers for each group is set as $L_g = 6$ for all the cases. The results of PM and RS are obtained by averaging 100 random channel realizations. In Fig. 3.1, harvested power threshold is constant at $\mu = 10\mu W$. PM results significantly larger minimum SNR compared to RS, reaching 6 dB SNR gain as G increases. It is observed that the minimum SNR increases as G increases. This pattern is expected due to the increased diversity for the channel gains used in Algorithm 3.1 and occurs with a trade-off for the reduced number of subcarriers assigned to each group. As

shown in Fig. 3.1, SNR increase saturates for high G.

In Fig. 3.2, harvested power threshold, μ is varied in $[10 - 50]\mu$W while the number of users in each group is set as $K/G = 4$. PM again performs significantly better than RS reaching 6 dB SNR gain for $G = 5$ and 6. As μ increases, the minimum SNR decreases where the decrease becomes sharper after 40μW.

Table 3.1: Minimum SNR (in dB) for ES, PM, and RS

		$K = 2G$		$K = 6G$	
		$\mu = 10\mu$W	$\mu = 50\mu$W	$\mu = 10\mu$W	$\mu = 50\mu$W
$G = 2, N = 12,$	ES	22.9253	18.7824	17.7832	12.7114
	PM	22.8402	18.7775	17.7832	12.0107
$L_1 = 4, L_2 = 6$	RS	22.0213	17.0060	17.0742	12.0077
$G = 3, N = 10,$	ES	21.3965	21.5973	20.4585	14.4606
$L_1 = 2,$	PM	21.3965	21.3271	20.0951	13.7069
$L_2 = 3, L_3 = 3$	RS	16.4344	20.8998	17.4180	11.2356
$G = 4, N = 8,$	ES	27.7030	25.5907	21.4508	16.4895
$L_1 = 1, L_2 = 1$	PM	27.7030	25.0281	21.2298	15.0438
$L_3 = 2, L_4 = 2$	RS	23.6696	18.5454	17.7935	7.0994
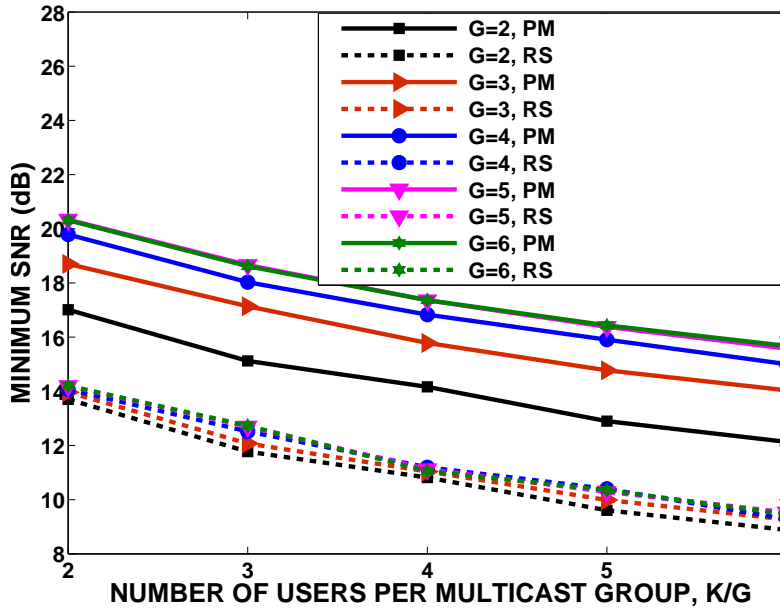
Figure 3.1: Minimum SNR for $\mu = 10\mu$W.
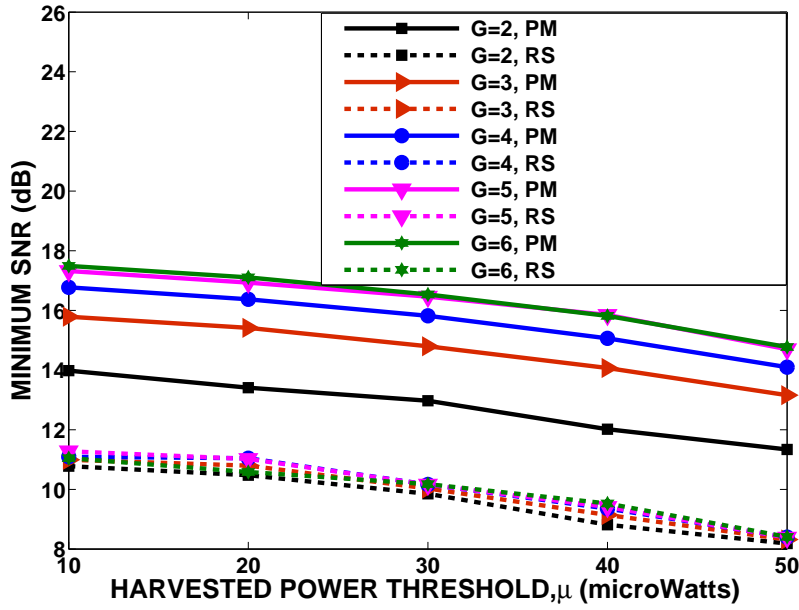
Figure 3.2: Minimum SNR for $K/G = 4$.

3.6 Conclusion

In this chapter, the joint design of resource allocation and PS ratios have been considered for multi-group multicast OFDM systems. The problem is solved in two parts. An efficient algorithm is proposed for subcarrier allocation as a first step. In the second stage, the optimum power allocation and PS ratios are found by expressing the problem in a convex form. The minimum SNR obtained by the complete procedure is very close to the optimum solution which has extremely high complexity. Moreover, the proposed method performs significantly better than the random selection approach.

Algorithm 3.1 Subcarrier Assignment for Multi-Group Multicasting (SA-MGM)

1: Let $\widetilde{h}_{g,n}$ denote the minimum of channel power gain for the nth subcarrier among the users in the gth multicast group, i.e., $\widetilde{h}_{g,n} = \min_{k \in \mathcal{G}_g} h_{k,n}$, $g = 1, ..., G$, $n = 1, ..., N$.

2: Set $\mathcal{N}_g = \emptyset$ for $g = 1, ..., G$.

3: Construct the set $\mathcal{H}_g = \{\widetilde{h}_{g,1}, ..., \widetilde{h}_{g,N}\}$ for $g = 1, ..., G$. Let $\mathcal{I}_g(i)$ denote the subcarrier index of the ith greatest element of $\mathcal{H}_g$, $g = 1, ..., G$. Construct the sets $\mathcal{I}'_g = \{\mathcal{I}_g(1), ..., \mathcal{I}_g(L_g)\}$, $g = 1, ..., G$.

4: **repeat**

5:     **for** $n = 1, ..., N$ **do**

6:         **if** $n \in \mathcal{N}_{g'}$ for some g' where $|\mathcal{N}_{g'}| > L_{g'}$ or $n \notin \mathcal{N}_g$, $\forall g \in \{1, ..., G\}$ **then**

7:             Construct the set $\mathcal{F}_n = \{g \mid n \in \mathcal{I}'_g$ and $|\mathcal{N}_g| < L_g\}$.

8:             **if** $\mathcal{F}_n = \emptyset$ **then**

9:                 Construct $\mathcal{D} = \{g \mid |\mathcal{N}_g| < L_g$ and $\forall n' \in \mathcal{I}'_g$, $n' \in \mathcal{N}_{\breve{g}}$ for some $\breve{g}$ s.t. $|\mathcal{N}_{\breve{g}}| \leq L_{\breve{g}}\}$.

10:                 **if** $\mathcal{D} \neq \emptyset$ **then**

11:                     Set $\widehat{g} = \operatorname*{argmax}\limits_{g \in \mathcal{D}} \widetilde{h}_{g,n}$.

12:                 **else**

13:                     Set $\widehat{g} = \operatorname*{argmax}\limits_{g \in \{1,...,G\}} \widetilde{h}_{g,n}$.

14:                 **end if**

15:             **else if** $|\mathcal{F}_n| = 1$ **then**

16:                 Set $\widehat{g}$ to the only element of $\mathcal{F}_n$.

17:             **else**

18:                 • $\forall g \in \mathcal{F}_n$ set $\mathcal{T}_g = \{\widetilde{h}_{g,\breve{n}} \mid \breve{n} \neq n, \breve{n} \in \mathcal{N}_{\breve{g}}$ for some $\breve{g}$ s.t. $|\mathcal{N}_{\breve{g}}| > L_{\breve{g}}$ or $\breve{n} \notin \mathcal{N}_{\breve{g}} \forall \breve{g} = \{1, ..., G\}\}$.

19:                 • Let $\mathcal{T}_g(i)$ denote the ith greatest element of $\mathcal{T}_g$, $g \in \mathcal{F}_n$.

20:                 • Set $\widehat{g} = \operatorname*{argmin}\limits_{g \in \mathcal{F}_n} \mathcal{T}_g(L_g - |\mathcal{N}_g|)$.

21:                 • Update $\mathcal{I}'_g \leftarrow \mathcal{I}'_g \cup \{\breve{n}\}$ for $\breve{n}$ such that $\mathcal{T}_g(i) = \widetilde{h}_{g,\breve{n}}$, $i = 1, ..., L_g - |\mathcal{N}_g|$, for $g \in \mathcal{F}_n \setminus \{\widehat{g}\}$.

22:             **end if**

57

23:                Update the subcarrier set of $(g')^{th}$ multicast group as $\mathcal{N}_{g'} \leftarrow \mathcal{N}_{g'} \setminus \{n\}$ if $n \in \mathcal{N}_{g'}$ for some g'.

24:                Update the subcarrier set of $(\widehat{g})^{th}$ multicast group as $\mathcal{N}_{\widehat{g}} \leftarrow \mathcal{N}_{\widehat{g}} \cup \{n\}$.

25:       **end if**

26:     **end for**

27: **until** $|\mathcal{N}_g| \geq L_g, \forall g = \{1, ..., G\}$

OPTIMUM QOS-AWARE BEAMFORMER DESIGN FOR FULL-DUPLEX RELAY WITH SELF-ENERGY RECYCLING

In this chapter, quality of service (QoS)-aware beamformer design is introduced for full-duplex wireless-powered relay with self-energy recycling. In the first phase of communication, information signal is transmitted from the source to the relay. In the second phase, the relay forwards this signal using beamforming while it harvests energy via self recycling and from the source. The aim is to satisfy signal-to-noise ratio (SNR) requirement of the destination with minimum transmission power from the relay's own battery. A closed-form solution for the optimum relay beamformer is derived and the feasibility conditions are obtained. The effects of different system parameters on the relay's performance are discussed in the simulation results.

4.1 Introduction

In [19], a two-phase protocol is proposed for full-duplex WPR without any time switching (TS) or power splitting (PS) device which enables uninterrupted information transmission. This self-energy recycling based protocol and similar ones are studied for different scenarios [4], [22], [61].

In this chapter, we consider the two-phase amplify-and-forward (AF) protocol in [19] as shown in Fig. 4.1. In the first phase, information signal is transmitted from the source (**S**) to the relay (**R**). Then, **R** forwards its received signal to the destination (**D**) and harvests energy by using both the dedicated energy signal sent from **S** and self-recycling. Since information reception and forwarding occur in different slots, no self-interference cancellation is required in this scheme. Note that in [19], only

one antenna is used at **R** for information reception while the remaining antennas are not in use in the first phase. In this chapter, we modify the system such that all the antennas of **R** are employed for better performance. In addition, we propose QoS-aware design approach different from [19] which considers SNR maximization. The design problem is cast to satisfy the SNR requirement of the destination using the minimum amount of power from the relay's battery with the help of harvested energy.

The main contributions of this chapter can be outlined as follows. First, the closed-form optimum solution is derived for the QoS-aware beamformer design problem. Compared to the SNR maximization problem in [19], the proposed design has two main advantages. The problem in [19] imposes the constraint that the transmission power of the relay is less than the harvested power. However, this is a strict and usually unrealizable condition when the desired SNR of the destination is greater than the one that can be supplied by the harvested power. Unlike [19], we find the optimum relay beamformer including the cases which require more power than the harvested. Furthermore, the amount of power required for the relay's own battery is found. Secondly, transmission power limit of the relay is not considered in [19]. In order to be more practical, we introduce maximum power constraint to the QoS-aware optimization problem. In addition to finding the closed-form optimum solution, we derive feasibility conditions for the source power and the relay's maximum power limit. Simulation results show that energy harvesting assists the relay by reducing the external power supply need. For most of the scenarios, transmission power is greater than the harvested power showing the strictness of the constraint in [19] and the importance of the proposed approach.
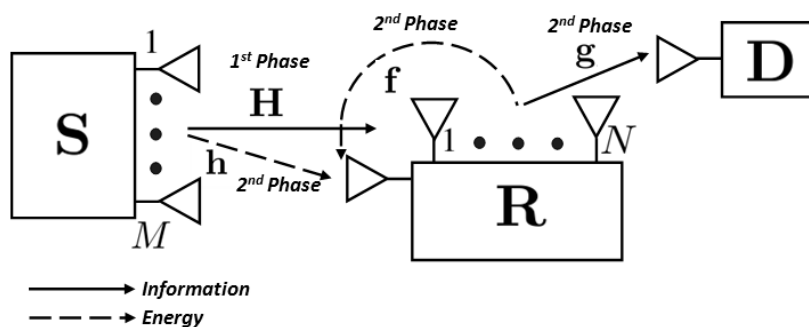
Figure 4.1: System model.

60

4.2 System Model and Problem Formulation

As shown in Fig. 4.1, **S** and **R** are equipped with M and $N + 1$ antennas, respectively whereas **D** has a single antenna. In the first phase, information signal is transmitted from **S** to **R** employing all the antennas at **S** and **R**. Let $\mathbf{H} \in \mathbb{C}^{M \times (N+1)}$ be the baseband equivalent channel from **S** to **R**. Assuming that **H** is known at **S** and **R**, the optimal transmit and receive beamformers are the left and right singular vectors corresponding to the largest singular value of **H**, i.e. λ_H, respectively. If P_s denotes the transmission power of **S**, the received signal at **R** in the first phase is given by,

$$y_{r,1} = \sqrt{P_s} \lambda_H x_{s,1} + n_{r,1}, \tag{4.1}$$

where $x_{s,1}$ is the information symbol sent by **S** and it is assumed to be circularly-symmetric complex Gaussian distributed with zero mean and unit variance, i.e., $x_{s,1} \sim \mathcal{CN}(0, 1)$. $n_{r,1}$ is the noise at **R** after receive beamforming and $n_{r,1} \sim \mathcal{CN}(0, \sigma_r^2)$.

In the second phase, the received signal in (4.1) is amplified and forwarded to **D** by N transmitting antennas shown on the top of **R** in Fig. 4.1 with relay beamforming vector $\mathbf{v}_r \in \mathbb{C}^{N \times 1}$. The transmitted signal is given in vector form as follows,

$$\mathbf{y}_t = \mathbf{v}_r y_{r,1} = \mathbf{v}_r (\sqrt{P_s} \lambda_H x_{s,1} + n_{r,1}). \tag{4.2}$$

Assuming that $n_{r,1}$ is independent from the information symbol $x_{s,1}$, the transmission power of **R**, i.e. P_r, is given by,

$$P_r = ||\mathbf{v}_r||^2 (P_s \lambda_H^2 + \sigma_r^2). \tag{4.3}$$

If $\mathbf{g} \in \mathbb{C}^{N \times 1}$ denotes the channel from transmitting antennas of **R** to **D**, the received signal at **D** in the second phase is given by,

$$y_d = \mathbf{g}^H \mathbf{y}_t + n_d = \mathbf{g}^H \mathbf{v}_r (\sqrt{P_s} \lambda_H x_{s,1} + n_{r,1}) + n_d \tag{4.4}$$

where $n_d \sim \mathcal{CN}(0, \sigma_d^2)$ is the noise at **D**. Assuming that it is independent from the information symbol and $n_{r,1}$, the received SNR at **D** is given by,

$$SNR_d = \frac{P_s \lambda_H^2 |\mathbf{g}^H \mathbf{v}_r|^2}{\sigma_r^2 |\mathbf{g}^H \mathbf{v}_r|^2 + \sigma_d^2}. \tag{4.5}$$

In the second phase, energy harvesting is done at the remaining single antenna of **R**. Note that using only one antenna for energy harvesting requires only one rectifier at

R and maximum number of antennas can be employed for an effective beam steering towards **D** and energy harvesting antenna. In this phase, an energy-bearing signal is sent from **S** to **R** and $\mathbf{y}_t$ is used as an energy source. Let $\mathbf{h} \in \mathbb{C}^{M \times 1}$ denote the channel from **S** to the energy harvesting antenna of **R**. In this case, the optimal source beamforming vector is $\sqrt{P_s}\mathbf{h}/||\mathbf{h}||$. If the self-recycling channel from N transmitting antennas to the energy harvesting antenna is denoted by $\mathbf{f} \in \mathbb{C}^{N \times 1}$, the received signal at **R** in the second phase is expressed as,

$$
\begin{aligned}
y_{r,2} &= \sqrt{P_s}||\mathbf{h}||x_{s,2} + \mathbf{f}^H\mathbf{y}_t + n_{r,2} \\
&= \sqrt{P_s}(||\mathbf{h}||x_{s,2} + \lambda_H\mathbf{f}^H\mathbf{v}_r x_{s,1}) + \mathbf{f}^H\mathbf{v}_r n_{r,1} + n_{r,2}
\end{aligned} \tag{4.6}
$$

where $x_{s,2} \sim \mathcal{CN}(0,1)$ denotes the symbol sent from **S** for energy harvesting. Let us neglect the harvested energy from the noise terms $n_{r,1}$ and $n_{r,2}$ in accordance with [19]. As shown in [19], the harvested power is maximized when $x_{s,2} = x_{s,1}e^{j\angle\mathbf{f}^H\mathbf{v}_r}$. In this case, the harvested power at **R** can be given by,

$$
P_h = \eta P_s(||\mathbf{h}|| + \lambda_H|\mathbf{f}^H\mathbf{v}_r|)^2 \tag{4.7}
$$

where $0 < \eta \leq 1$ denotes the energy harvesting efficiency at **R**.

In this chapter, we adopt QoS-aware design approach for the relay beamformer vector, $\mathbf{v}_r$. The goal is to minimize the relay transmission power used by the relay's own battery, i.e., $P_r - P_h$, such that SNR requirement of the destination is satisfied. Additionally, P_r should not exceed both the transmission power limit of the relay, i.e., P_{max}, and the power budget which is the sum of the harvested power, P_h, and a conventional power supply P_c. The optimization of $\mathbf{v}_r$ for this design objective can be stated as follows,

$$
\min_{\mathbf{v}_r} \ ||\mathbf{v}_r||^2(P_s\lambda_H^2 + \sigma_r^2) - \eta P_s(||\mathbf{h}|| + \lambda_H|\mathbf{f}^H\mathbf{v}_r|)^2 \tag{4.8a}
$$

$$
s.t. \ \frac{P_s\lambda_H^2|\mathbf{g}^H\mathbf{v}_r|^2}{\sigma_r^2|\mathbf{g}^H\mathbf{v}_r|^2 + \sigma_d^2} \geq \gamma, \tag{4.8b}
$$

$$
||\mathbf{v}_r||^2(P_s\lambda_H^2 + \sigma_r^2) \leq P_{max}, \tag{4.8c}
$$

$$
||\mathbf{v}_r||^2(P_s\lambda_H^2 + \sigma_r^2) - \eta P_s(||\mathbf{h}|| + \lambda_H|\mathbf{f}^H\mathbf{v}_r|)^2 \leq P_c \tag{4.8d}
$$

where γ is the target SNR for **D**. Note that the left side of (4.8d) is minimized by the optimum solution of the reduced problem (4.8a-c). Hence, the optimum solution

of (4.8) is the same as that of (4.8a-c) if it satisfies (4.8d). The problem in (4.8) can be solved by considering (4.8a-c) and then checking (4.8d) for feasibility. If (4.8d) is satisfied, then optimum and feasible solution is found for (4.8). Otherwise, the problem (4.8) is infeasible.

4.3 Closed-Form Optimum Solution of (4.8)

In the following, we will ignore (4.8d) and find the optimum solution of (4.8a-c). Then, we will check the feasibility of the problem (4.8) using this optimum solution. In order to simplify the Kuhn-Tucker conditions for (4.8a-c), let us express the relay beamformer vector as $\mathbf{v}_r = \sum_{i=1}^{N} \beta_i e^{j\theta_i} \boldsymbol{\Phi}_i$ where $\beta_i \geq 0$, $i = 1, ..., N$ and $\{\boldsymbol{\Phi}_i\}_{i=1}^{N}$ is an orthonormal basis for $\mathbb{C}^{N \times 1}$ such that $\boldsymbol{\Phi}_1 = \frac{\mathbf{f}}{||\mathbf{f}||}$ and $\boldsymbol{\Phi}_2 = \frac{\mathbf{g} - \boldsymbol{\Phi}_1 \boldsymbol{\Phi}_1^H \mathbf{g}}{||\mathbf{g} - \boldsymbol{\Phi}_1 \boldsymbol{\Phi}_1^H \mathbf{g}||}$. Then, we have the following result.

Lemma 4.1: The optimum relay beamformer vector for (4.8a-c) is given in the form $\mathbf{v}_r = \beta_1 \boldsymbol{\Phi}_1 + \beta_2 e^{j\angle \mathbf{g}^H \mathbf{f}} \boldsymbol{\Phi}_2$, where $\beta_1 \geq 0$ and $\beta_2 \geq 0$.

Proof: First, let us express the problem (4.8a-c) in terms of $\{\boldsymbol{\Phi}_i\}_{i=1}^{N}$ as follows,

$$\min_{\{\beta_i \geq 0, \theta_i\}_{i=1}^{N}} (P_s \lambda_H^2 + \sigma_r^2) \sum_{i=1}^{N} \beta_i^2 - \eta P_s(||\mathbf{h}|| + \lambda_H ||\mathbf{f}|| \beta_1)^2 \tag{4.9a}$$

$$s.t. \quad \left| \frac{\mathbf{g}^H \mathbf{f}}{||\mathbf{f}||} \beta_1 e^{j\theta_1} + \frac{\mathbf{g}^H \mathbf{g} - \mathbf{g}^H \boldsymbol{\Phi}_1 \boldsymbol{\Phi}_1^H \mathbf{g}}{||\mathbf{g} - \boldsymbol{\Phi}_1 \boldsymbol{\Phi}_1^H \mathbf{g}||} \beta_2 e^{j\theta_2} \right| \geq \sqrt{\tilde{\gamma}} \tag{4.9b}$$

$$(P_s \lambda_H^2 + \sigma_r^2) \sum_{i=1}^{N} \beta_i^2 \leq P_{max} \tag{4.9c}$$

where $\tilde{\gamma} = \gamma \sigma_d^2 / (P_s \lambda_H^2 - \gamma \sigma_r^2)$. Note that $\{\beta_i\}_{i=3}^{N}$ do not affect the constraint (4.9b). It is obviously seen that for optimum $\mathbf{v}_r$, $\{\beta_i\}_{i=3}^{N}$ should be zero. Suppose that this is not the case for the optimum solution. In this case, $\{\beta_i\}_{i=3}^{N}$ can be set to zero by improving the objective function without violating (4.9b) and (4.9c). Note that θ_1 can be selected as 0 since any phase rotation of $\mathbf{v}_r$ does not change the optimality. Now, we will prove that optimum θ_2 is $\angle \mathbf{g}^H \mathbf{f}$ by contradiction. Suppose that $\{\beta_1^\star, \beta_2^\star, \theta_2^\star \neq \angle \mathbf{g}^H \mathbf{f}\}$ is optimum for (4.9). In this case, the left side of (4.9b) is strictly less than the following

expression

$$\frac{|\mathbf{g}^H\mathbf{f}|}{||\mathbf{f}||}\beta_1^\star + \frac{\mathbf{g}^H\mathbf{g} - \mathbf{g}^H\boldsymbol{\Phi}_1\boldsymbol{\Phi}_1^H\mathbf{g}}{||\mathbf{g} - \boldsymbol{\Phi}_1\boldsymbol{\Phi}_1^H\mathbf{g}||}\beta_2^\star. \tag{4.10}$$

Note that both terms in (4.10) are positive. Let us consider an alternative solution like $\{\beta_1^\star, \beta_2^\star, \theta_2 = \angle\mathbf{g}^H\mathbf{f}\}$. Note that this solution aligns the second term with the first term in (4.9b) and (4.9b) becomes equal to (4.10). Since (4.10) is strictly greater than $\sqrt{\tilde{\gamma}}$, $\beta_2^\star$ can be decreased until (4.10) is equal to $\sqrt{\tilde{\gamma}}$ without violating (4.9b) and (4.9c) . However, this results a solution which is better than the optimum which contradicts the optimality of $\theta_2^\star \neq \angle\mathbf{g}^H\mathbf{f}$. ∎

Now, let us express (4.9) in terms of β_1 and β_2 as follows,

$$\min_{\beta_1,\beta_2} \ b_1\beta_1^2 + b_2\beta_2^2 + b_3\beta_1 \tag{4.11a}$$

$$s.t. \ a_1\beta_1 + a_2\beta_2 \geq \sqrt{\tilde{\gamma}} \tag{4.11b}$$

$$b_2\beta_1^2 + b_2\beta_2^2 \leq P_{max} \tag{4.11c}$$

where $a_1 = |\mathbf{g}^H\mathbf{f}|/||\mathbf{f}||$, $a_2 = (\mathbf{g}^H\mathbf{g} - \mathbf{g}^H\boldsymbol{\Phi}_1\boldsymbol{\Phi}_1^H\mathbf{g})/||\mathbf{g} - \boldsymbol{\Phi}_1\boldsymbol{\Phi}_1^H\mathbf{g}||$, $b_1 = (1 - \eta||\mathbf{f}||^2)P_s\lambda_H^2 + \sigma_r^2$, $b_2 = P_s\lambda_H^2 + \sigma_r^2$, $b_3 = -2\eta P_s||\mathbf{h}||\lambda_H||\mathbf{f}||$ and the constant term in (4.9a) is ignored. It is easily seen that the optimum β_1 and β_2 should be nonnegative for (4.11) since $a_1 \geq 0$, $a_2 \geq 0$ and $b_3 < 0$. Hence, the constraints $\beta_1 \geq 0$ and $\beta_2 \geq 0$ are not included for simplicity. The Kuhn-Tucker necessary conditions for the optimum solution of (4.11) are given by,

$$2b_1\beta_1 + b_3 = \mu_1 a_1 - 2\mu_2 b_2\beta_1 \tag{4.12a}$$

$$2b_2\beta_2 = \mu_1 a_2 - 2\mu_2 b_2\beta_2 \tag{4.12b}$$

$$\mu_1 \geq 0, \quad \mu_2 \geq 0 \tag{4.12c}$$

$$\mu_1(a_1\beta_1 + a_2\beta_2 - \sqrt{\tilde{\gamma}}) = 0 \tag{4.12d}$$

$$\mu_2(b_2\beta_1^2 + b_2\beta_2^2 - P_{max}) = 0 \tag{4.12e}$$

$$(4.11b), (4.11c) \tag{4.12f}$$

where μ_1 and μ_2 are the Lagrange multipliers corresponding to (4.11b) and (4.11c), respectively. Now, let us consider different cases for the conditions in (4.12).

Case 1: $\mu_1 = 0$, $\mu_2 = 0$.

In this case, β_1 and β_2 are obtained from (4.12a-b) as $\beta_1 = -b_3/(2b_1)$ and $\beta_2 = 0$. Note that they should satisfy (4.12f) to be a candidate optimum solution.

Case 2: $\mu_1 > 0$, $\mu_2 = 0$.

In this case, by taking the ratio of both sides of (4.12a-b) and using the fact that (4.11b) is satisfied with equality, we obtain β_1 and β_2 as follows,

$$\beta_1 = \frac{2a_1 b_2 \sqrt{\bar{\gamma}} - a_2^2 b_3}{2(a_1^2 b_2 + a_2^2 b_1)}, \quad \beta_2 = \frac{2a_2 b_1 \sqrt{\bar{\gamma}} + a_1 a_2 b_3}{2(a_1^2 b_2 + a_2^2 b_1)}. \tag{4.13}$$

Note that in deriving (4.13) it is assumed that $a_1 > 0$ and $a_2 > 0$. However, it can be easily shown that (4.13) is also valid for other cases of a_1 and a_2. β_1 and β_2 given in (4.13) present a candidate optimum solution of (4.11) if they satisfy (4.11c) (They already satisfy (4.11b) since $\mu_1 > 0$.)

Case 3: $\mu_1 = 0$, $\mu_2 > 0$.

In this case, $\beta_2 = 0$ by (4.12b). Since $\mu_2 > 0$, (4.11c) is satisfied with equality, i.e., $\beta_1 = \sqrt{P_{max}/b_2}$. If β_1 and β_2 also satisfy (4.11b), they represent a candidate optimum solution for (4.11).

Case 4: $\mu_1 > 0$, $\mu_2 > 0$.

In this case, both (4.11b) and (4.11c) are satisfied with equality. Hence, $\beta_2 = (\sqrt{\bar{\gamma}} - a_1 \beta_1)/a_2$ if $a_2 > 0$. (If $a_2 = 0$, then we obtain $\beta_2 = 0$. In this case, either Case 2 or Case 3 is valid.) If we insert this β_2 into the equality $\beta_1^2 + \beta_2^2 = P_{max}/b_2$, we obtain a quadratic equation of β_1. If it exists, for each positive root of this equation, we obtain a candidate optimum solution for (4.11).

Let us construct the set $\mathcal{B}$ whose elements are the candidate $\{\beta_1, \beta_2\}$ pairs given in Case 1-4. If $\mathcal{B} \neq \emptyset$, the optimum solution of (4.11) is given by $\{\beta_1^\star, \beta_2^\star\} = \underset{\{\beta_1, \beta_2\} \in \mathcal{B}}{\text{argmin}} (b_1 \beta_1^2 + b_2 \beta_2^2 + b_3 \beta_1)$ and the optimum relay beamformer vector $\mathbf{v}_r$ for (4.8a-c) is $\mathbf{v}_r^\star = \beta_1^\star \boldsymbol{\Phi}_1 + \beta_2^\star e^{j \angle \mathbf{g}^H \mathbf{f}} \boldsymbol{\Phi}_2$. If $\mathbf{v}_r^\star$ satisfies (4.8d), it is the optimum solution of (4.8). If not, then the problem (4.8) is infeasible. For the considered design, the channel $\mathbf{H}$ should be available both at $\mathbf{S}$ and $\mathbf{R}$ whereas $\mathbf{f}$ and $\mathbf{g}$ should be estimated only by $\mathbf{R}$. In practice, the channel state information (CSI) can be acquired by pilot-assisted reverse link channel training [19]. In addition, the optimum $x_{s,2} = x_{s,1} e^{j \angle \mathbf{f}^H \mathbf{v}_r^\star} = x_{s,1}$

by $\angle \mathbf{f}^H \mathbf{v}_r^\star = 0$ and there is no need to send the angle information to $\mathbf{S}$.

4.4 Feasibility Conditions

In the following part, we investigate the feasibility conditions and find the bounds for P_{max} and P_s such that (4.8) is feasible. For the problem (4.8) to be feasible, (4.8a-c) should be feasible and the optimum solution of (4.8a-c) should satisfy (4.8d). Now, let us consider the feasibility conditions for the problem (4.8a-c). (4.8a-c) is feasible if and only if there exist $\beta_1 \geq 0$ and $\beta_2 \geq 0$ such that (4.11b) and (4.11c) are satisfied simultaneously. In order to check the existence of such β_1 and β_2, consider the following optimization problem,

$$\max_{\beta_1, \beta_2} \ a_1\beta_1 + a_2\beta_2 \tag{4.14a}$$

$$\text{s.t.} \ \ b_2\beta_1^2 + b_2\beta_2^2 \leq P_{max}. \tag{4.14b}$$

Note that the optimum β_1 and β_2 for (4.14) should be nonnegative since $a_1 \geq 0$ and $a_2 \geq 0$. Moreover, if the optimum objective value is greater than or equal to $\sqrt{\tilde{\gamma}}$, then we conclude that the problem (4.11a-c) and hence (4.8a-c) is feasible. Otherwise, they are infeasible since it is impossible to find other β_1 and β_2 which satisfy (4.14b) with greater objective value. The optimum solution of (4.14), $\{\beta_1^*, \beta_2^*\}$, is given by,

$$\beta_1^* = \sqrt{\frac{P_{max}}{b_2(a_1^2 + a_2^2)}} a_1, \quad \beta_2^* = \sqrt{\frac{P_{max}}{b_2(a_1^2 + a_2^2)}} a_2. \tag{4.15}$$

The feasibility condition for (4.8a-c) can be expressed as $a_1\beta_1^* + a_2\beta_2^* \geq \sqrt{\tilde{\gamma}}$ which is equivalent to,

$$P_{max}(a_1^2 + a_2^2) \geq b_2\tilde{\gamma}. \tag{4.16a}$$

We can use this condition to find P_s for a given target SNR, γ, and P_{max} to make the problem feasible. The first condition on P_s for a given γ is $P_s > \gamma\sigma_r^2/\lambda_H^2$ to make $\tilde{\gamma}$ positive. For the other condition, note that $a_1^2 + a_2^2 = ||\mathbf{g}||^2$ and the only terms in (4.16a) that depend on P_s are b_2 and $\tilde{\gamma}$. If we write (4.16a) in terms of P_s we obtain,

$$P_{max}||\mathbf{g}||^2 \geq \frac{(P_s\lambda_H^2 + \sigma_r^2)\gamma\sigma_d^2}{P_s\lambda_H^2 - \gamma\sigma_r^2}. \tag{4.16b}$$

Since the denominator in (4.16b) is positive by the first condition ($P_s > \gamma \sigma_r^2 / \lambda_H^2$), we can rearrange (4.16b) as follows,

$$(P_{max} ||\mathbf{g}||^2 - \gamma \sigma_d^2) \lambda_H^2 P_s \geq \gamma \sigma_r^2 (P_{max} ||\mathbf{g}||^2 + \sigma_d^2). \tag{4.16c}$$

As seen from (4.16c), $P_{max} ||\mathbf{g}||^2 > \gamma \sigma_d^2$ is required for the feasibility. Hence, the problem (4.8a-c) is feasible if and only if the following conditions are satisfied, i.e.,

$$P_{max} > \frac{\gamma \sigma_d^2}{||\mathbf{g}||^2}, \tag{4.17a}$$

$$P_s > \frac{\gamma \sigma_r^2}{\lambda_H^2}, \quad P_s \geq \frac{\gamma \sigma_r^2 (P_{max} ||\mathbf{g}||^2 + \sigma_d^2)}{(P_{max} ||\mathbf{g}||^2 - \gamma \sigma_d^2) \lambda_H^2}. \tag{4.17b}$$

The complete problem (4.8a-d) is feasible if (4.17) is satisfied and P_c is at least the objective value found by the optimum solution of (4.8a-c). Hence, a constant power source with a value greater than optimum value of (4.8a) is required by the relay for a feasible solution.

4.5 Simulation Results

In the simulations, we set $M = 4$, $\eta = 0.8$, $\sigma_r^2 = \sigma_d^2 = -100$ dBW, $P_{max} = 0.1$ W. We assume Rayleigh fading for the channels $\mathbf{H}$ and $\mathbf{g}$ with 60 dB path loss. The loop channel $\mathbf{f}$ is assumed to be line-of-sight (LOS) and is modeled as $\mathbf{f} = \sqrt{\beta_f^{-1}} [1 \ e^{j\pi \sin \theta} \ e^{j2\pi \sin \theta} \ ... \ e^{j(N-1)\pi \sin \theta}]^T$ where β_f is the path loss for $\mathbf{f}$. In the following figures, each point presents the average of randomly generated 1000 channels where θ for $\mathbf{f}$ is uniformly distributed in $[0, 2\pi)$. Unless otherwise stated, $P_s = 0$ dBW, $N = 4$, $\gamma = 10$ dB and $\beta_f = 10$ dB.

In Fig. 4.2-5, the transmission power of $\mathbf{R}$, P_r, harvested power, P_h, and their difference $P_r - P_h$ which is the objective function of our design are plotted by changing P_s, N, γ and β_f, respectively. $P_r - P_h$ shows the extra power required at $\mathbf{R}$ for a feasible design. Note that for the considered scenarios, it is almost always greater than zero showing the necessity of additional power supply. When $P_r - P_h > 0$, it is concluded that the maximum SNR obtained by the design in [19] is less than the target SNR for the QoS-aware design. Our proposed design enables us to find the optimum beamformer and the additional power for a given target SNR. Moreover, we reduce the power requirement of $\mathbf{R}$ as much as possible by minimizing $P_r - P_h$.

In Fig. 4.2, as the source power increases, P_r has an increasing pattern in general. However, the increase in P_s helps **R** to harvest more energy by decreasing $P_r - P_h$. Hence, our objective improves as P_s increases. Similarly, increasing the number of antennas at the transmitter of **R** enables more energy harvesting after $N = 4$ as shown in Fig. 4.3. Although P_r and P_h do not have a monotonic pattern, the required power at **R**, $P_r - P_h$, decreases significantly as N increases and becomes negative for $N = 12$. This means that the harvested power is more than the transmitted power. The reason of the sharp increase in P_r and P_h from $N = 10$ to $N = 12$ is to make the objective, $P_r - P_h$, as negative as possible for more power saving. Fig. 4.4 shows that increasing target SNR for **D**, γ, increases both P_r and P_h. However, the increase of P_h is negligible compared to P_r which increases $P_r - P_h$. Hence the required power at **R**'s battery has been increased. Similarly, increasing path loss for the loop channel results in more required power at **R** as shown in Fig. 4.5. However, after some point, the increase saturates. This is due to the fact that the effect of self-recycling diminishes and the path loss does not affect P_h considerably leaving only energy signal sent from **S** for harvesting.
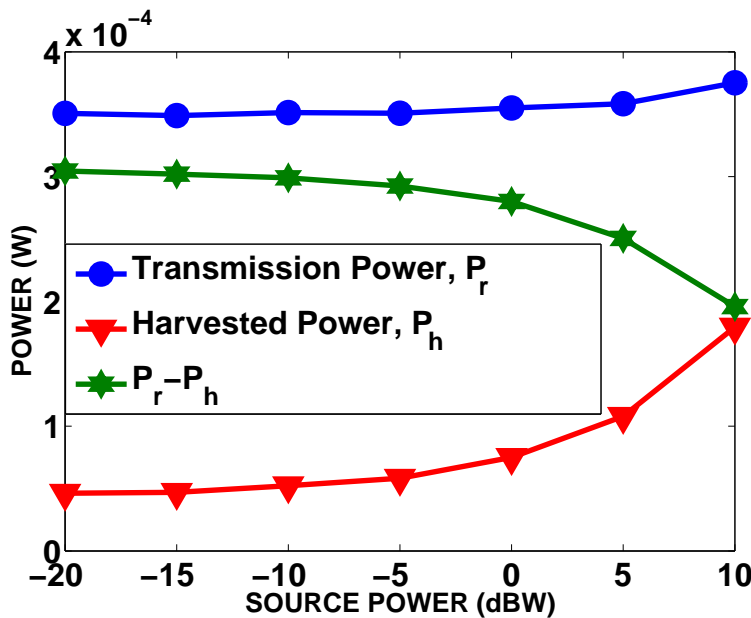
Figure 4.2: P_r, P_h and $P_r - P_h$ versus P_s.
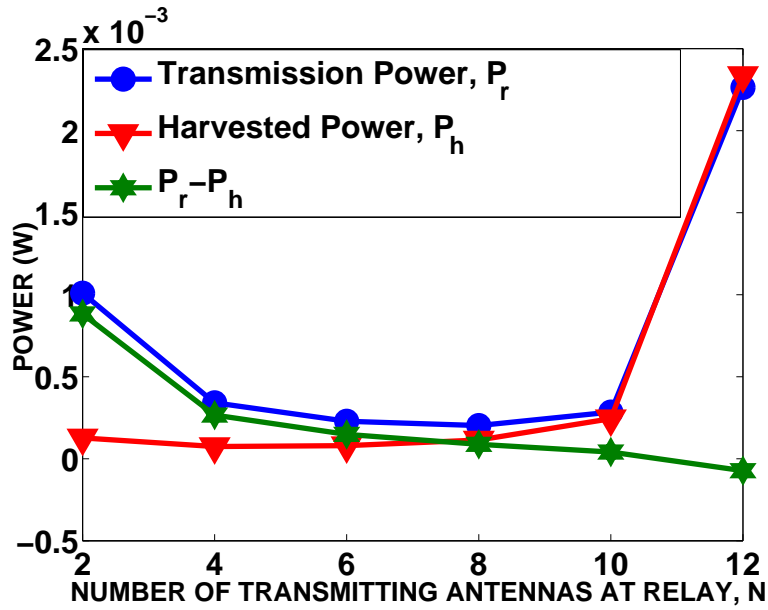
Figure 4.3: P_r, P_h and $P_r - P_h$ versus N.

4.6 Conclusion

In this chapter, the QoS-aware beamformer design is proposed for full-duplex WPR system with self-energy recycling. The objective is to minimize the power used by the relay's own battery such that the target SNR at the destination is satisfied under the transmission power limit of the relay. The closed-form optimum solution and the bounds for the source and maximum relay power are derived. The performance and the advantages of the proposed design are shown in the simulations. In summary, improving loop channel by increasing the number of antennas at the relay or decreasing the path loss decreases the power need of the relay. In fact, it is possible to save energy at some scenarios. Similarly, increasing source power improves the design objective by assisting the relay more. On the other hand, the increase in target SNR requires more additional power at the relay.
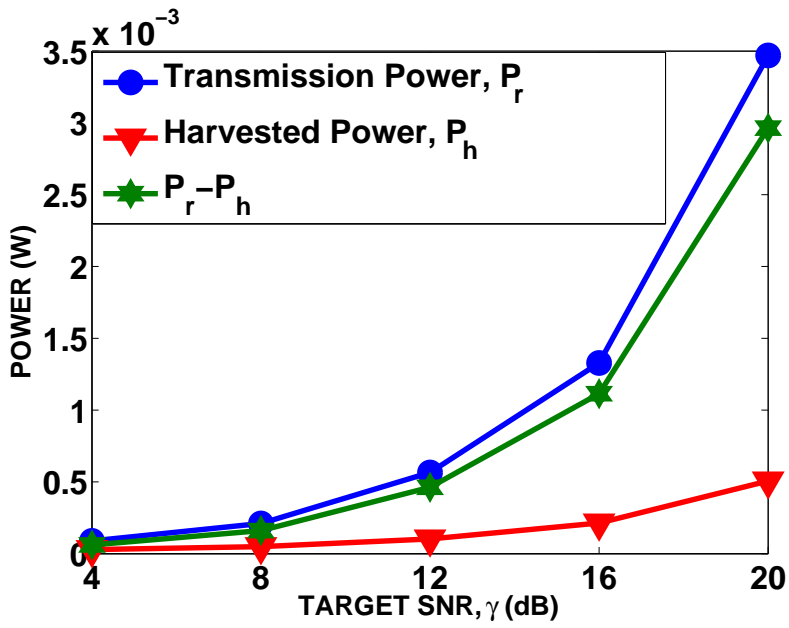
Figure 4.4: P_r, P_h and $P_r - P_h$ versus γ.
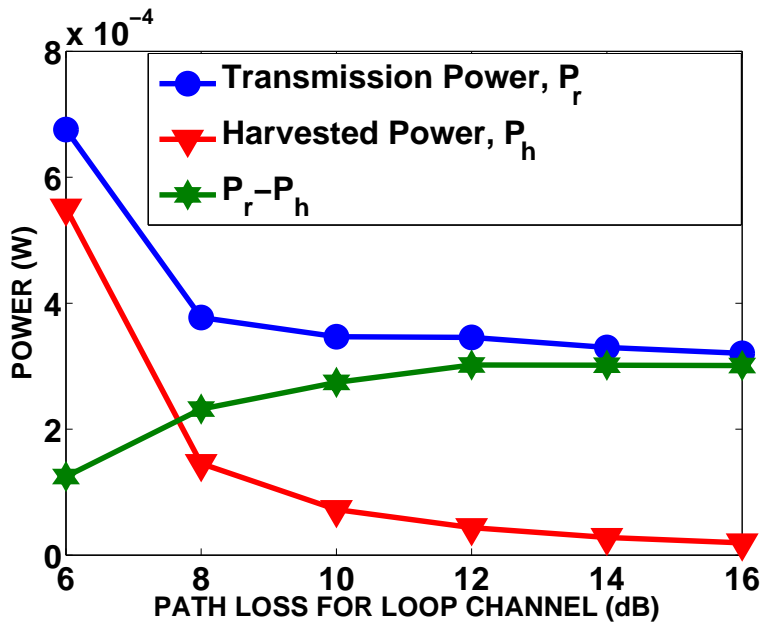
Figure 4.5: P_r, P_h and $P_r - P_h$ versus path loss for $\mathbf{f}$.

CHAPTER 5

OPTIMUM CLOSED-FORM BEAMFORMERS FOR SELF-ENERGY RECYCLING FULL-DUPLEX RELAY WITH A NEW POWER SPLITTING PROTOCOL

This chapter considers wireless-powered amplify-and-forward relaying where the relay harvests energy from the source and self-energy recycling. Two well-known protocols based on self-energy recycling and power splitting are investigated to present the closed-form optimum solutions. A new protocol combining self-energy recycling and power splitting is proposed to improve the energy efficiency and the signal-to-noise ratio at the destination. This new protocol provides up to 3 dB signal-to-noise ratio improvement. The transmit beamformer design for the multiple antenna relay is laid out as an optimization problem. The joint optimization for beamformer design and power splitting ratio is considered for the power splitting based protocols. The optimum closed-form solutions are obtained through signal-to-noise ratio maximization under the constraint that the transmitted power cannot exceed the harvested power. Energy harvesting is due to a dedicated energy signal from the source and the recycled transmitted signal of the relay. Phase alignment for the energy-bearing signal is considered which has a better performance in comparison to non-aligned energy signal. Furthermore, the joint optimum solutions for the beamformer and discrete power splitting ratio are presented for the two power splitting based protocols. Several simulations are done and the performances of different protocols and schemes are compared.

5.1   Related Works and Contributions

Simultaneous wireless information and power transfer (SWIPT) has been an appealing research topic in the context of wireless-powered relaying (WPR) in order to improve the lifetime of the relaying system. The works in [5], [20], [50] studied power splitting (PS) based SWIPT for wireless relaying whereas time switching (TS) protocol is considered in [20], [51]. All of these works are based on half-duplex (HD) relaying, where in the first phase, information and energy carrying RF signal is received and in the second phase, information signal is forwarded to the destination. Although HD relaying does not suffer from self-interference cancellation, it is inefficient in terms of spectral utilization compared to full-duplex (FD) relaying [22], [52]. FD relaying has gained great popularity in the context of SWIPT by using TS [53], [54], [55] and PS [23], [49], [52], [56], [57], [58] protocols.

In the above FD works, self-interference is the main design challenge which is handled by several analog, digital, and analog/digital self-interference cancellation techniques [59], [60]. One interesting approach different from TS and PS protocols is to take advantage of self-interference in self-energy recycling [59]. In [19], a two-phase self-energy recycling protocol is proposed for FD WPR. In the first phase, the source node transmits information signal to the relay. Then, the relay forwards the amplified signal to the destination in the second phase. At the same time, source transmits an energy-bearing signal to the relay and relay harvests energy from this dedicated signal as well as its self-interference loop channel. Since information transmission and energy reception occur at the same slot, FD name is used for this scheme. In this protocol, there are multiple-transmit antennas and a single receiving antenna at the relay. The problem is to design relay transmit beamformer such that its transmission power does not exceed the harvested power. Later, this idea is used in several works including [4], [21], [22], [61], [62]. In particular, signal-to-noise ratio (SNR) maximization problem for this protocol is considered for a more general case in which multiple receiving antennas are employed at the relay [4].

In this chapter, three SWIPT protocols are investigated. While the first two of these protocols are known in the literature, the third protocol is proposed in this chapter in order to improve the energy efficiency and the SNR at the destination. It is shown

that this new protocol achieves up to 3 dB SNR gain in comparison to the previous protocols. An important contribution in this chapter is the derivation of the closed-form expressions for the optimum relay transmit beamformers. In addition, optimum power splitting ratio is derived for the PS based protocols. While the optimum closed-form solutions are presented for real-valued PS ratios, discrete optimum solutions are also provided. Furthermore, the beamformer design problem is also considered for the optimized energy-bearing signal for multiple-receive antenna relay by presenting the closed-form solutions.

In the first part, we consider the same scenario in [4] where multiple-transmit and multiple-receive antenna relay assists the source-destination communication. In [4], the optimum solution of SNR maximization is found by solving a semidefinite programming (SDP) solver whose complexity increases by the number of transmit antennas. Furthermore, the number of variables is squared by matrix lifting which further increases the computational complexity. If the solution is not rank one, then a rank reduction iterative procedure is required in order to extract the solution. In this chapter, we first find the conditions which make the problem bounded and derive the closed-form optimum solution without resorting to any numerical solver. This single-line optimum solution is obviously more efficient compared to the approach in [4]. As a second contribution, we optimize the energy-bearing signal transmitted from the source. Using the optimum energy signal to increase the energy harvesting capability enables the relay to provide higher SNR at the destination. In this chapter, we derive the optimum closed-form solution for the optimized energy signal which is shown to perform significantly better compared to the non-optimized energy signal.

In [4], PS based beamformer design is also investigated as a benchmark and the joint optimization of the transmit beamformer vector and PS ratio is considered. The optimum solution is found by a full search over a single variable and a SDP problem is solved at each iteration. Hence, it is a computationally very expensive approach in general. In this chapter, we also present the closed-form optimum solution for this problem.

In addition to the existing protocols, we propose a novel unified framework for SWIPT. This new protocol combines PS and self-energy recycling. In the first phase of this

protocol, source node transmits the information signal to the relay. The relay splits the RF signal into two for information decoding and energy harvesting as in the conventional PS protocol. In the second phase, the amplified signal is forwarded to the destination while the energy is harvested at the multiple-receive antennas of the relay using the dedicated energy signal from the source as well as the self-energy recycling. We formulate the SNR maximization problem for the joint solution of the transmit beamformer vector and PS ratio. Both non-optimized and optimized energy signals are considered. For the former case, we derive the closed-form optimum solution while a near-optimum solution is presented for the latter case. In obtaining near-optimum solution, we ignore a relatively small term in the constraint of the problem and find the optimum solution of the approximate problem. Then, we update the solution such that the constraint is satisfied with the best objective value leading to a close-to-optimum solution.

In all the above PS based design problems, it is assumed that PS ratio can take any real value between zero and one, i.e., from a continuous set of PS ratios. In practice, PS ratios can take discrete levels [1]. In [1], the design of discrete PS ratios is also considered in addition to the continuous one. In this chapter, we also study the discrete PS ratio optimization together with the transmit beamformer vector for conventional PS and the proposed self-energy recycling assisted PS protocol. For both protocols, we present the joint optimum solution. Simulation results show that one can obtain a very close performance to the real-valued PS case even when four level discrete PS is used.

5.2   System Model and Problem Formulation

A multiple-antenna relay operating in full-duplex mode is considered for the transmission of a source signal to a destination using the amplify-and-forward scheme similar to [4]. As shown in Fig. 5.1, the source ($\mathbf{S}$) and destination ($\mathbf{D}$) nodes have both single antenna while the energy harvesting relay ($\mathbf{R}$) has multiple transmit and receive antennas. Let N_t and N_r denote the number of transmitting and receiving antennas at $\mathbf{R}$, respectively. $\mathbf{S}$ transmits message signal to $\mathbf{D}$ with the help of $\mathbf{R}$. Quasi-static block fading channel model with perfect channel state information at $\mathbf{R}$

is assumed in accordance with the related works [4], [19]. As shown in Fig. 5.1, $\mathbf{h}_r \in \mathbb{C}^{N_r \times 1}$ denotes the baseband equivalent channel vector from $\mathbf{S}$ to the receiving antennas of $\mathbf{R}$. $\mathbf{h}_d \in \mathbb{C}^{N_t \times 1}$ is the channel vector from transmitting antennas of $\mathbf{R}$ to $\mathbf{D}$ and $\mathbf{H}_{rr} \in \mathbb{C}^{N_r \times N_t}$ is the self-energy recycling loop channel matrix from N_t transmitting antennas to N_r receiving antennas.
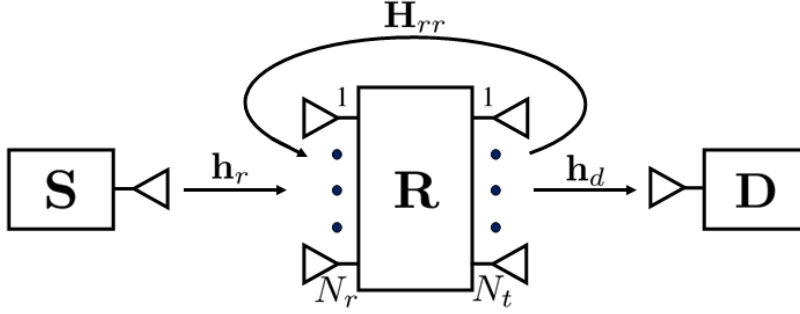
Figure 5.1: System model for self-energy recycling WPR.
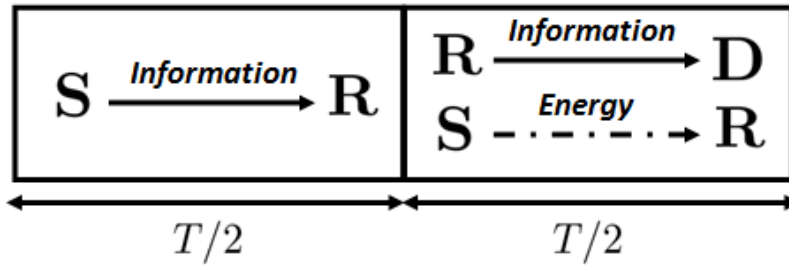
Figure 5.2: Self-energy recycling protocol for WPR.

As shown in Fig. 5.2, information signal is transmitted from $\mathbf{S}$ to $\mathbf{R}$ in the first phase which takes half of the complete cycle, i.e., $T/2$. The optimum receive beamformer is the maximal ratio combiner, i.e. $\mathbf{w}_r = \mathbf{h}_r / ||\mathbf{h}_r||$. After the receive beamforming, the received signal at $\mathbf{R}$ is given by,

$$y_{r,1} = \sqrt{P_s} ||\mathbf{h}_r|| x_s + n_{r,1} + n_b, \tag{5.1}$$

where P_s is the transmission power of $\mathbf{S}$ and x_s is the information symbol sent by $\mathbf{S}$. x_s is assumed to have unit power, i.e. $\mathbb{E}(|x_s|^2) = 1$. $n_{r,1}$ is the additive complex Gaussian noise at $\mathbf{R}$ after receive beamforming and $n_{r,1} \sim \mathcal{CN}(0, \sigma_{r,1}^2)$. n_b is the noise resulting from RF to baseband conversion with $n_b \sim \mathcal{CN}(0, \sigma_b^2)$.

In the second phase, the received signal in (5.1) is amplified and forwarded to $\mathbf{D}$ by N_t

75

transmitting antennas with relay transmit beamforming vector $\mathbf{w}_t \in \mathbb{C}^{N_t \times 1}$ as shown in Fig. 5.2. The transmitted signal, $\mathbf{y}_t$, in vector form can be expressed as follows,

$$\mathbf{y}_t = \mathbf{w}_t y_{r,1} = \mathbf{w}_t \left(\sqrt{P_s} ||\mathbf{h}_r|| x_s + n_{r,1} + n_b \right). \tag{5.2}$$

Assuming that $n_{r,1}$ and n_b are independent from each other and the information symbol x_s, the transmission power of $\mathbf{R}$ is given by,

$$P_r = ||\mathbf{w}_t||^2 \left(P_s ||\mathbf{h}_r||^2 + \sigma_{r,1}^2 + \sigma_b^2 \right). \tag{5.3}$$

The received signal at $\mathbf{D}$ in the second phase is given by,

$$y_d = \mathbf{h}_d^H \mathbf{y}_t + n_d = \mathbf{h}_d^H \mathbf{w}_t \left(\sqrt{P_s} ||\mathbf{h}_r|| x_s + n_{r,1} + n_b \right) + n_d \tag{5.4}$$

where $n_d \sim \mathcal{CN}(0, \sigma_d^2)$ is the additive complex Gaussian noise at $\mathbf{D}$. Assuming that it is independent from the information symbol and the other noise terms, the SNR at $\mathbf{D}$ is given by,

$$SNR_d = \frac{P_s ||\mathbf{h}_r||^2 |\mathbf{h}_d^H \mathbf{w}_t|^2}{(\sigma_{r,1}^2 + \sigma_b^2)|\mathbf{h}_d^H \mathbf{w}_t|^2 + \sigma_d^2}. \tag{5.5}$$

In the second phase, $\mathbf{R}$ harvests energy from the received RF signal at its receiving antennas. In this phase, an energy-bearing signal, x_e, is transmitted from $\mathbf{S}$ to $\mathbf{R}$. The received signal at $\mathbf{R}$ is given as

$$\begin{aligned} \mathbf{y}_{r,2} = & \sqrt{P_s} \mathbf{h}_r x_e + \mathbf{H}_{rr} \mathbf{y}_t + \mathbf{n}_{r,2} = \sqrt{P_s} \mathbf{h}_r x_e + \sqrt{P_s} ||\mathbf{h}_r|| \mathbf{H}_{rr} \mathbf{w}_t x_s \\ & + \mathbf{H}_{rr} \mathbf{w}_t n_{r,1} + \mathbf{H}_{rr} \mathbf{w}_t n_b + \mathbf{n}_{r,2} \end{aligned} \tag{5.6}$$

where $\mathbf{n}_{r,2} \sim \mathcal{CN}(\mathbf{0}, \sigma_{r,2}^2 \mathbf{I}_{N_r})$ is the additive complex Gaussian noise at the receiving antennas of $\mathbf{R}$. Energy signal sent from $\mathbf{S}$ is assumed to have unit power, i.e. $\mathbb{E}(|x_e|^2) = 1$. In this case, the harvested power at $\mathbf{R}$ is

$$P_h = \eta \left(P_s ||\mathbf{h}_r||^2 + P_s ||\mathbf{h}_r||^2 ||\mathbf{H}_{rr} \mathbf{w}_t||^2 + (\sigma_{r,1}^2 + \sigma_b^2) ||\mathbf{H}_{rr} \mathbf{w}_t||^2 + N_r \sigma_{r,2}^2 \right), \tag{5.7}$$

where $0 < \eta \leq 1$ denotes the energy harvesting efficiency.

In this chapter, we first consider the optimization problem to maximize the achievable rate at $\mathbf{D}$ under the transmission power constraint at $\mathbf{R}$ similar to [4]. The harvested power in (5.7) is assumed to be the only energy source at $\mathbf{R}$. Hence, the transmission power of $\mathbf{R}$, P_r, cannot exceed the harvested power, P_h. Furthermore, maximization of the achievable rate is equivalent to maximizing SNR at $\mathbf{D}$ which is the expression

in (5.5). Since the only optimization variable is the transmit beamforming vector $\mathbf{w}_t$ and SNR in (5.5) is an increasing function of $|\mathbf{h}_d^H \mathbf{w}_t|$, the optimization problem can be expressed as follows,

$$\max_{\mathbf{w}_t} \ |\mathbf{h}_d^H \mathbf{w}_t| \tag{5.8a}$$

$$s.t. \ ||\mathbf{w}_t||^2 - \eta ||\mathbf{H}_{rr} \mathbf{w}_t||^2 \leq \frac{\eta P_s ||\mathbf{h}_r||^2 + \eta N_r \sigma_{r,2}^2}{P_s ||\mathbf{h}_r||^2 + \sigma_{r,1}^2 + \sigma_b^2}. \tag{5.8b}$$

The problem in (5.8) is solved using SDP relaxation by expressing it in terms of a positive semidefinite matrix $\mathbf{X} \triangleq \mathbf{w}_t \mathbf{w}_t^H$ in [4]. Although optimum solution is guaranteed, the number of complex variables has been increased from N_t to $N_t^2/2$ in the SDP formulation. More importantly, a SDP solver is required which has growing complexity as N_t increases. In the following section, we will show that there is no need for a numerical solver by deriving the closed-form optimum solution for the problem in (5.8).

5.3 Closed-Form Optimum Solution of (5.8)

Before deriving the closed-form solution for (5.8), the following lemma is presented in order to obtain a bounded problem.

Lemma 5.1: The problem in (5.8) is bounded if the matrix $\mathbf{I}_{N_t} - \eta \mathbf{H}_{rr}^H \mathbf{H}_{rr}$ is positive definite.

Proof: Please see Appendix B.1 for the proof. ∎

The matrix $\mathbf{I}_{N_t} - \eta \mathbf{H}_{rr}^H \mathbf{H}_{rr}$ is invertible since all of its eigenvalues are assumed to be positive for a bounded solution. In this case, we can introduce the optimization variable $\widetilde{\mathbf{w}}_t \triangleq (\mathbf{I}_{N_t} - \eta \mathbf{H}_{rr}^H \mathbf{H}_{rr})^{1/2} \mathbf{w}_t$ and express (5.8) in terms of it as follows,

$$\max_{\widetilde{\mathbf{w}}_t} \ |\widetilde{\mathbf{h}}_d^H \widetilde{\mathbf{w}}_t| \tag{5.9a}$$

$$s.t. \ ||\widetilde{\mathbf{w}}_t||^2 \leq \gamma. \tag{5.9b}$$

where $\widetilde{\mathbf{h}}_d \triangleq (\mathbf{I}_{N_t} - \eta \mathbf{H}_{rr}^H \mathbf{H}_{rr})^{-1/2} \mathbf{h}_d$ and γ is defined in Appendix B.1. The optimum solution of (5.9) is easily found as

$$\widetilde{\mathbf{w}}_t^\star = \frac{\sqrt{\gamma}}{||\widetilde{\mathbf{h}}_d||} \widetilde{\mathbf{h}}_d. \tag{5.10}$$

As a result, the optimum relay transmit beamformer vector for (5.8) is given as

$$\mathbf{w}_t^\star = \sqrt{\frac{\gamma}{\mathbf{h}_d^H(\mathbf{I}_{N_t} - \eta\mathbf{H}_{rr}^H\mathbf{H}_{rr})^{-1}\mathbf{h}_d}}(\mathbf{I}_{N_t} - \eta\mathbf{H}_{rr}^H\mathbf{H}_{rr})^{-1}\mathbf{h}_d \qquad (5.11)$$

In the next section, we will consider the same optimization problem by designing dedicated energy-bearing signal x_e in order to improve the energy efficiency.

5.4 Beamforming Optimization for the Optimum Energy-Bearing Signal

In [4], harvested power expression in (5.7) is obtained by assuming that the energy-bearing signal x_e is independent from the information signal x_s. However, a power efficient approach is to adjust the phase of x_e to match it to x_s such that the harvested power is maximized for the given $\mathbf{y}_{r,2}$ expression in (5.6). Following an approach similar to the one in [19], the power harvested from the term $\sqrt{P_s}\mathbf{h}_r x_e + \sqrt{P_s}||\mathbf{h}_r||\mathbf{H}_{rr}\mathbf{w}_t x_s$ in (5.6) is maximized when $x_e = x_s e^{j\angle\mathbf{h}_r^H\mathbf{H}_{rr}\mathbf{w}_t}$. In this case, the harvested power at $\mathbf{R}$ is given by,

$$P_h = \eta\Big(P_s||\mathbf{h}_r||^2 + P_s||\mathbf{h}_r||^2||\mathbf{H}_{rr}\mathbf{w}_t||^2 + 2P_s||\mathbf{h}_r|||\mathbf{h}_r^H\mathbf{H}_{rr}\mathbf{w}_t|$$

$$+ (\sigma_{r,1}^2 + \sigma_b^2)||\mathbf{H}_{rr}\mathbf{w}_t||^2 + N_r\sigma_{r,2}^2 \Big). \qquad (5.12)$$

Now, SNR maximization problem in (5.8) can be expressed using the updated P_h in (5.12) as follows,

$$\max_{\mathbf{w}_t} \ |\mathbf{h}_d^H\mathbf{w}_t| \qquad (5.13a)$$

$$s.t. \ \gamma_1\big(||\mathbf{w}_t||^2 - \eta||\mathbf{H}_{rr}\mathbf{w}_t||^2\big) - 2\eta P_s||\mathbf{h}_r|||\mathbf{h}_r^H\mathbf{H}_{rr}\mathbf{w}_t| \leq \gamma_2 \qquad (5.13b)$$

where $\gamma_1 \triangleq P_s||\mathbf{h}_r||^2 + \sigma_{r,1}^2 + \sigma_b^2$ and $\gamma_2 \triangleq \eta P_s||\mathbf{h}_r||^2 + \eta N_r\sigma_{r,2}^2$. In order to simplify the optimization problem in (5.13), let us introduce $\widetilde{\mathbf{w}}_t \triangleq (\mathbf{I}_{N_t} - \eta\mathbf{H}_{rr}^H\mathbf{H}_{rr})^{1/2}\mathbf{w}_t$ as in the previous section and reformulate (5.13) as follows,

$$\max_{\widetilde{\mathbf{w}}_t} \ |\widetilde{\mathbf{h}}_d^H\widetilde{\mathbf{w}}_t| \qquad (5.14a)$$

$$s.t. \ \gamma_1||\widetilde{\mathbf{w}}_t||^2 - 2\eta P_s||\mathbf{h}_r|||\widetilde{\mathbf{h}}_r^H\widetilde{\mathbf{w}}_t| \leq \gamma_2. \qquad (5.14b)$$

where $\widetilde{\mathbf{h}}_d$ is the same as in (5.9) and $\widetilde{\mathbf{h}}_r \triangleq (\mathbf{I}_{N_t} - \eta\mathbf{H}_{rr}^H\mathbf{H}_{rr})^{-1/2}\mathbf{H}_{rr}^H\mathbf{h}_r$. In order to simplify the Kuhn-Tucker conditions for (5.14), let us express $\widetilde{\mathbf{w}}_t$ as $\widetilde{\mathbf{w}}_t = \sum_{n=1}^{N_t}\beta_n e^{j\theta_n}\boldsymbol{\Phi}_n$

where $\beta_n \geq 0$, $n = 1, ..., N_t$ and $\{\boldsymbol{\Phi}_n\}_{n=1}^{N_t}$ is an orthonormal basis for $\mathbb{C}^{N_t \times 1}$ such that $\boldsymbol{\Phi}_1 = \widetilde{\mathbf{h}}_r/||\widetilde{\mathbf{h}}_r||$ and $\boldsymbol{\Phi}_2 = (\widetilde{\mathbf{h}}_d - \boldsymbol{\Phi}_1\boldsymbol{\Phi}_1^H\widetilde{\mathbf{h}}_d)/||\widetilde{\mathbf{h}}_d - \boldsymbol{\Phi}_1\boldsymbol{\Phi}_1^H\widetilde{\mathbf{h}}_d||$. Then, we have the following result.

Lemma 5.2: The optimum relay beamformer vector for (5.14) is given as $\widetilde{\mathbf{w}}_t = \beta_1\boldsymbol{\Phi}_1 + \beta_2 e^{j\angle\widetilde{\mathbf{h}}_d^H\widetilde{\mathbf{h}}_r}\boldsymbol{\Phi}_2$, where $\beta_1 \geq 0$ and $\beta_2 \geq 0$.

Proof: Please see Appendix B.2 for the proof. ∎

Now, let us express (5.14) in terms of β_1 and β_2 as follows,

$$\max_{\beta_1,\beta_2} \ a_1\beta_1 + a_2\beta_2 \tag{5.15a}$$

$$s.t. \ \gamma_1\beta_1^2 + \gamma_1\beta_2^2 - 2\eta P_s||\mathbf{h}_r||||\widetilde{\mathbf{h}}_r||\beta_1 \leq \gamma_2 \tag{5.15b}$$

where $a_1 = |\widetilde{\mathbf{h}}_d^H\widetilde{\mathbf{h}}_r|/||\widetilde{\mathbf{h}}_r||$, $a_2 = (\widetilde{\mathbf{h}}_d^H\widetilde{\mathbf{h}}_d - \widetilde{\mathbf{h}}_d^H\boldsymbol{\Phi}_1\boldsymbol{\Phi}_1^H\widetilde{\mathbf{h}}_d)/||\widetilde{\mathbf{h}}_d - \boldsymbol{\Phi}_1\boldsymbol{\Phi}_1^H\widetilde{\mathbf{h}}_d||$. It is easily seen that the optimum β_1 and β_2 should be nonnegative for (5.15) since $a_1 \geq 0$, $a_2 \geq 0$ and $-2\eta P_s||\mathbf{h}_r||||\widetilde{\mathbf{h}}_r|| < 0$. Hence, the constraints $\beta_1 \geq 0$ and $\beta_2 \geq 0$ are not included for simplicity. The Kuhn-Tucker necessary conditions for the optimum solution of (5.15) are given by,

$$a_1 = 2\mu\gamma_1\beta_1 - 2\mu\eta P_s||\mathbf{h}_r||||\widetilde{\mathbf{h}}_r||, \tag{5.16a}$$

$$a_2 = 2\mu\gamma_1\beta_2, \tag{5.16b}$$

$$\mu \geq 0, \quad \mu(\gamma_1\beta_1^2 + \gamma_1\beta_2^2 - 2\eta P_s||\mathbf{h}_r||||\widetilde{\mathbf{h}}_r||\beta_1 - \gamma_2) = 0 \tag{5.16c}$$

$$\gamma_1\beta_1^2 + \gamma_1\beta_2^2 - 2\eta P_s||\mathbf{h}_r||||\widetilde{\mathbf{h}}_r||\beta_1 \leq \gamma_2 \tag{5.16d}$$

where μ is the Lagrange multiplier corresponding to (5.15b). Note that there are two cases for μ which are $\mu = 0$ and $\mu > 0$. First, assume that $\mu = 0$ for the optimum solution. This is impossible since both $a_1 = 0$ and $a_2 = 0$ cannot be zero by $a_1^2 + a_2^2 = ||\widetilde{\mathbf{h}}_d||^2$. Hence, it is concluded that $\mu > 0$ and (5.16d) is satisfied with equality by (5.16c). By (5.16a-b), we obtain $\beta_1 = a_1/(2\gamma_1\mu) + \eta P_s||\mathbf{h}_r||||\widetilde{\mathbf{h}}_r||/\gamma_1$ and $\beta_2 = a_2/(2\gamma_1\mu)$. If we insert these into the equality $\gamma_1\beta_1^2 + \gamma_1\beta_2^2 - 2\eta P_s||\mathbf{h}_r||||\widetilde{\mathbf{h}}_r||\beta_1 =$

γ_2, we obtain the optimum β_1 and β_2 as follows,

$$\beta_1^\star = \frac{a_1 \sqrt{\eta^2 P_s^2 ||\mathbf{h}_r||^2 ||\widetilde{\mathbf{h}}_r||^2 + \gamma_1 \gamma_2}}{\gamma_1 \sqrt{a_1^2 + a_2^2}} + \frac{\eta P_s ||\mathbf{h}_r|| ||\widetilde{\mathbf{h}}_r||}{\gamma_1} \tag{5.17a}$$

$$\beta_2^\star = \frac{a_2 \sqrt{\eta^2 P_s^2 ||\mathbf{h}_r||^2 ||\widetilde{\mathbf{h}}_r||^2 + \gamma_1 \gamma_2}}{\gamma_1 \sqrt{a_1^2 + a_2^2}} \tag{5.17b}$$

Using (5.17a-b) and Lemma 5.2, the optimum relay transmit beamformer weight vector for (5.13) is given by

$$\mathbf{w}_t^\star = (\mathbf{I}_{N_t} - \eta \mathbf{H}_{rr}^H \mathbf{H}_{rr})^{-1/2} (\beta_1^\star \mathbf{\Phi}_1 + \beta_2^\star e^{j \angle \widetilde{\mathbf{h}}_d^H \widetilde{\mathbf{h}}_r} \mathbf{\Phi}_2). \tag{5.18}$$

(5.11) and (5.18) are the optimum beamformers for non-optimized and optimized energy-bearing signals for the first SWIPT protocol in Fig. 5.2. In the following section, the closed-form optimum transmit beamformer is derived for the second SWIPT protocol, namely, PS protocol.

5.5   Conventional Power Splitting Protocol

In [20], PS protocol is considered for a single antenna relay. This problem is generalized for multiple transmit and receiving antenna case in [4]. In order to tackle the joint optimization of the PS coefficient and relay transmit beamformer, full search is performed with respect to the PS coefficient and a semidefinite programming problem with $N_t N_r \times N_t N_r$ matrix variable is solved for each PS coefficient. This procedure has a high computational complexity especially when N_t and N_r are relatively big.

In this section, we will derive the closed-form optimum solution for the PS protocol considered in [4]. The conventional PS protocol is given in Fig. 5.3.

As shown in Fig. 5.3, there are two phases in each block. In the first phase of duration $T/2$, source signal is sent from $\mathbf{S}$ to $\mathbf{R}$. The received signal at the antennas of R is given by

$$\mathbf{y}_{r,1} = \sqrt{P_s} \mathbf{h}_r x_s + \mathbf{n}_{r,1}. \tag{5.19}$$

The received signal $\mathbf{y}_{r,1}$ is split into two for information decoding and energy harvesting. If $0 \leq \rho < 1$ denotes the fraction of power for energy harvesting, the signal at
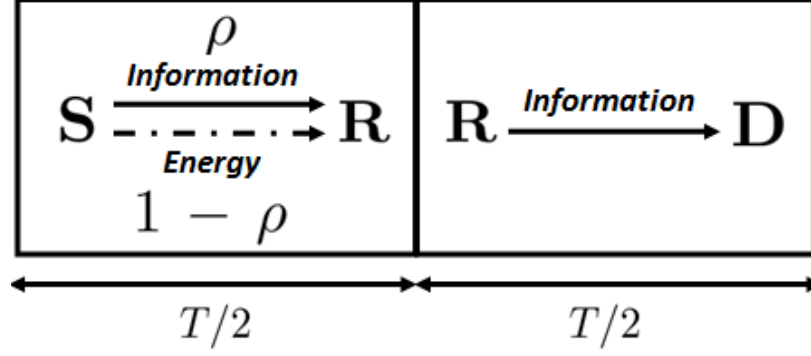
Figure 5.3: Conventional PS protocol for WPR.

the energy harvesting receiver is given by,

$$\mathbf{y}_{r,1}^E = \sqrt{\rho}\left(\sqrt{P_s}\mathbf{h}_r x_s + \mathbf{n}_{r,1}\right). \tag{5.20}$$

In this case, the total harvested power at $\mathbf{R}$ in the first phase is given by

$$P_{h,1} = \eta\rho\left(P_s||\mathbf{h}_r||^2 + N_r\sigma_{r,1}^2\right). \tag{5.21}$$

The received signal at the information decoder after optimum receive beamforming by $\mathbf{w}_r = \mathbf{h}_r/||\mathbf{h}_r||$ is,

$$y_{r,1}^I = \sqrt{1-\rho}\left(\sqrt{P_s}||\mathbf{h}_r||x_s + \tilde{n}_{r,1}\right) + n_b. \tag{5.22}$$

Here, $\tilde{n}_{r,1} \triangleq \mathbf{w}_r^H \mathbf{n}_{r,1}$ and it has the variance $\sigma_{r,1}^2$. n_b is the additive complex Gaussian noise due to baseband conversion. In the second phase of duration $T/2$, information signal $y_{r,1}^I$ is amplified and forwarded to $\mathbf{D}$ by the transmit beamformer $\mathbf{w}_t$ and the transmitted signal is given as follows,

$$\mathbf{y}_t = \mathbf{w}_t y_{r,1}^I = \mathbf{w}_t\left(\sqrt{1-\rho}\left(\sqrt{P_s}||\mathbf{h}_r||x_s + \tilde{n}_{r,1}\right) + n_b\right). \tag{5.23}$$

The transmission power of the relay is given as

$$P_r = ||\mathbf{w}_t||^2\left((1-\rho)P_s||\mathbf{h}_r||^2 + (1-\rho)\sigma_{r,1}^2 + \sigma_b^2\right). \tag{5.24}$$

In the second phase, the received signal at $\mathbf{D}$ is given as follows,

$$y_d = \mathbf{h}_d^H \mathbf{w}_t\left(\sqrt{1-\rho}\left(\sqrt{P_s}||\mathbf{h}_r||x_s + \tilde{n}_{r,1}\right) + n_b\right) + n_d. \tag{5.25}$$

Using (5.25), SNR at **D** is written as

$$SNR_d = \frac{P_s||\mathbf{h}_r||^2|\mathbf{h}_d^H\mathbf{w}_t|^2}{\sigma_{r,1}^2|\mathbf{h}_d^H\mathbf{w}_t|^2 + \frac{\sigma_b^2|\mathbf{h}_d^H\mathbf{w}_t|^2+\sigma_d^2}{1-\rho}}. \tag{5.26}$$

The SNR maximization problem for the conventional PS is formulated as follows,

$$\max_{\mathbf{w}_t,\rho} \quad \frac{P_s||\mathbf{h}_r||^2|\mathbf{h}_d^H\mathbf{w}_t|^2}{\sigma_{r,1}^2|\mathbf{h}_d^H\mathbf{w}_t|^2 + \frac{\sigma_b^2|\mathbf{h}_d^H\mathbf{w}_t|^2+\sigma_d^2}{1-\rho}} \tag{5.27a}$$

$$s.t. \quad ||\mathbf{w}_t||^2\left(P_s||\mathbf{h}_r||^2 + \sigma_{r,1}^2 + \frac{\sigma_b^2}{1-\rho}\right) \le \eta\frac{\rho}{1-\rho}(P_s||\mathbf{h}_r||^2 + N_r\sigma_{r,1}^2) \tag{5.27b}$$

$$0 \le \rho < 1. \tag{5.27c}$$

Let us express $\mathbf{w}_t$ as $\mathbf{w}_t = \sum_{n=1}^{N_t}\beta_n e^{j\theta_n}\mathbf{\Psi}_n$ where $\beta_n \ge 0$, $n = 1, ..., N_t$ and $\{\mathbf{\Psi}_n\}_{n=1}^{N_t}$ is an orthonormal basis for $\mathbb{C}^{N_t\times 1}$ such that $\mathbf{\Psi}_1 = \mathbf{h}_d/||\mathbf{h}_d||$. Furthermore define $x \triangleq \sqrt{\frac{\rho}{1-\rho}}$ in order to eliminate (5.27c) and simplify Kuhn-Tucker conditions. (5.27) can be expressed in terms of $\{\beta_n\}_{n=1}^{N_t}$ and x as follows,

$$\max_{\{\beta_n\}_{n=1}^{N_t},x} \quad \frac{\beta_1^2}{\delta_1\beta_1^2 x^2 + \delta_2\beta_1^2 + \sigma_d^2(x^2+1)} \tag{5.28a}$$

$$s.t. \quad \sigma_b^2 x^2\sum_{n=1}^{N_t}\beta_n^2 + \pi_1\sum_{n=1}^{N_t}\beta_n^2 - \pi_2 x^2 \le 0. \tag{5.28b}$$

where the following terms are defined for the ease of notation, i.e.,

$$\delta_1 = ||\mathbf{h}_d||^2\sigma_b^2, \quad \delta_2 = ||\mathbf{h}_d||^2(\sigma_{r,1}^2 + \sigma_b^2),$$
$$\pi_1 = P_s||\mathbf{h}_r||^2 + \sigma_{r,1}^2 + \sigma_b^2, \quad \pi_2 = \eta(P_s||\mathbf{h}_r||^2 + N_r\sigma_{r,1}^2) \tag{5.29}$$

Note that $0 \le \rho < 1$ region maps to $0 \le x < \infty$ and the problem (5.28) is independent of the sign of x. Hence, there is no constraint for the region of the introduced variable x. The Kuhn-Tucker conditions necessitate the following constraints for the optimum solution of (5.28), i.e.,

$$\frac{2\sigma_d^2(x^2+1)\beta_1}{(\delta_1\beta_1^2 x^2 + \delta_2\beta_1^2 + \sigma_d^2(x^2+1))^2} = 2\mu(\sigma_b^2 x^2 + \pi_1)\beta_1 \tag{5.30a}$$

$$2\mu(\sigma_b^2 x^2 + \pi_1)\beta_n = 0, \quad n = 2, ..., N_t \tag{5.30b}$$

$$\mu \ge 0, \quad \mu\left(\sigma_b^2 x^2\sum_{n=1}^{N_t}\beta_n^2 + \pi_1\sum_{n=1}^{N_t}\beta_n^2 - \pi_2 x^2\right) = 0 \tag{5.30c}$$

where μ is the Lagrange multiplier corresponding to the inequality in (5.28b). Note that μ should be strictly greater than zero for the optimum solution of (5.28). If $\mu = 0$, then $\beta_1 = 0$ by (5.30a) and this results zero SNR as seen from (5.28a). Hence, $\mu > 0$. Using this fact and (5.30b), it is seen that $\beta_n = 0$, $n = 2, ..., N_t$ for the optimum solution. Furthermore, the inequality in (5.28b) should be satisfied with equality by (5.30c). Hence, $\sigma_b^2 x^2 \beta_1^2 + \pi_1 \beta_1^2 - \pi_2 x^2 = 0$. Using this, we obtain $\beta_1^2 = \frac{\pi_2 x^2}{\sigma_b^2 x^2 + \pi_1}$. If we insert this relation into (5.28a), the following unconstrained optimization problem is obtained, i.e.,

$$\max_{x} \quad \frac{x^2}{A_4 x^4 + A_2 x^2 + A_0} \tag{5.31}$$

where $A4$, $A2$, and $A0$ are defined as follows,

$$A4 = \sigma_d^2 \sigma_b^2 + \pi_2 \delta_1, \quad A2 = \sigma_d^2 \sigma_b^2 + \sigma_d^2 \pi_1 + \pi_2 \delta_2, \quad A0 = \sigma_d^2 \pi_1 \tag{5.32}$$

If we take the derivative of the objective function in (5.31) and equate it to zero, we obtain the equation

$$A_4 x^5 = A_0 x \tag{5.33}$$

One of the critical points that satisfy (5.33) is $x = 0$ which corresponds to $\rho = 0$, i.e., no energy harvesting. Hence, it results zero SNR as seen from (5.31). The other critical point is the optimum solution and it is given as follows,

$$x^\star = \left(\frac{A_0}{A_4} \right)^{1/4} \tag{5.34}$$

Note that we are only interested in the range $0 \le x < \infty$ for the critical points since the objective in (5.31) is a function of $x^2 = \rho/(1 - \rho)$. In this case, the optimum relay transmit beamformer vector and PS ratio are given as follows,

$$\mathbf{w}_t^\star = \beta_1^\star \mathbf{\Psi}_1 = \frac{\sqrt{\pi_2} x^\star}{\sqrt{\sigma_b^2 (x^\star)^2 + \pi_1} ||\mathbf{h}_d||} \mathbf{h}_d, \quad \rho^\star = \frac{(x^\star)^2}{(x^\star)^2 + 1} \tag{5.35}$$

(5.35) gives the closed-form solution for the PS based protocol. In the following section, a new SWIPT protocol is presented in order to improve the energy efficiency as well as the SNR at the destination.
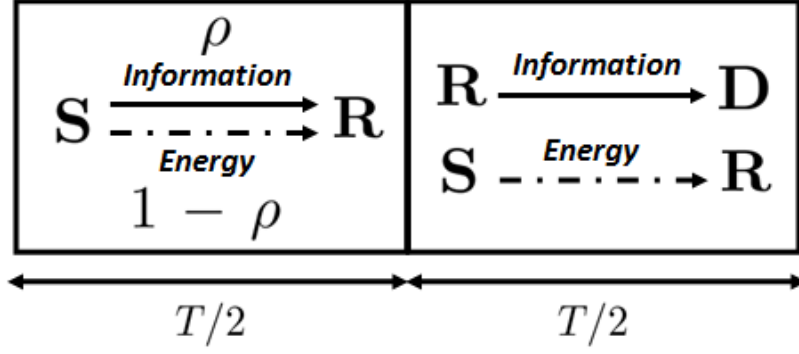
Figure 5.4: Self-energy recycling assisted PS protocol for WPR.

5.6 Beamforming Optimization for the Self-Energy Recycling Assisted Power Splitting Protocol

In this section, we propose a new protocol which is based on both conventional power splitting relaying in [4], [20] and self-energy recycling. The motivation for this unified framework lies in the fact that the performance of conventional PS protocol falls behind the self-energy recycling protocol considered in the previous section. In order to improve PS protocol, we employ the receiving antennas of **R** in the second phase different from the conventional protocol. In the conventional PS protocol in [4], **R** harvests energy in the first phase only. In this section, we modify the conventional PS protocol such that **S** sends an energy signal to **R** in the second phase as well and self-energy recycling is taken into account in the design of the transmit beamformer as shown in Fig. 5.4. In this case, the received signal at the receiving antennas of **R** in the second phase is given by

$$
\begin{aligned}
\mathbf{y}_{r,2} &= \sqrt{P_s}\mathbf{h}_R x_e + \mathbf{H}_{rr}\mathbf{y}_t + \mathbf{n}_{r,2} \\
&= \sqrt{P_s}\mathbf{h}_r x_e + \sqrt{1-\rho}\sqrt{P_s}\|\mathbf{h}_r\|\mathbf{H}_{rr}\mathbf{w}_t x_s + \sqrt{1-\rho}\mathbf{H}_{rr}\mathbf{w}_t \tilde{n}_{r,1} + \mathbf{H}_{rr}\mathbf{w}_t n_b + \mathbf{n}_{r,2}.
\end{aligned}
$$

(5.36)

In the following two subsections, we will consider the beamformer design for the non-optimized and optimum energy-bearing signal, x_e, respectively. Non-optimized energy-bearing signal case leads to a simpler formulation and a single-line optimum solution can be found. In case of optimized energy-bearing signal, a bisection search is performed and a near-optimum solution is obtained. While the latter design is expected to perform better, it has an additional overhead and requires feedback signaling

from **R** to **S** for phase alignment. Note that this overhead is small since it is required to transfer only a single phase value as the channel varies.

5.6.1 Beamforming Design for the Non-Optimized Energy-Bearing Signal

In this part, we will assume that x_e is independent from the information signal x_s as in Section 5.3. The harvested power at **R** in the second phase is given by

$$P_{h,2} = \eta\left(P_s||\mathbf{h}_r||^2 + (1-\rho)P_s||\mathbf{h}_r||^2||\mathbf{H}_{rr}\mathbf{w}_t||^2 + (1-\rho)\sigma_{r,1}^2||\mathbf{H}_{rr}\mathbf{w}_t||^2\right.$$
$$\left. + \sigma_b^2||\mathbf{H}_{rr}\mathbf{w}_t||^2 + N_r\sigma_{r,2}^2\right). \tag{5.37}$$

The total available power for each transmission block is the summation of the harvested powers in the first and second phase, which is $P_{h,1} + P_{h,2}$ where $P_{h,1}$ is given in (5.21). Then the SNR maximization problem is formulated as follows,

$$\max_{\mathbf{w}_t,\rho} \quad \frac{P_s||\mathbf{h}_r||^2|\mathbf{h}_d^H\mathbf{w}_t|^2}{\sigma_{r,1}^2|\mathbf{h}_d^H\mathbf{w}_t|^2 + \frac{\sigma_b^2|\mathbf{h}_d^H\mathbf{w}_t|^2+\sigma_d^2}{1-\rho}} \tag{5.38a}$$

$$s.t. \quad \left(||\mathbf{w}_t||^2 - \eta||\mathbf{H}_{rr}\mathbf{w}_t||^2\right)\left(P_s||\mathbf{h}_r||^2 + \sigma_{r,1}^2 + \frac{\sigma_b^2}{1-\rho}\right)$$
$$\leq \eta\frac{\rho\left(P_s||\mathbf{h}_r||^2 + N_r\sigma_{r,1}^2\right) + P_s||\mathbf{h}_r||^2 + N_r\sigma_{r,2}^2}{1-\rho} \tag{5.38b}$$

$$0 \leq \rho < 1. \tag{5.38c}$$

Note that the second term in the numerator of (5.38b) is due to the energy signal in the second phase as shown in Fig. 5.4. By introducing the optimization variable $\widetilde{\mathbf{w}}_t \triangleq (\mathbf{I}_{N_t} - \eta\mathbf{H}_{rr}^H\mathbf{H}_{rr})^{1/2}\mathbf{w}_t$ and defining $x \triangleq \sqrt{\frac{\rho}{1-\rho}}$ as in the previous section, the problem in (5.38) can be reformulated as follows,

$$\max_{\widetilde{\mathbf{w}}_t,x} \quad \frac{P_s||\mathbf{h}_r||^2|\widetilde{\mathbf{h}}_d^H\widetilde{\mathbf{w}}_t|^2}{\sigma_{r,1}^2|\widetilde{\mathbf{h}}_d^H\widetilde{\mathbf{w}}_t|^2 + (\sigma_b^2|\widetilde{\mathbf{h}}_d^H\widetilde{\mathbf{w}}_t|^2 + \sigma_d^2)(x^2+1)} \tag{5.39a}$$

$$s.t. \quad ||\widetilde{\mathbf{w}}_t||^2\left(P_s||\mathbf{h}_r||^2 + \sigma_{r,1}^2 + \sigma_b^2(x^2+1)\right)$$
$$\leq \eta\left(P_s||\mathbf{h}_r||^2 + N_r\sigma_{r,1}^2\right)x^2 + \eta\left(P_s||\mathbf{h}_r||^2 + N_r\sigma_{r,2}^2\right)(x^2+1) \tag{5.39b}$$

where $\widetilde{\mathbf{h}}_d$ is as in (5.9). The problem in (5.39) is similar to the problem in (5.27). Using the same argument in the previous section, the optimum $\widetilde{\mathbf{w}}_t$ is given in the

form $\widetilde{\mathbf{w}}_t = \beta_1 \widetilde{\mathbf{h}}_d / ||\widetilde{\mathbf{h}}_d||$ where $\beta_1 \geq 0$. Furthermore, (5.38b) should be satisfied with equality for the optimum solution and thus $\beta_1^2 = \frac{(\pi_2 + \pi_3)x^2 + \pi_3}{\sigma_b^2 x^2 + \pi_1}$, where π_1, π_2 are as in (5.29) and $\pi_3 \triangleq \eta(P_s||\mathbf{h}_r||^2 + N_r \sigma_{r,2}^2)$. Then, we obtain the following unconstrained optimization problem in terms of x, i.e.,

$$\max_x \frac{B_2 x^2 + B_0}{C_4 x^4 + C_2 x^2 + C_0} \tag{5.40}$$

where B_2, B_0, C_4, C_2, and C_0 are introduced for ease of notation as follows,

$$B2 = \pi_2 + \pi_3, \quad B0 = \pi_3 \tag{5.41a}$$

$$C4 = \sigma_d^2 \sigma_b^2 + (\pi_2 + \pi_3)||\widetilde{\mathbf{h}}_d||^2 \sigma_b^2 \tag{5.41b}$$

$$C2 = \sigma_d^2 \sigma_b^2 + \sigma_d^2 \pi_1 + (\pi_2 + \pi_3)||\widetilde{\mathbf{h}}_d||^2 (\sigma_{r,1}^2 + \sigma_b^2) + \pi_3 ||\widetilde{\mathbf{h}}_d||^2 \sigma_b^2 \tag{5.41c}$$

$$C0 = \sigma_d^2 \pi_1 + \pi_3 ||\widetilde{\mathbf{h}}_d||^2 (\sigma_{r,1}^2 + \sigma_b^2). \tag{5.41d}$$

If we take the derivative of the function in (5.40) and equate it to zero, we obtain the equation

$$B_2 C_4 x^5 + 2 B_0 C_4 x^3 + (B_0 C_2 - B_2 C_0)x = 0 \tag{5.42}$$

One of the critical points that satisfy (5.42) is $x = 0$ which corresponds to $\rho = 0$ and hence no energy harvesting in the first phase. This case corresponds to the conventional self-energy recycling protocol without power splitting. The other critical point is $x = \sqrt{r^\star}$ where $r^\star$ is the positive root of the second order polynomial $B_2 C_4 r^2 + 2 B_0 C_4 r + (B_0 C_2 - B_2 C_0)$. The only positive root $r^\star$ exists if $(B_0 C_2 - B_2 C_0) \leq 0$. Then, the optimum solution of (5.40) is $x = 0$ or $x = \sqrt{r^\star}$ which maximizes the objective function in (5.40), i.e.,

$$x^\star = \arg \max_{x \in \{0, \sqrt{r^\star}\}} \frac{B_2 x^2 + B_0}{C_4 x^4 + C_2 x^2 + C_0} \tag{5.43}$$

In this case, the optimum relay transmit beamformer vector and the optimum power splitting ratio are given as follows,

$$\mathbf{w}_t^\star = \sqrt{\frac{(\pi_2 + \pi_3)(x^\star)^2 + \pi_3}{\sigma_b^2 (x^\star)^2 + \pi_1}} \frac{(\mathbf{I}_{N_t} - \eta \mathbf{H}_{rr}^H \mathbf{H}_{rr})^{-1} \mathbf{h}_d}{\sqrt{\mathbf{h}_d^H (\mathbf{I}_{N_t} - \eta \mathbf{H}_{rr}^H \mathbf{H}_{rr})^{-1} \mathbf{h}_d}}, \quad \rho^\star = \frac{(x^\star)^2}{(x^\star)^2 + 1} \tag{5.44}$$

5.6.2 Beamforming Design for the Optimum Energy-Bearing Signal

In this part, we will consider the relay beamformer design for the optimum energy-bearing signal which is $x_e = x_s e^{j \angle \mathbf{h}_r^H \mathbf{H}_{rr} \mathbf{w}_t}$. In this case, the harvested power in the

second phase for $\mathbf{R}$ is given as

$$P_{h,2} = \eta\left(P_s||\mathbf{h}_r||^2 + (1-\rho)P_s||\mathbf{h}_r||^2||\mathbf{H}_{rr}\mathbf{w}_t||^2 + 2\sqrt{1-\rho}P_s||\mathbf{h}_r|||\mathbf{h}_r^H\mathbf{H}_{rr}\mathbf{w}_t|\right.$$

$$\left. + (1-\rho)\sigma_{r,1}^2||\mathbf{H}_{rr}\mathbf{w}_t||^2 + \sigma_b^2||\mathbf{H}_{rr}\mathbf{w}_t||^2 + N_r\sigma_{r,2}^2\right). \tag{5.45}$$

SNR maximization problem in terms of $\widetilde{\mathbf{w}}_t = (\mathbf{I}_{N_t} - \eta\mathbf{H}_{rr}^H\mathbf{H}_{rr})^{1/2}\mathbf{w}_t$ and ρ can be formulated as follows,

$$\max_{\widetilde{\mathbf{w}}_t,\rho} \quad \frac{P_s||\mathbf{h}_r||^2|\widetilde{\mathbf{h}}_d^H\widetilde{\mathbf{w}}_t|^2}{\sigma_{r,1}^2|\widetilde{\mathbf{h}}_d^H\widetilde{\mathbf{w}}_t|^2 + \frac{\sigma_b^2|\widetilde{\mathbf{h}}_d^H\widetilde{\mathbf{w}}_t|^2+\sigma_d^2}{1-\rho}} \tag{5.46a}$$

$$s.t. \quad ||\widetilde{\mathbf{w}}_t||^2\left((P_s||\mathbf{h}_r||^2 + \sigma_{r,1}^2)(1-\rho) + \sigma_b^2\right)$$

$$\leq \eta\left(P_s||\mathbf{h}_r||^2 + N_r\sigma_{r,1}^2\right)\rho + \eta\left(P_s||\mathbf{h}_r||^2 + N_r\sigma_{r,2}^2\right) + 2\eta P_s||\mathbf{h}_r|||\widetilde{\mathbf{h}}_r^H\widetilde{\mathbf{w}}_t|\sqrt{1-\rho} \tag{5.46b}$$

$$0 \leq \rho < 1 \tag{5.46c}$$

where $\widetilde{\mathbf{h}}_d$ and $\widetilde{\mathbf{h}}_r$ are as in (5.9) and (5.14), respectively. Let us express $\widetilde{\mathbf{w}}_t = \sum_{n=1}^{N_t}\beta_n e^{j\theta_n}\boldsymbol{\Psi}_n$ where $\beta_n \geq 0$, $n = 1, ..., N_t$ and $\{\boldsymbol{\Psi}_n\}_{n=1}^{N_t}$ is an orthonormal basis for $\mathbb{C}^{N_t\times 1}$ such that $\boldsymbol{\Psi}_1 = \widetilde{\mathbf{h}}_d/||\widetilde{\mathbf{h}}_d||$ and $\boldsymbol{\Psi}_2 = (\widetilde{\mathbf{h}}_r - \boldsymbol{\Psi}_1\boldsymbol{\Psi}_1^H\widetilde{\mathbf{h}}_r)/||\widetilde{\mathbf{h}}_r - \boldsymbol{\Psi}_1\boldsymbol{\Psi}_1^H\widetilde{\mathbf{h}}_r||$. Then we have the following result.

Lemma 5.3: The optimum $\widetilde{\mathbf{w}}_t$ for (5.46) is given in the form $\widetilde{\mathbf{w}}_t = \beta_1\boldsymbol{\Psi}_1 + \beta_2 e^{j\angle\widetilde{\mathbf{h}}_r^H\widetilde{\mathbf{h}}_d}\boldsymbol{\Psi}_2$.

Proof: The proof is similar to the one for Lemma 5.2. ∎

Let us express (5.46) in terms of β_1, β_2 and ρ as follows,

$$\max_{\beta_1,\beta_2,\rho} \quad \frac{P_s||\mathbf{h}_r||^2||\widetilde{\mathbf{h}}_d||^2\beta_1^2}{\sigma_{r,1}^2||\widetilde{\mathbf{h}}_d||^2\beta_1^2 + \frac{\sigma_b^2||\widetilde{\mathbf{h}}_d||^2\beta_1^2+\sigma_d^2}{1-\rho}} \tag{5.47a}$$

$$s.t. \quad (\beta_1^2 + \beta_2^2)\left((P_s||\mathbf{h}_r||^2 + \sigma_{r,1}^2)(1-\rho) + \sigma_b^2\right)$$

$$\leq \eta\left(P_s||\mathbf{h}_r||^2 + N_r\sigma_{r,1}^2\right)\rho + \eta\left(P_s||\mathbf{h}_r||^2 + N_r\sigma_{r,2}^2\right) + (\tilde{a}_1\beta_1 + \tilde{a}_2\beta_2)\sqrt{1-\rho} \tag{5.47b}$$

$$0 \leq \rho < 1 \tag{5.47c}$$

where $\tilde{a}_1 = 2\eta P_s||\mathbf{h}_r|||\widetilde{\mathbf{h}}_r^H\widetilde{\mathbf{h}}_d|/||\widetilde{\mathbf{h}}_d||$, $\tilde{a}_2 = 2\eta P_s||\mathbf{h}_r||(\widetilde{\mathbf{h}}_r^H\widetilde{\mathbf{h}}_r - \widetilde{\mathbf{h}}_r^H\boldsymbol{\Psi}_1\boldsymbol{\Psi}_1^H\widetilde{\mathbf{h}}_r)/||\widetilde{\mathbf{h}}_r - \boldsymbol{\Psi}_1\boldsymbol{\Psi}_1^H\widetilde{\mathbf{h}}_r||$.

Note that the closed-form optimum solution of (5.47) is difficult to obtain in its current form due to the highly coupled variables and the square root function in (5.47b). In the

following part, we will define new optimization variables and obtain the closed-form optimum solution for an approximate problem of (5.47). Let us define the following set of variables for the reformulation of (5.47), i.e.,

$$\widetilde{\beta}_1 \triangleq \beta_1 \sqrt{1-\rho}, \quad \widetilde{\beta}_2 \triangleq \beta_2 \sqrt{1-\rho}. \tag{5.48}$$

Using the newly introduced variables in (5.48), the problem (5.47) can be expressed as,

$$\min_{\widetilde{\beta}_1, \widetilde{\beta}_2, \rho} \quad \frac{\widetilde{\delta}_1}{1-\rho} + \frac{\widetilde{\delta}_2}{\widetilde{\beta}_1^2} \tag{5.49a}$$

$$s.t. \quad \left(\tilde{\pi}_1 + \frac{\sigma_b^2}{1-\rho}\right)(\widetilde{\beta}_1^2 + \widetilde{\beta}_2^2) \leq \pi_2\rho + \pi_3 + \tilde{a}_1\widetilde{\beta}_1 + \tilde{a}_2\widetilde{\beta}_2 \tag{5.49b}$$

$$0 \leq \rho < 1 \tag{5.49c}$$

where $\widetilde{\delta}_1 = \sigma_b^2/(P_s||\mathbf{h}_r||^2)$ and $\widetilde{\delta}_2 = \sigma_d^2/(P_s||\mathbf{h}_r||^2||\widetilde{\mathbf{h}}_d||^2)$. $\pi_2 = \eta(P_s||\mathbf{h}_r||^2 + N_r\sigma_{r,1}^2)$ and $\pi_3 = \eta(P_s||\mathbf{h}_r||^2 + N_r\sigma_{r,2}^2)$ are as defined before. $\tilde{\pi}_1 = P_s||\mathbf{h}_r||^2 + \sigma_{r,1}^2$. In (5.49a), we take the multiplicative inverse of the objective function in (5.47a) for simplification. Note that it is difficult to obtain a closed-form solution due to the term on the left side of (5.49b), $\frac{\sigma_b^2}{1-\rho}$. Since $\sigma_b^2 \ll \tilde{\pi}_1$, it is a safe assumption to ignore this term for a simpler problem. In this case, the problem in (5.49) can be rewritten after some arrangements as follows,

$$\min_{\widetilde{\beta}_1, \widetilde{\beta}_2, \rho} \quad \frac{\widetilde{\delta}_1}{1-\rho} + \frac{\widetilde{\delta}_2}{\widetilde{\beta}_1^2} \tag{5.50a}$$

$$s.t. \quad \left(\sqrt{\tilde{\pi}_1}\widetilde{\beta}_1 - \frac{\tilde{a}_1}{2\sqrt{\tilde{\pi}_1}}\right)^2 + \left(\sqrt{\tilde{\pi}_1}\widetilde{\beta}_2 - \frac{\tilde{a}_2}{2\sqrt{\tilde{\pi}_1}}\right)^2 \leq \pi_2\rho + \pi_3 + \frac{\tilde{a}_1^2 + \tilde{a}_2^2}{4\tilde{\pi}_1} \tag{5.50b}$$

$$0 \leq \rho < 1. \tag{5.50c}$$

It can be easily verified that the optimum solution of (5.50) should satisfy the inequality in (5.50b) with equality. If we assume that it is not the case, then, we can increase the value of $\widetilde{\beta}_1$ until (5.50b) becomes an equality with an improved objective function. Hence, (5.50b) is an equality for the optimum solution. Furthermore, optimum $\widetilde{\beta}_2$ should be $\widetilde{\beta}_2^\star = \frac{\tilde{a}_2}{2\tilde{\pi}_1}$. This value minimizes the second term on the left side of (5.50b) and makes it zero. Note that $\widetilde{\beta}_2$ only appears in this term and the optimum $\widetilde{\beta}_2$ should minimize this term. Otherwise, we can decrease this term and increase $\widetilde{\beta}_1$ without violating the constraint in (5.50b) with a decreased objective function which

88

is a contradiction. After inserting optimum $\widetilde{\beta}_2^\star$ into (5.50b), we obtain the following equality by (5.50b), i.e.,

$$\rho = \left(\sqrt{\frac{\tilde{\pi}_1}{\pi_2}} \widetilde{\beta}_1 - \frac{\tilde{a}_1}{2\sqrt{\tilde{\pi}_1\pi_2}} \right)^2 - \frac{4\tilde{\pi}_1\pi_3 + \tilde{a}_1^2 + \tilde{a}_2^2}{4\tilde{\pi}_1\pi_2} \tag{5.51}$$

If we insert ρ in (5.51) into the objective function in (5.50a) we obtain the following optimization problem in terms of $\widetilde{\beta}_1$ only, i.e.,

$$\min_{\widetilde{\beta}_1} \quad \frac{\widetilde{\delta}_1}{-\left(\sqrt{\frac{\tilde{\pi}_1}{\pi_2}} \widetilde{\beta}_1 - \frac{\tilde{a}_1}{2\sqrt{\tilde{\pi}_1\pi_2}} \right)^2 + \frac{4\tilde{\pi}_1(\pi_2+\pi_3)+\tilde{a}_1^2+\tilde{a}_2^2}{4\tilde{\pi}_1\pi_2}} + \frac{\widetilde{\delta}_2}{\widetilde{\beta}_1^2} \tag{5.52a}$$

$$s.t. \quad 0 \le \left(\sqrt{\frac{\tilde{\pi}_1}{\pi_2}} \widetilde{\beta}_1 - \frac{\tilde{a}_1}{2\sqrt{\tilde{\pi}_1\pi_2}} \right)^2 - \frac{4\tilde{\pi}_1\pi_3 + \tilde{a}_1^2 + \tilde{a}_2^2}{4\tilde{\pi}_1\pi_2} < 1. \tag{5.52b}$$

One of the critical points corresponds to $\rho = 0$ in (5.51). For this case, let us note the objective value and the solution as a candidate. This solution will be used later on for determining the final best solution. For other critical points, $\rho \ne 0$ and (5.52b) becomes a strict inequality. Hence, Lagrange multiplier corresponding to (5.52b) becomes 0 for the other critical points. In this case, we can simply take the derivative of (5.52a) and equate it to zero. Firstly, define the following parameters for the ease of notation, i.e.,

$$D_1 \triangleq \sqrt{\frac{\tilde{\pi}_1}{\pi_2}}, \quad D_2 \triangleq \frac{\tilde{a}_1}{2\sqrt{\tilde{\pi}_1\pi_2}}, \quad D_3 \triangleq \frac{4\tilde{\pi}_1(\pi_2 + \pi_3) + \tilde{a}_1^2 + \tilde{a}_2^2}{4\tilde{\pi}_1\pi_2} \tag{5.53}$$

Now, if we take the derivative of (5.52a) and equate it to zero, we obtain

$$\frac{2\widetilde{\delta}_1 D_1(D_1\widetilde{\beta}_1 - D_2)}{\left((D_1\widetilde{\beta}_1 - D_2)^2 - D_3 \right)^2} = \frac{2\widetilde{\delta}_2}{\widetilde{\beta}_1^3} \tag{5.54}$$

If we rearrange (5.54), we can write (5.54) as quartic equation, i.e.,

$$E_4\widetilde{\beta}_1^4 + E_3\widetilde{\beta}_1^3 + E_2\widetilde{\beta}_1^2 + E_1\widetilde{\beta}_1 + E_0 = 0 \tag{5.55}$$

where E_4, E_3, E_2, E_1 and E_0 are given as follows,

$$E_4 = \widetilde{\delta}_1 D_1^2 - \widetilde{\delta}_2 D_1^4, \quad E_3 = -\widetilde{\delta}_1 D_1 D_2 + 4\widetilde{\delta}_2 D_1^3 D_2, \quad E_2 = 2\widetilde{\delta}_2 D_1^2(D_3 - 3D_2^2) \tag{5.56a}$$

$$E_1 = 4\widetilde{\delta}_2 D_1 D_2(D_2^2 - D_3), \quad E_0 = -\widetilde{\delta}_2(D_2^2 - D_3)^2 \tag{5.56b}$$

Now, we will show that we need only one zero of the quartic equation given in (5.55).

89

Lemma 5.4: The quartic function in (5.55) is monotonically increasing in the region where $0 \leq \rho < 1$.

Proof: Please see Appendix B.3 for the proof. ∎

By Lemma 5.4, there is only one zero if it exists inside the feasible region of the problem. Hence, there is no need to find the other roots of the polynomial in (5.55). A simple bisection search is presented to find this root in Algorithm 5.1 given below. In Algorithm 5.1, $\widetilde{\beta}_1^{(r)}$ shows the value of $\widetilde{\beta}_1$ at the rth iteration and $f(\widetilde{\beta}_1) \triangleq E_4\widetilde{\beta}_1^4 + E_3\widetilde{\beta}_1^3 + E_2\widetilde{\beta}_1^2 + E_1\widetilde{\beta}_1 + E_0$. Note that initial lower and upper bounds are selected such that ρ in (5.51) is 0 and 1, respectively. If $f(L^{(0)}) > 0$ or $f(U^{(0)}) < 0$, the Algorithm 5.1 is not implemented since there is no zero of (5.55) inside the feasible region. In this case, the only critical point is $\rho = 0$ as mentioned before and it is the optimum solution. We will give the solution for $\rho = 0$ case later in this section.

Algorithm 5.1: Bisection Search for Finding the Root of (5.55)

Initialization: Set initial lower and upper bounds as $L^{(0)} = (\sqrt{D_3 - 1} + D_2)/D_1$ and $U^{(0)} = (\sqrt{D_3} + D_2)/D_1$, respectively. If $f(L^{(0)}) > 0$ or $f(U^{(0)}) < 0$, terminate. Otherwise take the initial $\widetilde{\beta}_1$ as $\widetilde{\beta}_1^{(0)} = (L^{(0)} + U^{(0)})/2$. Set the iteration number $r \leftarrow 0$.
Repeat

    If $f(\widetilde{\beta}_1^{(r)}) < 0$, set $L^{(r+1)} = \widetilde{\beta}_1^{(r)}$.

    ElseIf $f(\widetilde{\beta}_1^{(r)}) > 0$, set $U^{(r+1)} = \widetilde{\beta}_1^{(r)}$.

    Else Terminate.

$\widetilde{\beta}_1^{(r+1)} = (L^{(r+1)} + U^{(r+1)})/2$

Set $r \leftarrow r + 1$.
Until convergence criterion is met.

Let $\widetilde{\beta}_1^{\dagger}$ denote the root of (5.55) inside the region $0 \leq \rho < 1$. In this case, we obtain

$\rho^\dagger$ by inserting $\widetilde{\beta}_1^\dagger$ into (5.51). At this point, we have obtained the candidate optimum solution of the approximate problem given in (5.50) using $\{\rho^\dagger, \widetilde{\beta}_1^\dagger\}$. In order to obtain a solution to the original problem in (5.47), we can keep $\rho^\dagger$ constant and update β_1 and β_2, respectively. For a given $\rho^\dagger$, the problem in (5.47) can be reformulated in terms of β_1 and β_2 as follows,

$$\max_{\beta_1, \beta_2} \quad \beta_1^2 \tag{5.57a}$$

$$s.t. \quad f_1(\rho^\dagger)(\beta_1^2 + \beta_2^2) - f_2(\rho^\dagger)\beta_1 - f_3(\rho^\dagger)\beta_2 \leq f_4(\rho^\dagger) \tag{5.57b}$$

where $f_1(\rho)$, $f_2(\rho)$, $f_3(\rho)$, and $f_4(\rho)$ are the functions defined as follows,

$$f_1(\rho) \triangleq (P_s\|\mathbf{h}_r\|^2 + \sigma_{r,1}^2)(1 - \rho) + \sigma_b^2 \tag{5.58a}$$

$$f_2(\rho) \triangleq \tilde{a}_1\sqrt{1 - \rho}, \quad f_3(\rho) \triangleq \tilde{a}_2\sqrt{1 - \rho} \tag{5.58b}$$

$$f_4(\rho) \triangleq \eta\left(P_s\|\mathbf{h}_r\|^2 + N_r\sigma_{r,1}^2\right)\rho + \eta\left(P_s\|\mathbf{h}_r\|^2 + N_r\sigma_{r,2}^2\right) \tag{5.58c}$$

Similar to the problem in (5.50), optimum β_2 minimizes the left side of (5.57b) and (5.57b) is satisfied with equality. Hence, the optimum β_1 and β_2 are given by

$$\beta_1^\dagger = \frac{\sqrt{4f_1(\rho^\dagger)f_4(\rho^\dagger) + f_2^2(\rho^\dagger) + f_3^2(\rho^\dagger)} + f_2(\rho^\dagger)}{2f_1(\rho^\dagger)} \tag{5.59a}$$

$$\beta_2^\dagger = \frac{f_3(\rho^\dagger)}{2f_1(\rho^\dagger)} \tag{5.59b}$$

$\{\widetilde{\beta}_1^\dagger, \widetilde{\beta}_2^\dagger, \rho^\dagger \neq 0\}$ is the one candidate solution. The other possible solution corresponds to the other critical point $\rho = 0$. Overall, near-optimum solution of (5.47) is given by

$$\rho^\star = \arg\min_{\rho \in \{0, \rho^\dagger\}} \frac{\widetilde{\delta}_1}{1 - \rho} + \frac{\widetilde{\delta}_2}{(1 - \rho)\left(\frac{\sqrt{4f_1(\rho)f_4(\rho) + f_2^2(\rho) + f_3^2(\rho)} + f_2(\rho)}{2f_1(\rho)}\right)^2} \tag{5.60a}$$

$$\beta_1^\star = \frac{\sqrt{4f_1(\rho^\star)f_4(\rho^\star) + f_2^2(\rho^\star) + f_3^2(\rho^\star)} + f_2(\rho^\star)}{2f_1(\rho^\star)}, \quad \beta_2^\star = \frac{f_3(\rho^\star)}{2f_1(\rho^\star)} \tag{5.60b}$$

Using (5.60b), near-optimum relay transmit beamformer vector is given by

$$\mathbf{w}_t^\star = (\mathbf{I}_{N_t} - \eta\mathbf{H}_{rr}^H\mathbf{H}_{rr})^{-1/2}(\beta_1^\star\boldsymbol{\Psi}_1 + \beta_2^\star e^{j\angle\widetilde{\mathbf{h}}_r^H\widetilde{\mathbf{h}}_d}\boldsymbol{\Psi}_2). \tag{5.61}$$

The performance of this near-optimum solution for optimized energy-bearing signal is compared with the non-optimized case in the simulations in section 5.8. In the following part, we will investigate the discrete PS ratio.

5.7 Beamforming Optimization over Discrete Power Splitting Ratio Set

In the previous sections, power splitting ratio, ρ is assumed to be a continuous variable. In practice, ρ can be chosen from a discrete set in order to simplify the system hardware design. In this part, we consider conventional (Fig. 5.3) and the proposed self-energy recycling assisted power splitting protocol (Fig. 5.4) for the discrete set of power splitting ratios. We will consider both of the protocols in sequence. Note that optimum solution is found for all the optimization problems in this section thanks to the closed-form solutions derived in the previous sections.

5.7.1 Conventional Power Splitting Protocol

Consider the simplified unconstrained optimization problem in (5.31) in terms of $x = \sqrt{\frac{\rho}{1-\rho}}$. In this case, optimum discrete PS ratio can be simply found as follows,

$$x^\star = \arg\max_{x \in \mathcal{P}_x} \frac{x^2}{A_4 x^4 + A_2 x^2 + A_0} \tag{5.62a}$$

$$\rho^\star = \frac{(x^\star)^2}{(x^\star)^2 + 1} \tag{5.62b}$$

where $\mathcal{P}_x$ is the discrete set whose elements are the corresponding $x = \sqrt{\frac{\rho}{1-\rho}}$ for the discrete PS ratios, ρ. The optimum beamformer weight vector is obtained by (5.32) and (5.35) using the optimum discrete x.

5.7.2 Self-Energy Recycling Assisted Power Splitting Protocol for the Non-Optimized Energy-Bearing Signal

Consider the unconstrained optimization problem given in (5.40) in terms of x only. Similar to the previous section, optimum discrete PS ratio can be simply found as follows,

$$x^\star = \arg\max_{x \in \mathcal{P}_x} \frac{B_2 x^2 + B_0}{C_4 x^4 + C_2 x^2 + C_0} \tag{5.63a}$$

$$\rho^\star = \frac{(x^\star)^2}{(x^\star)^2 + 1} \tag{5.63b}$$

The optimum beamformer weight vector is obtained by (5.41) and (5.44) using the optimum discrete x.

5.7.3 Self-Energy Recycling Assisted Power Splitting Protocol for the Optimum Energy-Bearing Signal

Given the discrete PS ratio, we can solve (5.57a-b) and choose the best discrete ρ which results the best objective function given in (5.60a). Hence, optimum discrete PS ratio can be found as

$$\rho^\star = \arg \min_{\rho \in \mathcal{P}_\rho} \frac{\widetilde{\delta}_1}{1 - \rho} + \frac{\widetilde{\delta}_2}{(1 - \rho)\left(\frac{\sqrt{4f_1(\rho)f_4(\rho)+f_2^2(\rho)+f_3^2(\rho)}+f_2(\rho)}{2f_1(\rho)}\right)^2} \tag{5.64}$$

where $\mathcal{P}_\rho$ is the set of discrete PS ratios. The optimum beamformer weight vector is obtained by (5.60b) and (5.61) using the optimum discrete ρ. Note that the optimum discrete PS ratios in (5.62), (5.63), and (5.64) can be found by only evaluating the corresponding equations for a finite set of $\rho \in \mathcal{P}_\rho$ values.

5.8 Simulation Results

In this section, the SNR performance of the proposed beamformers is evaluated for the considered protocols. In the simulations, the parameters are selected as follows. We set all the noise powers as $\sigma_{r,1}^2 = \sigma_{r,2}^2 = \sigma_b^2 = \sigma_d^2 = -110$ dBW. The energy harvesting efficiency is $\eta = 0.7$. Rayleigh fading is assumed for all the channels, i.e., $\mathbf{h}_r$, $\mathbf{H}_{rr}$, and $\mathbf{h}_d$. Unless otherwise stated, the number of transmitting and receiving antennas of $\mathbf{R}$ are $N_t = 4$ and $N_r = 4$, respectively. Source power is $P_s = 0$ dBW. In addition, the path loss, PL, for the channels $\mathbf{h}_r$ (S-R), $\mathbf{h}_d$ (R-D), and the loop channel $\mathbf{H}_{rr}$ are $\text{PL}_{\mathbf{h}_r} = 60$ dB, $\text{PL}_{\mathbf{h}_d} = 60$ dB, and $\text{PL}_{\mathbf{H}_{rr}} = 15$ dB, respectively. In the figures, each point represents the average of randomly generated 1000 channel realizations. In order to obtain bounded solution, 1000 channels for which $\mathbf{Q} = \mathbf{I}_{N_t} - \eta \mathbf{H}_{rr}^H \mathbf{H}_{rr}$ is positive definite are considered. Note that if $\mathbf{Q}$ is not positive definite, unbounded solution is also obtained for the SDP problem proposed in [4].

In the following figures, destination SNR, SNR_d is presented for different system

parameters. In the labels, SE-N stands for the optimum closed-form solution given in (5.11) for the self-energy recycling problem in [4] and (5.8). Note that this protocol is based on non-optimized energy-bearing signal. SE-N (SDP) is the solution obtained by the numerical SDP solver as proposed in [4]. The performances of these two methods are exactly the same in all the scenarios verifying that the relay beamformer in (5.11) is the optimum solution of the problem in (5.8). The main advantage of the proposed closed-form beamformer, SE-N, is that it does not require a numerical solver to give the optimum result. SE-O corresponds to the closed-form solution in (5.18) derived for the optimized energy-bearing signal. PS-CON is the optimum solution for conventional power splitting protocol which is given in (5.35). PS-SE-N and PS-SE-O are the solutions in (5.44) and (5.61), respectively corresponding to the self-energy recycling assisted power splitting protocols with non-optimized and optimized energy signals. The PS ratio sets for the discrete optimization problems in Section 5.7 are taken as $\mathcal{P}_\rho = \{0, 1/R, 2/R, ..., 1 - 1/R\}$ where R is the cardinality of the set $\mathcal{P}_\rho$ and the PS ratios are the endpoints of R uniform intervals of 0-1. In the figures, R is given as the level number inside the parentheses.

In Fig. 5.5, SNR_d is plotted in terms of the source power, P_s. As expected, SNR increases with P_s for all the methods and SE-N and SE-N (SDP) give the same result. In accordance with [4], PS-CON performs slightly worse, i.e, there is an approximately 0.5 dB gap between SE-N and PS-CON. When phase alignment is used to obtain optimum energy signal, harvested power is maximized and 1.6 dB SNR improvement is obtained for SE-O in comparison to SE-N. When we look at the performance of the newly proposed self-energy recycling assisted power splitting protocol, it is observed that up to 3 dB and 2.4 dB SNR gain is possible for PS-SE-N and PS-SE-O compared to SE-N and SE-O, respectively showing the effectiveness of this unified framework. The reason for this can be easily explained as follows. Power splitting option in the first phase allows for more energy harvesting compared to the conventional self-energy recycling protocol. The special case $\rho = 0$ for PS-SE corresponds to SE. This shows that the feasible region is enlarged by the new protocol.

In Fig. 5.6, the same results for PS-CON, PS-SE-N, and PS-SE-O are repeated with their discrete counterparts. We use $R = 4$ and $R = 8$ levels for the discrete PS ratio set. The difference between continuous and 4 level discrete case is 1.2 dB for PS-

CON, and it is only about 0.5 dB for the PS-SE. When we increase R to 8, the gap becomes smaller and this shows that choosing PS ratio from a finite set is a quite effective approach.
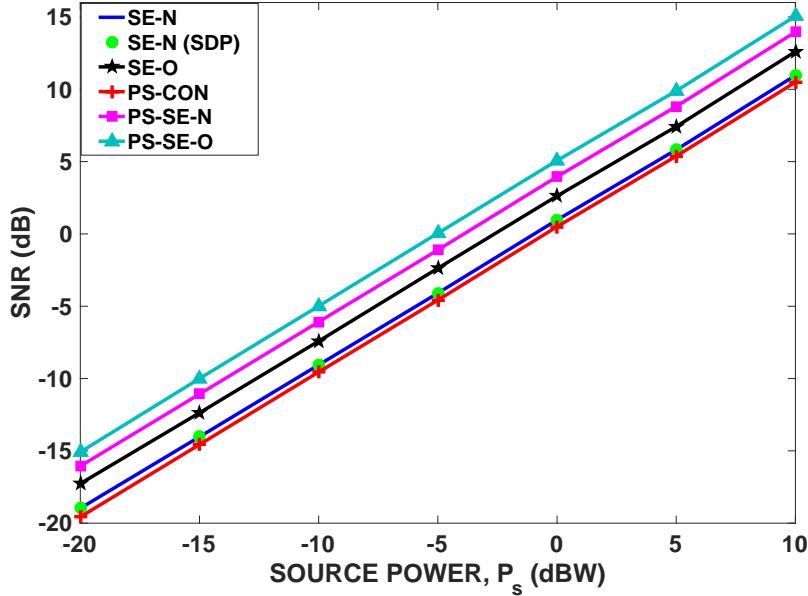
Figure 5.5: Destination SNR versus source power, P_s.

In Fig. 5.7, path loss for the self-energy recycling loop channel $\mathbf{H}_{rr}$ is changed from 10 dB to 20 dB in 2 dB steps. As expected, PS-CON is not affected by this change since it does not consider loop channel in designing beamformer. As an important observation, when path loss is 10 dB, both SE-O and PS-SE-O drastically outperform the other methods. This is due to the fact that increase in the norm of $\mathbf{H}_{rr}$ boosts the effect of phase-adjusted optimized energy-bearing signal. Since, loop channel is very strong, energy need is met from self-energy recycling in PS-SE-O protocol and PS coefficient ρ can be selected near 0 in order to amplify the information signal. In this case, we expect PS-SE-O and SE-O perform nearly the same since the case $\rho = 0$ in PS-SE-O corresponds to SE-O. As path loss increases, this effect decreases and the gap between the protocols with non-optimized and optimized energy signal also decreases.

In Fig. 5.8, the same results for PS-CON and PS-SE-N and PS-SE-O are repeated with their discrete counterparts. The results are similar to Fig. 5.6. The SNR gap between continuous and discrete designs is higher for PS-CON in comparison to the
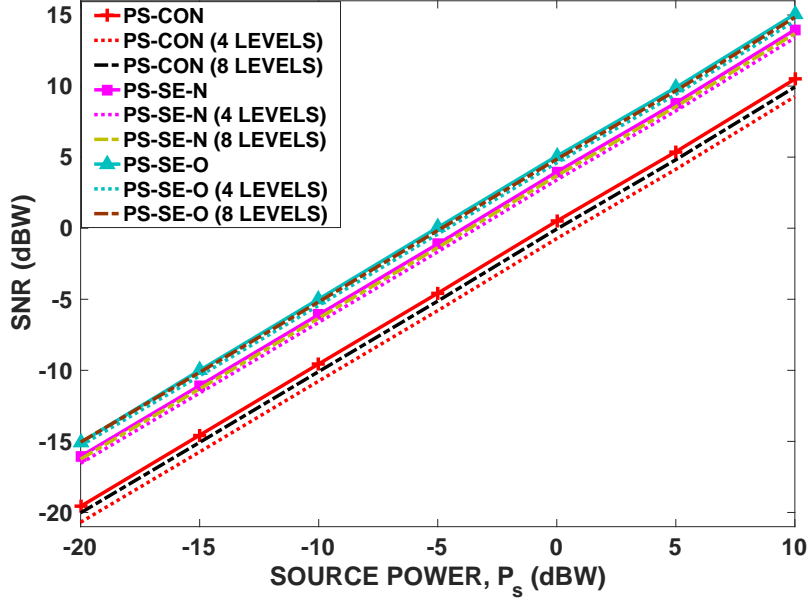
Figure 5.6: Destination SNR versus source power, P_s for discrete PS ratio design.

others. When we increase R from 4 to 8, the performance of the discrete design approaches to its continuous counterpart.

In Fig. 5.9, we vary the path loss for $\mathbf{h}_r$. As the path loss increases, SNR for all the methods decreases accordingly. Similar to the previous scenarios, the proposed PS-SE protocol outperforms the existing protocols.

In Fig. 5.10, we repeat the previous experiment by changing the path loss for $\mathbf{h}_d$. As it can be seen from Fig. 5.10, we obtain a similar SNR characteristics with the Fig. 5.9. SNR degrades nearly at the same proportion as the path loss increases. Hence, we conclude that the channel between the source-relay and relay-destination have similar effect on the performance.

In Fig. 5.11, the number of transmitting antennas at $\mathbf{R}$, N_t, is varied while the other parameters are kept constant. Increasing N_t enhances spatial diversity and as a result, the performance of relay transmit beamformer improves yielding greater SNR. The main difference in Fig. 5.11 in comparison to Fig. 5.5 is that SE-O outperforms PS-SE-N for high values of N_t. This result is due to the fact that increasing the number of transmitting antennas strengthens the loop channel $\mathbf{H}_{rr}$ and this leads to an increase in energy harvesting as well as relay transmitted power. Note that the effect of optimized
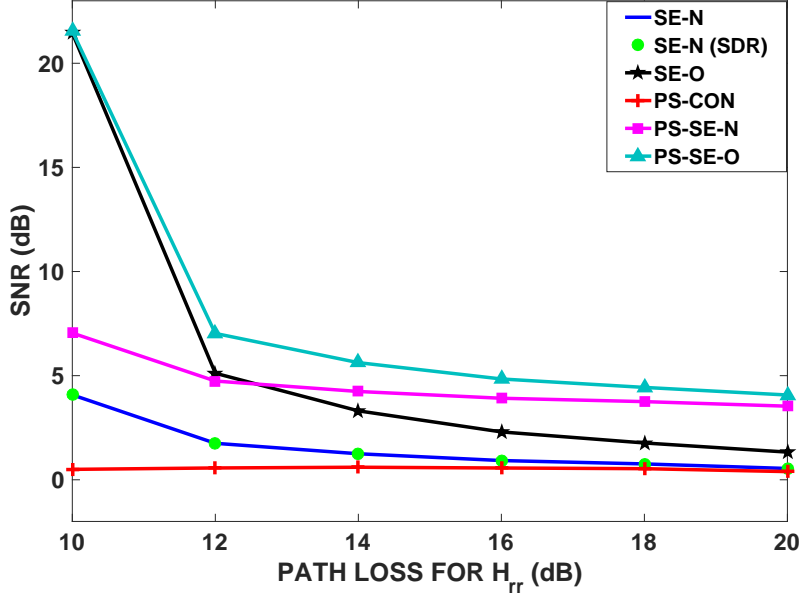
Figure 5.7: Destination SNR versus path loss for $\mathbf{H}_{rr}$.

energy signal becomes more dominant. An important observation in Fig. 5.10 is the SNR gain obtained by the PS-SE which reaches up to 3 dB in comparison to the other protocols.

In Fig. 5.12, we vary the number of receiving antennas, N_r and obtain a slightly different characteristics from Fig. 5.11. Now, SE-O always results less SNR compared to PS-SE-N similar to Fig. 5.5 and different from Fig. 5.11. However, the gap between them decreases as N_r increases verifying the boosting effect of the optimized energy signal. Different from Fig. 5.11, the performance gap between SE-N and PS-CON increases significantly with increase in N_r, reaching 2.4 dB difference at $N_r = 16$. This results from the fact that in PS-CON, only a portion of the source signal received at the N_r antennas of $\mathbf{R}$ can be used whereas all the source energy signal is harvested in SE. The gap between these two protocols become visible as the number of energy harvesting units, i.e N_r, increases.

5.9 Conclusion

In this chapter, relay transmit beamformer design is considered in order to maximize SNR at the destination node under the transmission power constraint for wireless-

97
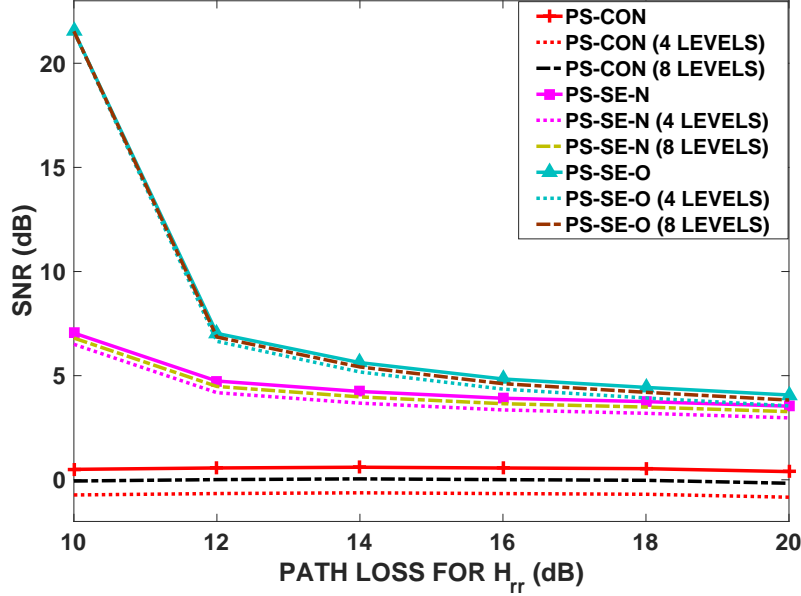
Figure 5.8: Destination SNR versus path loss for $\mathbf{H}_{rr}$ for discrete PS ratio design.

powered full-duplex relaying. The relay has multiple transmit and receive antennas. Two conventional amplify-and-forward based WPR protocols are investigated and optimum closed-form solutions for the relay transmit beamformers as well as the power splitting ratios are presented. Furthermore, a new protocol is proposed to improve the efficiency and SNR performance. The first protocol is a self-energy recycling protocol while the second one is a PS based protocol. The third protocol is both a self-energy recycling and PS one which allows energy harvesting in two phases. For the first protocol, the optimum closed-form solutions are derived for two beamformer design problems. These two problems correspond to the non-optimized and optimized energy-bearing signals from the source. It is shown that significant SNR improvement can be achieved in case of optimized energy-bearing signal. Conventional PS protocol is considered as a second protocol and the joint optimization of the relay transmit beamformer and PS ratio is considered. The optimum closed-form solution is derived. It is shown that self-energy recycling protocol performs better than conventional PS protocol for the destination SNR. The third protocol considered in this chapter unifies the self-energy recycling and PS protocols in order to improve efficiency and destination SNR. This self-energy recycling assisted PS protocol achieves significantly higher SNR reaching up to 3 dB in comparison to the previous two protocols. For the power splitting based protocols, the optimum solution is presented and
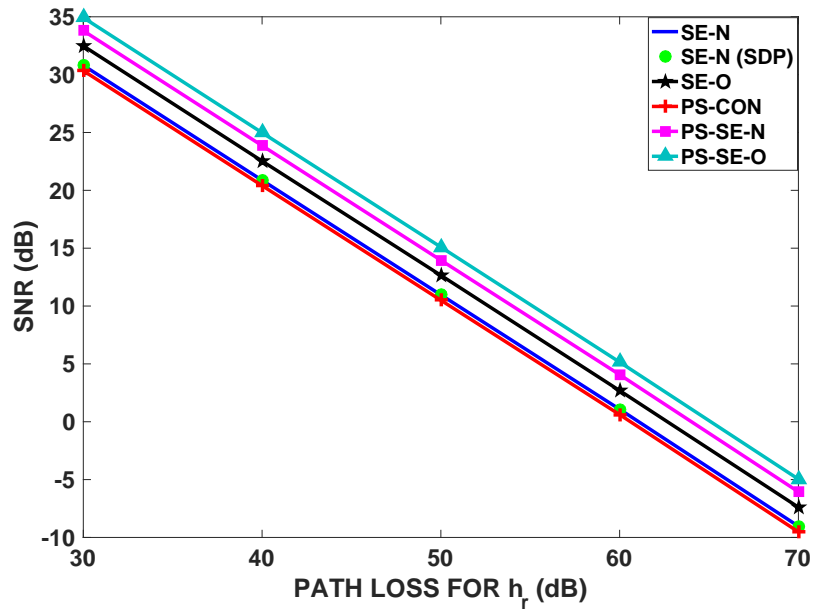
Figure 5.9: Destination SNR versus path loss for $\mathbf{h}_r$.

the simulation results indicate that the performance of the discrete design is close to the continuous one for most of the scenarios.
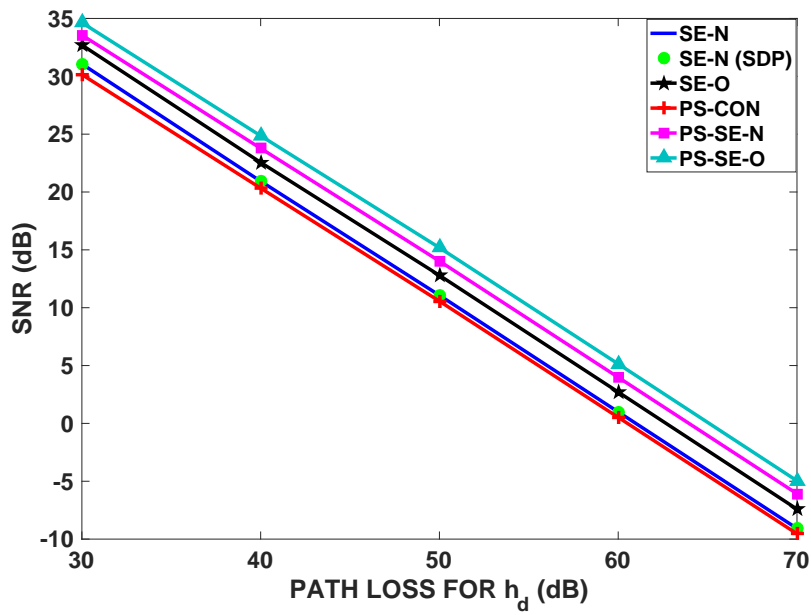
Figure 5.10: Destination SNR versus path loss for $\mathbf{h}_d$.
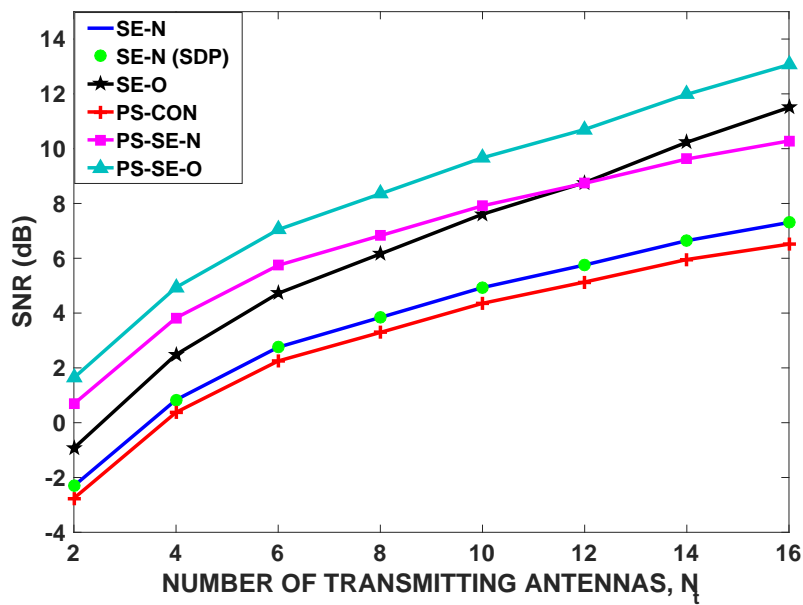
Figure 5.11: Destination SNR versus the number of transmitting antennas, N_t.
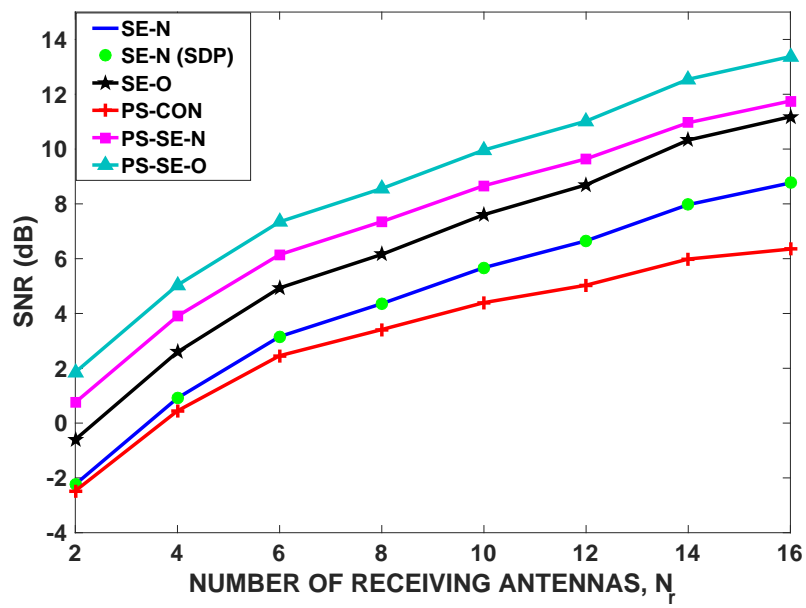
Figure 5.12: Destination SNR versus the number of receiving antennas, N_r.

CHAPTER 6

JOINT SOURCE POWER ALLOCATION AND RELAY BEAMFORMER DESIGN FOR WIRELESS-POWERED RELAYING WITH SELF-ENERGY RECYCLING

This chapter considers a wireless-powered relaying system where the multiple-antenna relay amplifies and forwards the information signal of the source node to the destination. Relay uses both the dedicated energy signal sent from the source and its own transmitted signal as an energy source. This self-energy recycling protocol is investigated using equal power allocation between the information and energy transmission phases of the source in the literature. In this chapter, we propose the joint power allocation optimization with relay transmit beamformer in order to improve the performance. Two optimization problems, namely signal-to-noise ratio (SNR) maximization and quality-of-service (QoS)-aware design are considered. The joint optimum solution for the former problem is presented while using an approximation, a near-optimum joint solution is obtained for the latter problem. Simulation results show that the proposed method achieves 3 dB higher SNR at the destination compared to equal power allocation. For QoS-aware problem, the required power by the relay's own battery is decreased by 2 for the proposed method. An improvement by 2 is obtained for power saving in comparison to the equal power allocation strategy.

6.1   Related Works and Contributions

In [19], a new wireless powered relaying (WPR) protocol based on self-energy recycling is proposed in order to take advantage of self-interference different from power splitting (PS) and time swithcing (TS) protocols. In the first phase of this protocol,

source node transmits the information symbol to the relay and relay amplifies and forwards this signal to the destination in the second phase. For this purpose, it uses beamforming with the help of multiple transmit antennas. In the second phase, source sends an energy signal to assist the relay and relay also uses a part of its transmitted signal as an energy source with its receiving antenna. Since information transfer and energy reception occur in the same phase, this protocol belongs to full-duplex WPR.

In [19], the optimization problem in terms of relay transmit beamformer is formulated to maximize destination signal-to-noise ratio (SNR) subject to the constraint that transmission power of the relay cannot exceed its harvested power. In the first phase, only the single receiving antenna is used for information reception while the remaining antennas of the relay are idle. In [21] and [62], this system is modified such that all antennas are used in the first phase for a more efficient system. Furthermore, transmission power limit is not considered in [19]. [21] included this constraint for the quality-of-service (QoS)-aware problem to be more practical. In SNR maximization, the transmission power of the relay is constrained to be less than the harvested power. However, this is a strict condition when the desired SNR of the destination is greater than the one that can be supplied by the harvested power. In QoS-aware design, the objective that is minimized is the difference between the transmitted and the harvested power. Hence, the amount of the required power by the relay's own battery is minimized. This allows one to find solutions for cases which require more power than the harvested and this becomes an important difference between the SNR maximization and QoS-aware design problems.

In all the above works and similar ones in [4], [22], [59], [62], it is assumed that equal power is used for information and energy transfer at the source side. As a more power efficient approach, power allocation optimization can be realized [55], [63], [64] in addition to relay transmit beamformer. In [63], power allocation between information and energy transfer phases is considered for self-energy recycling assisted full-duplex relaying. In this work, beamforming optimization is not taken into account since there is only one transmitting antenna at the relay. Furthermore, only SNR maximization is considered. In this chapter, we jointly optimize the relay transmit beamformer and power division parameter for both SNR maximization and QoS-aware design problem. The problem formulations for both of the problems are simplified in an

equivalent manner in order to obtain the optimum solution. Karush Kuhn Tucker (KKT) conditions are obtained to better analyze the problems via several lemmas. For the SNR maximization problem, the joint optimum solution is derived. For the QoS-aware problem, an approximation is needed for some of the KKT conditions and a near-optimum joint solution is found. Simulation results verify the effectiveness of the proposed methods compared to equal power allocation scheme. The proposed method achieves 3 dB SNR improvement for the SNR maximization problem. For the QoS-aware problem, the required power of the relay's own battery is decreased by 2. Furthermore, additional power savings are achieved.

6.2 System Model

Fig. 6.1 shows a wireless-powered relaying system where source node $\mathbf{S}$ transmits information to the destination node $\mathbf{D}$ through the relay node $\mathbf{R}$ [19]. $\mathbf{S}$ and $\mathbf{R}$ are equipped with M and $N+1$ antennas, respectively whereas $\mathbf{D}$ has a single antenna. In [19], a two-phase amplify-and-forward (AF) protocol is proposed for this wireless-powered relaying system. If T denotes the total transmission time, information signal is transmitted from $\mathbf{S}$ to $\mathbf{R}$ in the first $T/2$ sec. In this phase, single receiving antenna of $\mathbf{R}$ shown on the left side in Fig. 6.1 is used for information reception while all the antennas of $\mathbf{S}$ are used for transmission. In [21] and [62] this protocol is improved by employing all the antennas at $\mathbf{R}$ for information reception. In this chapter, we will adapt this modified protocol.

In the second phase with duration $T/2$ sec., N transmitting antennas of $\mathbf{R}$ are used for information forwarding to $\mathbf{D}$ while the remaining single antenna harvests energy from the dedicated energy signal sent from $\mathbf{S}$ and self-energy recycling via loop channel $\mathbf{f}$. In the proposed protocol [19], equal power is allocated at $\mathbf{S}$ for both information and power transfer. In this chapter, we generalize this protocol by introducing a power division parameter, $0 < \alpha \leq 1$, to be designed together with relay transmit beamformer vector to increase the performance of the system. In this chapter, the improved protocol and the joint design of power division parameter and the relay transmit beamformer will be considered in detail.
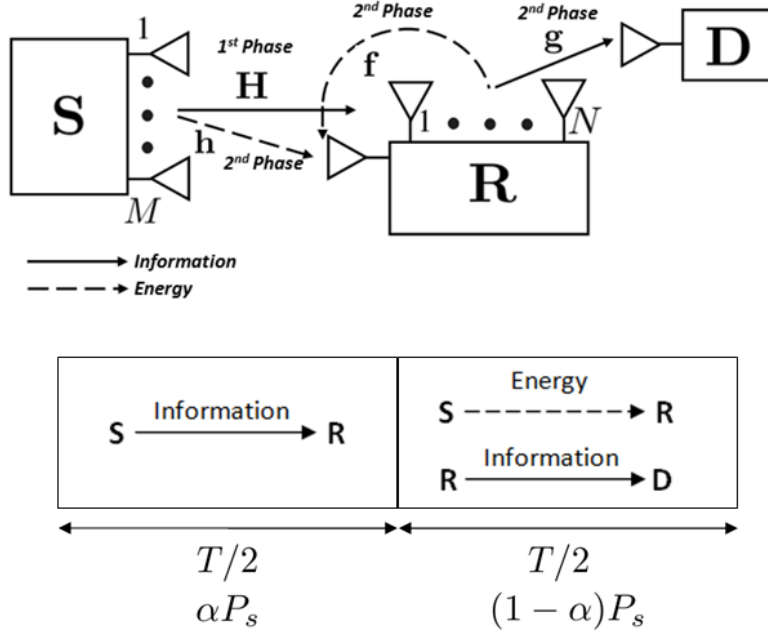
Figure 6.1: System model and self-energy recycling based wireless-powered relaying protocol with power allocation.

Let $\mathbf{H} \in \mathbb{C}^{M \times (N+1)}$ be the baseband equivalent channel from $\mathbf{S}$ to $\mathbf{R}$. Assuming that $\mathbf{H}$ is known at $\mathbf{S}$ and $\mathbf{R}$, the optimum transmit and receive beamformers are the left and right singular vectors corresponding to the largest singular value of $\mathbf{H}$, i.e., λ_H, respectively. After receive beamforming, the information symbol received at $\mathbf{R}$ in the first phase is given by

$$y_{r,1} = \sqrt{P_s \alpha} \lambda_H x_{s,1} + n_{r,1} \tag{6.1}$$

where P_s denotes the total transmission power of $\mathbf{S}$ during two phases. $0 < \alpha \leq 1$ is the portion of P_s for the first phase as shown in Fig. 6.1. $x_{s,1}$ is the information symbol sent by $\mathbf{S}$ and it is assumed to have unit average power without loss of generality. $n_{r,1}$ is circularly-symmetric complex Gaussian noise at the receiver of $\mathbf{R}$ in the first phase with zero mean and σ_r^2 variance, i.e., $n_{r,1} \sim \mathcal{CN}(0, \sigma_r^2)$.

In the second phase, the received signal in (6.1) is amplified and forwarded to $\mathbf{D}$ by N transmitting antennas of $\mathbf{R}$ with beamforming relay vector $\mathbf{v}_r \in \mathbb{C}^{N \times 1}$. The transmitted signal from $\mathbf{R}$ is given in vector form as follows,

$$\mathbf{y}_t = \mathbf{v}_r y_{r,1} = \mathbf{v}_r (\sqrt{P_s \alpha} \lambda_H x_{s,1} + n_{r,1}) \tag{6.2}$$

106

Assuming that $n_{r,1}$ is independent from the information symbol $x_{s,1}$, the transmission power of $\mathbf{R}$, i.e. P_r is given by,

$$P_r = ||\mathbf{v}_r||^2(P_s\alpha\lambda_H^2 + \sigma_r^2) \tag{6.3}$$

If $\mathbf{g} \in \mathbb{C}^{N \times 1}$ denotes the channel from the transmitting antennas of $\mathbf{R}$ to $\mathbf{D}$, the received signal at $\mathbf{D}$ in the second phase is given by,

$$y_d = \mathbf{g}^H\mathbf{y}_t + n_d = \mathbf{g}^H\mathbf{v}_r(\sqrt{P_s\alpha}\lambda_H x_{s,1} + n_{r,1}) + n_d \tag{6.4}$$

where $n_d \sim \mathcal{CN}(0, \sigma_d^2)$ is the circularly symmetric complex Gaussian noise at the receiver of $\mathbf{D}$. Assuming that n_d is independent from the information symbol and $n_{r,1}$, the received signal-to-noise ratio (SNR) is given by,

$$SNR_d = \frac{P_s\lambda_H^2\alpha|\mathbf{g}^H\mathbf{v}_r|^2}{\sigma_r^2|\mathbf{g}^H\mathbf{v}_r|^2 + \sigma_d^2} \tag{6.5}$$

While the information is being forwarded from the transmitting antennas of $\mathbf{R}$ to $\mathbf{D}$, energy harvesting is done at the single antenna of $\mathbf{R}$ in the second phase. For this purpose, an energy-bearing signal is sent from $\mathbf{S}$ to $\mathbf{R}$. In addition, a portion of $\mathbf{y}_t$ is used as an energy source due to self-energy recycling. Let $\mathbf{h} \in \mathbb{C}^{M \times 1}$ denote the channel from $\mathbf{S}$ to the energy harvesting antenna of $\mathbf{R}$. In this case, the optimum transmit beamformer vector is $\sqrt{P_s(1-\alpha)}\mathbf{h}/||\mathbf{h}||$ [19]. If the channel between N transmitting and energy harvesting antennas of $\mathbf{R}$ is denoted by $\mathbf{f} \in \mathbb{C}^{N \times 1}$, the received signal at $\mathbf{R}$ is expressed as,

$$
\begin{aligned}
y_{r,2} &= \sqrt{P_s(1-\alpha)}||\mathbf{h}||x_{s,2} + \mathbf{f}^H\mathbf{y}_t + n_{r,2} \\
&= \sqrt{P_s}\left(||\mathbf{h}||\sqrt{1-\alpha}x_{s,2} + \lambda_H\sqrt{\alpha}\mathbf{f}^H\mathbf{v}_r x_{s,1}\right) + \mathbf{f}^H\mathbf{v}_r n_{r,1} + n_{r,2}
\end{aligned} \tag{6.6}
$$

where $x_{s,2}$ denotes the unit power symbol sent from $\mathbf{S}$ for energy harvesting. Let us neglect the harvested energy from the noise terms $n_{r,1}$ and $n_{r,2}$ in accordance with [19]. As shown in [19], the harvested power is maximized when $x_{s,2} = x_{s,1}e^{j\angle\mathbf{f}^H\mathbf{v}_r}$. In this case, the harvested power at $\mathbf{R}$ can be given by,

$$P_h = \eta P_s\left(||\mathbf{h}||\sqrt{1-\alpha} + \lambda_H\sqrt{\alpha}|\mathbf{f}^H\mathbf{v}_r|\right)^2 \tag{6.7}$$

where $0 < \eta \leq 1$ denotes the energy harvesting efficiency at $\mathbf{R}$. In [19], SNR maximization problem is considered where the aim is to maximize the received SNR at $\mathbf{D}$

under the constraint that transmission power is below the harvested power. In [21], QoS-aware design problem is elaborated where the power used by the relay's own battery is minimized under SNR and transmission power limits constraints. In both works, equal power allocation between two phases at **S** is assumed. In this chapter, we will study both the SNR maximization and QoS-aware optimization problems with the transmission power limit constraint for the joint power allocation and beamformer design. Hence, in this chapter a more general outline is followed and solutions are presented for the aforementioned problems.

6.3 SNR Maximization

As in [19], our target is to maximize the received SNR of **D** such that P_r does not exceed the harvested power at **R** for a given P_s. Note that we also include the constraint for transmission power limit, P_{max} at **R** which is a practical consideration different from [19]. In addition to the design of relay beamformer, $\mathbf{v}_r$, in [19], we also consider the optimization of power allocation at **S** between the two transmission phases by keeping α as a variable. The optimization problem for this design objective can be written as follows,

$$\max_{\mathbf{v}_r, \alpha} \frac{\alpha |\mathbf{g}^H \mathbf{v}_r|^2}{\sigma_r^2 |\mathbf{g}^H \mathbf{v}_r|^2 + \sigma_d^2} \tag{6.8a}$$

$$s.t. \ ||\mathbf{v}_r||^2 (P_s \alpha \lambda_H^2 + \sigma_r^2) \leq \eta P_s \left(||\mathbf{h}|| \sqrt{1-\alpha} + \lambda_H \sqrt{\alpha} |\mathbf{f}^H \mathbf{v}_r| \right)^2 \tag{6.8b}$$

$$||\mathbf{v}_r||^2 (P_s \alpha \lambda_H^2 + \sigma_r^2) \leq P_{max} \tag{6.8c}$$

$$0 < \alpha \leq 1 \tag{6.8d}$$

where constant term $P_s \lambda_H^2$ is removed in the numerator of (6.8a) for simplicity. In the following, we propose certain lemmas and transformations to solve the problem in (6.8).

Let us express the relay beamformer vector as $\mathbf{v}_r = \sum_{n=1}^N \beta_n e^{j\theta_n} \boldsymbol{\Psi}_n$ where $\beta_n \geq 0$, $n = 1, ..., N$ and $\{\boldsymbol{\Psi}_n\}_{n=1}^N$ is an orthonormal basis for $\mathbb{C}^{N \times 1}$ such that $\boldsymbol{\Psi}_1 = \frac{\mathbf{g}}{||\mathbf{g}||}$ and $\boldsymbol{\Psi}_2 = \frac{\mathbf{f} - \boldsymbol{\Psi}_1 \boldsymbol{\Psi}_1^H \mathbf{f}}{||\mathbf{f} - \boldsymbol{\Psi}_1 \boldsymbol{\Psi}_1^H \mathbf{f}||}$. Then, the following Lemma presents the form of optimum relay beamformer.

Lemma 6.1: The optimum relay beamformer vector, $\mathbf{v}_r^\star$, for the problem (6.8) is given by the form $\mathbf{v}_r^\star = \beta_1 \boldsymbol{\Psi}_1 + \beta_2 e^{j \angle \mathbf{f}^H \mathbf{g}} \boldsymbol{\Psi}_2$, where $\beta_1 \geq 0$ and $\beta_2 \geq 0$.

Proof: The proof is similar to the one in [21]. ∎

Using Lemma 6.1, the problem in (6.8) can be expressed in an equivalent manner in terms of β_1, β_2 and α as follows,

$$\max_{\beta_1, \beta_2, \alpha} \frac{\alpha \|\mathbf{g}\|^2 \beta_1^2}{\sigma_r^2 \|\mathbf{g}\|^2 \beta_1^2 + \sigma_d^2} \tag{6.9a}$$

$$s.t. \ (\beta_1^2 + \beta_2^2)(P_s \alpha \lambda_H^2 + \sigma_r^2) \leq \eta P_s \left(\|\mathbf{h}\| \sqrt{1-\alpha} + \lambda_H \sqrt{\alpha}(c_1 \beta_1 + c_2 \beta_2) \right)^2 \tag{6.9b}$$

$$(\beta_1^2 + \beta_2^2)(P_s \alpha \lambda_H^2 + \sigma_r^2) \leq P_{max} \tag{6.9c}$$

$$0 < \alpha \leq 1 \tag{6.9d}$$

where $c_1 = |\mathbf{f}^H \boldsymbol{\Psi}_1| = |\mathbf{f}^H \mathbf{g}|/\|\mathbf{g}\|$ and $c_2 = \mathbf{f}^H \boldsymbol{\Psi}_2 = \frac{\mathbf{f}^H \mathbf{f} - \mathbf{f}^H \boldsymbol{\Psi}_1 \boldsymbol{\Psi}_1^H \mathbf{f}}{\|\mathbf{f} - \boldsymbol{\Psi}_1 \boldsymbol{\Psi}_1^H \mathbf{f}\|}$. Note that c_1 and c_2 are real and nonnegative. Hence, optimum β_1 and β_2 for (6.9) should be nonnegative in order to maximize SNR in (6.9a). This result can be easily obtained by contradiction. Assume that this case is not valid, i.e., at least one of β_1 and β_2 is negative. In this case, the right side of (6.9b) can be increased by changing the sign of β_1 and β_2 to positive. In this way, we enlarge the feasible region of the problem and (6.9a) can possibly be increased. Hence, the optimum solution should satisfy $\beta_1 \geq 0$ and $\beta_2 \geq 0$ for (6.9). This is the reason why we do not include nonnegativity as separate constraints in (6.9) for simplicity.

For α, there are two main cases to be evaluated.

Case 1: Assume that the inequality in (6.9d) is satisfied with an equality, i.e., $\alpha = 1$. In this case, the problem in (6.9) can be reformulated as follows,

$$\max_{\beta_1, \beta_2} \beta_1 \tag{6.10a}$$

$$s.t. \ (P_s \lambda_H^2 + \sigma_r^2)(\beta_1^2 + \beta_2^2) \leq \eta P_s \lambda_H^2 (c_1 \beta_1 + c_2 \beta_2)^2 \tag{6.10b}$$

$$(P_s \lambda_H^2 + \sigma_r^2)(\beta_1^2 + \beta_2^2) \leq P_{max} \tag{6.10c}$$

The solution of this problem constitutes a candidate optimum solution for the problem (6.9a-d). KKT necessary optimality conditions for the problem in (6.10a-c) are given

by

$$1 = 2\mu_1\left((P_s\lambda_H^2 + \sigma_r^2 - P_s\lambda_H^2\eta c_1^2)\beta_1 - P_s\lambda_H^2\eta c_1 c_2\beta_2\right) + 2\mu_2(P_s\lambda_H^2 + \sigma_r^2)\beta_1 \quad (6.11\text{a})$$

$$0 = 2\mu_1\left((P_s\lambda_H^2 + \sigma_r^2 - P_s\lambda_H^2\eta c_2^2)\beta_2 - P_s\lambda_H^2\eta c_1 c_2\beta_1\right) + 2\mu_2(P_s\lambda_H^2 + \sigma_r^2)\beta_2 \quad (6.11\text{b})$$

$$\mu_1 \geq 0, \quad \mu_2 \geq 0 \quad (6.11\text{c})$$

$$\mu_1\left((P_s\lambda_H^2 + \sigma_r^2)(\beta_1^2 + \beta_2^2) - \eta P_s\lambda_H^2(c_1\beta_1 + c_2\beta_2)^2\right) = 0 \quad (6.11\text{d})$$

$$\mu_2\left((P_s\lambda_H^2 + \sigma_r^2)(\beta_1^2 + \beta_2^2) - P_{max}\right) = 0 \quad (6.11\text{e})$$

$$(6.10\text{b})\text{-}(6.10\text{c}) \quad (6.11\text{f})$$

where μ_1 and μ_2 are the Lagrange multipliers corresponding to the inequality constraints in (6.10b) and (6.10c), respectively. Now, we will consider four sub-cases according to the values of μ_1 and μ_2 in sequel.

Case 1a: $\mu_1 = 0$, $\mu_2 = 0$.
This case results a contradiction in (6.11a). Hence, this case cannot happen.

Case 1b: $\mu_1 = 0$, $\mu_2 > 0$.
In this case by (6.11b), we obtain, $\beta_2 = 0$. Furthermore, (6.10c) should be satisfied with equality by (6.11e). Hence, we obtain

$$\beta_1 = \sqrt{\frac{P_{max}}{P_s\lambda_H^2 + \sigma_r^2}}, \quad \beta_2 = 0. \quad (6.13)$$

If (6.13) satisfies the inequality in (6.10b), it constitutes a candidate optimum solution.

Case 1c: $\mu_1 > 0$, $\mu_2 = 0$.
In this case by (6.11b), we obtain

$$\beta_2 = \frac{P_s\lambda_H^2\eta c_1 c_2}{P_s\lambda_H^2 + \sigma_r^2 - P_s\lambda_H^2\eta c_2^2}\beta_1. \quad (6.14)$$

By (6.11d), (6.10b) is satisfied with equality for this solution. If we insert (6.14) into the equality in (6.11d), we obtain $\beta_1 = 0$ which results zero SNR. Hence, we eliminate this case.

Case 1d: $\mu_1 > 0$, $\mu_2 > 0$.
In this case, both (6.10b) and (6.10c) are satisfied with equality. If $c_2 = 0$, c_1 cannot

be zero since $c_1 = |\mathbf{f}^H \mathbf{\Psi}_1|$, $c_2 = \mathbf{f}^H \mathbf{\Psi}_2$, and $c_1^2 + c_2^2 = ||\mathbf{f}||^2$. Hence, we obtain $\beta_1 = \sqrt{\frac{P_{max}}{\eta c_1^2 P_s \lambda_H^2}}$ and $\beta_2 = \sqrt{\frac{P_{max}}{P_s \lambda_H^2 + \sigma_r^2} - \frac{P_{max}}{\eta c_1^2 P_s \lambda_H^2}}$ by (6.11d-e). If $\eta c_1^2 P_s \lambda_H^2 \geq P_s \lambda_H^2 + \sigma_r^2$ this is a candidate solution for the case $c_2 = 0$.

If $c_2 > 0$, we obtain by (6.11d-e)

$$\beta_2 = \sqrt{\frac{P_{max}}{\eta P_s \lambda_H^2 c_2^2}} - \frac{c_1}{c_2}\beta_1 \tag{6.15}$$

If we insert (6.15) into the equality in (6.11e), we obtain the following quadratic equation, i.e.,

$$(P_s \lambda_H^2 + \sigma_r^2)\frac{c_1^2 + c_2^2}{c_2^2}\beta_1^2 - (P_s \lambda_H^2 + \sigma_r^2)\frac{2c_1}{c_2}\sqrt{\frac{P_{max}}{\eta P_s \lambda_H^2 c_2^2}}\beta_1$$

$$+ (P_s \lambda_H^2 + \sigma_r^2)\frac{P_{max}}{\eta P_s \lambda_H^2 c_2^2} - P_{max} = 0 \tag{6.16}$$

Let $\beta_1^{r_1}$ and $\beta_1^{r_2}$ be the roots of the quadratic equation in (6.16). For each positive root, we can find the corresponding β_2 as in (6.15). If the resulting $\beta_2 < 0$, we eliminate that solution. Otherwise, it is a candidate optimum solution.

Now, let us consider the second main case where $0 < \alpha < 1$ in the following part.

Case 2: In this case, $\alpha < 1$ and the Lagrange multiplier corresponding to the constraint in (6.9d) is zero by complementary slackness. The candidate solution corresponding to this case can be found by solving (6.9a-c) and checking whether the solution satisfies (6.9d) or not. In order to simplify the problem, let us define $\tilde{\beta}_1 \triangleq \sqrt{\alpha}\beta_1$, $\tilde{\beta}_2 \triangleq \sqrt{\alpha}\beta_2$, and $x \triangleq \sqrt{1 - \alpha}$. Then, (6.9a-c) can be reformulated as follows,

$$\min_{\tilde{\beta}_1, \tilde{\beta}_2, x} \frac{\sigma_r^2}{1 - x^2} + \frac{\sigma_d^2}{||\mathbf{g}||^2 \tilde{\beta}_1^2} \tag{6.17a}$$

$$s.t. \left(d_1 + \frac{\sigma_r^2}{1 - x^2}\right)(\tilde{\beta}_1^2 + \tilde{\beta}_2^2) \leq (d_2 x + d_3\tilde{\beta}_1 + d_4\tilde{\beta}_2)^2 \tag{6.17b}$$

$$\left(d_1 + \frac{\sigma_r^2}{1 - x^2}\right)(\tilde{\beta}_1^2 + \tilde{\beta}_2^2) \leq P_{max} \tag{6.17c}$$

where we take the multiplicative inverse of (6.9a) and obtain a minimization problem. $d_1 \triangleq P_s \lambda_H^2$, $d_2 \triangleq \sqrt{\eta P_s}||\mathbf{h}||$, $d_3 \triangleq \sqrt{\eta P_s}\lambda_H c_1$, and $d_4 \triangleq \sqrt{\eta P_s}\lambda_H c_2$ are defined for

ease of notation. KKT conditions for (6.17a-c) are given as follows,

$$\frac{2\sigma_d^2}{\|\mathbf{g}\|^2 \tilde{\beta}_1^3} = 2\mu_1\left((d_1 + \frac{\sigma_r^2}{1-x^2})\tilde{\beta}_1 - d_3(d_2 x + d_3\tilde{\beta}_1 + d_4\tilde{\beta}_2)\right) + 2\mu_2(d_1 + \frac{\sigma_r^2}{1-x^2})\tilde{\beta}_1$$
$$(6.18a)$$

$$0 = 2\mu_1\left((d_1 + \frac{\sigma_r^2}{1-x^2})\tilde{\beta}_2 - d_4(d_2 x + d_3\tilde{\beta}_1 + d_4\tilde{\beta}_2)\right) + 2\mu_2(d_1 + \frac{\sigma_r^2}{1-x^2})\tilde{\beta}_2 \quad (6.18b)$$

$$\frac{2\sigma_r^2 x}{(1-x^2)^2} = 2\mu_1 d_2(d_2 x + d_3\tilde{\beta}_1 + d_4\tilde{\beta}_2) - 2\mu_1 \frac{(\tilde{\beta}_1^2 + \tilde{\beta}_2^2)\sigma_r^2 x}{(1-x^2)^2} - 2\mu_2 \frac{(\tilde{\beta}_1^2 + \tilde{\beta}_2^2)\sigma_r^2 x}{(1-x^2)^2}$$
$$(6.18c)$$

$$\mu_1 \geq 0, \quad \mu_2 \geq 0 \tag{6.18d}$$

$$\mu_1\left((d_1 + \frac{\sigma_r^2}{1-x^2})(\tilde{\beta}_1^2 + \tilde{\beta}_2^2) - (d_2 x + d_3\tilde{\beta}_1 + d_4\tilde{\beta}_2)^2\right) = 0 \tag{6.18e}$$

$$\mu_2\left((d_1 + \frac{\sigma_r^2}{1-x^2})(\tilde{\beta}_1^2 + \tilde{\beta}_2^2) - P_{max}\right) = 0 \tag{6.18f}$$

(6.17b)-(6.17c) $\hspace{9cm}$ (6.18g)

where μ_1 and μ_2 are the Lagrange multipliers corresponding to the inequalities in (6.17b) and (6.17c), respectively. According to the values of μ_1 and μ_2, we will consider four sub-cases similar to the previous part.

Case 2a: $\mu_1 = 0, \mu_2 = 0$.
This case makes a contradiction for (6.18a) and thus it is not possible.

Case 2b: $\mu_1 = 0, \mu_2 > 0$.
In this case, we obtain $x = 0$ by (6.18c). $x = 0$ corresponds to $\alpha = 1$ and this case is considered in Case 1.

Case 2c: $\mu_1 > 0, \mu_2 = 0$.
Now, (6.17b) is satisfied with equality by (6.18e). In addition, if $d_4 > 0$, we obtain the following relation by (6.18b), i.e.,

$$d_2 x + d_3\tilde{\beta}_1 + d_4\tilde{\beta}_2 = \frac{d_1 + \frac{\sigma_r^2}{1-x^2}}{d_4}\tilde{\beta}_2. \tag{6.19}$$

If we insert right side of (6.19) into the equality in (6.18e), we obtain

$$(d_1 + \frac{\sigma_r^2}{1-x^2})(\tilde{\beta}_1^2 + \tilde{\beta}_2^2) - \frac{\left(d_1 + \frac{\sigma_r^2}{1-x^2}\right)^2}{d_4^2}\tilde{\beta}_2^2 = 0. \tag{6.20}$$

112

By (6.20), we obtain

$$\tilde{\beta}_1 = \frac{\sqrt{d_1 - d_4^2 + \frac{\sigma_r^2}{1-x^2}}}{d_4} \tilde{\beta}_2. \tag{6.21}$$

If we insert (6.21) into (6.19) we obtain

$$\tilde{\beta}_2 = \frac{d_2 d_4}{d_1 - d_4^2 + \frac{\sigma_r^2}{1-x^2} - d_3\sqrt{d_1 - d_4^2 + \frac{\sigma_r^2}{1-x^2}}} x. \tag{6.22}$$

If we insert (6.21) and (6.22) into the objective function in (6.17a), we obtain the following unconstrained optimization problem, i.e.,

$$\min_{0 \le x < 1} \frac{\sigma_r^2}{1 - x^2} + \frac{\sigma_d^2\left(\sqrt{d_1 - d_4^2 + \frac{\sigma_r^2}{1-x^2}} - d_3\right)^2}{||\mathbf{g}||^2 d_2^2 x^2} \tag{6.23}$$

Let us find the minimizer of the function in (6.23) and check whether it satisfies $0 \le x < 1$ or not. In order to simplify the derivative operation, let us define $y \triangleq \sqrt{d_1 - d_4^2 + \frac{\sigma_r^2}{1-x^2}}$ and express (6.23) in terms of y as follows,

$$\min_y \; y^2 + \frac{\sigma_d^2(y - d_3)^2(y^2 - d_1 + d_4^2)}{||\mathbf{g}||^2 d_2^2(y^2 - d_1 + d_4^2 - \sigma_r^2)} \tag{6.24}$$

If we equate the derivative of the function in (6.24) to zero, we obtain

$$2y + \frac{\sigma_d^2}{||\mathbf{g}||^2 d_2^2} \frac{\left(4y^3 - 6d_3 y^2 + 2(d_3^2 + d_4^2 - d_1)y + 2d_3(d_1 - d_4^2)\right)\left(y^2 - d_1 + d_4^2 - \sigma_r^2\right)}{(y^2 - d_1 + d_4^2 - \sigma_r^2)^2}$$
$$-\frac{\sigma_d^2}{||\mathbf{g}||^2 d_2^2} \frac{2y\left(y^4 - 2d_3 y^3 + (d_3^2 + d_4^2 - d_1)y^2 + 2d_3(d_1 - d_4^2)y + d_3^2(d_4^2 - d_1)\right)}{(y^2 - d_1 + d_4^2 - \sigma_r^2)^2} = 0 \tag{6.25}$$

If we rearrange the terms in (6.25), we obtain the following fifth order polynomial, i.e.,

$$A_5 y^5 + A_4 y^4 + A_3 y^3 + A_2 y^2 + A_1 y + A_0 = 0 \tag{6.26}$$

113

where A_5, A_4, A_3, A_2, A_1, and A_0 are defined for ease of notation as follows

$$A_5 = 1 + \frac{\sigma_d^2}{||\mathbf{g}||^2 d_2^2}, \quad A_4 = \frac{-d_3 \sigma_d^2}{||\mathbf{g}||^2 d_2^2}, \quad A_3 = -2(d_1 - d_4^2 + \sigma_r^2) - \frac{2(d_1 - d_4^2 + \sigma_r^2)\sigma_d^2}{||\mathbf{g}||^2 d_2^2},$$
$$\text{(6.27a)}$$

$$A_2 = \frac{\left(3d_3(d_1 - d_4^2 + \sigma_r^2) - d_3(d_1 - d_4^2) \right)\sigma_d^2}{||\mathbf{g}||^2 d_2^2}, \quad \text{(6.27b)}$$

$$A_1 = (d_1 - d_4^2 + \sigma_r^2)^2 + \frac{\left(d_3^2(d_1 - d_4^2) - (d_3^2 + d_4^2 - d_1)(d_1 - d_4^2 + \sigma_r^2) \right)\sigma_d^2}{||\mathbf{g}||^2 d_2^2}, \quad \text{(6.27c)}$$

$$A_0 = \frac{-d_3(d_1 - d_4^2)(d_1 - d_4^2 + \sigma_r^2)\sigma_d^2}{||\mathbf{g}||^2 d_2^2}. \quad \text{(6.27d)}$$

After finding the positive roots of (6.26), we can determine each candidate x using the relation $x = \sqrt{\frac{y^2 - d_1 + d_4^2 - \sigma_r^2}{y^2 - d_1 + d_4^2}}$. We note the corresponding solution as a candidate for each positive root if it satisfies $0 \le x < 1$, $\tilde{\beta}_2 \ge 0$ in (6.22) and the constraint in (6.17c).

If $d_4 = 0$, we obtain $\tilde{\beta}_2 = 0$ by (6.18b). Then, we obtain $\tilde{\beta}_1 = \frac{d_2 x}{\sqrt{d_1 + \frac{\sigma_r^2}{1-x^2} - d_3}}$ by (6.18e). If we insert this $\tilde{\beta}_1$ into (6.17a), we obtain the same optimization problem in (6.23) with $d_4 = 0$. For each positive root of (6.26), we note the corresponding solution as a candidate if it satisfies $0 \le x < 1$, $\tilde{\beta}_1 = \frac{d_2 x}{\sqrt{d_1 + \frac{\sigma_r^2}{1-x^2} - d_3}} > 0$ and the constraint in (6.17c).

Case 2d: $\mu_1 > 0$, $\mu_2 > 0$.

In this case, both (6.17b) and (6.17c) are satisfied with equality. Hence, by subtracting one of the equalities from the other, we obtain

$$\tilde{\beta}_2 = \frac{\sqrt{P_{max}} - d_2 x - d_3 \tilde{\beta}_1}{d_4} \quad \text{(6.28)}$$

Here, we have assumed that $d_4 > 0$. If $d_4 = 0$, $\beta_2 = 0$ by (6.18b). Continuing with

114

$d_4 > 0$, if we insert (6.28) into the equality in (6.18f), we obtain,

$$\left(d_1 + \frac{\sigma_r^2}{1-x^2}\right)\left(\tilde{\beta}_1^2 + \frac{(\sqrt{P_{max}} - d_2 x - d_3\tilde{\beta}_1)^2}{d_4^2}\right) = P_{max} \tag{6.29a}$$

$$\left(d_1 + \frac{\sigma_r^2}{1-x^2}\right)\left((d_3^2 + d_4^2)\tilde{\beta}_1^2 + 2d_3(d_2 x - \sqrt{P_{max}})\tilde{\beta}_1 + (d_2 x - \sqrt{P_{max}})^2\right)$$
$$- P_{max}d_4^2 = 0 \tag{6.29b}$$

$$\tilde{\beta}_1^2 + \frac{2d_3}{d_3^2 + d_4^2}(d_2 x - \sqrt{P_{max}})\tilde{\beta}_1 + \frac{(d_2 x - \sqrt{P_{max}})^2}{d_3^2 + d_4^2} - \frac{P_{max}d_4^2}{\left(d_1 + \frac{\sigma_r^2}{1-x^2}\right)(d_3^2 + d_4^2)} = 0 \tag{6.29c}$$

$$\left(\tilde{\beta}_1 + \frac{d_3}{d_3^2 + d_4^2}(d_2 x - \sqrt{P_{max}})\right)^2 + \frac{d_4^2(d_2 x - \sqrt{P_{max}})^2}{(d_3^2 + d_4^2)^2} - \frac{P_{max}d_4^2}{\left(d_1 + \frac{\sigma_r^2}{1-x^2}\right)(d_3^2 + d_4^2)} = 0 \tag{6.29d}$$

$$\left(\tilde{\beta}_1 + D_1 x - D_2\right)^2 + D_3(D_1 x - D_2)^2 - \frac{D_4}{d_1 + \frac{\sigma_r^2}{1-x^2}} = 0 \tag{6.29e}$$

where D_1, D_2, D_3, D_4 are defined for ease of notation, i.e.,

$$D_1 \triangleq \frac{d_2 d_3}{d_3^2 + d_4^2}, \quad D_2 \triangleq \frac{\sqrt{P_{max}}d_3}{d_3^2 + d_4^2}, \quad D_3 \triangleq \frac{d_4^2}{d_3^2}, \quad D_4 \triangleq \frac{P_{max}d_4^2}{(d_3^2 + d_4^2)} \tag{6.30}$$

Note that (6.29e) is also valid for $d_4 = 0$, i.e., $\sqrt{P_{max}} - d_2 x - d_3\tilde{\beta}_1 = 0$ by (6.18e-f) with $\tilde{\beta}_2 = 0$. By (6.29e) we obtain $\tilde{\beta}_1$ as follows,

$$\tilde{\beta}_1 = \sqrt{\frac{D_4}{d_1 + \frac{\sigma_r^2}{1-x^2}} - D_3(D_1 x - D_2)^2} - (D_1 x - D_2) \tag{6.31}$$

If we insert (6.31) into the objective function in (6.17a), we obtain the following optimization problem in terms of x only as follows,

$$\min_{0 \le x < 1} \frac{\sigma_r^2}{1-x^2} + \frac{\sigma_d^2}{||\mathbf{g}||^2\left(\sqrt{\frac{D_4}{d_1 + \frac{\sigma_r^2}{1-x^2}} - D_3(D_1 x - D_2)^2} - (D_1 x - D_2)\right)^2} \tag{6.32}$$

First, let us find the minimizer of the above function in (6.32) ignoring $0 \le x < 1$. If the solution satisfies $0 \le x < 1$, then it is the optimum solution of (6.32). Otherwise, boundary point $x = 0$ should be considered which is already analyzed in Case 1. Let us take the derivative of the function in (6.32) and equate it to zero, i.e.,

$$f(x) = \frac{2\sigma_r^2 x}{(1-x^2)^2} - \frac{2\sigma_d^2 f_1'(x)}{||\mathbf{g}||^2 f_1^3(x)} = 0 \tag{6.33}$$

115

where $f_1(x) \triangleq \sqrt{\dfrac{D_4}{d_1 + \frac{\sigma_r^2}{1-x^2}} - D_3(D_1 x - D_2)^2} - (D_1 x - D_2)$ is defined for ease of notation and the derivative of it is given by

$$f_1'(x) = \frac{\dfrac{-D_4 \frac{\sigma_r^2 x}{(1-x^2)^2}}{\left(d_1 + \frac{\sigma_r^2}{1-x^2}\right)^2} - D_1 D_3(D_1 x - D_2)}{\sqrt{\dfrac{D_4}{d_1 + \frac{\sigma_r^2}{1-x^2}} - D_3(D_1 x - D_2)^2}} - D_1 \tag{6.34}$$

Now, we will show that $f(x)$ is monotonically increasing in the region of interest in Lemma 6.2.

Lemma 6.2: $f(x)$ is monotonically increasing in the region specified by $\tilde{\beta}_1 > 0$ and $0 \le x < 1$.

Proof: Proof can be found in Appendix C.1. ∎

By Lemma 6.2, we can find the zeros of $f(x)$ inside the region of interest by using bisection search as outlined in Algorithm 6.1. Note that $D_1 x - D_2$ is negative inside the region specified by $\tilde{\beta}_1 > 0$ and $\tilde{\beta}_2 \ge 0$ by (6.28) using the definitions in (6.30). Hence, upper bound for x is given as $\min\left\{1, \frac{D_2}{D_1}\right\}$. When $D_1 x - D_2 \le 0$, we see that $\tilde{\beta}_1$ is real and positive if $\frac{D_4}{d_1 + \frac{\sigma_r^2}{1-x^2}} - D_3(D_1 x - D_2)^2 \ge 0$ by (6.31). In order to find the intervals in which this function is nonnegative, let us find its zeros, i.e.,

$$\frac{D_4}{d_1 + \frac{\sigma_r^2}{1-x^2}} - D_3(D_1 x - D_2)^2 = 0 \tag{6.35}$$

If we rearrange the terms in (6.35), we obtain the following quartic equation, i.e.,

$$-D_1^2 D_3 d_1 x^4 + 2D_1 D_2 D_3 d_1 x^3 + \left(D1^2 D_3(d_1 + \sigma_r^2) - D_2^2 D_3 d_1 + D_4\right) x^2$$
$$-2D_1 D_2 D_3(d_1 + \sigma_r^2)x + D_2^2 D_3(d_1 + \sigma_r^2) - D_4 = 0 \tag{6.36}$$

At this point, the intervals, in which the function in (6.35) is nonnegative, are chosen for bisection search in order to obtain candidate solutions by considering the sign of $f(x)$ at the end points of the intervals.

Algorithm 6.1: Bisection Search for Finding the Zeros of $f(x)$

Initialization: Find the real and nonnegative roots of the quartic equation in (6.36) which are less than $\min\left\{1, \frac{D_2}{D_1}\right\}$. Choose the interval between the roots such that the function in (6.35) is nonnegative and $f(x)$ is nonpositive and nonnegative at the left and right endpoints, respectively. If there is no such an interval, terminate. If it exists, for each interval, set initial lower and upper bounds, $L^{(0)}$ and $U^{(0)}$, as the left and right endpoints, respectively. Take the initial x as $x^{(0)} = (L^{(0)} + U^{(0)})/2$. Set the iteration number $i \leftarrow 0$.

Repeat

    If $f(x^{(i)}) < 0$, set $L^{(i+1)} = x^{(i)}$.

    ElseIf $f(x^{(i)}) > 0$, set $U^{(i+1)} = x^{(i)}$.

    Else Terminate.

$x^{(i+1)} = (L^{(i+1)} + U^{(i+1)})/2$

Set $i \leftarrow i + 1$.

Until convergence criterion is met.

Note the corresponding solutions as candidate for each zero found by Algorithm 6.1.

Let us construct the set $\mathcal{S}$ whose elements are the candidate $\{\beta_1, \beta_2, \alpha\}$ given in Case (1a-1d) and Case (2a-2d). Note that $\tilde{\beta}_1$, $\tilde{\beta}_2$ and x found in Cases (2a-2d) are converted β_1, β_2, and α in constructing the set $\mathcal{S}$. If $\mathcal{S} \neq \emptyset$, then the optimum solution of (6.9) is obtained as follows,

$$\{\beta_1^\star, \beta_2^\star, \alpha^\star\} = \arg \max_{\{\beta_1, \beta_2, \alpha\} \in \mathcal{S}} \frac{\alpha ||\mathbf{g}||^2 \beta_1^2}{\sigma_r^2 ||\mathbf{g}||^2 \beta_1^2 + \sigma_d^2}. \tag{6.37}$$

Using (6.37), optimum beamformer $\mathbf{v}_r^\star$ for the problem in (6.8) is obtained by Lemma 6.1 as $\mathbf{v}_r^\star = \beta_1^\star \mathbf{\Psi}_1 + \beta_2^\star e^{j \angle \mathbf{f}^H \mathbf{g}} \mathbf{\Psi}_2$.

117

6.4 QoS-Aware Design Problem

QoS-aware design for the considered self-energy recycling protocol is considered for the optimization of only relay beamformer in [21]. In this chapter, we consider the joint design of power allocation and relay beamforming weight vector. In this problem, the aim is to minimize the relay transmission power used by the relay's own battery, $P_r - P_h$, such that the SNR requirement at $\mathbf{D}$ and maximum power limit constraint at $\mathbf{R}$ are satisfied. The addressed optimization problem can be written as follows,

$$\min_{\mathbf{v}_r, \alpha} \ ||\mathbf{v}_r||^2 (P_s \alpha \lambda_H^2 + \sigma_r^2) - \eta P_s \left(||\mathbf{h}|| \sqrt{1-\alpha} + \lambda_H \sqrt{\alpha} |\mathbf{f}^H \mathbf{v}_r| \right)^2 \tag{6.38a}$$

$$s.t. \ \frac{P_s \lambda_H^2 \alpha |\mathbf{g}^H \mathbf{v}_r|^2}{\sigma_r^2 |\mathbf{g}^H \mathbf{v}_r|^2 + \sigma_d^2} \geq \gamma \tag{6.38b}$$

$$||\mathbf{v}_r||^2 (P_s \alpha \lambda_H^2 + \sigma_r^2) \leq P_{max} \tag{6.38c}$$

$$0 < \alpha \leq 1 \tag{6.38d}$$

where γ is the target SNR at $\mathbf{D}$. Let us express the relay beamformer vector as $\mathbf{v}_r = \sum_{n=1}^N \beta_n e^{j\theta_n} \mathbf{\Psi}_n$ where $\beta_n \geq 0$, $n = 1, ..., N$ and $\{\mathbf{\Psi}_n\}_{n=1}^N$ is an orthonormal basis for $\mathbb{C}^{N \times 1}$ such that $\mathbf{\Psi}_1 = \frac{\mathbf{g}}{||\mathbf{g}||}$ and $\mathbf{\Psi}_2 = \frac{\mathbf{f} - \mathbf{\Psi}_1 \mathbf{\Psi}_1^H \mathbf{f}}{||\mathbf{f} - \mathbf{\Psi}_1 \mathbf{\Psi}_1^H \mathbf{f}||}$. Then, we have the following Lemma similar to Lemma 6.1.

Lemma 6.3: The optimum beamformer relay vector, $\mathbf{v}_r^\star$, for the problem (6.38) is given by the form $\mathbf{v}_r^\star = \beta_1 \mathbf{\Psi}_1 + \beta_2 e^{j\angle \mathbf{f}^H \mathbf{g}} \mathbf{\Psi}_2$, where $\beta_1 \geq 0$ and $\beta_2 \geq 0$.

Proof: A similar proof can be found in [21]. ∎

Using Lemma 6.3, the problem in (6.38) can be expressed in terms of β_1, β_2 and α as follows,

$$\min_{\beta_1, \beta_2, \alpha} \ (\beta_1^2 + \beta_2^2)(P_s \alpha \lambda_H^2 + \sigma_r^2) - \eta P_s \left(||\mathbf{h}|| \sqrt{1-\alpha} + \lambda_H \sqrt{\alpha}(c_1 \beta_1 + c_2 \beta_2) \right)^2 \tag{6.39a}$$

$$s.t. \ \frac{P_s \lambda_H^2 \alpha ||\mathbf{g}||^2 \beta_1^2}{\sigma_r^2 ||\mathbf{g}||^2 \beta_1^2 + \sigma_d^2} \geq \gamma \tag{6.39b}$$

$$(\beta_1^2 + \beta_2^2)(P_s \alpha \lambda_H^2 + \sigma_r^2) \leq P_{max} \tag{6.39c}$$

$$0 < \alpha \leq 1 \tag{6.39d}$$

where $c_1 = |\mathbf{f}^H \mathbf{\Psi}_1| = |\mathbf{f}^H \mathbf{g}|/||\mathbf{g}||$ and $c_2 = \mathbf{f}^H \mathbf{\Psi}_2 = \frac{\mathbf{f}^H \mathbf{f} - \mathbf{f}^H \mathbf{\Psi}_1 \mathbf{\Psi}_1^H \mathbf{f}}{||\mathbf{f} - \mathbf{\Psi}_1 \mathbf{\Psi}_1^H \mathbf{f}||}$ are as defined before.

Note that c_1 and c_2 are real and nonnegative. Hence, optimum β_1 and β_2 for (6.39) should be nonnegative in order to maximize harvested power expression in (6.39a). This is the reason why we do not include nonnegativity constraints in (6.39).

Now, there are two main cases to be evaluated as in the previous section.

Case 1: Assume $\alpha = 1$. In this case, the problem in (6.39) can be reformulated as follows,

$$\min_{\beta_1, \beta_2} (P_s \lambda_H^2 + \sigma_r^2)(\beta_1^2 + \beta_2^2) - \eta P_s \lambda_H^2 (c_1 \beta_1 + c_2 \beta_2)^2 \tag{6.40a}$$

$$s.t. \quad \frac{P_s \lambda_H^2 ||\mathbf{g}||^2 \beta_1^2}{\sigma_r^2 ||\mathbf{g}||^2 \beta_1^2 + \sigma_d^2} \geq \gamma \tag{6.40b}$$

$$(P_s \lambda_H^2 + \sigma_r^2)(\beta_1^2 + \beta_2^2) \leq P_{max} \tag{6.40c}$$

The solution of this problem constitutes a candidate optimum solution for the problem (6.39a-d). KKT necessary optimality conditions for the problem in (6.40a-c) are given by

$$2\left((P_s \lambda_H^2 + \sigma_r^2)\beta_1 - \eta P_s \lambda_H^2 c_1 (c_1 \beta_1 + c_2 \beta_2)\right)$$
$$= \frac{2\mu_1 P_s \lambda_H^2 ||\mathbf{g}||^2 \sigma_d^2 \beta_1}{(\sigma_r^2 ||\mathbf{g}||^2 \beta_1^2 + \sigma_d^2)^2} - 2\mu_2 (P_s \lambda_H^2 + \sigma_r^2)\beta_1 \tag{6.41a}$$

$$2\left((P_s \lambda_H^2 + \sigma_r^2)\beta_2 - \eta P_s \lambda_H^2 c_2 (c_1 \beta_1 + c_2 \beta_2)\right) = -2\mu_2 (P_s \lambda_H^2 + \sigma_r^2)\beta_2 \tag{6.41b}$$

$$\mu_1 \geq 0, \quad \mu_2 \geq 0 \tag{6.41c}$$

$$\mu_1 \left(\frac{P_s \lambda_H^2 ||\mathbf{g}||^2 \beta_1^2}{\sigma_r^2 ||\mathbf{g}||^2 \beta_1^2 + \sigma_d^2} - \gamma \right) = 0 \tag{6.41d}$$

$$\mu_2 \left((P_s \lambda_H^2 + \sigma_r^2)(\beta_1^2 + \beta_2^2) - P_{max} \right) = 0 \tag{6.41e}$$

$$(6.40b)\text{-}(6.40c) \tag{6.41f}$$

where μ_1 and μ_2 are the Lagrange multipliers corresponding to the inequality constraints in (6.40b) and (6.40c), respectively. Now, we will consider four sub-cases.

Case 1a: $\mu_1 = 0$, $\mu_2 = 0$.
If $c_1 = 0$, $\beta_1 = 0$ by (6.41a), and (6.40b) cannot be satisfied. Hence, if $c_1 = 0$, we do

not consider this case. Otherwise, we obtain the following relations by (6.41a-b), i.e.,

$$\beta_2 = \frac{c_2}{c_1}\beta_1 \tag{6.42a}$$

$$\left(P_s\lambda_H^2(1 - \eta c_1^2) + \sigma_r^2\right)\beta_1 = P_s\lambda_H^2\eta c_2^2\beta_1 \tag{6.42b}$$

If $P_s\lambda_H^2(1 - \eta c_1^2) + \sigma_r^2 \neq P_s\lambda_H^2\eta c_2^2$, this case results zero SNR by $\beta_1 = 0$. Hence, we eliminate this case. Otherwise if $P_s\lambda_H^2(1 - \eta c_1^2) + \sigma_r^2 = P_s\lambda_H^2\eta c_2^2$, then if we multiply (6.41a) and (6.41b) by β_1 and β_2, respectively and add them up we obtain the objective function as zero for any β_1 and β_2 as in (6.42a). In this case, we should check other conditions. β_1 should be at least $\sqrt{\frac{\gamma\sigma_d^2}{(P_s\lambda_H^2 - \gamma\sigma_r^2)\|\mathbf{g}\|^2}}$ in order to satisfy (6.40b). If this β_1 and the corresponding β_2 in (6.42a) also satisfy (6.40c), they are noted as a candidate solution.

Case 1b: $\mu_1 = 0$, $\mu_2 > 0$.

Note that c_1 and c_2 cannot be zero at the same time since $c_1 = |\mathbf{f}^H\mathbf{\Psi}_1|$, $c_2 = \mathbf{f}^H\mathbf{\Psi}_2$, and $c_1^2 + c_2^2 = \|\mathbf{f}\|^2$. If $c_1 = 0$, we obtain $\beta_1 = 0$ by (6.41a) which results zero SNR. Hence, we do not consider this case if $c_1 = 0$. If $c_2 = 0$, we obtain $\beta_2 = 0$ by (6.41b) and $\beta_1 = \sqrt{\frac{P_{max}}{P_s\lambda_H^2 + \sigma_r^2}}$ by (6.41e). If they also satisfy (6.40b), they are noted as a candidate solution. If $c_1 > 0$ and $c_2 > 0$, both β_1 and β_2 are nonzero by (6.41a-b) and (6.41e). In this case, if we divide both sides of (6.41a) by (6.41b) and rearrange the terms, we obtain

$$-\eta c_1^2\beta_1\beta_2 - \eta c_1 c_2\beta_2^2 = -\eta c_2^2\beta_1\beta_2 - \eta c_1 c_2\beta_1^2 \tag{6.43}$$

We can divide both sides of (6.43) by $\eta c_1 c_2$ and obtain

$$\beta_2^2 + \frac{(c_1^2 - c_2^2)}{c_1 c_2}\beta_1\beta_2 - \beta_1^2 = 0 \tag{6.44}$$

Let r be the only nonnegative root of the quadratic equation in (6.44), i.e., $\beta_2 = r\beta_1$. Note that (6.40c) is satisfied with equality by (6.41e) and if we insert this relation into the equality in (6.41e), we obtain

$$\beta_1 = \sqrt{\frac{P_{max}}{(P_s\lambda_H^2 + \sigma_r^2)(1 + r^2)}} \tag{6.45}$$

If this solution satisfies SNR constraint in (6.40b), it is a candidate solution.

120

Case 1c: $\mu_1 > 0$, $\mu_2 = 0$.

Since $\mu_1 > 0$, (6.40b) is satisfied with equality. Hence, we obtain

$$\beta_1 = \sqrt{\frac{\gamma \sigma_d^2}{(P_s \lambda_H^2 - \gamma \sigma_r^2)||\mathbf{g}||^2}} \tag{6.46}$$

If $P_s \lambda_H^2 (1 - \eta c_2^2) + \sigma_r^2 = 0$ and $c_1 > 0$, then we obtain $\beta_1 = 0$ by (6.41b) which contradicts with (6.46). Hence, we do not consider this case for $P_s \lambda_H^2 (1 - \eta c_2^2) + \sigma_r^2 = 0$ and $c_1 > 0$. If $P_s \lambda_H^2 (1 - \eta c_2^2) + \sigma_r^2 = 0$ and $c_1 = 0$, then the objective function in (6.40a) is independent of β_2 and $\beta_2 = 0$ with β_1 in (6.46) is a candidate solution if they also satisfy (6.40c). Otherwise if $P_s \lambda_H^2 (1 - \eta c_2^2) + \sigma_r^2 \neq 0$, we obtain by (6.41b)

$$\beta_2 = \frac{\eta c_1 c_2 P_s \lambda_H^2}{P_s \lambda_H^2 (1 - \eta c_2^2) + \sigma_r^2} \beta_1. \tag{6.47}$$

Note that for (6.46) and (6.47) to be a candidate solution, it is required that $P_s \lambda_H^2 (1 - \eta c_2^2) + \sigma_r^2 > 0$ and (6.40c) is satisfied.

Case 1d: $\mu_1 > 0$, $\mu_2 > 0$.

In this case, both (6.40b) and (6.40c) are satisfied with equality. Hence, we obtain

$$\beta_1 = \sqrt{\frac{\gamma \sigma_d^2}{(P_s \lambda_H^2 - \gamma \sigma_r^2)||\mathbf{g}||^2}} \tag{6.48a}$$

$$\beta_2 = \sqrt{\frac{P_{max}}{P_s \lambda_H^2 + \sigma_r^2} - \frac{\gamma \sigma_d^2}{(P_s \lambda_H^2 - \gamma \sigma_r^2)||\mathbf{g}||^2}} \tag{6.48b}$$

If the term inside the square root function in (6.48b) is nonnegative, this constitutes a candidate solution. Now, let us consider the other case where $0 < \alpha < 1$.

Case 2: In this case, we will solve (6.39a-c) and check whether the solution satisfies (6.39d) or not. We will express (6.39a-c) in terms of $\tilde{\beta}_1 \triangleq \sqrt{\alpha}\beta_1$, $\tilde{\beta}_2 \triangleq \sqrt{\alpha}\beta_2$, and $x \triangleq \sqrt{1 - \alpha}$ as in the previous section. (6.39a-c) can be reformulated as follows,

$$\min_{\tilde{\beta}_1, \tilde{\beta}_2, x} \left(d_1 + \frac{\sigma_r^2}{1 - x^2} \right)(\tilde{\beta}_1^2 + \tilde{\beta}_2^2) - (d_2 x + d_3 \tilde{\beta}_1 + d_4 \tilde{\beta}_2)^2 \tag{6.49a}$$

$$s.t. \quad \frac{P_s \lambda_H^2 ||\mathbf{g}||^2 \tilde{\beta}_1^2}{\sigma_r^2 ||\mathbf{g}||^2 \frac{\tilde{\beta}_1^2}{1-x^2} + \sigma_d^2} \geq \gamma \tag{6.49b}$$

$$\left(d_1 + \frac{\sigma_r^2}{1 - x^2} \right)(\tilde{\beta}_1^2 + \tilde{\beta}_2^2) \leq P_{max} \tag{6.49c}$$

where $d_1 \triangleq P_s \lambda_H^2$, $d_2 \triangleq \sqrt{\eta P_s}||\mathbf{h}||$, $d_3 \triangleq \sqrt{\eta P_s} \lambda_H c_1$, and $d_4 \triangleq \sqrt{\eta P_s} \lambda_H c_2$ are as defined before. KKT conditions for (6.49a-c) are given as follows,

$$2\left(d_1 + \frac{\sigma_r^2}{1-x^2}\right)\tilde{\beta}_1 - 2d_3(d_2 x + d_3\tilde{\beta}_1 + d_4\tilde{\beta}_2)$$
$$= 2\mu_1 \frac{P_s \lambda_H^2 ||\mathbf{g}||^2 \sigma_d^2 \tilde{\beta}_1}{(\sigma_r^2 ||\mathbf{g}||^2 \frac{\tilde{\beta}_1^2}{1-x^2} + \sigma_d^2)^2} - 2\mu_2\left(d_1 + \frac{\sigma_r^2}{1-x^2}\right)\tilde{\beta}_1 \tag{6.50a}$$

$$2\left(d_1 + \frac{\sigma_r^2}{1-x^2}\right)\tilde{\beta}_2 - 2d_4(d_2 x + d_3\tilde{\beta}_1 + d_4\tilde{\beta}_2) = -2\mu_2\left(d_1 + \frac{\sigma_r^2}{1-x^2}\right)\tilde{\beta}_2 \tag{6.50b}$$

$$2\frac{\sigma_r^2 x(\tilde{\beta}_1^2 + \tilde{\beta}_2^2)}{(1-x^2)^2} - 2d_2(d_2 x + d_3\tilde{\beta}_1 + d_4\tilde{\beta}_2)$$
$$= -2\mu_1 \frac{P_s \lambda_H^2 ||\mathbf{g}||^4 \sigma_r^2 \frac{\tilde{\beta}_1^4 x}{(1-x^2)^2}}{(\sigma_r^2 ||\mathbf{g}||^2 \frac{\tilde{\beta}_1^2}{1-x^2} + \sigma_d^2)^2} - 2\mu_2 \frac{\sigma_r^2 x(\tilde{\beta}_1^2 + \tilde{\beta}_2^2)}{(1-x^2)^2} \tag{6.50c}$$

$$\mu_1 \geq 0, \quad \mu_2 \geq 0 \tag{6.50d}$$

$$\mu_1\left(\frac{P_s \lambda_H^2 ||\mathbf{g}||^2 \tilde{\beta}_1^2}{\sigma_r^2 ||\mathbf{g}||^2 \frac{\tilde{\beta}_1^2}{1-x^2} + \sigma_d^2} - \gamma\right) = 0 \tag{6.50e}$$

$$\mu_2\left(\left(d_1 + \frac{\sigma_r^2}{1-x^2}\right)(\tilde{\beta}_1^2 + \tilde{\beta}_2^2) - P_{max}\right) = 0 \tag{6.50f}$$

$$(6.49b)\text{-}(6.49c) \tag{6.50g}$$

where μ_1 and μ_2 are the Lagrange multipliers corresponding to the inequalities in (6.49b) and (6.49c), respectively. According to μ_1 and μ_2, we will consider 4 sub-cases.

Case 2a: $\mu_1 = 0$, $\mu_2 = 0$.

If $d_3 = 0$, we obtain $\tilde{\beta}_1 = 0$ by (6.50a). In this case, the SNR constraint in (6.49b) cannot be satisfied. Hence, we will not consider this case if $d_3 = 0$. If $d_3 \neq 0$, we obtain by (6.50a-b)

$$\tilde{\beta}_2 = \frac{d_4}{d_3}\tilde{\beta}_1 \tag{6.51}$$

If we insert (6.51) into (6.50a), we obtain the following relation, i.e.,

$$\tilde{\beta}_1 = \frac{d_2 d_3}{d_1 - d_3^2 - d_4^2 + \frac{\sigma_r^2}{1-x^2}} x \tag{6.52}$$

By (6.50a) and (6.50c), we obtain

$$\frac{d_3 \sigma_r^2 x(\tilde{\beta}_1^2 + \tilde{\beta}_2^2)}{(1-x^2)^2} = d_2\left(d_1 + \frac{\sigma_r^2}{1-x^2}\right)\tilde{\beta}_1 \tag{6.53}$$

If we insert (6.51) into (6.53), we obtain

$$\tilde{\beta}_1 = \frac{d_2 d_3 (1 - x^2)}{\sigma_r^2 x (d_3^2 + d_4^2)} (d_1 + \sigma_r^2 - d_1 x^2) \tag{6.54}$$

If we equate both sides of (6.52) and (6.54), we obtain

$$\frac{d_2 d_3 (1 - x^2) x}{d_1 - d_3^2 - d_4^2 + \sigma_r^2 - (d_1 - d_3^2 - d_4^2) x^2} = \frac{d_2 d_3 (1 - x^2)}{\sigma_r^2 x (d_3^2 + d_4^2)} (d_1 + \sigma_r^2 - d_1 x^2) \tag{6.55}$$

By rearranging the terms in (6.55), we obtain the following quadratic polynomial of x^2, i.e.,

$$B_2 x^4 + B_1 x^2 + B_0 = 0 \tag{6.56}$$

where B_2, B_1, and B_0 are defined as follows

$$B_2 = d_1 (d_1 - d_3^2 - d_4^2), \tag{6.57a}$$

$$B_1 = -d_1 (d_1 - d_3^2 - d_4^2 + \sigma_r^2) - (d_1 + \sigma_r^2)(d_1 - d_3^2 - d_4^2) - \sigma_r^2 (d_3^2 + d_4^2) \tag{6.57b}$$

$$B_0 = (d_1 + \sigma_r^2)(d_1 - d_3^2 - d_4^2 + \sigma_r^2) \tag{6.57c}$$

For each root of (6.56) such that $0 \leq x < 1$, we can find the corresponding $\tilde{\beta}_1$ and $\tilde{\beta}_2$ by (6.52) and (6.51), respectively. We note each solution as candidate if it satisfies the constraints in (6.49b) and (6.49c).

Case 2b: $\mu_1 = 0$, $\mu_2 > 0$.

If $d_3 = 0$, we obtain $\tilde{\beta}_1 = 0$. In this case, the SNR constraint in (6.49b) cannot be satisfied. Hence, we will not consider this case if $d_3 = 0$. If $d_3 \neq 0$, we obtain (6.51) by (6.50a-b). By dividing both sides of (6.50a) and (6.50c), we obtain the relation in (6.54). Additionally, by (6.50f) and (6.51), we obtain

$$\tilde{\beta}_1 = \sqrt{\frac{P_{max} d_3^2}{\left(d_1 + \frac{\sigma_r^2}{1 - x^2}\right)(d_3^2 + d_4^2)}} \tag{6.58}$$

If we equate the right sides of (6.54) and (6.58), we obtain

$$\frac{P_{max} d_3^2 (1 - x^2)}{\left(d_1 + \sigma_r^2 - d_1 x^2\right)(d_3^2 + d_4^2)} = \frac{d_2^2 d_3^2 (1 - x^2)^2}{\sigma_r^4 x^2 (d_3^2 + d_4^2)^2} (d_1 + \sigma_r^2 - d_1 x^2)^2 \tag{6.59}$$

If we rearrange the terms in (6.59), we obtain the following quartic polynomial of x^2, i.e.,

$$C_4 x^8 + C_3 x^6 + C_2 x^4 + C_1 x^2 + C_0 = 0 \tag{6.60}$$

123

where C_4, C_3, C_2, C_1, and C_0 are given as follows

$$C_4 = d_1^3 d_2^2, \quad C_3 = -3d_1^2 d_2^2(d_1 + \sigma_r^2) - d_1^3 d_2^2, \tag{6.61a}$$

$$C_2 = 3d_1 d_2^2(d_1 + \sigma_r^2)^2 + 3d_1^2 d_2^2(d_1 + \sigma_r^2), \tag{6.61b}$$

$$C_1 = -3d_1 d_2^2(d_1 + \sigma_r^2)^2 - d_2^2(d_1 + \sigma_r^2)^3 - P_{max}\sigma_r^4(d_3^2 + d_4^2), \quad C_0 = d_2^2(d_1 + \sigma_r^2)^3 \tag{6.61c}$$

For each root of (6.60) such that $0 \leq x < 1$, we can find the corresponding $\tilde{\beta}_1$ and $\tilde{\beta}_2$ by (6.58) and (6.51), respectively. We note each solution as candidate if it satisfies the constraint in (6.49b). In the following two sub-cases, we will ignore the term $\frac{\sigma_r^2}{1-x^2}$ in (6.49a) and (6.49c) in order to simplify the problem. At the end, we will include this term and update the solution for these two cases. Note that $\frac{\sigma_r^2}{1-x^2}$ term is relatively small compared to $P_s\lambda_H^2$ term and we will obtain a near-optimum solution of the problem in this way.

Case 2c: $\mu_1 > 0$, $\mu_2 = 0$.
If $d_1 - d_4^2 \leq 0$, we obtain $\tilde{\beta}_1 \leq 0$ by (6.50b). Hence either $\tilde{\beta}_1$ becomes negative or SNR becomes zero. Hence, we do not consider this case for a candidate solution if $d_1 - d_4^2 \leq 0$. Otherwise by (6.50b), we obtain $\tilde{\beta}_2$ as follows,

$$\tilde{\beta}_2 = \frac{d_2 d_4}{d_1 - d_4^2} x + \frac{d_3 d_4}{d_1 - d_4^2} \tilde{\beta}_1. \tag{6.62}$$

By the equality in (6.50e), x is obtained in terms of $\tilde{\beta}_1$ as follows,

$$x = \sqrt{\frac{(P_s\lambda_H^2||\mathbf{g}||^2 - \gamma\sigma_r^2||\mathbf{g}||^2)\tilde{\beta}_1^2 - \gamma\sigma_d^2}{P_s\lambda_H^2||\mathbf{g}||^2\tilde{\beta}_1^2 - \gamma\sigma_d^2}} = \sqrt{\frac{(E_1 - E_2)\tilde{\beta}_1^2 - E_3}{E_1\tilde{\beta}_1^2 - E_3}} \tag{6.63}$$

where $E_1 \triangleq P_s\lambda_H^2||\mathbf{g}||^2$, $E_2 \triangleq \gamma\sigma_r^2||\mathbf{g}||^2$, and $E_3 \triangleq \gamma\sigma_d^2$ are defined for ease of notation. Note that E_1, E_2, and E_3 are positive. If we insert (6.62) and (6.63) into the objective function in (6.49a), we obtain the following unconstrained optimization

124

problem, i.e.,

$$\min_{\tilde{\beta}_1} \quad d_1\tilde{\beta}_1^2 + d_1\left(\frac{d_2 d_4}{d_1 - d_4^2}\sqrt{\frac{(E_1 - E_2)\tilde{\beta}_1^2 - E_3}{E_1\tilde{\beta}_1^2 - E_3}} + \frac{d_3 d_4}{d_1 - d_4^2}\tilde{\beta}_1\right)^2$$
$$-\left(\frac{d_1 d_2}{d_1 - d_4^2}\sqrt{\frac{(E_1 - E_2)\tilde{\beta}_1^2 - E_3}{E_1\tilde{\beta}_1^2 - E_3}} + \frac{d_1 d_3}{d_1 - d_4^2}\tilde{\beta}_1\right)^2 \tag{6.64a}$$

$$\min_{\tilde{\beta}_1} \quad d_1\tilde{\beta}_1^2 - \frac{d_1}{d_1 - d_4^2}\left(d_2\sqrt{\frac{(E_1 - E_2)\tilde{\beta}_1^2 - E_3}{E_1\tilde{\beta}_1^2 - E_3}} + d_3\tilde{\beta}_1\right)^2 \tag{6.64b}$$

$$\min_{\tilde{\beta}_1} \quad \frac{d_1(d_1 - d_3^2 - d_4^2)}{d_1 - d_4^2}\tilde{\beta}_1^2 - \frac{2 d_1 d_2 d_3}{d_1 - d_4^2}\tilde{\beta}_1\sqrt{\frac{(E_1 - E_2)\tilde{\beta}_1^2 - E_3}{E_1\tilde{\beta}_1^2 - E_3}}$$
$$-\frac{d_1 d_2^2}{d_1 - d_4^2}\frac{(E_1 - E_2)\tilde{\beta}_1^2 - E_3}{E_1\tilde{\beta}_1^2 - E_3} \tag{6.64c}$$

Now, let us take the derivative of the function in (6.64c) and equate it to zero and obtain

$$g(\tilde{\beta}_1) = \frac{2 d_1(d_1 - d_3^2 - d_4^2)}{d_1 - d_4^2}\tilde{\beta}_1 - \frac{2 d_1 d_2 d_3}{d_1 - d_4^2}\sqrt{g_1(\tilde{\beta}_1)} - \frac{d_1 d_2 d_3}{d_1 - d_4^2}\frac{\tilde{\beta}_1 g_1'(\tilde{\beta}_1)}{\sqrt{g_1(\tilde{\beta}_1)}}$$
$$-\frac{d_1 d_2^2}{d_1 - d_4^2}g_1'(\tilde{\beta}_1) = 0 \tag{6.65}$$

where $g_1(\tilde{\beta}_1) \triangleq \frac{(E_1 - E_2)\tilde{\beta}_1^2 - E_3}{E_1\tilde{\beta}_1^2 - E_3}$ is defined for ease of notation and its derivative is given by $g_1'(\tilde{\beta}_1) = \frac{2 E_2 E_3 \tilde{\beta}_1}{(E_1\tilde{\beta}_1^2 - E_3)^2}$.

Now, we will claim that $g(\tilde{\beta}_1)$ is monotonically increasing in the region of interest in Lemma 6.4.

Lemma 6.4: $g(\tilde{\beta}_1)$ is monotonically increasing in the region specified by $\tilde{\beta}_1 > 0$ and $0 \leq x < 1$.

Proof: Proof can be found in Appendix C.2. ∎

As shown in the proof of Lemma 6.4, it is required that $d_1 \geq d_3^2 + d_4^2$ for this case to result a candidate solution. By Lemma 6.4, we can find the unique zero of $g(\tilde{\beta}_1)$ inside the region of interest using a bisection search whose steps are outlined in Algorithm 6.2 if it exists. Note that (6.63) requires that lower bound of $\tilde{\beta}_1$ is $\sqrt{\frac{E_3}{E_1 - E_2}}$. $g(\tilde{\beta}_1)$ goes to minus infinity when $\tilde{\beta}_1$ approaches this lower bound from the right. Hence, if $g\left(\sqrt{\frac{P_{max}}{d_1}}\right) \geq 0$, there is a unique zero inside the region of interest where $\sqrt{\frac{P_{max}}{d_1}}$ is the

125

upper bound for $\tilde{\beta}_1$ by (6.49c). If there is no zero, then we do not consider this case for a candidate solution.

Algorithm 6.2: Bisection Search for Finding the Unique Zero of $g(\tilde{\beta}_1)$

Initialization: Set initial lower and upper bounds as $L^{(0)} = \sqrt{\frac{E_3}{E_1 - E_2}}$ and $U^{(0)} = \sqrt{\frac{P_{max}}{d_1}}$, respectively. If $g(U^{(0)}) < 0$ or $U^{(0)} < L^{(0)}$ terminate. Otherwise, take the initial $\tilde{\beta}_1$ as $\tilde{\beta}_1^{(0)} = (L^{(0)} + U^{(0)})/2$. Set iteration number $i \leftarrow 0$.

Repeat

        If $g(\tilde{\beta}_1^{(i)}) < 0$, set $L^{(i+1)} = \tilde{\beta}_1^{(i)}$.

        ElseIf $g(\tilde{\beta}_1^{(i)}) > 0$, set $U^{(i+1)} = \tilde{\beta}_1^{(i)}$.

        Else Terminate.

$\tilde{\beta}_1^{(i+1)} = (L^{(i+1)} + U^{(i+1)})/2$.

Set $i \leftarrow i + 1$.

Until convergence criterion is met.

The solution corresponding to the zero found by Algorithm 6.2 is noted as a candidate if it satisfies (6.49c).

Case 2d: $\mu_1 > 0$, $\mu_2 > 0$.

In this case, both (6.49b) and (6.49c) are satisfied with equality. We again obtain x as in (6.63) by the equality in (6.50e). Furthermore, $\tilde{\beta}_2 = \sqrt{\frac{P_{max}}{d_1} - \tilde{\beta}_1^2}$. If $d_4 = 0$, we obtain $\tilde{\beta}_2 = 0$ by (6.50b). Then, $\tilde{\beta}_1 = \sqrt{\frac{P_{max}}{d_1}}$. For $d_4 > 0$ case, inserting $\tilde{\beta}_2$ and (6.63) into (6.49a), we obtain the following unconstrained optimization problem in terms of $\tilde{\beta}_1$, i.e.,

$$\max_{\tilde{\beta}_1} \quad d_2 \sqrt{\frac{(E_1 - E_2)\tilde{\beta}_1^2 - E_3}{E_1 \tilde{\beta}_1^2 - E_3}} + d_3 \tilde{\beta}_1 + d_4 \sqrt{\frac{P_{max}}{d_1} - \tilde{\beta}_1^2} \qquad (6.66)$$

126

Let us take the derivative of the objective function in (6.66) and equate it to zero, i.e.,

$$h(\tilde{\beta}_1) = d_2 \frac{g_1'(\tilde{\beta}_1)}{2\sqrt{g_1(\tilde{\beta}_1)}} + d_3 - \frac{d_4 \tilde{\beta}_1}{\sqrt{\frac{P_{max}}{d_1} - \tilde{\beta}_1^2}} = 0 \qquad (6.67)$$

where $g_1(\tilde{\beta}_1) = \frac{(E_1-E_2)\tilde{\beta}_1^2 - E_3}{E_1\tilde{\beta}_1^2 - E_3}$ is as defined in the previous part. Its derivative is given by $g_1'(\tilde{\beta}_1) = \frac{2E_2 E_3 \tilde{\beta}_1}{(E_1\tilde{\beta}_1^2 - E_3)^2}$. Now, we will claim that $h(\tilde{\beta}_1)$ is monotonically decreasing in the region of interest in Lemma 6.5.

Lemma 6.5: $h(\tilde{\beta}_1)$ is monotonically decreasing in the region specified by $\tilde{\beta}_1 > 0$, $\tilde{\beta}_2 \geq 0$ and $0 \leq x < 1$.

Proof: Proof can be found in Appendix C.3. ∎

By Lemma 6.5, we can find the unique zero of $h(\tilde{\beta}_1)$ inside the region of interest using a bisection search whose steps are outlined in Algorithm 6.3. Note that (6.63) requires that lower bound of $\tilde{\beta}_1$ is $\sqrt{\frac{E_3}{E_1-E_2}}$. $h(\tilde{\beta}_1)$ goes to plus infinity when $\tilde{\beta}_1$ approaches this lower bound from the right. Furthermore, $h\left(\sqrt{\frac{P_{max}}{d_1}}\right)$ is minus infinity which shows that there always exists a zero inside the region of interest.

Algorithm 6.3: Bisection Search for Finding the Unique Zero of $h(\tilde{\beta}_1)$

Initialization: Set initial lower and upper bounds as $L^{(0)} = \sqrt{\frac{E_3}{E_1-E_2}}$ and $U^{(0)} = \sqrt{\frac{P_{max}}{d_1}}$, respectively. If $U^{(0)} < L^{(0)}$ terminate. Otherwise, take the initial $\tilde{\beta}_1$ as $\tilde{\beta}_1^{(0)} = (L^{(0)} + U^{(0)})/2$. Set iteration number $i \leftarrow 0$.

Repeat

    If $h(\tilde{\beta}_1^{(i)}) > 0$, set $L^{(i+1)} = \tilde{\beta}_1^{(i)}$.

    ElseIf $h(\tilde{\beta}_1^{(i)}) < 0$, set $U^{(i+1)} = \tilde{\beta}_1^{(i)}$.

    Else Terminate.

$\tilde{\beta}_1^{(i+1)} = (L^{(i+1)} + U^{(i+1)})/2$.

Set $i \leftarrow i + 1$.

Until convergence criterion is met.

For the Case 2c and Case 2d, we will keep x constant for each candidate solution and include the ignored term $\frac{\sigma_r^2}{1-x^2}$ as in the original problem in (6.49). Then, we will obtain a near-optimum candidate solution by solving (6.49). KKT conditions for constant x is given as (6.50a-b), (6.50d-g). We will now briefly go over all cases.

Case 1: $\mu_1 = 0$, $\mu_2 = 0$.
If $d_3 = 0$, we obtain $\tilde{\beta}_1 = 0$ by (6.50a) which results zero SNR. Hence, we do not consider this case if $d_3 = 0$. Otherwise, we obtain

$$\tilde{\beta}_2 = \frac{d_4}{d_3}\tilde{\beta}_1 \tag{6.68a}$$

$$d_2 x + d_3 \tilde{\beta}_1 + d_4 \tilde{\beta}_2 = \frac{d_1 + \frac{\sigma_r^2}{1-x^2}}{d_3}\tilde{\beta}_1 \tag{6.68b}$$

If we insert (6.68a) into (6.68b), we obtain $\tilde{\beta}_1$ and thus $\tilde{\beta}_2$ from (6.68a). If they satisfy (6.49b) and (6.49c), they are noted as a candidate solution.

Case 2: $\mu_1 = 0$, $\mu_2 > 0$.
If $d_3 = 0$, we again obtain $\tilde{\beta}_1 = 0$ which is not a candidate solution. For $d_3 > 0$, by (6.50a-b), we obtain (6.68a). In addition, (6.49c) should be satisfied with equality. Hence, we obtain $\tilde{\beta}_1$ as follows,

$$\tilde{\beta}_1 = \sqrt{\frac{P_{max} d_3^2}{(d_1 + \frac{\sigma_r^2}{1-x^2})(d_3^2 + d_4^2)}}. \tag{6.69}$$

If this solution satisfies also (6.49b), it is a candidate solution.

Case 3: $\mu_1 > 0$, $\mu_2 = 0$.
In this case, (6.49b) is satisfied with equality. Hence, we obtain

$$\tilde{\beta}_1 = \sqrt{\frac{\gamma \sigma_d^2}{P_s \lambda_H^2 ||\mathbf{g}||^2 - \frac{\gamma \sigma_r^2 ||\mathbf{g}||^2}{1-x^2}}}. \tag{6.70}$$

We can obtain $\tilde{\beta}_2$ easily by (6.50b). For this solution to be candidate, it is required that (6.49c) is satisfied.

Case 4: $\mu_1 > 0$, $\mu_2 > 0$.

In this case, both (6.49b) and (6.49c) are satisfied with equality. In this case, $\tilde{\beta}_1$ is given in (6.70). And $\tilde{\beta}_2$ is found by (6.50f).

Now, using these last four cases, we can construct $\mathcal{S}_u$ whose elements are the corresponding candidate pairs $\{\beta_1, \beta_2\}$ which are obtained as $\beta_1 = \frac{\tilde{\beta}_1}{\sqrt{\alpha}}$ and $\beta_2 = \frac{\tilde{\beta}_2}{\sqrt{\alpha}}$ where $\alpha = 1 - x^2$. In this case, we can update β_1 and β_2 as follows,

$$\{\beta_1^\star, \beta_2^\star\} = \arg\min_{\{\beta_1,\beta_2\}\in\mathcal{S}_u} (\beta_1^2 + \beta_2^2)(P_s\alpha\lambda_H^2 + \sigma_r^2)$$
$$-\eta P_s\left(||\mathbf{h}||\sqrt{1-\alpha} + \lambda_H\sqrt{\alpha}(c_1\beta_1 + c_2\beta_2)\right)^2. \tag{6.71}$$

Let us construct the set $\mathcal{S}$ whose elements are the candidate $\{\beta_1, \beta_2, \alpha\}$ obtained from Case (1a-1d) and Case (2a-2d). If $\mathcal{S} \neq \emptyset$, then the near-optimum solution of (6.39) is given as follows,

$$\{\beta_1^\star, \beta_2^\star, \alpha^\star\} = \arg\min_{\{\beta_1,\beta_2,\alpha\}\in\mathcal{S}} (\beta_1^2 + \beta_2^2)(P_s\alpha\lambda_H^2 + \sigma_r^2)$$
$$-\eta P_s\left(||\mathbf{h}||\sqrt{1-\alpha} + \lambda_H\sqrt{\alpha}(c_1\beta_1 + c_2\beta_2)\right)^2. \tag{6.72}$$

Using (6.72), near-optimum beamformer $\mathbf{v}_r^\star$ for the problem in (6.38) is obtained by Lemma 6.3 as $\mathbf{v}_r^\star = \beta_1^\star\mathbf{\Psi}_1 + \beta_2^\star e^{j\angle\mathbf{f}^H\mathbf{g}}\mathbf{\Psi}_2$.

6.5 Simulation Results

In this section, the performance of the proposed joint power allocation and beamforming is evaluated for several scenarios. The simulation parameters are selected as follows. There are $M = 32$ antennas at $\mathbf{S}$. The variances of the $\mathbf{R}$ and $\mathbf{D}$ noises are set as $\sigma_r^2 = \sigma_d^2 = -110$ dBW. The energy harvesting efficiency and transmission power limit of $\mathbf{R}$ are $\eta = 0.2$ and $P_{max} = -10$ dBW, respectively. The target SNR at $\mathbf{D}$ is $\gamma = 10$ dB for QoS-aware optimization problem. Rayleigh fading is assumed for the all channels, i.e., $\mathbf{H}$, $\mathbf{h}$, $\mathbf{g}$, and $\mathbf{f}$. The path loss for the channels $\mathbf{H}$, $\mathbf{h}$, and $\mathbf{g}$ are 60 dB. Unless otherwise stated, the path loss for the self-energy recycling loop channel,

$\mathbf{f}$, is 10 dB. The number of transmit antennas of $\mathbf{R}$ is $N = 8$. The source power is $P_s = 0$ dBW. In the following figures, each point represents the average of randomly generated 1000 channel realizations.

In the first part of the simulations, SNR maximization problem is considered. In Fig. 6.2, destination SNR is plotted in terms of the source power, P_s and the performances of several methods are compared. "PM for JPA-B" stands for the proposed method for the joint power allocation and relay transmit beamforming which is presented in Section 6.3. "EPA with TPC" is equal power allocation approach with transmission power limit constraint included as in the proposed method. The result of this method is obtained by taking α constant at 0.5 and solving the problem by using the KKT conditions given in Section 6.3. The same procedure is applied for "EPA without TPC" without including transmit power limit constraint. This method is equivalent to the one in [19]. In the considered scenarios, these two methods give the same result as expected. As shown in Fig. 6.2 , the proposed method provides 3 dB higher SNR compared to the equal power division approach. In addition, EPA with TPC and without TPC perform the same indicating the transmission power limit P_{max} does not restrict the optimization problem.

In Fig. 6.3, we compare the destination SNR for the above methods by varying path loss for the loop channel. As expected, increase in path loss decreases SNR by limiting energy harvested by self-energy recycling via loop channel $\mathbf{f}$. Similarly, there is a 3 dB SNR gain provided by the proposed method compared to its equal power allocation counterpart.

In Fig. 6.4, we change the number of transmit antennas at $\mathbf{R}$ from $N = 8$ to $N = 40$. For N less than 32, the SNR gain of the proposed method is 3 dB. As N increases, the gain becomes smaller. From $N = 8$ until $N = 32$, EPA without TPC gives the same result with EPA without TPC showing that transmission power limit constraint does not affect the optimality of the optimization problem. However, EPA without TPC results significantly higher SNR for $N = 40$ case. However, this is not a fair comparison. In fact, the average transmission power for EPA without TPC is 0.3471 W which is 3.471 times of P_{max}. Since there is no constraint for transmission power limit in the method of [19], higher SNR is resulted. Our proposed method also takes
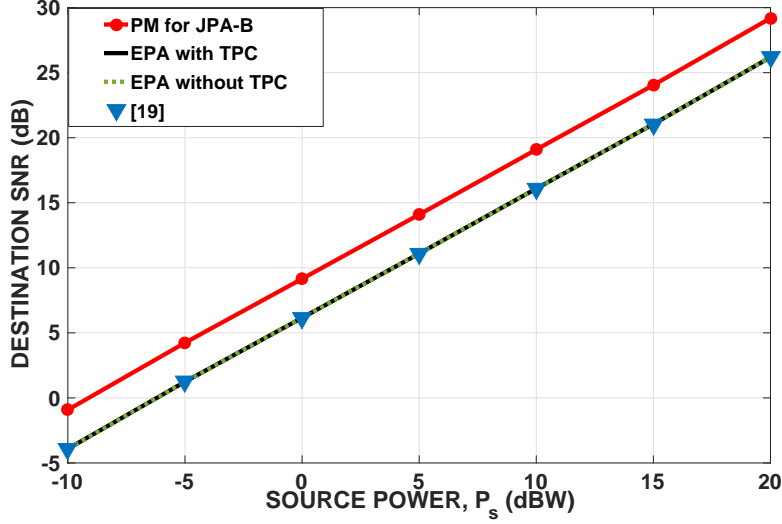
Figure 6.2: Destination SNR versus source power, P_s.

into account the transmission power constraint and hence presents a more practical solution.

In Fig. 6.5, 6.6, and 6.7 we consider QoS-aware optimization problem presented in Section 6.4. We select the method in [21] as benchmark for our comparison. The method in [21] assumes equal power allocation and includes transmission power constraint. EPA with TPC solves the same optimization problem by applying the KKT conditions presented in this chapter. We verify that they are equal in the following scenarios. In Fig. 6.5, we plot transmission power minus the harvested power, $P_r - P_h$, which is the objective function of the QoS-aware optimization problem. The PM always performs better and the difference between PM and EPA increases with P_s. $P_r - P_h$ is usually negative and this means that the harvested power is greater compared to the transmitted power. Hence, power saving is possible for these scenarios. As it can be seen from Fig. 6.5, the difference between harvested and transmitted power is approximately two times greater for the proposed method showing its efficiency in terms of power saving.

In Fig. 6.6, path loss for the loop channel $\mathbf{f}$ is varied. When path loss is 6 dB, power saving is possible for the proposed method since harvested power is greater than the transmitted power while the reverse is true for equal power allocation method. As the path loss increases, the power required by the relay's own battery increases for both

131
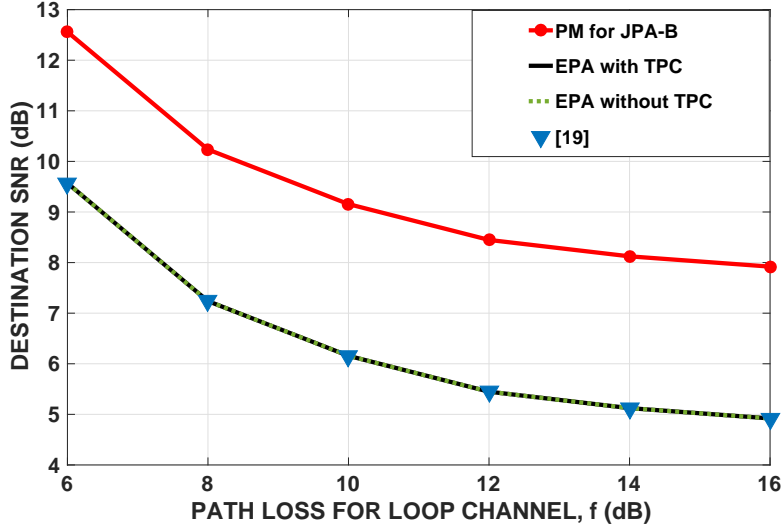
Figure 6.3: Destination SNR versus path loss for loop channel, **f**.

methods. However, the extra power needed for PM is about two times less compared to EPA.

In Fig. 6.7, we change the number of transmit antennas at **R**, N. As N increases, the difference between the transmitted and harvested power decreases for both methods. At $N = 28$, the difference becomes about 2.4 times more negative for PM compared to EPA. When N becomes 32, power saving significantly increases due to strong self-energy recycling channel between transmit and energy harvesting antennas at **R**.

6.6   Conclusion

In this chapter, the joint optimization of power allocation between information and energy signals at the source side and the relay transmit beamformer is considered for the self-energy recycling wireless-powered relaying. Two design approaches are adopted. The first one aims at maximizing destination SNR subject to the constraint that transmission power is less than the maximum power limit and the harvested power. The joint optimum power division parameter and relay transmit beamformer are derived for this problem. The second problem minimizes the difference of transmitted and harvested power at the relay subject to the SNR and maximum power limit constraints. A near-optimum joint solution is found for this QoS-aware design prob-
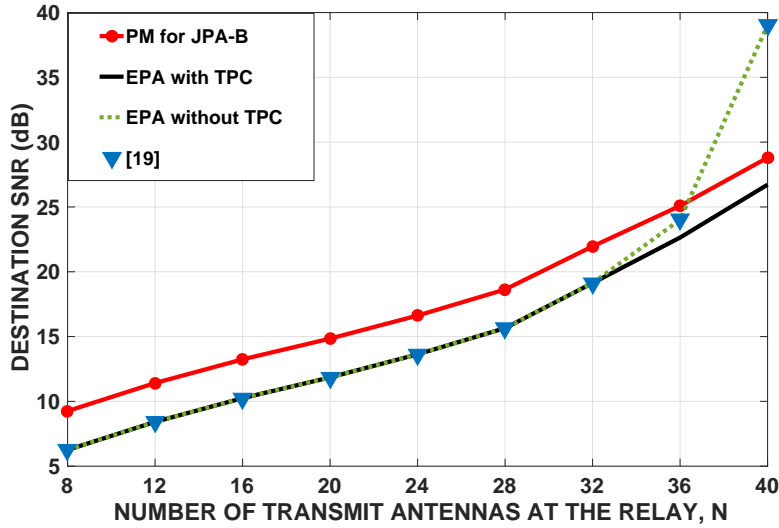
Figure 6.4: Destination SNR versus number of transmit antennas at the relay, N.

lem. As shown in the simulations, the proposed method provides 3 dB higher SNR for the SNR maximization problem compared to the equal power allocation whereas it results two times less power by the relay's own battery and two times more power savings when the objective is negative valued.
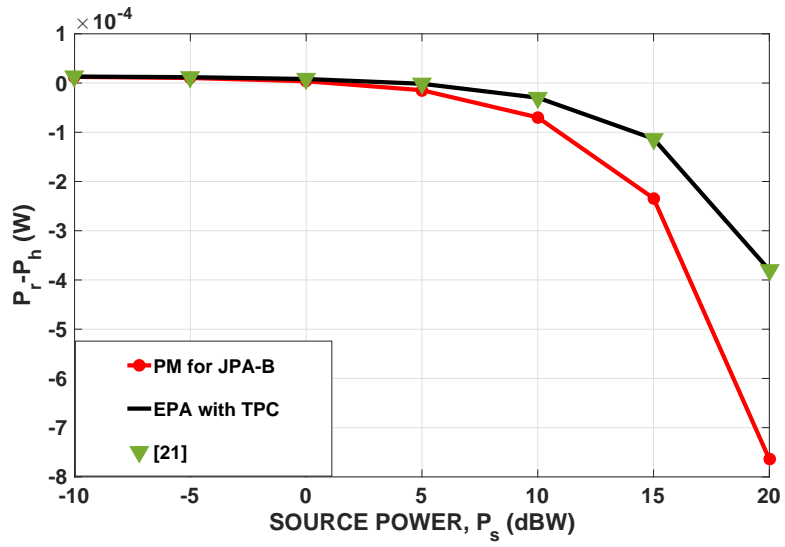
Figure 6.5: $P_r - P_h$ versus source power, P_s.
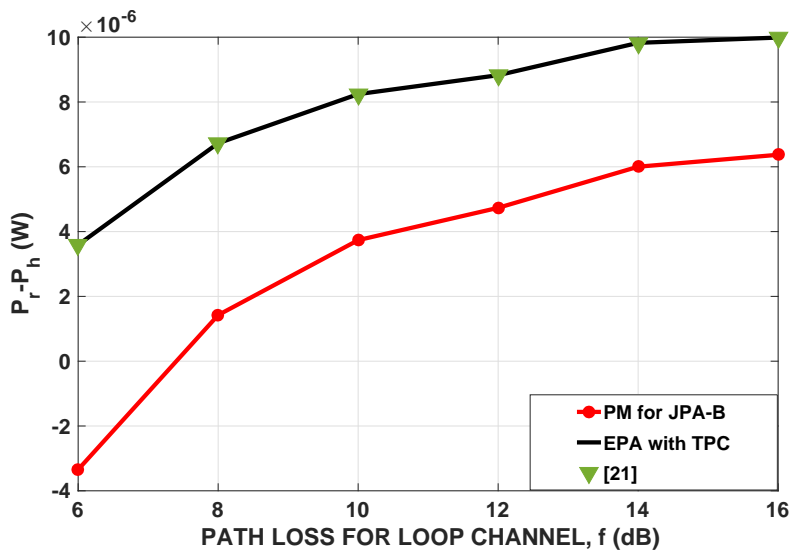
Figure 6.6: $P_r - P_h$ versus path loss for loop channel, $\mathbf{f}$.

134
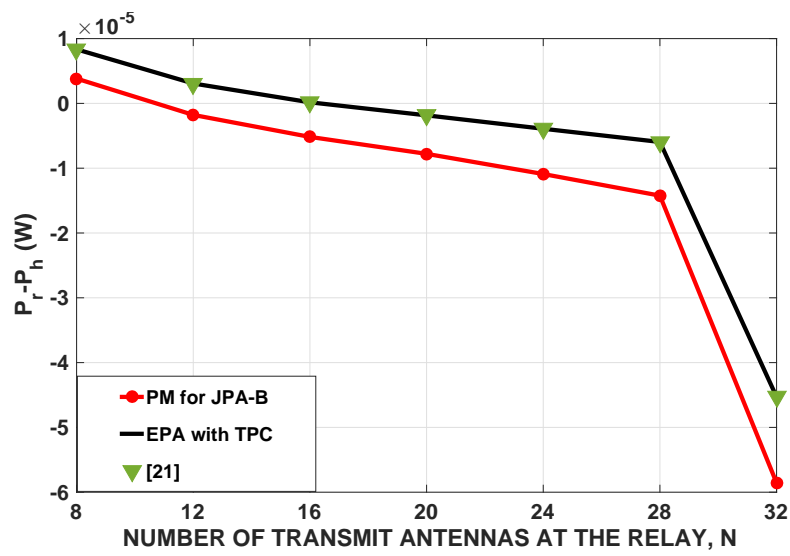
Figure 6.7: $P_r - P_h$ versus number of transmit antennas at the relay, N.

CHAPTER 7

OPTIMUM AND NEAR-OPTIMUM BEAMFORMERS FOR DECODE-AND-FORWARD FULL-DUPLEX MULTI-ANTENNA RELAY WITH SELF-ENERGY RECYCLING

In this chapter, we consider the full-duplex decode-and-forward wireless-powered relaying system which employs energy harvesting protocol with power splitting. The joint optimum relay transmit beamformer and power splitting factor are obtained for the quality of service (QoS)-aware problem for the first time in the literature. The optimum solution is found by analyzing the Karush-Kuhn-Tucker conditions thanks to the effective reformulation of the problem in an equivalent and simplified manner. In addition, the signal-to-interference-plus-noise ratio (SINR) maximization problem is investigated in order to find the joint optimum solution. Simulation results verify the optimality of the proposed method compared to the sub-optimum one which is presented in [49]. In the next part of the chapter, the considered system is generalized by employing multiple receive antennas at the relay. Both QoS-aware and SINR maximization problems are considered. The near-optimum relay transmit and receive beamformers as well as power splitting factor are found by optimizing the variables alternately. First, transmit beamformer and power splitting factor are found optimally for a given initial receive beamformer. Then, the optimum receive beamformer is obtained. Relay with multiple-receive antennas is shown to perform better than the single receive antenna relay in terms of SINR and transmission power.

7.1 Introduction

In [65], power splitting (PS)-based SWIPT with decode-and-forward full duplex (FD) relaying is considered for single transmit and single receive antenna relay. Then in [49], this scenario is generalized by employing multiple transmit antennas at the relay. A sub-optimum solution is presented for signal-to-interference-plus-noise ratio (SINR) maximization problem.

Unlike SINR maximization, quality-of-service (QoS)-aware design problem is not considered in the literature for the above mentioned system to the best of authors' knowledge. In this chapter, we first study the QoS-aware design optimization and present the optimum solution. In this problem, the aim is to minimize the transmission power used by the relay's own battery such that the effective SINR of the system is above a certain threshold. The optimization variables are the relay transmit beamformer and power splitting ratio. The joint optimum solution is found by reformulating the original problem to obtain and equivalent but simple form. Using a proper basis for the transmit beamformer and reducing the dimension of the problem size enables us to analyze Karush-Kuhn-Tucker (KKT) conditions easily. In the following part of the chapter, we revisit the SINR maximization problem whose sub-optimum solution is given in [49]. Using bisection search over SINR threshold for QoS-aware problem, we obtain the optimum solution for the SINR maximization as well. In the simulation results, the proposed optimum solution always perform better than the sub-optimum one in [49] and for some scenarios the performance difference between the two methods becomes significantly large.

In the above problems, it is assumed that there are multiple transmit antennas whereas there is a single receive antenna at the relay. There are several works in the literature which prove the efficiency of multiple receive antennas in energy harvesting systems [66], [67]. In this chapter, we further study QoS-aware and SINR maximization problems for multiple-receive antenna case. Since the joint optimum solution is difficult to obtain, we follow an alternating optimization approach for the design of transmit and receive beamformers together with power splitting factor. First, receive beamformer is initialized properly and the joint optimum transmit beamformer and power splitting factor are found by keeping the receive beamformer constant. Then, trans-

mit beamformer and power splitting factor are kept constant and the optimum receive beamformer is obtained. This procedure results a near-optimum solution to the QoS-aware problem. Then, using a bisection search similar to the single antenna case, we present a near-optimum solution for SINR maximization problem. Several simulations are performed and it is shown that using multiple receive antennas increases the SINR and energy performance of the system. As the number of antennas increases, the improvement becomes more significant.

7.2 System Model

We consider the full-duplex relaying system shown in Fig. 7.1 where the relay node **R** assists source node **S** for information transmission to the single-antenna destination, **D**. **S** and **R** have M and N transmitting antennas, respectively. In addition, **R** has a single receive antenna. While **S** sends information signal to **R**, **R** harvests energy from some portion of its received signal. **R** uses the remaining portion of the RF received signal for decode-and-forward (DF) protocol to transmit the information to **D**. In this chapter, block fading channels and perfect channel state information (CSI) are assumed in accordance with [49]. This will enable us to find the theoretical performance limit of the considered system. Let $s[i]$ denote the information symbol

Figure 7.1: System model.
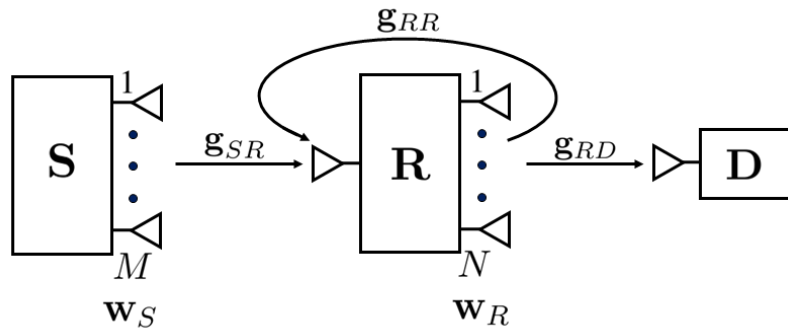
to be transmitted at time instant i. $s[i]$ is assumed to have unit average power, i.e., $\mathbb{E}\{|s[i]|^2\} = 1$. As in [49], we assume that the information symbol is correctly decoded at **R**. In this case, the forwarded symbol by **R** is given by $s[i-\tau]$ where $\tau \geq 1$ is the processing delay introduced by **R**. Note that the optimum transmit beamformer for

139

S is the maximal ratio combiner given by $\mathbf{w}_S = \sqrt{P_S}\mathbf{g}_{SR}/\|\mathbf{g}_{SR}\|$ where $\mathbf{g}_{SR} \in \mathbb{C}^{M \times 1}$ is the baseband equivalent channel from **S** to the single receiving antenna of **R** as shown in Fig. 7.1. Let $\mathbf{w}_R \in \mathbb{C}^{N \times 1}$ denote the relay transmit beamforming vector. In this case, transmission power of **R** is given by $P_R = \mathbf{w}_R^H \mathbf{w}_R$. The baseband equivalent received signal at **R** is given by

$$y_R[i] = \sqrt{P_S}\|\mathbf{g}_{SR}\|s[i] + \mathbf{w}_R^H \mathbf{g}_{RR} s[i - \tau] + n_{RA}[i] \tag{7.1}$$

where $\mathbf{g}_{RR} \in \mathbb{C}^{N \times 1}$ is the loop interference channel between transmitting and receiving antennas of **R**. $n_{RA}[i]$ is the additive complex Gaussian noise at the receiving antenna of **R**, i.e., $n_{RA}[i] \sim \mathbb{CN}(0, \sigma_{RA}^2)$. The received signal at **D** is given by

$$y_D[i] = \mathbf{w}_R^H \mathbf{g}_{RD} s[i - \tau] + n_D[i] \tag{7.2}$$

where $\mathbf{g}_{RD} \in \mathbb{C}^{N \times 1}$ is the channel from **R** to **D**. Note that the direct link between **S** and **D** is ignored as in [49] due to severe attenuation. $n_D[i] \sim \mathbb{CN}(0, \sigma_D^2)$ is the additive noise at the receiver of **D**.

A portion of the received signal $y_R[i]$ is used for energy harvesting while the remaining part is used for information decoding. If we consider power splitting ratio as $0 \le \alpha \le 1$, the signal for energy harvesting is given by $y_R^E[i] = \sqrt{\alpha}y_R[i]$. Neglecting the noise power as in [49], the harvested power at **R** is expressed as

$$P_H = \eta\alpha\left(P_S\|\mathbf{g}_{SR}\|^2 + \left|\mathbf{w}_R^H \mathbf{g}_{RR}\right|^2\right) \tag{7.3}$$

where $0 < \eta < 1$ denotes the energy conversion efficiency of the energy harvesting circuit at **R**. In [49], a portion variable β is defined and the relation $P_R = \zeta\beta P_H$ is enforced where P_R is the transmission power of the relay and $0 < \zeta < 1$ is the energy utilization efficiency. In this chapter, we will use the constraint $P_R = \mathbf{w}_R^H \mathbf{w}_R \le \zeta P_H$ instead of this relation in SINR maximization problem where β is not introduced as a separate variable. Now, consider the remaining portion of the received relay signal for information decoding as given by

$$y_R^I[i] = \sqrt{1-\alpha}y_R[i] + n_{RI}[i] \tag{7.4a}$$

$$= \sqrt{(1-\alpha)P_S}\|\mathbf{g}_{SR}\|s[i] + \sqrt{1-\alpha}\mathbf{w}_R^H \mathbf{g}_{RR} s[i-\tau] + \sqrt{1-\alpha}n_{RA}[i] + n_{RI}[i] \tag{7.4b}$$

where $n_{RI}[i] \sim \mathbb{CN}(0, \sigma_{RI}^2)$ is the additive noise introduced by the digital baseband processor. In [49], antenna noise $\mathbf{n}_{RA}$ is neglected since $\sigma_{RA}^2 \ll \sigma_{RI}^2$ in practical systems [102]. Furthermore, ideal self-interference cancellation is not assumed in [49]. Instead, the following model is used for the received signal at the information decoder,

$$y_R^I[i] = \sqrt{(1-\alpha)P_S}||\mathbf{g}_{SR}||s[i] + \sqrt{1-\alpha}g_{LI}s[i - \tau] + n_{RI}[i] \qquad (7.5)$$

where g_{LI} denotes the estimation error of $\mathbf{w}_R^H\mathbf{g}_{RR}$ and if μ denotes the residual self interference level, g_{LI} can be modeled as $g_{LI} \sim \mathbb{CN}(0, \mu|\mathbf{w}_R^H\mathbf{g}_{RR}|^2)$ [103]. In this case, the signal-to-interference-plus-noise ratio (SINR) at the information decoder of $\mathbf{R}$ can be expressed as

$$\text{SINR}_R = \frac{(1-\alpha)P_S||\mathbf{g}_{SR}||^2}{(1-\alpha)\mu|\mathbf{w}_R^H\mathbf{g}_{RR}|^2 + \sigma_{RI}^2}. \qquad (7.6)$$

Similarly, signal-to-noise ratio (SNR) for $\mathbf{D}$ is given as follows,

$$\text{SNR}_D = \frac{|\mathbf{w}_R^H\mathbf{g}_{RD}|^2}{\sigma_D^2}. \qquad (7.7)$$

Note that the effective SINR of the system is determined by the minimum of SINR_R and SNR_D, i.e., $\text{SINR}_{eff} = \min\{\text{SINR}_R, \text{SNR}_D\}$. In the following section, we will first consider QoS-aware power minimization in order to find the joint optimum solution. Then, we will study the SINR maximization problem as in [49] and find the optimum solution in order to compare it with the suboptimal solution in [49].

7.3 QoS-Aware Design Optimization

In QoS-aware problem, the aim is to satisfy the constraint that the effective SINR is above some predetermined target threshold, γ. We will select the objective as to minimize the relay transmission power used by the relay's own battery, i.e., $P_R - \zeta P_H$. The addressed optimization problem can be formulated as follows,

$$\min_{\mathbf{w}_R, \alpha} \quad \mathbf{w}_R^H\mathbf{w}_R - \zeta\eta\alpha\left(P_S||\mathbf{g}_{SR}||^2 + |\mathbf{w}_R^H\mathbf{g}_{RR}|^2\right) \qquad (7.8a)$$

$$\text{s.t.} \quad \min\{\text{SINR}_R, \text{SNR}_D\} \geq \gamma \qquad (7.8b)$$

$$0 \leq \alpha \leq 1. \qquad (7.8c)$$

141

Note that the constraint in (7.8b) can be reformulated as two constraints, i.e.,

$$\min_{\mathbf{w}_R, \alpha} \quad \mathbf{w}_R^H \mathbf{w}_R - \zeta \eta \alpha \left(P_S ||\mathbf{g}_{SR}||^2 + \left| \mathbf{w}_R^H \mathbf{g}_{RR} \right|^2 \right) \tag{7.9a}$$

$$\text{s.t.} \quad \frac{(1-\alpha)P_S ||\mathbf{g}_{SR}||^2}{(1-\alpha)\mu \left| \mathbf{w}_R^H \mathbf{g}_{RR} \right|^2 + \sigma_{RI}^2} \geq \gamma \tag{7.9b}$$

$$\frac{\left| \mathbf{w}_R^H \mathbf{g}_{RD} \right|^2}{\sigma_D^2} \geq \gamma \tag{7.9c}$$

$$0 \leq \alpha \leq 1. \tag{7.9d}$$

In the following, we will first express (7.9) in a simple equivalent form and derive the optimum closed-form solution. In order to simplify the problem, let us express the relay beamformer vector as $\mathbf{w}_R = \sum_{n=1}^{N} \beta_n e^{j\theta_n} \mathbf{\Phi}_n$ by adopting the procedure in [21]. Here $\beta_n \geq 0$, $n = 1, ..., N$ and $\{\mathbf{\Phi}_n\}_{n=1}^{N}$ is an orthonormal basis for $\mathbb{C}^{N \times 1}$ such that $\mathbf{\Phi}_1 = \frac{\mathbf{g}_{RR}}{||\mathbf{g}_{RR}||}$ and $\mathbf{\Phi}_2 = \frac{\mathbf{g}_{RD} - \mathbf{\Phi}_1 \mathbf{\Phi}_1^H \mathbf{g}_{RD}}{||\mathbf{g}_{RD} - \mathbf{\Phi}_1 \mathbf{\Phi}_1^H \mathbf{g}_{RD}||}$. The remaining vectors are arbitrary. Then, optimum beamformer vector is given as in Lemma 7.1.

Lemma 7.1: The optimum relay beamformer vector for (7.9) is given in the form $\mathbf{w}_R = \beta_1 \mathbf{\Phi}_1 + \beta_2 e^{j \angle (\mathbf{g}_{RD}^H \mathbf{g}_{RR})} \mathbf{\Phi}_2$, where $\beta_1 \geq 0$ and $\beta_2 \geq 0$.

Proof: Let us first express the problem (7.9) in terms of $\{\beta_n, \theta_n\}_{n=1}^{N}$ as follows,

$$\min_{\{\beta_n, \theta_n\}_{n=1}^{N}, \alpha} \quad \sum_{n=1}^{N} \beta_n^2 - \zeta \eta \alpha \left(P_S ||\mathbf{g}_{SR}||^2 + ||\mathbf{g}_{RR}||^2 \beta_1^2 \right) \tag{7.10a}$$

$$\text{s.t.} \quad \frac{(1-\alpha)P_S ||\mathbf{g}_{SR}||^2}{(1-\alpha)\mu ||\mathbf{g}_{RR}||^2 \beta_1^2 + \sigma_{RI}^2} \geq \gamma \tag{7.10b}$$

$$\left| \beta_1 e^{-j\theta_1} \frac{\mathbf{g}_{RR}^H \mathbf{g}_{RD}}{||\mathbf{g}_{RR}||} + \beta_2 e^{-j\theta_2} \frac{\mathbf{g}_{RD}^H \mathbf{g}_{RD} - \mathbf{g}_{RD}^H \mathbf{\Phi}_1 \mathbf{\Phi}_1^H \mathbf{g}_{RD}}{||\mathbf{g}_{RD} - \mathbf{\Phi}_1 \mathbf{\Phi}_1^H \mathbf{g}_{RD}||} \right| \geq \sqrt{\gamma \sigma_D^2}. \tag{7.10c}$$

Note that any common phase rotation of $\{\theta_n\}_{n=1}^{N}$ does not change the optimality of the problem (7.10). Hence, θ_1 can be selected as zero without loss of generality. Let us first prove that optimum θ_2 is given by $\theta_2 = \angle \mathbf{g}_{RD}^H \mathbf{g}_{RR}$. This angle aligns the phase of the two terms inside the parentheses in (7.10c). Assume that the terms are not phase aligned. In this case, by aligning their phases, (7.10c) can be made a strict inequality. By this way, β_2 can be decreased still satisfying (7.10c) and improving the objective function. Hence, optimum θ_2 should be $\angle \mathbf{g}_{RD}^H \mathbf{g}_{RR}$. Now, suppose that at least one of β_n for $n = 3, ..., N$ is positive for the optimum solution. This β_n can be made zero by improving the objective function without violating any constraint. This contradicts

with the optimality of positive β_n for $n = 3, ..., N$. Hence, $\beta_n = 0$, $n = 3, ..., N$ for the optimum solution. ∎

Now, let us express (7.10) in terms of β_1, β_2, and α as follows,

$$\min_{\beta_1, \beta_2, \alpha} \quad \beta_1^2 + \beta_2^2 - \zeta\eta\alpha\left(P_S||\mathbf{g}_{SR}||^2 + ||\mathbf{g}_{RR}||^2\beta_1^2\right) \tag{7.11a}$$

$$\text{s.t.} \quad \frac{(1-\alpha)P_S||\mathbf{g}_{SR}||^2}{(1-\alpha)\mu||\mathbf{g}_{RR}||^2\beta_1^2 + \sigma_{RI}^2} \geq \gamma \tag{7.11b}$$

$$c_1\beta_1 + c_2\beta_2 \geq \sqrt{\gamma\sigma_D^2} \tag{7.11c}$$

$$0 \leq \alpha \leq 1 \tag{7.11d}$$

where $c_1 \triangleq \frac{\left|\mathbf{g}_{RR}^H\mathbf{g}_{RD}\right|}{||\mathbf{g}_{RR}||}$ and $c_2 = \frac{\mathbf{g}_{RD}^H\mathbf{g}_{RD} - \mathbf{g}_{RD}^H\Phi_1\Phi_1^H\mathbf{g}_{RD}}{||\mathbf{g}_{RD} - \Phi_1\Phi_1^H\mathbf{g}_{RD}||}$. Note that both c_1 and c_2 are nonnegative and it can be easily seen that optimum β_1 and β_2 for (7.11) should be nonnegative. Consider the contrary case where at least one of them is negative. Note that if both are negative, then (7.11c) cannot be satisfied. If only $\beta_1 < 0$, we can change its sign and (7.11c) becomes a strict inequality without changing other constraints and the objective function. In this case, we can decrease β_2 such that (7.11c) is an equality with an improved objective function. Hence, this results a contradiction. The other case when $\beta_2 < 0$ is similar. As a result, we didn't include extra nonnegativity constraints for β_1 and β_2 for simplicity.

For the ease of notation, define also $d_1 \triangleq \zeta\eta P_S||\mathbf{g}_{SR}||^2$, $d_2 \triangleq \zeta\eta||\mathbf{g}_{RR}||^2$, $d_3 \triangleq \frac{\mu||\mathbf{g}_{RR}||^2}{P_S||\mathbf{g}_{SR}||^2}$, and $d_4 \triangleq \frac{\sigma_{RI}^2}{P_S||\mathbf{g}_{SR}||^2}$. Using these parameters, Karush-Kuhn-Tucker (KKT)

necessary optimality conditions are given as follows,

$$2(1 - d_2\alpha)\beta_1 = \mu_1 \frac{-2(1 - \alpha)^2 d_3 \beta_1}{\left((1 - \alpha)d_3\beta_1^2 + d_4\right)^2} + \mu_2 c_1 \tag{7.12a}$$

$$2\beta_2 = \mu_2 c_2 \tag{7.12b}$$

$$- d_1 - d_2\beta_1^2 = \mu_1 \frac{-d_4}{\left((1 - \alpha)d_3\beta_1^2 + d_4\right)^2} + \mu_3 - \mu_4 \tag{7.12c}$$

$$\mu_1\left(\frac{1 - \alpha}{(1 - \alpha)d_3\beta_1^2 + d_4} - \gamma\right) = 0 \tag{7.12d}$$

$$\mu_2\left(c_1\beta_1 + c_2\beta_2 - \sqrt{\gamma\sigma_D^2}\right) = 0 \tag{7.12e}$$

$$\mu_3\alpha = 0, \quad \mu_4(1 - \alpha) = 0 \tag{7.12f}$$

$$\mu_1 \geq 0, \quad \mu_2 \geq 0, \quad \mu_3 \geq 0, \quad \mu_4 \geq 0 \tag{7.12g}$$

$$\text{(7.11b)-(7.11d)} \tag{7.12h}$$

where μ_1 and μ_2 are the Lagrange multipliers corresponding to the inequalities in (7.11b) and (7.11c), respectively. μ_3 and μ_4 are the Lagrange multipliers for $0 \leq \alpha$ and $\alpha \leq 1$, respectively. Note that if $\alpha = 1$, (7.11b) cannot be satisfied. Hence, $\alpha < 1$. This results $\mu_4 = 0$ by (7.12f). Now, we will consider two main cases by evaluating the value of α.

Case 1: $\alpha = 0$

Note that μ_1 cannot be zero as seen from (7.12c) since the sign of two sides are different in case $\mu_1 = 0$. Hence $\mu_1 > 0$ and (7.11b) is satisfied with equality by (7.12d). Additionally, μ_2 also cannot be zero. If it were zero, we would obtain $\beta_1 = \beta_2 = 0$ by (7.12a-b) which cannot satisfy the SINR constraints. Hence, $\mu_2 > 0$ and the inequality in (7.11c) is also an equality. By (7.12d) and (7.12e), we obtain,

$$\beta_1 = \sqrt{\frac{1}{\gamma d_3} - \frac{d_4}{d_3}}, \tag{7.13a}$$

$$\beta_2 = \frac{\sqrt{\gamma\sigma_D^2}}{c_2} - \frac{c_1}{c_2}\sqrt{\frac{1}{\gamma d_3} - \frac{d_4}{d_3}}. \tag{7.13b}$$

If β_1 and β_2 given in (7.13a-b) are both real and nonnegative, we note them as a candidate solution in order to use them later on.

Case 2: $0 < \alpha < 1$

In this case, both μ_3 and μ_4 are zero by (7.12f). μ_1 still cannot be zero by (7.12c).

Hence, (7.11b) is satisfied with equality. For the value of μ_2, we will consider two sub-cases as follows.

Case 2a: $\mu_2 = 0$

In this case, $\beta_2 = 0$ by (7.12b). Hence, β_1 should be positive in order to satisfy (7.11c). If we divide both sides of (7.12a) and (7.12c), we obtain the following relation,

$$\frac{1 - d_2\alpha}{-d_1 - d_2\beta_1^2} = \frac{(1 - \alpha)^2 d_3}{d_4}. \tag{7.14}$$

Furthermore, by the equality in (7.12d), we obtain

$$\beta_1^2 = \frac{1}{d_3\gamma} - \frac{d_4}{d_3(1 - \alpha)}. \tag{7.15}$$

If we insert the right side of (7.15) into (7.14) and rearrange the terms, we obtain the following quadratic equation, i.e.,

$$e_2\alpha^2 + e_1\alpha + e_0 = 0 \tag{7.16}$$

where e_2, e_1, and e_0 are defined as follows,

$$e_2 = d_1 d_3 + \frac{d_2}{\gamma}, \tag{7.17a}$$

$$e_1 = -2d_1 d_3 - 2\frac{d_2}{\gamma}, \tag{7.17b}$$

$$e_0 = d_4 + d_1 d_3 + \frac{d_2}{\gamma} - d_2 d_4. \tag{7.17c}$$

For each root of (7.16) which is between zero and one, we find β_1 by (7.15). If β_1 satisfies (7.11c) and it is real and nonnegative, we note the solution as a candidate.

Case 2b: $\mu_2 > 0$

In this case, (7.11c) is satisfied with equality by (7.12e). By the equalities in (7.12d) and (7.12e), we obtain

$$\alpha = \frac{1 - \gamma d_4 - \gamma d_3\beta_1^2}{1 - \gamma d_3\beta_1^2} \tag{7.18a}$$

$$\beta_2 = \frac{\sqrt{\gamma\sigma_D^2}}{c_2} - \frac{c_1}{c_2}\beta_1. \tag{7.18b}$$

Note that $0 < \alpha < 1$ if $1 - \gamma d_4 - \gamma d_3\beta_1^2 > 0$. We will use this condition to determine the candidate solutions in the following part. Now, if we insert (7.18a-b) into the objective

function in (7.11a), we obtain the following unconstrained optimization problem

$$\min_{\beta_1} \; \beta_1^2 + \left(\frac{\sqrt{\gamma \sigma_D^2}}{c_2} - \frac{c_1}{c_2} \beta_1 \right)^2 - (d_1 + d_2 \beta_1^2) \frac{1 - \gamma d_4 - \gamma d_3 \beta_1^2}{1 - \gamma d_3 \beta_1^2}. \tag{7.19}$$

Let us take the derivative of the objective function in (7.19) and equate it to zero, i.e.,

$$2\beta_1 - \frac{2c_1}{c_2} \left(\frac{\sqrt{\gamma \sigma_D^2}}{c_2} - \frac{c_1}{c_2} \beta_1 \right) - 2d_2 \beta_1 \frac{1 - \gamma d_4 - \gamma d_3 \beta_1^2}{1 - \gamma d_3 \beta_1^2}$$

$$+ (d_1 + d_2 \beta_1^2) \frac{2\gamma^2 d_3 d_4 \beta_1}{(1 - \gamma d_3 \beta_1^2)^2} = 0. \tag{7.20}$$

By rearranging the terms in (7.20), we obtain the following fifth order polynomial, i.e.,

$$f_5 \beta_1^5 + f_4 \beta_1^4 + f_3 \beta_1^3 + f_2 \beta_1^2 + f_1 \beta_1 + f_0 = 0 \tag{7.21}$$

where f_5, f_4, f_3, f_2, f_1, and f_0 are given as follows,

$$f_5 = \gamma^2 d_3^2 \left(1 + \frac{c_1^2}{c_2^2} - d_2 \right), \tag{7.22a}$$

$$f_4 = -\frac{\gamma^2 d_3^2 c_1 \sqrt{\gamma \sigma_D^2}}{c_2^2}, \tag{7.22b}$$

$$f_3 = -2\gamma d_3 \left(1 + \frac{c_1^2}{c_2^2} \right) + 2\gamma d_2 d_3, \tag{7.22c}$$

$$f_2 = \frac{2\gamma d_3 c_1 \sqrt{\gamma \sigma_D^2}}{c_2^2}, \tag{7.22d}$$

$$f_1 = \left(1 + \frac{c_1^2}{c_2^2} \right) + d_2(\gamma d_4 - 1) + \gamma^2 d_1 d_3 d_4, \tag{7.22e}$$

$$f_0 = \frac{-c_1 \sqrt{\gamma \sigma_D^2}}{c_2^2}. \tag{7.22f}$$

For each root of the polynomial in (7.21) check whether the condition $1 - \gamma d_4 - \gamma d_3 \beta_1^2 > 0$, which ensures α to be in the $0 < \alpha < 1$ range, is satisfied or not. Also check whether $\beta_2 \geq 0$ in (7.18b). If all the conditions are satisfied, then note the solution as a candidate optimum.

Let us construct the set $\mathcal{S}$ whose elements are the candidate $\{\beta_1, \beta_2, \alpha\}$ sets given in Case 1-3. If $\mathcal{S} \neq \emptyset$, the optimum solution of (7.11) and the optimum relay transmit

beamformer are given by

$$\{\beta_1^\star, \beta_2^\star, \alpha^\star\} = \underset{\{\beta_1, \beta_2, \alpha\} \in \mathbb{S}}{\operatorname{argmin}} \ \beta_1^2 + \beta_2^2 - d_1\alpha - d_2\alpha\beta_1^2, \tag{7.23a}$$

$$\mathbf{w}_R^\star = \beta_1^\star \boldsymbol{\Phi}_1 + \beta_2^\star e^{j\angle(\mathbf{g}_{RD}^H \mathbf{g}_{RR})} \boldsymbol{\Phi}_2. \tag{7.23b}$$

7.4 SINR Maximization

In SINR maximization problem, the aim is to maximize the effective SINR of the system under the power constraint given by $P_R \leq \zeta P_H$. The addressed optimization problem in terms of $\mathbf{w}_R$ and α can be formulated as follows,

$$\underset{\mathbf{w}_R, \alpha}{\max} \ \min\{\mathrm{SINR}_R, \mathrm{SNR}_D\} \tag{7.24a}$$

$$\text{s.t. } \mathbf{w}_R^H \mathbf{w}_R \leq \zeta\eta\alpha\left(P_S||\mathbf{g}_{SR}||^2 + \left|\mathbf{w}_R^H \mathbf{g}_{RR}\right|^2\right) \tag{7.24b}$$

$$0 \leq \alpha \leq 1. \tag{7.24c}$$

Similar to the previous part, let us express the relay beamformer vector as $\mathbf{w}_R = \sum_{n=1}^N \beta_n e^{j\theta_n} \boldsymbol{\Phi}_n$ where $\{\boldsymbol{\Phi}_n\}_{n=1}^N$ is the same orthonormal set as in the previous section. Then, optimum beamformer can be expressed in the following Lemma.

Lemma 7.2: The optimum relay beamformer vector for (7.24) is given in the form $\mathbf{w}_R = \beta_1 \boldsymbol{\Phi}_1 + \beta_2 e^{j\angle(\mathbf{g}_{RD}^H \mathbf{g}_{RR})} \boldsymbol{\Phi}_2$, where $\beta_1 \geq 0$ and $\beta_2 \geq 0$.

Proof: The proof is similar to that of Lemma 7.1. ∎

Let us express the optimization problem in terms of β_1, β_2, and α as follows,

$$\underset{\beta_1, \beta_2, \alpha}{\max} \ \min\left\{\frac{(1-\alpha)P_S||\mathbf{g}_{SR}||^2}{(1-\alpha)\mu||\mathbf{g}_{RR}||^2\beta_1^2 + \sigma_{RI}^2}, \frac{(c_1\beta_1 + c_2\beta_2)^2}{\sigma_D^2}\right\} \tag{7.25a}$$

$$\text{s.t} \quad \beta_1^2 + \beta_2^2 \leq \zeta\eta\alpha\left(P_S||\mathbf{g}_{SR}||^2 + ||\mathbf{g}_{RR}||^2\beta_1^2\right) \tag{7.25b}$$

$$0 \leq \alpha \leq 1. \tag{7.25c}$$

The problem in (7.25) can be equivalently reformulated as follows,

$$\max_{\beta_1,\beta_2,\alpha,t} \quad t \tag{7.26a}$$

$$\text{s.t.} \quad \frac{(1-\alpha)P_S\|\mathbf{g}_{SR}\|^2}{(1-\alpha)\mu\|\mathbf{g}_{RR}\|^2\beta_1^2 + \sigma_{RI}^2} \geq t \tag{7.26b}$$

$$\frac{(c_1\beta_1 + c_2\beta_2)^2}{\sigma_D^2} \geq t \tag{7.26c}$$

$$\beta_1^2 + \beta_2^2 \leq \zeta\eta\alpha\left(P_S\|\mathbf{g}_{SR}\|^2 + \|\mathbf{g}_{RR}\|^2\beta_1^2\right) \tag{7.26d}$$

$$0 \leq \alpha \leq 1. \tag{7.26e}$$

Now, consider the following problem for a fixed $t = t_0$, i.e.,

$$\min_{\beta_1,\beta_2,\alpha} \quad \beta_1^2 + \beta_2^2 - \zeta\eta\alpha\left(P_S\|\mathbf{g}_{SR}\|^2 + \|\mathbf{g}_{RR}\|^2\beta_1^2\right) \tag{7.27a}$$

$$\text{s.t.} \quad \frac{(1-\alpha)P_S\|\mathbf{g}_{SR}\|^2}{(1-\alpha)\mu\|\mathbf{g}_{RR}\|^2\beta_1^2 + \sigma_{RI}^2} \geq t_0 \tag{7.27b}$$

$$\frac{(c_1\beta_1 + c_2\beta_2)^2}{\sigma_D^2} \geq t_0 \tag{7.27c}$$

$$0 \leq \alpha \leq 1. \tag{7.27d}$$

If the optimum objective value in (7.27a) is less than zero, we can deduce that the optimum value of (7.26a) is greater than or equal to t_0. Using a bisection search over t by solving (7.27) at each point, we can obtain the optimum solution of (7.26) numerically. The steps of the proposed method are outlined in Algorithm 7.1. Note that solving (7.27) for a fixed t is equivalent to solving QoS-aware optimization problem in (7.11a-d) and the optimum solution at each iteration can be easily found.

Algorithm 7.1: Bisection Search for Finding the Optimum Solution of (7.26)

Initialization: Set initial lower bound as $L^{(0)} = 0$ and a proper upper bound $U^{(0)}$. Take the initial t as $t^{(0)} = (L^{(0)} + U^{(0)})/2$. Set the iteration number $r \leftarrow 0$.
Repeat

    If (7.27) for $t_0 = t^{(r)}$ is feasible and the optimum objective value is less than 0, set $L^{(r+1)} = t^{(r)}$ and $U^{(r+1)} = 3t^{(r)}$.

Else Set $U^{(r+1)} = t^{(r)}$.

$t^{(r+1)} = (L^{(r+1)} + U^{(r+1)})/2$

Set $r \leftarrow r + 1$.

Until convergence criterion is met.

Now, consider the following Lemma.

Lemma 7.3: The bisection search presented in Algorithm 7.1 converges to the optimum solution of (7.26).

Proof: In order to prove the Lemma, it is sufficient to show that if (7.27) is not feasible or results positive objective value for any t_0, the optimum objective value of (7.26a) should be less than t_0. We will prove this claim by contradiction. Suppose that (7.27) is not feasible or results positive objective value for $t_0 = t_0^1$. Suppose also the optimum objective value of (7.26a) is $t_0^2 > t_0^1$. In this case, (7.27) is feasible and has nonpositive optimum objective value for $t_0 = t_0^2$. By increasing α, we can make (7.27b) equal to t_0^1. This increase improves the objective function. Hence, (7.27) is both feasible and has nonpositive objective value for $t_0 = t_0^1$ which results a contradiction. ∎

7.5 Multiple Receive Antenna Case

In this section, we generalize the system in the previous section by employing multiple receive antennas at the relay. Multiple receive antennas at the relay increases spatial diversity and improves performance at the expense of system complexity.

Let K denote the number of receive antennas at **R** as shown in Fig. 7.2. In addition, let $\mathbf{G}_{SR} \in \mathbb{C}^{M \times K}$ be the channel from **S** to **R** and $\mathbf{w}_S$ be the source transmit beamformer vector such that $||\mathbf{w}_S|| = 1$. In this case, the received signal after receive beamforming at **R** is given by,

$$y_R[i] = \sqrt{P_S}\mathbf{w}_S^H \mathbf{G}_{SR}\mathbf{z}_R s[i] + \mathbf{w}_R^H \mathbf{G}_{RR}\mathbf{z}_R s[i - \tau] + n_{RA}[i] \tag{7.28}$$
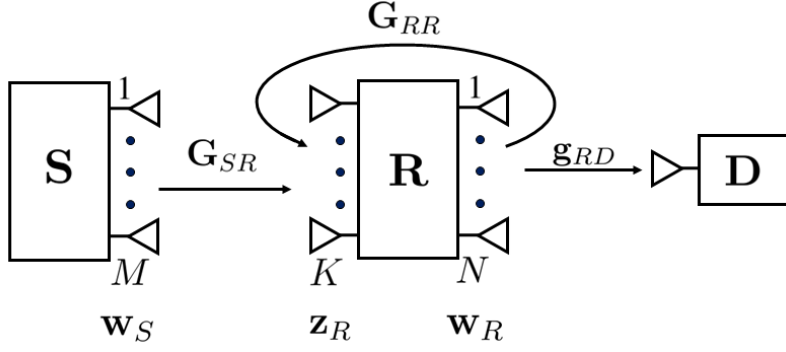
Figure 7.2: System model for multiple receive antenna case.

where $\mathbf{G}_{RR} \in \mathbb{C}^{N \times K}$ is the loop interference channel between transmitting and receiving antennas of $\mathbf{R}$. $\mathbf{z}_R \in \mathbb{C}^{K \times 1}$ is the receive beamformer weight vector at $\mathbf{R}$ such that $||\mathbf{z}_R|| = 1$. $n_{RA}[i]$ is the effective additive complex Gaussian noise after receive beamforming at $\mathbf{R}$ following $n_{RA}[i] \sim \mathbb{CN}(0, \sigma_{RA}^2)$. The received signal at $\mathbf{D}$ is the same as the previous section and is given by

$$y_D[i] = \mathbf{w}_R^H \mathbf{g}_{RD} s[i - \tau] + n_D[t]. \tag{7.29}$$

SNR for $\mathbf{D}$ is the same as in the previous section and given as follows,

$$\text{SNR}_D = \frac{|\mathbf{w}_R^H \mathbf{g}_{RD}|^2}{\sigma_D^2}. \tag{7.30}$$

The received relay signal for information decoding is given by

$$y_R^I[i] = \sqrt{(1 - \alpha)P_S} \mathbf{w}_S^H \mathbf{G}_{SR} \mathbf{z}_R s[i] + \sqrt{1 - \alpha} \mathbf{w}_R^H \mathbf{G}_{RR} \mathbf{z}_R s[i - \tau]$$
$$+ \sqrt{1 - \alpha} n_{RA}[i] + n_{RI}[i]. \tag{7.31}$$

In this chapter, we will design relay transmit and receive beamformers in a joint manner. Source transmit beamformer can be designed such that it enhances the desired signal $\mathbf{w}_S^H \mathbf{G}_{SR} \mathbf{z}_R s[i]$. In order to simplify the design procedure, we will select source beamformer $\mathbf{w}_S$ as the left singular vector of $\mathbf{G}_{SR}$ corresponding to the largest singular value. Let $\mathbf{G}_{SR} = \mathbf{U} \mathbf{\Lambda} \mathbf{V}^H$ be the singular value decomposition of $\mathbf{G}_{SR}$. Let λ_1 be the largest singular value and $\mathbf{v}_1$ be the corresponding right singular vector of $\mathbf{G}_{SR}$. Using the same assumptions and residual self interference model as in the previous section, the SINR at the information decoder of $\mathbf{R}$ is given by

$$\text{SINR}_R = \frac{(1 - \alpha)P_S \lambda_1^2 |\mathbf{v}_1^H \mathbf{z}_R|^2}{(1 - \alpha)\mu |\mathbf{w}_R^H \mathbf{G}_{RR} \mathbf{z}_R|^2 + \sigma_{RI}^2} \tag{7.32}$$

150

where μ is the residual self interference level. The RF signal for energy harvesting is $y_R^E[i] = \sqrt{\alpha} y_R[i]$ and the harvested power is given by

$$P_H = \eta \alpha \left(P_S \lambda_1^2 |\mathbf{v}_1^H \mathbf{z}_R|^2 + |\mathbf{w}_R^H \mathbf{G}_{RR} \mathbf{z}_R|^2 \right) \tag{7.33}$$

where η is the energy conversion efficiency.

In the following subsections, we will first analyze QoS-aware power minimization. Then, SINR maximization problem will be considered. Near-optimum solutions for both of these problems are presented in sequel.

7.5.1 QoS-Aware Optimization Problem

The QoS-aware design problem in terms of relay transmit and receive beamformers for multiple receive antenna can be formulated as follows,

$$\min_{\mathbf{w}_R, \mathbf{z}_R, \alpha} \quad \mathbf{w}_R^H \mathbf{w}_R - \zeta \eta \alpha \left(P_S \lambda_1^2 |\mathbf{v}_1^H \mathbf{z}_R|^2 + |\mathbf{w}_R^H \mathbf{G}_{RR} \mathbf{z}_R|^2 \right) \tag{7.34a}$$

$$\text{s.t.} \quad \frac{(1-\alpha) P_S \lambda_1^2 |\mathbf{v}_1^H \mathbf{z}_R|^2}{(1-\alpha)\mu |\mathbf{w}_R^H \mathbf{G}_{RR} \mathbf{z}_R|^2 + \sigma_{RI}^2} \geq \gamma \tag{7.34b}$$

$$\frac{|\mathbf{w}_R^H \mathbf{g}_{RD}|^2}{\sigma_D^2} \geq \gamma \tag{7.34c}$$

$$0 \leq \alpha \leq 1 \tag{7.34d}$$

$$||\mathbf{z}_R|| = 1. \tag{7.34e}$$

The joint optimum solution for (7.34) is not easy to obtain due to highly coupled terms of optimization variables. Instead, we will employ alternating optimization in order to obtain a solution. We first find the optimum transmit beamformer and power splitting ratio for a given receive beamformer. Then, we will update the receive beamformer optimally using the previous transmit beamformer and power splitting ratio. A good initial receive beamformer can be $\mathbf{z}_R^0 = \frac{\mathbf{v}_1 + \beta e^{j\angle \tilde{\mathbf{v}}_1^H \mathbf{v}_1} \tilde{\mathbf{v}}_1}{||\mathbf{v}_1 + \beta e^{j\angle \tilde{\mathbf{v}}_1^H \mathbf{v}_1} \tilde{\mathbf{v}}_1||}$ where $\tilde{\mathbf{v}}_1$ is the right singular vector corresponding to the largest singular value of $\mathbf{G}_{RR}$. With this selection, $\mathbf{v}_1$ and $\tilde{\mathbf{v}}_1$ vectors are phase aligned and the objective value in (7.34a) is enhanced. $\beta > 0$ parameter is selected to be less than one since $|\mathbf{w}_R^H \mathbf{G}_{RR} \mathbf{z}_R|$ term is to be minimized in

(7.34b) unlike (7.34a). In this case, we obtain the following optimization problem,

$$\min_{\mathbf{w}_R, \alpha} \quad \mathbf{w}_R^H \mathbf{w}_R - \zeta\eta\alpha\left(P_S\lambda_1^2|\mathbf{v}_1^H\mathbf{z}_R^0|^2 + |\mathbf{w}_R^H\mathbf{G}_{RR}\mathbf{z}_R^0|^2\right) \tag{7.35a}$$

$$\text{s.t.} \quad \frac{(1-\alpha)P_S\lambda_1^2|\mathbf{v}_1^H\mathbf{z}_R^0|^2}{(1-\alpha)\mu\left|\mathbf{w}_R^H\mathbf{G}_{RR}\mathbf{z}_R^0\right|^2 + \sigma_{RI}^2} \geq \gamma \tag{7.35b}$$

$$\frac{\left|\mathbf{w}_R^H\mathbf{g}_{RD}\right|^2}{\sigma_D^2} \geq \gamma \tag{7.35c}$$

$$0 \leq \alpha \leq 1. \tag{7.35d}$$

The above problem is similar to the one in (7.10) and the optimum solution can be easily found by following the same steps in the previous section. Let $\mathbf{w}_R^\star$ and $\alpha^\star$ denote the optimum transmit beamformer and power splitting ratio for (7.35), respectively. In this case, the optimization of $\mathbf{z}_R$ given $\mathbf{w}_R^\star$ and $\alpha^\star$ can be formulated as follows,

$$\min_{\mathbf{z}_R} \quad -P_S\lambda_1^2|\mathbf{v}_1^H\mathbf{z}_R|^2 - |(\mathbf{w}_R^\star)^H\mathbf{G}_{RR}\mathbf{z}_R|^2 \tag{7.36a}$$

$$\text{s.t.} \quad \frac{(1-\alpha^\star)P_S\lambda_1^2|\mathbf{v}_1^H\mathbf{z}_R|^2}{(1-\alpha^\star)\mu\left|(\mathbf{w}_R^\star)^H\mathbf{G}_{RR}\mathbf{z}_R\right|^2 + \sigma_{RI}^2} \geq \gamma \tag{7.36b}$$

$$||\mathbf{z}_R|| = 1. \tag{7.36c}$$

Let us express the relay beamformer vector as $\mathbf{z}_R = \sum_{k=1}^K \beta_k e^{j\theta_k}\mathbf{\Psi}_k$. Here $\beta_k \geq 0$, $k = 1, ..., K$, and $\{\mathbf{\Psi}_k\}_{k=1}^K$ is an orthonormal basis for $\mathbb{C}^{K\times 1}$ such that $\mathbf{\Psi}_1 = \frac{\mathbf{G}_{RR}^H\mathbf{w}_R^\star}{||\mathbf{G}_{RR}^H\mathbf{w}_R^\star||}$ and $\mathbf{\Psi}_2 = \frac{\mathbf{v}_1 - \mathbf{\Psi}_1\mathbf{\Psi}_1^H\mathbf{v}_1}{||\mathbf{v}_1 - \mathbf{\Psi}_1\mathbf{\Psi}_1^H\mathbf{v}_1||}$. The following lemma is presented to characterize the optimum solution.

Lemma 7.4: The optimum relay beamformer vector for (7.36) is given in the form $\mathbf{z}_R = \beta_1\mathbf{\Psi}_1 + \beta_2 e^{j\angle\mathbf{v}_1^H\mathbf{G}_{RR}^H\mathbf{w}_R^\star}\mathbf{\Psi}_2$.

Proof: Let us first express the problem (7.36) in terms of $\{\beta_k, \theta_k\}_{k=1}^K$ as follows,

$$\min_{\{\beta_k, \theta_k\}_{k=1}^K} \quad -P_S\lambda_1^2\left|\mathbf{v}_1^H\mathbf{\Psi}_1\beta_1 e^{j\theta_1} + \mathbf{v}_1^H\mathbf{\Psi}_2\beta_2 e^{j\theta_2}\right|^2 - ||\mathbf{G}_{RR}^H\mathbf{w}_R^\star||^2\beta_1^2 \tag{7.37a}$$

$$\text{s.t.} \quad (1-\alpha^\star)P_S\lambda_1^2\left|\mathbf{v}_1^H\mathbf{\Psi}_1\beta_1 e^{j\theta_1} + \mathbf{v}_1^H\mathbf{\Psi}_2\beta_2 e^{j\theta_2}\right|^2$$
$$- \gamma(1-\alpha^\star)\mu||\mathbf{G}_{RR}^H\mathbf{w}_R^\star||^2\beta_1^2 - \gamma\sigma_{RI}^2 \geq 0 \tag{7.37b}$$

$$\sum_{k=1}^K \beta_k^2 = 1. \tag{7.37c}$$

Note that any common phase rotation of $\{\theta_k\}_{k=1}^K$ does not change the optimality of the problem (7.37). Hence, θ_1 can be selected as zero without loss of generality. Let us first prove that optimum θ_2 is given by $\theta_2 = \angle \mathbf{v}_1^H \mathbf{G}_{RR}^H \mathbf{w}_R^\star$. This angle aligns the phase of the two terms in $\mathbf{v}_1^H \mathbf{\Psi}_1 \beta_1 e^{j\theta_1} + \mathbf{v}_1^H \mathbf{\Psi}_2 \beta_2 e^{j\theta_2}$. Assume that the terms are not phase aligned. In this case, by aligning their phases, objective function can be improved without changing the constraints. Hence, optimum θ_2 should be $\angle \mathbf{v}_1^H \mathbf{G}_{RR}^H \mathbf{w}_R^\star$. Now, suppose that at least one of β_k for $k = 3, ..., K$ is positive for the optimum solution. This β_k can be made zero by increasing the value of β_2 such that (7.37c) is still satisfied. In this case, the constraint in (7.37b) is not violated and the objective function improves which contradicts with the optimality. Hence, $\beta_k = 0$ is found for $k = 3, ..., K$ for the optimum solution. ∎

Let us express (7.37) in a simpler way using Lemma 7.4, i.e.,

$$\min_{\beta_1, \beta_2} \quad -(h_1\beta_1 + h_2\beta_2)^2 - h_3\beta_1^2 \tag{7.38a}$$

$$\text{s.t.} \quad k_1(h_1\beta_1 + h_2\beta_2)^2 - k_2\beta_1^2 - k_3 \geq 0 \tag{7.38b}$$

$$\beta_1^2 + \beta_2^2 = 1 \tag{7.38c}$$

where $h_1 \triangleq \sqrt{P_S}\lambda_1|\mathbf{v}_1^H\mathbf{\Psi}_1|$, $h_2 \triangleq \sqrt{P_S}\lambda_1\mathbf{v}_1^H\mathbf{\Psi}_2$, $h_3 = ||\mathbf{G}_{RR}^H\mathbf{w}_R^\star||^2$, $k_1 = (1 - \alpha^\star)$, $k_2 = \gamma(1-\alpha^\star)\mu||\mathbf{G}_{RR}^H\mathbf{w}_R^\star||^2$, and $k_3 = \gamma\sigma_{RI}^2$ are defined for the simplicity of notation. It is obviously seen that the optimum β_1 and β_2 should be nonnegative for (7.38). Hence, we did not include nonnegativity constraints for simplicity. KKT conditions for the problem (7.38) are given as follows

$$-2h_1(h_1\beta_1 + h_2\beta_2) - 2h_3\beta_1 = 2\mu_1\big(k_1h_1(h_1\beta_1 + h_2\beta_2) - k_2\beta_1\big) - 2\mu_2\beta_1 \tag{7.39a}$$

$$-2h_2(h_1\beta_1 + h_2\beta_2) = 2\mu_1 k_1 h_2(h_1\beta_1 + h_2\beta_2) - 2\mu_2\beta_2 \tag{7.39b}$$

$$\mu_1 \geq 0 \tag{7.39c}$$

$$\mu_1\bigg(k_1(h_1\beta_1 + h_2\beta_2)^2 - k_2\beta_1^2 - k_3\bigg) = 0 \tag{7.39d}$$

$$(7.38b)\text{-}(7.38c) \tag{7.39e}$$

where μ_1 and μ_2 are the Lagrange multipliers corresponding to the inequality and equality in (7.38b) and (7.38c), respectively. Now, we will consider three different cases for the candidate solutions.

Case 1: $\mu_1 = 0$, $\mu_2 = 0$

In this case, we obtain $\beta_1 = \beta_2 = 0$ by (7.39a-b) which cannot satisfy the constraint in (7.38b). Hence, we do not consider this case for a candidate.

Case 2: $\mu_1 = 0$, $\mu_2 \neq 0$

If we divide both sides of (7.39a) by (7.39b), we obtain

$$\frac{(h_1^2 + h_3)\beta_1 + h_1 h_2 \beta_2}{h_1 h_2 \beta_1 + h_2^2 \beta_2} = \frac{\beta_1}{\beta_2}. \tag{7.40}$$

If we rearrange the terms in (7.40) we obtain

$$h_1 h_2 \beta_1^2 + (-h_1^2 + h_2^2 - h_3)\beta_1 \beta_2 - h_1 h_2 \beta_2^2 = 0. \tag{7.41}$$

Let r denote the only nonnegative root of the quadratic equation in (7.41), i.e., $\beta_1 = r\beta_2$. Then we obtain $\beta_1 = \frac{r}{\sqrt{r^2+1}}$ and $\beta_2 = \frac{1}{\sqrt{r^2+1}}$ by (7.38c). This solution is noted as a candidate if it further satisfies (7.38b).

Case 3: $\mu_1 > 0$

In this case, the inequality in (7.38b) is satisfied with equality by the condition in (7.39d). Together with (7.38c), we can determine candidate solutions. By (7.38c), $\beta_2 = \sqrt{1 - \beta_1^2}$. If we insert this into (7.39d), we obtain

$$\frac{(k_1 h_1^2 - k_1 h_2^2 - k_2)\beta_1^2 + k_1 h_2^2 - k_3}{-2k_1 h_1 h_2 \beta_1} = \sqrt{1 - \beta_1^2}. \tag{7.42}$$

If we take the square of both sides we obtain

$$\frac{\left((k_1 h_1^2 - k_1 h_2^2 - k_2)\beta_1^2 + k_1 h_2^2 - k_3\right)^2}{4k_1^2 h_1^2 h_2^2 \beta_1^2} = 1 - \beta_1^2. \tag{7.43}$$

After rearranging the terms in (7.43), we obtain the following quadratic equation of β_1^2, i.e.,

$$l_2 \beta_1^4 + l_1 \beta_1^2 + l_0 = 0 \tag{7.44}$$

where l_2, l_1, and l_0 are given by

$$l_2 = (k_1 h_1^2 - k_1 h_2^2 - k_2)^2 + 4k_1^2 h_1^2 h_2^2, \tag{7.45a}$$

$$l_1 = 2(k_1 h_1^2 - k_1 h_2^2 - k_2)(k_1 h_2^2 - k_3) - 4k_1^2 h_1^2 h_2^2, \tag{7.45b}$$

$$l_0 = (k_1 h_2^2 - k_3)^2. \tag{7.45c}$$

We can solve (7.44) easily to find the candidate β_1. The roots of (7.44) should be between zero and one in order to be a candidate. Then, β_2 can be easily found by the relation $\beta_2 = \sqrt{1 - \beta_1^2}$.

Let us construct the set $\mathcal{S}$ whose elements are the candidate $\{\beta_1, \beta_2\}$ couples given in Case 1-3 above. If $\mathcal{S} \neq \emptyset$, the optimum solution of (7.38) is given by

$$\{\beta_1^\star, \beta_2^\star\} = \underset{\{\beta_1, \beta_2\} \in \mathcal{S}}{\operatorname{argmin}} - (h_1\beta_1 + h_2\beta_2)^2 - h_3\beta_1^2. \tag{7.46}$$

The optimum relay beamformer is then given as

$$\mathbf{z}_R^\star = \beta_1^\star \boldsymbol{\Psi}_1 + \beta_2^\star e^{j\angle \mathbf{v}_1^H \mathbf{G}_{RR}^H \mathbf{w}_R^\star} \boldsymbol{\Psi}_2. \tag{7.47}$$

7.5.2 SINR Maximization Problem

This part is similar to the Section 7.4. We can use a similar algorithm like Algorithm 7.1 and the solution of QoS-aware design problem presented in (7.46-47) to find the near-optimum solution of SINR maximization problem.

7.6 Simulation Results

In this section, several simulations are implemented in order to observe the performance of the proposed methods for power-splitting based decode-and-forward full-duplex relaying. In the simulations, PM-SA and PM-MA correspond to the proposed method with single receive antenna and multiple receive antenna, respectively. Note that PM-SA is a joint optimum method for both QoS-aware and SINR maximization problems. PM-MA is a near-optimum solution for the same problems where the relay has multiple receive antennas. For single receive antenna scenarios, we take the sub-optimum solution in [49] as a benchmark for comparison with the proposed optimum solution. The simulation parameters are selected as follows. There are $M = 32$ antennas at $\mathbf{S}$. The variances of the $\mathbf{R}$ and $\mathbf{D}$ noises are set as $\sigma_{RI}^2 = \sigma_D^2 = -110$ dBW. The energy conversion and utilization efficiencies are both selected as $\eta = \zeta = 0.7$. Rayleigh fading is assumed for the all channels. The path loss from $\mathbf{S}$ to $\mathbf{R}$ and $\mathbf{R}$ to $\mathbf{D}$ is 60 dB. Unless otherwise stated, the path loss for the loop interference channel

is 10 dB. The number of transmit and receive antennas at **R** is $N = 32$ and $K = 4$, respectively. The source power is $P_S = 0$ dBW. The SINR threshold is $\gamma = 10$ dB for QoS-aware design problems. In the following figures, each point represents the average of randomly generated 100 channel realizations.
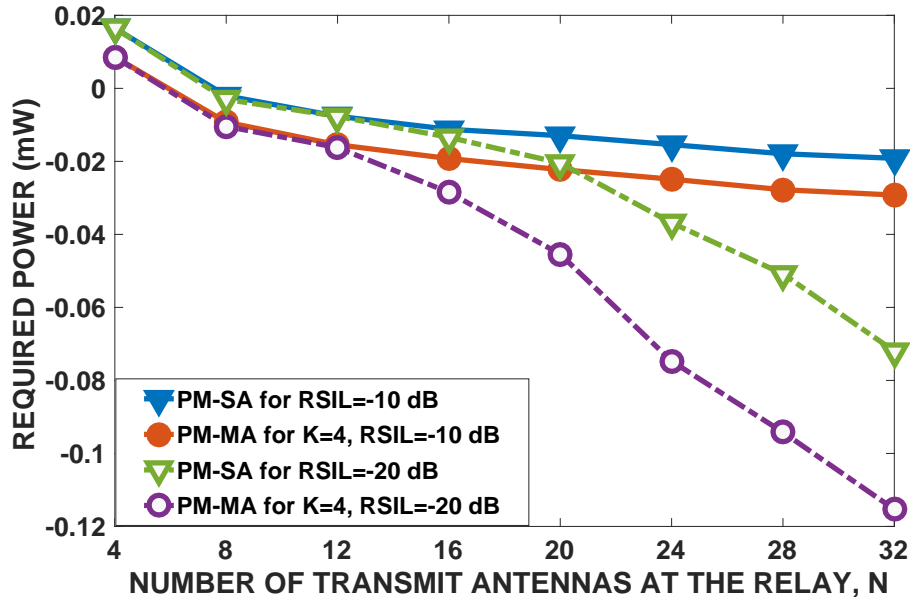

Figure 7.3: The required power by the relay's own battery, $P_R - \zeta P_H$, versus number of transmit antennas at the relay, N, for RSIL=-10 dB and RSIL=-20 dB.

In the first four figures, i.e. Fig. 7.3-6, we evaluate the performance of the proposed QoS-aware design problems for both single and multiple receive antenna scenarios. In Fig. 7.3, the number of transmit antennas at the relay is varied from $N = 4$ to $N = 32$ and the required power by the relay's own battery is plotted. The objective of the QoS-aware problem is $P_R - \zeta P_H$ and this is also the required power extracted from the relay's own battery. It can be positive or negative based on the system requirements. When it is positive, additional transmit power is required in order to satisfy the SINR need of the system. On the other hand, power saving is possible when it is negative. Therefore, the transmit power is less than the harvested power. In Fig. 7.3, the results of the proposed method for single, $K = 1$, and $K = 4$ receive antennas are shown for two different residual self interference level (RSIL), μ. When the number of transmit antennas at the relay is small, i.e., $N = 4$, relay battery should supply power in addition to the harvested power. As N increases, the harvested power becomes more
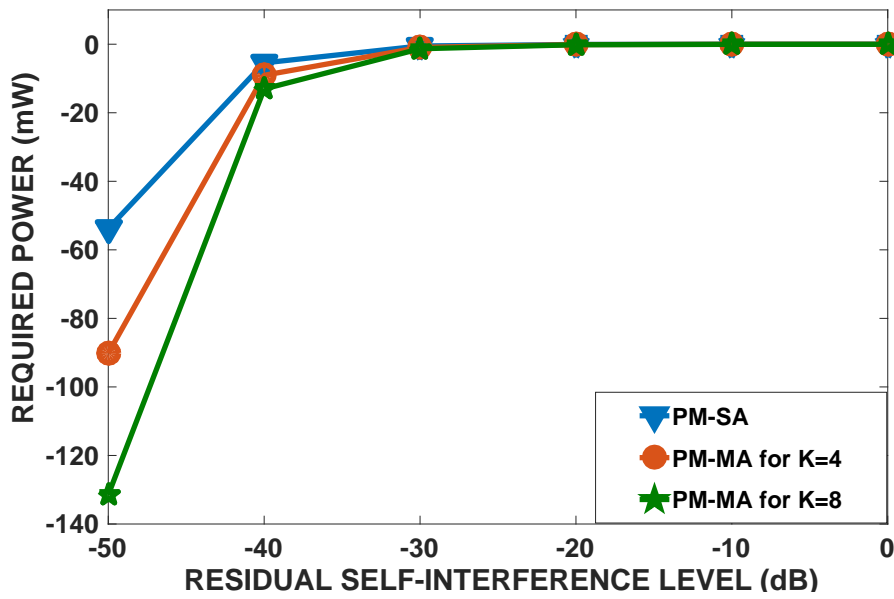
Figure 7.4: The required power by the relay's own battery, $P_R - \zeta P_H$, versus RSIL.

than necessary to satisfy the SINR constraints. Furthermore, the required power is significantly less for small RSIL values as expected. When it comes to comparing single and multiple receive antenna scenarios, the performance improvement with $K = 4$ is clearly seen for both RSIL levels. It is seen that PM-MA leads to significant power savings even though PS-SA is the joint optimum solution.
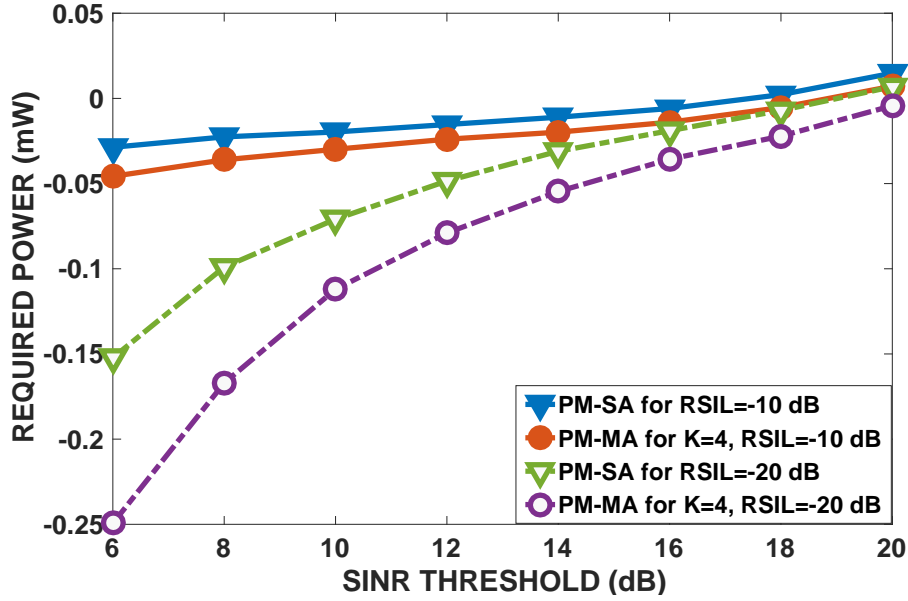
Figure 7.5: The required power by the relay's own battery, $P_R - \zeta P_H$, versus SINR threshold, γ, for RSIL=-10 dB and RSIL=-20 dB.
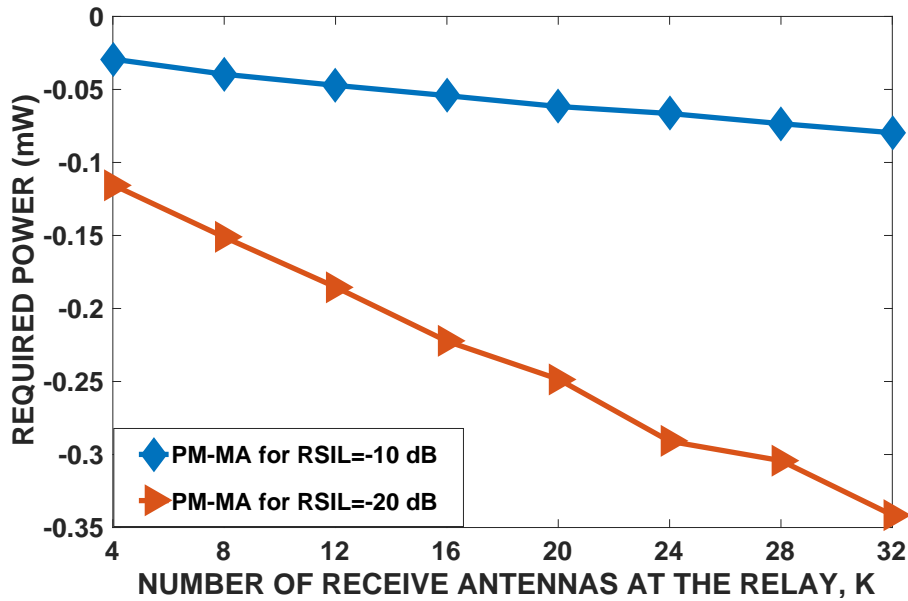

Figure 7.6: The required power by the relay's own battery, $P_R - \zeta P_H$, versus number of receive antennas at the relay, K, for RSIL=-10 dB and RSIL=-20 dB.

In Fig. 7.4, we increase RSIL from -50 dB to 0 dB. Different number of receive antennas are used, namely, $K = 1$, $K = 4$, and $K = 8$, respectively. The required power

for all these cases are negative for small RSIL and increases as RSIL is increased. The number of receive antennas is very important to improve the power savings. In fact, $K = 8$ case leads to 2.44 times power saving in comparison to $K = 1$ case for RSIL=-50 dB.

In Fig. 7.5, SINR threshold, γ is changed from 6 dB to 20 dB and the required power is plotted for $K = 1$ and $K = 4$ receive antennas when we set RSIL=-10 dB and -20 dB, respectively. As γ increases, the required power increases for all the solutions and become positive at $\gamma = 20$ dB for all the solutions except PM-MA with RSIL=-20 dB. As the target SINR becomes more demanding, additional power is required in order to satisfy the SINR constraint. Similar to the previous graphs, the required power is significantly less for multiple receive antenna case.

Fig. 7.6 is presented in order to observe the effect of the receive antennas at the relay in detail. As the number of receive antennas, K increases, the required power becomes more negative showing that more power savings from the energy harvesting is possible with large number of receive antennas. Furthermore, RSIL has an important effect determining the amount of power savings.

In the remaining figures, i.e., Fig. 7.7-10, we present the results for the proposed optimum solution and the sub-optimum one in [49] for SINR maximization problem. In addition, the proposed near-optimum solution is presented for the same problem with multiple-receive antenna case. In Fig. 7.7, the effective SINR of the system is plotted in terms of the number of transmit antennas at the relay, N. For different RSIL values, the proposed optimum solution for single receive antenna always performs better compared to the sub-optimum solution in [49]. As N increases, the performance gap between two solutions becomes larger especially for RSIL=-20 dB. Moreover, the proposed solution for multiple receive antenna provides higher SINR than that for single antenna solutions.
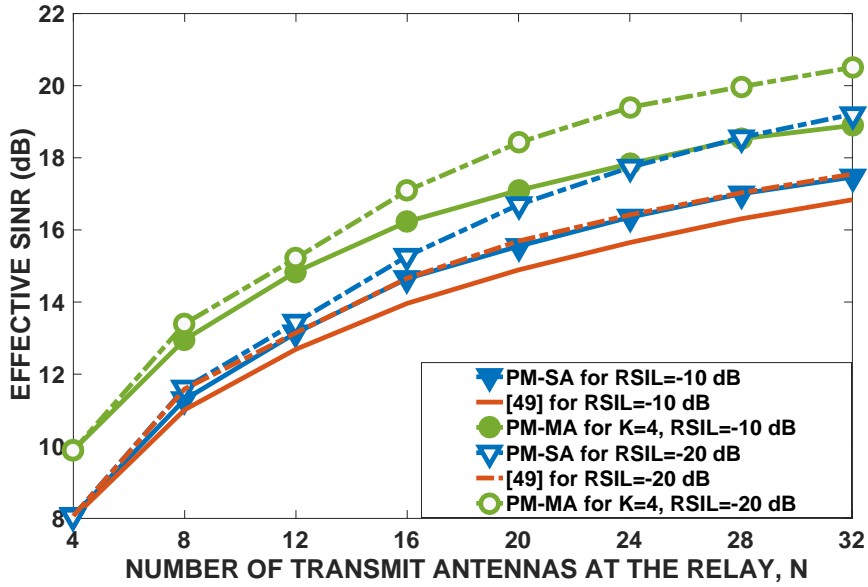
Figure 7.7: Effective SINR versus number of transmit antennas at the relay, N, for RSIL=-10 dB and RSIL=-20 dB.
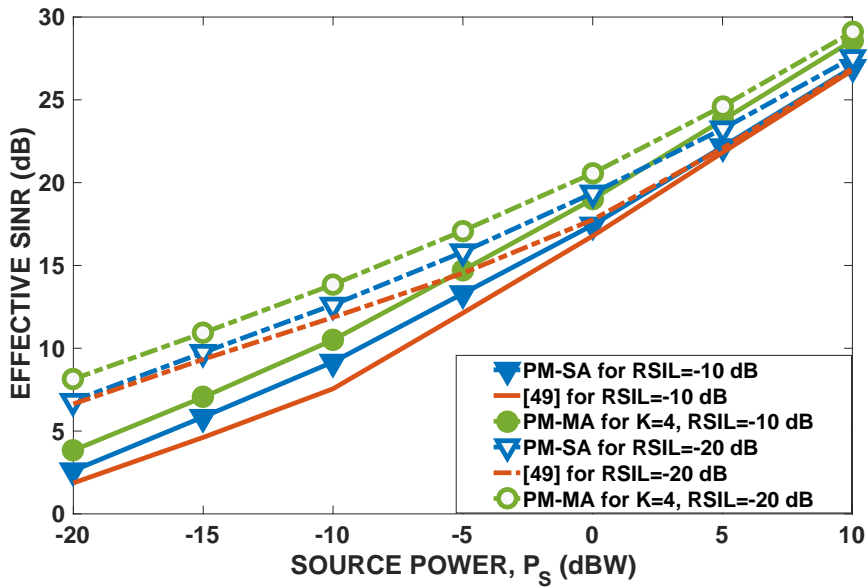

Figure 7.8: Effective SINR versus source power, P_S, for RSIL=-10 dB and RSIL=-20 dB.

In Fig. 7.8, source power, P_S is varied and SINR performance of the three methods are compared. Similar to the previous graph, the proposed optimum method always

results higher SINR compared to the sub-optimum solution in [49] for both RSIL values. Although the results for RSIL=-20 dB have higher effective SINR, the performance gap between two RSIL values decreases as the source power increases. This shows that supplying more source power compensates the adverse effect of high RSIL after some point. Note that the difference between PM-SA and PM-MA remains almost the same as P_S increases. Furthermore, employing more receive antennas at the relay improves the SINR by increasing spatial diversity and energy harvesting capability.

In Fig. 7.9, RSIL is increased from -50 dB to 0 dB and the effective SINR is plotted for all the methods. There are two results for multiple receive antenna case, namely, for $K = 4$ and $K = 8$, respectively. As RSIL increases, the effective SINR falls as expected. However, it is possible to improve SINR by employing more receive antennas at the relay for all the RSIL values.

Figure 7.9: Effective SINR versus RSIL.
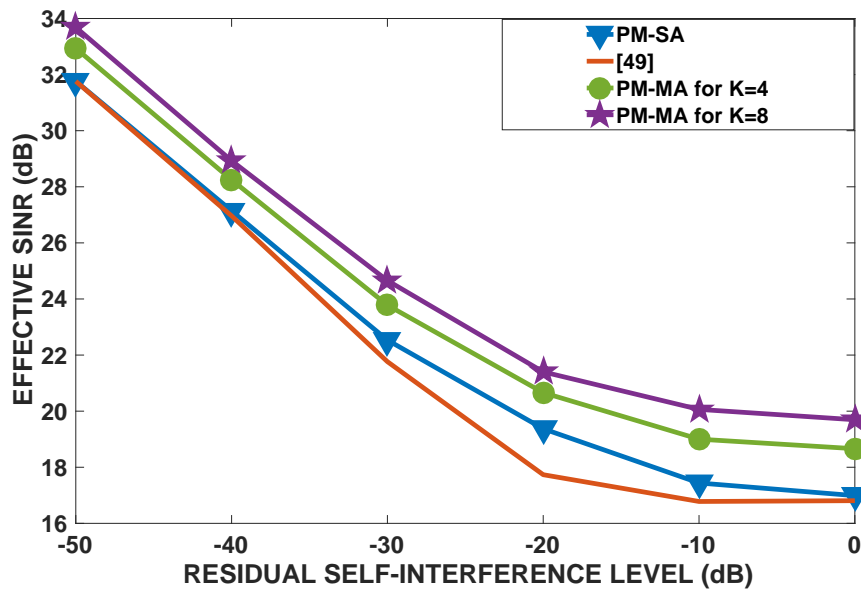
Finally, we increase the number of receive antennas at the relay, K, and plot the effective SINR of the proposed method for two RSIL values in Fig. 7.10. Increasing K from 4 to 32 provides up to 3.2 and 3.8 dB SINR improvement for RSIL=-20 dB and RSIL=-10 dB, respectively. This shows that employing large number of receive antennas improves the QoS of the system significantly.

161
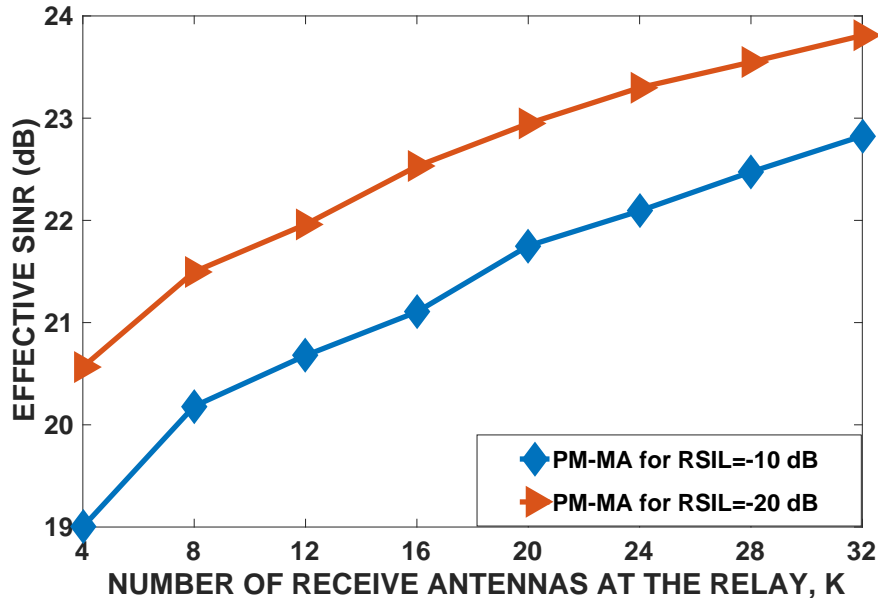
Figure 7.10: Effective SINR versus number of receive antennas at the relay, K, for RSIL=-10 dB and RSIL=-20 dB.

7.7 Conclusion

This chapter considers the joint optimization of relay transmit beamformer and power splitting factor for wireless-powered multi-antenna relay. The relay uses decode-and-forward protocol and power splitting is used to harvest some part of the received RF signal. Two different types of optimization problems are studied. The first one is the QoS-aware design problem where the aim is to satisfy the effective SINR need of the system by minimizing the transmission power used by the relay's own battery. This problem is solved optimally by reformulating it in an efficient form. Secondly, SINR maximization problem is elaborated for which a sub-optimum solution exists in the literature [49]. The optimum solution of this problem is also obtained in this chapter by using a bisection search and employing the solution of QoS-aware problem at each iteration. Simulation results show that the proposed optimum solution leads to better performance in SINR and transmit power. As an another contribution of this chapter, multiple-receive antenna relaying system is considered in addition to the single receive antenna case. The joint near-optimum solution is presented for the relay transmit and receive beamformers together with power splitting factor. First, optimum

transmit beamformer and power splitting factor are found for a given receive beam-former. Then, receive beamformer is optimally obtained by keeping other variables constant. Due to the increase in spatial diversity, multiple-receive antenna approach performs significantly better compared to the single antenna case. The performance improvement increases with the number of receive antennas.

CHAPTER 8

IMPROVED ADMM-BASED ALGORITHMS FOR MULTI-GROUP MULTICASTING IN LARGE-SCALE ANTENNA SYSTEMS WITH EXTENSION TO HYBRID BEAMFORMING

In this chapter, multi-group multicast beamforming is considered for full digital and hybrid beamforming. The wireless system comprises of a multiple-antenna base station and single-antenna users. Quality of service (QoS)-aware design is investigated where the optimization objective is to minimize the total transmitted power subject to signal-to-interference-plus-noise ratio (SINR) constraint at each user. In addition to SINR constraints, per-antenna power constraint is included for each antenna of the base station. The original optimization problem for full digital beamforming is transformed into an equivalent form such that alternating direction method of multipliers (ADMM) can be applied in an effective and computationally inexpensive manner for large-scale antenna systems. In this new formulation, the beamformer weight vectors are decomposed into two subspaces in order to decrease the number of dual variables and multiplications. The optimum update equations are obtained for the proposed ADMM algorithm. This new reformulation is used for two different hybrid beamforming structures employing phase shifters and vector modulators. Optimum updates are derived for each system. The proposed algorithms decrease computational complexity of the existing ADMM algorithms due to the effective reformulation as well as the direct solution of the nonconvex problem. In the simulation results, it is shown that the proposed methods have better convergence behavior and less computational time than the benchmark algorithms. Furthermore, the proposed method for hybrid beamforming with vector modulators performs better than its counterpart in the literature in terms of transmitted power.

8.1 Related Works and Contributions

Single-group multicast beamforming problem is first proposed in [24] and then extended to multi-group multicast beamforming case in [25]. Both problems are shown to be NP-hard and semidefinite relaxation (SDR) is applied in order to obtain a solution. Unfortunately, the optimum solution is not guaranteed and the performance of the SDR solution degrades as the size of problem increases. Secondly, SDR requires lifting of the problem to a high dimension and it is computationally inefficient for large-scale antenna and user systems [69]. In order to improve the performance and computational complexity, feasible point pursuit and successive convex approximation is developed in [34]. Then in [88] and [104], more efficient algorithms are proposed for single-group multicast beamforming problem. In [68], a consensus alternating directions method of multipliers (ADMM) algorithm is presented for efficient and fast solution of general quadratically constrained quadratic programming (QCQP) problems. Since, multi-group multicast beamforming can be formulated as a QCQP problem, ADMM is a good candidate for this problem. In [69], a more efficient ADMM method is developed for multi-group multicast beamforming by reducing the number of dual variables in the algorithm. This work is the current state of the art algorithm for single base station multi-group multicast beamforming problem and we will take it as our benchmark in this chapter.

Multicast beamforming is also considered for large scale antenna systems for a more efficient system design [71]. In [72], a conic quadratic programming approach is developed for large scale antenna multicasting systems. In this work, single group multicasting is considered. In [32], noncooperative multi-cell network is considered for massive MIMO multicasting. [29] and [73] investigated max-min fair multicast beamforming for large-scale arrays. [28] developed efficient algorithms for reducing the complexity of multicasting in large scale antenna systems. In our benchmark [69], ADMM-based fast algorithm is presented for large scale wireless systems. Finally in [26], joint unicast and multicast transmission is elaborated in massive MIMO systems.

In this chapter, we consider multi-group multicast beamforming for large-scale antenna systems. We adopt QoS-aware design approach also by including per-antenna power constraints to the problem to be more practical as in the works [69], [73], and

[74]. In the first part of the chapter, we consider full digital beamforming where each antenna is connected to a separate RF chain. Full digital beamforming achieves higher performance compared to analog and hybrid beamforming. This comes from the fact that the elements of each beamformer weight vector can be chosen as an arbitrary complex number without any restriction except the per-antenna power constraints. For full digital beamforming, we decompose each beamformer weight vector into two orthogonal subspaces. In this case, the SINR constraints become dependent only one of the subspaces. When the number of antennas is very high compared to the rank of the overall channel matrix, which is a practical scenario for large-scale antenna systems, the dimension of this subspace becomes significantly small compared to that of the orthogonal complement subspace. Then, we present the optimum updates for the ADMM framework and arrange the algorithm for a more memory efficient implementation. This together with the proposed decomposition brings us a computational advantage compared to the algorithm in [69] which uses the original problem formulation. Secondly, we deal with the nonconvex original problem directly instead of applying two-layer optimization as in [69]. The motivation behind this is the efficient use of ADMM for nonconvex problems [75], [76], [77], [78], [79]. Since, we use one-layer iteration sequence, our proposed algorithm has a faster and better convergence than the alternatives in the literature. In the second part of this chapter, we focus on two hybrid beamforming systems.

Hybrid beamforming design is considered for several scenarios including point-to-point MIMO and multi-user MIMO systems [85], [86], [87], [89]. In [88], [90], [105], it is investigated for single group multicasting. [80] considered hybrid beamforming design for joint unicast and multicast transmission. [27] proposed a fully-connected structure for multi-group multicasting. In this structure, two times more phase shifters are used compared to its conventional counterpart. Max-min hybrid beamforming design for multi-group multicasting is considered in [82]. In Chapter 2 ([10]), a new partially-connected hybrid beamforming structure is proposed for multi-group multicasting systems. In [10], SDR and successive convex approximation (SCA) based algorithms are proposed for the considered system. In this chapter, we propose an efficient ADMM based algorithm and solve each subproblem of it optimally by adopting this system. In [81], an alternating minimization algorithm

based on ADMM is realized over two different optimization problems each of which requires solving a two-layer optimization problem for a partially-connected hybrid structure with vector modulators. Vector modulators are used in place of the phase shifter and power amplifier. In this chapter, we formulate this problem according to our proposed efficient ADMM form and tackle the nonconvex problem directly instead of a three-layer optimization framework as in [81]. Simulation results show that our proposed algorithm performs significantly better in terms of both base station transmission power and computational complexity.

8.2 System Model

We consider a multicasting system comprising a base station (BS) equipped with N transmit antennas and M multicast groups of single-antenna users. The BS transmits a common multicast message to the users in each group. Let $\mathcal{G}_m$ denote the mth multicast group of users for all $m \in \mathcal{M} = \{1, ..., M\}$ and assume that there are K users in total. Each user is in only one multicast group, i.e., $\mathcal{G}_m \bigcap \mathcal{G}_{m'} = \emptyset$ for $m \neq m'$. Note that the special case $M = 1$ corresponds to single group multicasting scenario. Narrowband block-fading channel is considered. The signal transmitted from the antenna array of BS is $\mathbf{x} = \sum_{m=1}^{M} \mathbf{w}_m s_m$ where s_m is the information signal for the users in $\mathcal{G}_m$ and $\mathbf{w}_m$ is the corresponding $N \times 1$ complex beamformer weight vector for the mth multicast group. It is assumed that the information signals $\{s_m\}_{m=1}^{M}$ are mutually uncorrelated each with zero mean and unit variance, $\sigma_{s_m}^2 = 1$. In this case, the total average transmitted power is $P_{tot} = \sum_{m=1}^{M} \mathbf{w}_m^H \mathbf{w}_m$. The received signal at the kth user is given as,

$$y_k = \mathbf{h}_k^H \mathbf{x} + n_k, \quad \forall k \in \mathcal{K} \tag{8.1}$$

where $\mathbf{h}_k$ is the $N \times 1$ complex channel vector between BS and the kth user. $\mathcal{K} = \{1, ..., K\}$ is the index set of all the users. n_k is the additive zero mean Gaussian noise at the kth user's antenna with variance σ_k^2. n_k is assumed to be uncorrelated with the information signals. The received signal-to-interference-plus-noise ratio (SINR) of the kth user is expressed as,

$$\text{SINR}_k = \frac{|\mathbf{h}_k^H \mathbf{w}_{m_k}|^2}{\sum_{m' \neq m_k} |\mathbf{h}_k^H \mathbf{w}_{m'}|^2 + \sigma_k^2}, \quad \forall k \in \mathcal{K} \tag{8.2}$$

168

where m_k denotes the index of multicast group to which the kth user belongs. In this chapter, we first consider quality-of-service (QoS)-aware full digital beamformer design where the aim is to minimize the total average transmitted power subject to receive-SINR and per-antenna power constraints.

8.3 QoS-Aware Beamformer Design

The OoS-aware design problem can be formulated as follows,

$$\min_{\{\mathbf{w}_m\}_{m=1}^M} \quad \sum_{m=1}^{M} \mathbf{w}_m^H \mathbf{w}_m \tag{8.3a}$$

$$s.t. \quad \frac{|\mathbf{h}_k^H \mathbf{w}_{m_k}|^2}{\sum_{m' \neq m_k} |\mathbf{h}_k^H \mathbf{w}_{m'}|^2 + \sigma_k^2} \geq \gamma_k, \quad \forall k \in \mathcal{K} \tag{8.3b}$$

$$\sum_{m=1}^{M} |w_{m,n}|^2 \leq P_n, \ \forall n \in \mathcal{N} \tag{8.3c}$$

where γ_k is the minimum required SINR for the kth user and P_n is the maximum allowable power at the nth transmit antenna of BS. $w_{m,n}$ is the nth element of the vector $\mathbf{w}_m$ and $\mathcal{N} = \{1, ..., N\}$ is the index set for all the transmit antennas. The problem in (8.3) is not convex and hence should be handled appropriately for an effective and fast solution. Note that (8.3b) can be rewritten as a quadratic constraint. The current state-of-art methods for the QCQP problem (8.3) are the ADMM-based algorithms proposed in [68] and [69]. In the following section, we will briefly go over these algorithms before introducing our improved ADMM-based algorithm which results less computational time.

8.3.1 Prior ADMM-Based Algorithms for (8.3)

Recently, an efficient ADMM-based algorithm is proposed for general QCQP problems by using consensus optimization and decomposing the original problem into QCQP subproblems with only one constraint [68]. Later in [69], an improved technique is proposed for multi-group multicasting problem in (8.3). Let us mention these algorithms in turn in the following subsections.

8.3.1.1 Consensus-ADMM for General QCQP

In [68], consensus optimization is considered using ADMM for the following general QCQP,

$$\min_{\mathbf{x}} \quad \mathbf{x}^H \mathbf{A}_0 \mathbf{x} - 2\Re\{\mathbf{b}_0^H \mathbf{x}\} \tag{8.4a}$$

$$s.t. \quad \mathbf{x}^H \mathbf{A}_i \mathbf{x} - 2\Re\{\mathbf{b}_i^H \mathbf{x}\} \leq c_i, \quad i = 1, ..., I. \tag{8.4b}$$

First, (8.4) is transformed to the following consensus form by introducing auxiliary variables $\{\mathbf{z}_i\}_{i=1}^I$ for each constraint, i.e.,

$$\min_{\mathbf{x}, \{\mathbf{z}_i\}_{i=1}^I} \quad \mathbf{x}^H \mathbf{A}_0 \mathbf{x} - 2\Re\{\mathbf{b}_0^H \mathbf{x}\} \tag{8.5a}$$

$$s.t. \quad \mathbf{z}_i^H \mathbf{A}_i \mathbf{z}_i - 2\Re\{\mathbf{b}_i^H \mathbf{z}_i\} \leq c_i, \quad i = 1, ..., I, \tag{8.5b}$$

$$\mathbf{z}_i = \mathbf{x}, \quad i = 1, ..., I. \tag{8.5c}$$

The steps of consensus-ADMM algorithm for (8.5) in scaled form [106] are given as follows,

$$\mathbf{x} \leftarrow \arg\min_{\mathbf{x}} \mathbf{x}^H \mathbf{A}_0 \mathbf{x} - 2\Re\{\mathbf{b}_0^H \mathbf{x}\} + \rho \sum_{i=1}^I ||\mathbf{z}_i - \mathbf{x} + \mathbf{u}_i||^2 \tag{8.6a}$$

$$\mathbf{z}_i \leftarrow \arg\min_{\mathbf{z}_i} ||\mathbf{z}_i - \mathbf{x} + \mathbf{u}_i||^2$$

$$s.t. \quad \mathbf{z}_i^H \mathbf{A}_i \mathbf{z}_i - 2\Re\{\mathbf{b}_i^H \mathbf{z}_i\} \leq c_i,$$

$$i = 1, ..., I \tag{8.6b}$$

$$\mathbf{u}_i \leftarrow \mathbf{u}_i + \mathbf{z}_i - \mathbf{x}, \quad i = 1, ..., I \tag{8.6c}$$

where $\mathbf{u}_i$ is the scaled dual variable corresponding to the equality constraint $\mathbf{z}_i = \mathbf{x}$ in (8.5c) for $i = 1, ..., I$. $\rho > 0$ is the penalty parameter used in augmented Lagrangian [106]. In [68], the updates for (8.6b) are solved optimally. Moreover, a memory-efficient implementation of the consensus-ADMM algorithm is presented for single group multicast beamforming problem where $M = 1$ in (8.3) and there is no interference in (8.3b).

The algorithmic framework in [68] summarized above can also be used for multi-group multicast beamforming problem in (8.3). However, recently a more efficient method is proposed for this specific problem in [69].

8.3.1.2 Convex-Concave Procedure ADMM (CCP-ADMM) for Multi-Group Multicast Beamforming

As stated in [69], one of the main disadvantages of consensus-ADMM algorithm is that it requires a local copy of the optimization variables and a corresponding dual vector variable for each constraint. In [69], a new ADMM framework which requires less auxiliary variables is proposed by introducing $\{\{\Gamma_{k,m} = \mathbf{h}_k^H \mathbf{w}_m\}_{k=1}^K\}_{m=1}^M$ and expressing the SINR constraints in (8.3b) in terms of them. This new ADMM is applied for a sequence of convex subproblems obtained by CCP. The method in [69] performs significantly better compared to [68] with less computational complexity. In this chapter, we reduce the computational complexity more by an effective reformulation of the problem. Our new algorithm directly deals with the original problem different than [69] which solves a sequence of subproblems and requires both inner and outer loop iterations. It is shown that the performance is improved significantly in terms of computational saving.

8.3.2 Improved ADMM-Based Algorithm for (8.3)

Note that all the ADMM updates are carried through $N \times 1$ vectors for the algorithm in [68]. Similarly, $N \times 1$ vectors are used for the update of the main variables and per-antenna power constraints in [69]. When the number of antennas, N, is very large, these updates become extremely costly due to matrix inversions and multiplications. In this chapter, we reduce the complexity of the ADMM iterations by decomposing beamformer vectors into the subspace spanned by the channel vectors and its nullspace. For this method to be efficient, it is required that the dimension of the subspace of the channel vectors to be less than N. Let $\mathbf{H}$ denote the $N \times K$ matrix which is formed by stacking all the channel vectors $\mathbf{h}_k$, $\forall k \in \mathcal{K}$, as its columns, i.e., $\mathbf{H} = [\mathbf{h}_1 \ \mathbf{h}_2 \ ... \ \mathbf{h}_K]$. If L denotes the dimension of the column space of $\mathbf{H}$, there are two possible cases for $L < N$. In case the number of antennas, N, is greater than the number of users, K, L is always less than N. This is a very practical scenario in modern wireless communications which involves massive antenna systems. For the second case, i.e., $N < K$, L may not be less than N. However, it is possible for the scenarios where some users are clustered in close groups. In such a case, the corre-

sponding channel vectors are highly correlated and the rank of $\mathbf{H}$ gets smaller. Now, let us consider the singular value decomposition of $\mathbf{H}$ as follows,

$$\mathbf{H} = \begin{bmatrix} \mathbf{U}_A & \mathbf{U}_B \end{bmatrix} \begin{bmatrix} \Sigma_A & \mathbf{0} \\ \mathbf{0} & \Sigma_B \end{bmatrix} \begin{bmatrix} \mathbf{V}_A^H \\ \mathbf{V}_B^H \end{bmatrix} \tag{8.7}$$

where Σ_A and Σ_B are the diagonal matrices whose elements are the positive and zero singular values of $\mathbf{H}$, respectively. Let us express $\{\mathbf{w}_m\}_{m=1}^M$ as $\mathbf{w}_m = \mathbf{U}_A \mathbf{v}_{A,m} + \mathbf{v}_{B,m}$ where $\mathbf{v}_{A,m} \in \mathbb{C}^L$ and $\mathbf{v}_{B,m} \in \mathbb{C}^N$ for $m \in \mathcal{M}$ are the newly introduced auxiliary variables. $\mathbf{v}_{B,m}$ is in the nullspace of $\mathbf{U}_A$, i.e., $\mathbf{U}_A^H \mathbf{v}_{B,m} = \mathbf{0}$. The optimization problem in (8.3) can be reformulated as follows,

$$\min_{\{\mathbf{w}_m, \mathbf{v}_{A,m}, \mathbf{v}_{B,m}\}_{m=1}^M} \sum_{m=1}^M \mathbf{w}_m^H \mathbf{w}_m \tag{8.8a}$$

$$s.t. \quad \frac{|(\Sigma_A \mathbf{V}_A^H)_k^H \mathbf{v}_{A,m_k}|^2}{\sum_{m' \neq m_k} |(\Sigma_A \mathbf{V}_A^H)_k^H \mathbf{v}_{A,m'}|^2 + \sigma_k^2} \geq \gamma_k, \quad \forall k \in \mathcal{K} \tag{8.8b}$$

$$\mathbf{w}_m = \mathbf{U}_A \mathbf{v}_{A,m} + \mathbf{v}_{B,m}, \; \forall m \in \mathcal{M} \tag{8.8c}$$

$$\mathbf{U}_A^H \mathbf{v}_{B,m} = \mathbf{0}, \; \forall m \in \mathcal{M} \tag{8.8d}$$

$$\sum_{m=1}^M |w_{m,n}|^2 \leq P_n, \; \forall n \in \mathcal{N} \tag{8.8e}$$

where $(\Sigma_A \mathbf{V}_A^H)_k$ denotes the kth column of $\Sigma_A \mathbf{V}_A^H$. In order to make the problem in (8.8) appropriate for ADMM algorithm, we will define additional auxiliary variables $\Gamma_{k,m} \triangleq (\Sigma_A \mathbf{V}_A^H)_k^H \mathbf{v}_{A,m}, \forall k \in \mathcal{K}, \forall m \in \mathcal{M}$ using the same approach in [69]. In addition, we introduce $\tilde{\mathbf{v}}_{A,m} \triangleq \mathbf{U}_A \mathbf{v}_{A,m}$ and $\tilde{\mathbf{v}}_{B,m} \triangleq \mathbf{v}_{B,m}$. These definitions will allow us to obtain efficient and closed-form optimum ADMM updates. Using the new variables,

the problem in (8.8) can be expressed as follows,

$$\min_{\substack{\left\{\mathbf{v}_{A,m},\tilde{\mathbf{v}}_{A,m},\mathbf{v}_{B,m},\tilde{\mathbf{v}}_{B,m}, \\ \{\Gamma_{k,m}\}_{k=1}^{K}\right\}_{m=1}^{M}}} \sum_{m=1}^{M}(\tilde{\mathbf{v}}_{A,m}^{H}\tilde{\mathbf{v}}_{A,m} + \tilde{\mathbf{v}}_{B,m}^{H}\tilde{\mathbf{v}}_{B,m}) \tag{8.9a}$$

$$s.t. \ \Gamma_{k,m} = (\Sigma_A \mathbf{V}_A^H)_k^H \mathbf{v}_{A,m}, \ \forall k \in \mathcal{K}, \forall m \in \mathcal{M} \tag{8.9b}$$

$$\frac{|\Gamma_{k,m_k}|^2}{\sum_{m' \neq m_k} |\Gamma_{k,m'}|^2 + \sigma_k^2} \geq \gamma_k, \quad \forall k \in \mathcal{K} \tag{8.9c}$$

$$\tilde{\mathbf{v}}_{A,m} = \mathbf{U}_A \mathbf{v}_{A,m}, \ \forall m \in \mathcal{M} \tag{8.9d}$$

$$\tilde{\mathbf{v}}_{B,m} = \mathbf{v}_{B,m}, \ \forall m \in \mathcal{M} \tag{8.9e}$$

$$\mathbf{U}_A^H \tilde{\mathbf{v}}_{B,m} = \mathbf{0}, \ \forall m \in \mathcal{M} \tag{8.9f}$$

$$\mathbf{U}_B^H \tilde{\mathbf{v}}_{A,m} = \mathbf{0}, \ \forall m \in \mathcal{M} \tag{8.9g}$$

$$\sum_{m=1}^{M} |\tilde{v}_{A,m,n} + \tilde{v}_{B,m,n}|^2 \leq P_n, \ \forall n \in \mathcal{N}. \tag{8.9h}$$

Note that the constraint in (8.9g) is redundant. However, the inclusion of it will simplify the updates in ADMM algorithm. Similar to [69], the variables in (8.9) can be split into two blocks, $\{\mathbf{v}_{A,m}, \mathbf{v}_{B,m}\}_{m=1}^{M}$ and $\{\{\Gamma_{k,m}\}_{k=1}^{K}, \tilde{\mathbf{v}}_{A,m}, \tilde{\mathbf{v}}_{B,m}\}_{m=1}^{M}$ such that the updates of ADMM algorithm are separable. Now, the steps of ADMM algorithm for

173

the problem (8.9) in scaled-form [106] can be given as follows,

$$\{\Gamma_{k,m}\}_{m=1}^{M} \leftarrow \underset{\{\Gamma_{k,m}\}_{m=1}^{M}}{\arg\min} \sum_{m=1}^{M} |\Gamma_{k,m} - (\Sigma_A \mathbf{V}_A^H)_k^H \mathbf{v}_{A,m} + \lambda_{k,m}|^2$$

$$s.t. \ |\Gamma_{k,m_k}|^2 \geq \gamma_k \sum_{m' \neq m_k} |\Gamma_{k,m'}|^2 + \gamma_k \sigma_k^2$$

$$\forall k \in \mathcal{K} \tag{8.10a}$$

$$\{\tilde{\mathbf{v}}_{A,m}, \tilde{\mathbf{v}}_{B,m}\}_{m=1}^{M} \leftarrow \underset{\{\tilde{\mathbf{v}}_{A,m}, \tilde{\mathbf{v}}_{B,m}\}_{m=1}^{M}}{\arg\min} \sum_{m=1}^{M} \left(\tilde{\mathbf{v}}_{A,m}^H \tilde{\mathbf{v}}_{A,m} + \tilde{\mathbf{v}}_{B,m}^H \tilde{\mathbf{v}}_{B,m} \right.$$

$$\left. + \rho ||\tilde{\mathbf{v}}_{A,m} - \mathbf{U}_A \mathbf{v}_{A,m} + \mathbf{z}_{A,m}||^2 + \rho ||\tilde{\mathbf{v}}_{B,m} - \mathbf{v}_{B,m} + \mathbf{z}_{B,m}||^2 \right)$$

$$s.t. \ \sum_{m=1}^{M} |\tilde{v}_{A,m,n} + \tilde{v}_{B,m,n}|^2 \leq P_n, \ \forall n \in \mathcal{N}$$

$$\mathbf{U}_A^H \tilde{\mathbf{v}}_{B,m} = \mathbf{0}, \ \mathbf{U}_B^H \tilde{\mathbf{v}}_{A,m} = \mathbf{0}, \ \forall m \in \mathcal{M} \tag{8.10b}$$

$$\mathbf{v}_{A,m} \leftarrow \underset{\mathbf{v}_{A,m}}{\arg\min} \sum_{k=1}^{K} |\Gamma_{k,m} - (\Sigma_A \mathbf{V}_A^H)_k^H \mathbf{v}_{A,m} + \lambda_{k,m}|^2$$

$$+ ||\tilde{\mathbf{v}}_{A,m} - \mathbf{U}_A \mathbf{v}_{A,m} + \mathbf{z}_{A,m}||^2, \qquad \forall m \in \mathcal{M} \tag{8.10c}$$

$$\mathbf{v}_{B,m} \leftarrow \underset{\mathbf{v}_{B,m}}{\arg\min} ||\tilde{\mathbf{v}}_{B,m} - \mathbf{v}_{B,m} + \mathbf{z}_{B,m}||^2, \ \forall m \in \mathcal{M} \tag{8.10d}$$

$$\lambda_{k,m} \leftarrow \lambda_{k,m} + \Gamma_{k,m} - (\Sigma_A \mathbf{V}_A^H)_k^H \mathbf{v}_{A,m}, \quad \forall k \in \mathcal{K}, \ \forall m \in \mathcal{M} \tag{8.10e}$$

$$\mathbf{z}_{A,m} \leftarrow \mathbf{z}_{A,m} + \tilde{\mathbf{v}}_{A,m} - \mathbf{U}_A \mathbf{v}_{A,m}, \qquad \forall m \in \mathcal{M} \tag{8.10f}$$

$$\mathbf{z}_{B,m} \leftarrow \mathbf{z}_{B,m} + \tilde{\mathbf{v}}_{B,m} - \mathbf{v}_{B,m}, \qquad \forall m \in \mathcal{M} \tag{8.10g}$$

where $\{\{\lambda_{k,m}\}_{k=1}^{K}\}_{m=1}^{M}$, $\{\mathbf{z}_{A,m}\}_{m=1}^{M}$ and $\{\mathbf{z}_{B,m}\}_{m=1}^{M}$ are the scaled dual variables corresponding to the equality constraints in (8.9b), (8.9d), and (8.9e), respectively. $\rho > 0$ is the penalty parameter used in augmented Lagrangian [106]. In the following, we will present the closed form expressions for the updates in (8.10a-d), respectively.

In [69], the solution of a similar optimization problem to (8.10a) is found. Here, we

omit the details and give only the result as follows,

$$\Gamma_{k,m_k} \leftarrow \begin{cases} \zeta_{k,m_k} & \text{if } \phi_k(0) \geq 0 \\ \frac{\zeta_{k,m_k}}{1-\mu_k^\star} & \text{if } \phi_k(0) < 0 \end{cases} \tag{8.11a}$$

$$\Gamma_{k,m'} \leftarrow \begin{cases} \zeta_{k,m'} & \text{if } \phi_k(0) \geq 0 \\ \frac{\zeta_{k,m'}}{1+\gamma_k\mu_k^\star} & \text{if } \phi_k(0) < 0 \end{cases}, \ \forall m' \neq m_k, \tag{8.11b}$$

$$\forall k \in \mathcal{K}$$

where $\zeta_{k,m} \triangleq (\Sigma_A V_A^H)_k^H v_{A,m} - \lambda_{k,m}$ is defined for ease of notation. In (8.11a-b), $\phi_k(\mu) = \frac{|\zeta_{k,m_k}|^2}{(1-\mu)^2} - \gamma_k \sum_{m' \neq m_k} \frac{|\zeta_{k,m'}|^2}{(1+\gamma_k\mu)^2} - \gamma_k\sigma_k^2$ and $\mu_k^\star$ is the unique solution of $\phi_k(\mu) = 0$ in $0 < \mu < 1$ in case $\phi_k(0) < 0$. Note that $\mu_k^\star$ can easily be found by solving a quartic equation.

Now, let us consider the optimization problem in (8.10b). In order to simplify (8.10b), let us assume that $z_{A,m}$ and $z_{B,m}$ are initialized such that they lie in the column space of U_A and U_B, respectively without loss of generality. Assume also that initial value of $v_{B,m}$ is selected from the column space of U_B in accordance with the constraints (8.9e-f). Following (8.10d) and (8.10f-g), $z_{A,m}$ and $z_{B,m}$ continue to remain in the same subspaces if they are initialized in this way. In this case, (8.10b) can be expressed as follows,

$$\min_{\{\tilde{v}_{A,m},\tilde{v}_{B,m}\}_{m=1}^M} \sum_{m=1}^M \left((\tilde{v}_{A,m} + \tilde{v}_{B,m})^H(\tilde{v}_{A,m} + \tilde{v}_{B,m}) \right.$$

$$\left. + \rho||\tilde{v}_{A,m} + \tilde{v}_{B,m} - (U_A v_{A,m} - z_{A,m} + v_{B,m} - z_{B,m})||^2 \right) \tag{8.12a}$$

$$s.t. \ \sum_{m=1}^M |\tilde{v}_{A,m,n} + \tilde{v}_{B,m,n}|^2 \leq P_n, \ \forall n \in \mathcal{N} \tag{8.12b}$$

$$U_A^H \tilde{v}_{B,m} = 0, \ U_B^H \tilde{v}_{A,m} = 0, \ \forall m \in \mathcal{M} \tag{8.12c}$$

Now, let us define $\tilde{w}_m \triangleq \tilde{v}_{A,m} + \tilde{v}_{B,m}$. If we further define $\tilde{z}_m \triangleq U_A v_{A,m} - z_{A,m} + v_{B,m} - z_{B,m}$ for ease of notation, the objective function in (8.12a) can be expressed as $(1+\rho)||\tilde{w}_m - \frac{\rho}{1+\rho}\tilde{z}_m||^2 + \frac{\rho}{1+\rho}||\tilde{z}_m||^2$. The second term is constant and can be removed. Note that $\tilde{v}_{A,m}$ and $\tilde{v}_{B,m}$ lie in the column space of U_A and U_B, respectively. Hence, they can be expressed in terms of new variables as $\tilde{v}_{A,m} = U_A v_{A,m}$ and $\tilde{v}_{B,m} = U_B v_{B,m}$.

175

Using these variables, (8.12) can be reformulated as follows,

$$\min_{\{\tilde{\mathbf{w}}_m, \boldsymbol{v}_{A,m}, \boldsymbol{v}_{B,m}\}_{m=1}^M} \sum_{m=1}^M \left\| \tilde{\mathbf{w}}_m - \frac{\rho}{1+\rho} \tilde{\mathbf{z}}_m \right\|^2 \tag{8.13a}$$

$$s.t. \quad \sum_{m=1}^M |\tilde{w}_{m,n}|^2 \le P_n, \quad \forall n \in \mathcal{N} \tag{8.13b}$$

$$\boldsymbol{v}_{A,m} = \mathbf{U}_A^H \tilde{\mathbf{w}}_m, \quad \boldsymbol{v}_{B,m} = \mathbf{U}_B^H \tilde{\mathbf{w}}_m, \quad \forall m \in \mathcal{M} \tag{8.13c}$$

In the formulation (8.13), it is clearly seen that (8.13c) does not have any affect on both the objective function and the other constraints in (8.13b). Hence, the optimum solution is found by solving (8.13a-b). (8.13c) is used to obtain the optimum $\{\tilde{\mathbf{v}}_{A,m}, \tilde{\mathbf{v}}_{B,m}\}_{m=1}^M$.

Note that the problem (8.13a-b) can be decomposed into N subproblems. If we define $\hat{\mathbf{w}}^n \triangleq [\ \tilde{w}_{1,n}\ \tilde{w}_{2,n}\ ...\ \tilde{w}_{M,n}\ ]^T$ and $\hat{\mathbf{z}}^n \triangleq [\ \tilde{z}_{1,n}\ \tilde{z}_{2,n}\ ...\ \tilde{z}_{M,n}\ ]^T$, $\forall n \in \mathcal{N}$, the nth subproblem is given as follows,

$$\min_{\hat{\mathbf{w}}^n} \left\| \hat{\mathbf{w}}^n - \frac{\rho}{1+\rho} \hat{\mathbf{z}}^n \right\|^2 \tag{8.14a}$$

$$s.t. \quad ||\hat{\mathbf{w}}^n||^2 \le P_n. \tag{8.14b}$$

Following [69], the optimum solution of (8.14) is given by $\hat{\mathbf{w}}^n = \min\left\{ \frac{\sqrt{P_n}}{||\hat{\mathbf{z}}^n||_2}, \frac{\rho}{1+\rho} \right\} \hat{\mathbf{z}}^n$. Using this and (8.13c), the optimum update in (8.10b) is given as,

$$\hat{\mathbf{w}}^n \leftarrow \min\left\{ \frac{\sqrt{P_n}}{||\hat{\mathbf{z}}^n||_2}, \frac{\rho}{1+\rho} \right\} \hat{\mathbf{z}}^n, \quad \forall n \in \mathcal{N} \tag{8.15a}$$

$$\tilde{\mathbf{w}}_m \leftarrow [\ \hat{w}_m^1\ \hat{w}_m^2\ ...\ \hat{w}_m^N\ ]^T, \quad \forall m \in \mathcal{M} \tag{8.15b}$$

$$\tilde{\mathbf{v}}_{A,m} \leftarrow \mathbf{U}_A \mathbf{U}_A^H \tilde{\mathbf{w}}_m, \quad \forall m \in \mathcal{M} \tag{8.15c}$$

$$\tilde{\mathbf{v}}_{B,m} \leftarrow \mathbf{U}_B \mathbf{U}_B^H \tilde{\mathbf{w}}_m, \quad \forall m \in \mathcal{M} \tag{8.15d}$$

Note that defining auxiliary variables $\tilde{\mathbf{v}}_{A,m}$ in (8.9d) and $\tilde{\mathbf{v}}_{B,m}$ in (8.9e), $\forall m \in \mathcal{M}$ resulted the Euclidean projection problem in (8.14) whose closed-form optimum solution exists.

The update in (8.10c) can easily be expressed as follows,

$$\mathbf{v}_{A,m} \leftarrow \left(\mathbf{I}_L + \Sigma_A^2\right)^{-1} \left(\mathbf{U}_A^H(\tilde{\mathbf{v}}_{A,m} + \mathbf{z}_{A,m})\right.$$

$$\left. + \sum_{k=1}^K (\Sigma_A \mathbf{V}_A^H)_k (\Gamma_{k,m} + \lambda_{k,m})\right), \quad \forall m \in \mathcal{M} \tag{8.16}$$

Note that matrix inverse in (8.16) is computationally efficient since the matrix inside the inverse operation is diagonal unlike its counterpart in [69]. Similarly, the update in (8.10d) is given as follows,

$$\mathbf{v}_{B,m} \leftarrow \tilde{\mathbf{v}}_{B,m} + \mathbf{z}_{B,m}, \quad \forall m \in \mathcal{M} \tag{8.17}$$

At this point, all the steps of ADMM algorithm are expressed in closed-form. In the following part, we will arrange the algorithm variables in order to further reduce its computational complexity.

First, let us consider the dual variable update in (8.10f). Here, $\mathbf{z}_{A,m}$ is a $N \times 1$ complex vector. In fact, it is possible to carry out the update through a low dimensional dual vector. Let us define $\mathbf{u}_m \triangleq \mathbf{U}_A^H \mathbf{z}_{A,m} \; \forall m \in \mathcal{M}$. Remember that $\mathbf{z}_{A,m}$ lies in the column space of $\mathbf{U}_A$ if it is initialized properly. Hence, we can write $\mathbf{z}_{A,m} = \mathbf{U}_A \mathbf{u}_m, \; \forall m \in \mathcal{M}$. Using this and (8.15c), the update in (8.10f) becomes

$$\mathbf{u}_m \leftarrow \mathbf{u}_m + \mathbf{U}_A^H \tilde{\mathbf{w}}_m - \mathbf{v}_{A,m}, \qquad \forall m \in \mathcal{M} \tag{8.18}$$

Using the newly introduced dual variable, the update in (8.16) can be expressed as follows,

$$\begin{aligned}
\mathbf{v}_{A,m} \leftarrow & \left(\mathbf{I}_L + \Sigma_A^2 \right)^{-1} \left(\mathbf{U}_A^H \tilde{\mathbf{w}}_m + \mathbf{u}_m \right. \\
& \left. + \sum_{k=1}^{K} (\Sigma_A \mathbf{V}_A^H)_k (\Gamma_{k,m} + \lambda_{k,m}) \right), \quad \forall m \in \mathcal{M}
\end{aligned} \tag{8.19}$$

Now, we can easily see that there is no need to compute $\tilde{\mathbf{v}}_{A,m}$. Furthermore, as we show in the following part, there is also no need for the dual variable $\mathbf{z}_{B,m}$ in the iterations. Suppose $\mathbf{z}_{B,m}^0$ is the initial value of the dual variable $\mathbf{z}_{B,m}$. Then, we obtain $\mathbf{v}_{B,m}^1 = \tilde{\mathbf{v}}_{B,m}^1 + \mathbf{z}_{B,m}^0$ in the first iteration by (8.17). After that, $\mathbf{z}_{B,m}$ is updated by (8.10g) as $\mathbf{z}_{B,m}^1 = \mathbf{z}_{B,m}^0 + \tilde{\mathbf{v}}_{B,m}^1 - \mathbf{v}_{B,m}^1 = \mathbf{z}_{B,m}^0 + \tilde{\mathbf{v}}_{B,m}^1 - (\tilde{\mathbf{v}}_{B,m}^1 + \mathbf{z}_{B,m}^0) = 0$. In the first iteration, $\mathbf{z}_{B,m}$ becomes 0 and it continues in this way. Hence, we can omit this dual variable in the algorithm. Now, the simplified steps of the ADMM algorithm are given below. Note that neither $\mathbf{v}_{B,m}$ nor $\tilde{\mathbf{v}}_{B,m}$ are kept in memory. Instead, $\tilde{\mathbf{w}}_m^j - \mathbf{U}_A \mathbf{U}_A^H \tilde{\mathbf{w}}_m^j$ is used in place of $\mathbf{v}_{B,m}^j$ in (8.20c). The number of dual complex variables in the counterpart algorithm in [69] is $M(N + K)$ whereas it is $M(L + K)$ in the proposed one as can be seen in (8.20f-g). Furthermore, in case $N \geq K$, the number of complex multiplications is $\mathcal{O}(MNK)$ per ADMM iteration in [69]. Here, it is $\mathcal{O}(MNL)$ which is always less than

or equal to $\mathcal{O}(MNK)$ due to $L \leq \min(N, K)$. Furthermore, the proposed algorithm requires only one loop for iterations whereas the iterations in [69] are implemented in two nested loops. This fact brings a huge computational advantage to the proposed algorithm.

Algorithm 8.1: ADMM for QoS-Aware Design Problem

Initialization: Initialize $\tilde{\mathbf{w}}_m^0 \sim \mathcal{CN}(\mathbf{0}, \mathbf{I}_N)$, $\mathbf{v}_{A,m}^0 = \mathbf{U}_A^H \tilde{\mathbf{w}}_m^0$, $\lambda_{k,m}^0 \leftarrow 0$, $\forall k \in \mathcal{K}$, $\mathbf{u}_m^0 \leftarrow \mathbf{0}$, $\forall m \in \mathcal{M}$. Set the iteration number $i \leftarrow 0$ and the penalty parameter ρ.

Repeat

$$\Gamma_{k,m_k}^{i+1} \leftarrow \begin{cases} \zeta_{k,m_k}^i & \text{if } \phi_k^i(0) \geq 0 \\ \frac{\zeta_{k,m_k}^i}{1-\mu_k^\star} & \text{if } \phi_k^i(0) < 0 \end{cases} \tag{8.20a}$$

$$\Gamma_{k,m'}^{i+1} \leftarrow \begin{cases} \zeta_{k,m'}^i & \text{if } \phi_k^i(0) \geq 0 \\ \frac{\zeta_{k,m'}^i}{1+\gamma_k\mu_k^\star} & \text{if } \phi_k^i(0) < 0 \end{cases}, \quad \forall m' \neq m_k, \tag{8.20b}$$

$\forall k \in \mathcal{K}$

$$\tilde{\mathbf{z}}_m^{i+1} \leftarrow \mathbf{U}_A(\mathbf{v}_{A,m}^i - \mathbf{u}_m^i) + \tilde{\mathbf{w}}_m^i - \mathbf{U}_A\mathbf{U}_A^H\tilde{\mathbf{w}}_m^i, \quad \forall m \in \mathcal{M} \tag{8.20c}$$

$$(\hat{\mathbf{w}}^n)^{i+1} \leftarrow \min\left\{\frac{\sqrt{P_n}}{||(\hat{\mathbf{z}}^n)^{i+1}||_2}, \frac{\rho}{1+\rho}\right\}(\hat{\mathbf{z}}^n)^{i+1}, \quad \forall n \in \mathcal{N} \tag{8.20d}$$

$$\mathbf{v}_{A,m}^{i+1} \leftarrow \left(\mathbf{I}_L + \Sigma_A^2\right)^{-1}\left(\mathbf{U}_A^H\tilde{\mathbf{w}}_m^{i+1} + \mathbf{u}_m^i\right.$$

$$\left. + \sum_{k=1}^K (\Sigma_A\mathbf{V}_A^H)_k(\Gamma_{k,m}^{i+1} + \lambda_{k,m}^i)\right), \quad \forall m \in \mathcal{M} \tag{8.20e}$$

$$\lambda_{k,m}^{i+1} \leftarrow \lambda_{k,m}^i + \Gamma_{k,m}^{i+1} - (\Sigma_A\mathbf{V}_A^H)_k^H\mathbf{v}_{A,m}^{i+1}, \quad \forall k \in \mathcal{K}, \forall m \in \mathcal{M} \tag{8.20f}$$

$$\mathbf{u}_m^{i+1} \leftarrow \mathbf{u}_m^i + \mathbf{U}_A^H\tilde{\mathbf{w}}_m^{i+1} - \mathbf{v}_{A,m}^{i+1}, \quad \forall m \in \mathcal{M} \tag{8.20g}$$

Set $i \leftarrow i + 1$.

Until stopping criterion is met.

8.4 Hybrid Beamforming with Phase Shifters

In this part, partially connected hybrid beamformer structure with phase shifters as shown in Fig. 8.1 is considered for multi-group multicasting scenario. This structure is used for a similar scenario in [10]. Here, we will consider ADMM algorithm and derive update equations for this model.
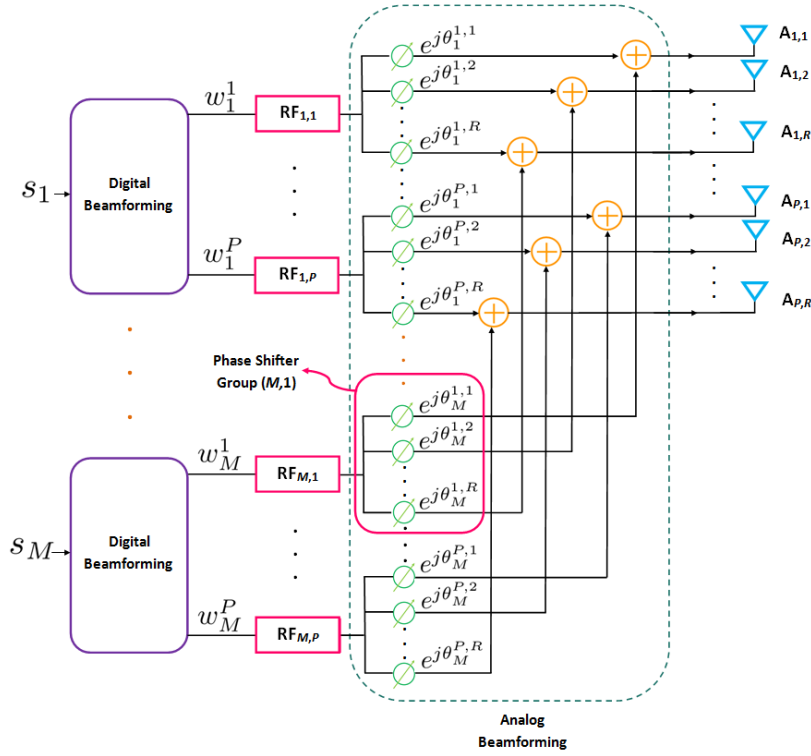
Figure 8.1: Hybrid Structure with Phase Shifters.

The hybrid structure in Fig. 8.1 consists of two stages, namely digital and analog beamformer which will be jointly designed. This structure presents a trade-off between performance and the number of RF chains. When the number of RF chains for each multicast stream is the same as the number of antennas (full digital beamformer), the best performance is achieved. If it is less than the number of antennas (i.e., hybrid beamformer), the system cost is decreased while there is a certain performance loss [10]. In Fig. 8.1, there are MP RF chains. Each RF chain is followed by R RF phase shifters. The analog signals coming from phase shifters of each multicast group are added up and the summed signal is fed into an antenna. As can be seen in Fig. 8.1, the total number of antennas is $N = PR$.

The beamforming weight vector for the mth multicast group is $PR \times 1$ complex vector $\mathbf{w}_m = [\ w_m^{1,1}\ w_m^{1,2}\ ...\ w_m^{1,R}\ w_m^{2,1}\ ...\ w_m^{2,R}\ ...\ w_m^{P,1}\ ...\ w_m^{P,R}\ ]^T$ where $w_m^{p,r} = w_m^p e^{j\theta_m^{p,r}}$. Here, w_m^p is the digital beamformer coefficient corresponding to the pth RF chain for the mth multicast stream. $\theta_m^{p,r}$ is the phase shift introduced by the rth phase shifter following the pth RF chain of the mth digital beamformer block. Hence, the elements of beamforming weight vectors, $\{\mathbf{w}_m\}_{m=1}^M$, are the phase shifted versions of the digital weights $\{w_m^1, w_m^2, ..., w_m^P\}_{m=1}^M$. As a result, the amplitude of complex weights inside each phase shifter group should be the same, i.e., $|w_m^p| = |w_m^{p,r}|$ for $r = 1, ..., R$, $p = 1, ..., P$, and $m = 1, ..., M$ where the phase shifters following $\text{RF}_{m,p}$ constitute the phase shifter group (m, p). The first weight of the phase shifter group (m, p), $w_m^{p,1}$, can be chosen as w_m^p, i.e., $w_m^{p,1} = w_m^p$ for $p = 1, ..., P$ and $m = 1, ..., M$ without loss of generality.

The QoS-aware hybrid beamforming design can be formulated as follows,

$$\min_{\{\mathbf{w}_m\}_{m=1}^M} \sum_{m=1}^M \mathbf{w}_m^H \mathbf{w}_m \tag{8.21a}$$

$$s.t. \quad \frac{|\mathbf{h}_k^H \mathbf{w}_{m_k}|^2}{\sum_{m' \neq m_k} |\mathbf{h}_k^H \mathbf{w}_{m'}|^2 + \sigma_k^2} \geq \gamma_k, \quad \forall k \in \mathcal{K} \tag{8.21b}$$

$$\sum_{m=1}^M |w_{m,n}|^2 \leq P_n, \ \forall n \in \mathcal{N} \tag{8.21c}$$

$$|w_m^{p,r}| = |w_m^{p,1}|, \quad \forall r \in \mathcal{R} \setminus \{1\}, \ \forall p \in \mathcal{P}, \ \forall m \in \mathcal{M} \tag{8.21d}$$

where $\mathcal{R} = \{1, ..., R\}$ and $\mathcal{P} = \{1, ..., P\}$. Similar to the previous part, (8.21) can be

reformulated appropriately for ADMM algorithm as follows,

$$\min_{\substack{\left\{\mathbf{v}_{A,m},\tilde{\mathbf{v}}_{A,m},\mathbf{v}_{B,m},\tilde{\mathbf{v}}_{B,m},\right. \\ \left.\{\Gamma_{k,m}\}_{k=1}^{K}\right\}_{m=1}^{M}}} \sum_{m=1}^{M} (\tilde{\mathbf{v}}_{A,m}^{H}\tilde{\mathbf{v}}_{A,m} + \tilde{\mathbf{v}}_{B,m}^{H}\tilde{\mathbf{v}}_{B,m}) \tag{8.22a}$$

$$s.t. \ \Gamma_{k,m} = (\Sigma_A \mathbf{V}_A^H)_k^H \mathbf{v}_{A,m}, \ \forall k \in \mathcal{K}, \forall m \in \mathcal{M} \tag{8.22b}$$

$$\frac{|\Gamma_{k,m_k}|^2}{\sum_{m' \neq m_k} |\Gamma_{k,m'}|^2 + \sigma_k^2} \geq \gamma_k, \quad \forall k \in \mathcal{K} \tag{8.22c}$$

$$\tilde{\mathbf{v}}_{A,m} = \mathbf{U}_A \mathbf{v}_{A,m}, \ \forall m \in \mathcal{M} \tag{8.22d}$$

$$\tilde{\mathbf{v}}_{B,m} = \mathbf{v}_{B,m}, \ \forall m \in \mathcal{M} \tag{8.22e}$$

$$\mathbf{U}_A^H \tilde{\mathbf{v}}_{B,m} = \mathbf{0}, \ \forall m \in \mathcal{M} \tag{8.22f}$$

$$\mathbf{U}_B^H \tilde{\mathbf{v}}_{A,m} = \mathbf{0}, \ \forall m \in \mathcal{M} \tag{8.22g}$$

$$\sum_{m=1}^{M} |\tilde{v}_{A,m,n} + \tilde{v}_{B,m,n}|^2 \leq P_n, \ \forall n \in \mathcal{N} \tag{8.22h}$$

$$|\tilde{v}_{A,m}^{p,r} + \tilde{v}_{B,m}^{p,r}| = |\tilde{v}_{A,m}^{p,1} + \tilde{v}_{B,m}^{p,1}|, \quad \forall r \in \mathcal{R} \setminus \{1\}, \ \forall p \in \mathcal{P}, \ \forall m \in \mathcal{M} \tag{8.22i}$$

As in the previous section, the variables in (8.22) can be split into two blocks, $\{\mathbf{v}_{A,m}, \mathbf{v}_{B,m}\}_{m=1}^{M}$ and $\{\{\Gamma_{k,m}\}_{k=1}^{K}, \tilde{\mathbf{v}}_{A,m}, \tilde{\mathbf{v}}_{B,m}\}_{m=1}^{M}$ such that the updates of ADMM algorithm are separable. Now, the steps of ADMM algorithm for the problem (8.22) in

scaled-form [106] are given as follows,

$$\{\Gamma_{k,m}\}_{m=1}^{M} \leftarrow \underset{\{\Gamma_{k,m}\}_{m=1}^{M}}{\arg\min} \sum_{m=1}^{M} |\Gamma_{k,m} - (\Sigma_A V_A^H)_k^H \mathbf{v}_{A,m} + \lambda_{k,m}|^2$$

$$s.t. \ |\Gamma_{k,m_k}|^2 \geq \gamma_k \sum_{m' \neq m_k} |\Gamma_{k,m'}|^2 + \gamma_k \sigma_k^2$$

$$\forall k \in \mathcal{K} \tag{8.23a}$$

$$\{\tilde{\mathbf{v}}_{A,m}, \tilde{\mathbf{v}}_{B,m}\}_{m=1}^{M} \leftarrow \underset{\{\tilde{\mathbf{v}}_{A,m}, \tilde{\mathbf{v}}_{B,m}\}_{m=1}^{M}}{\arg\min} \sum_{m=1}^{M} \Big(\tilde{\mathbf{v}}_{A,m}^H \tilde{\mathbf{v}}_{A,m} + \tilde{\mathbf{v}}_{B,m}^H \tilde{\mathbf{v}}_{B,m}$$

$$+ \rho||\tilde{\mathbf{v}}_{A,m} - \mathbf{U}_A \mathbf{v}_{A,m} + \mathbf{z}_{A,m}||^2 + \rho||\tilde{\mathbf{v}}_{B,m} - \mathbf{v}_{B,m} + \mathbf{z}_{B,m}||^2 \Big)$$

$$s.t. \ \sum_{m=1}^{M} |\tilde{v}_{A,m,n} + \tilde{v}_{B,m,n}|^2 \leq P_n, \ \forall n \in \mathcal{N}$$

$$|\tilde{v}_{A,m}^{p,r} + \tilde{v}_{B,m}^{p,r}| = |\tilde{v}_{A,m}^{p,1} + \tilde{v}_{B,m}^{p,1}|, \quad \forall r \in \mathcal{R} \setminus \{1\}, \ \forall p \in \mathcal{P}, \ \forall m \in \mathcal{M}$$

$$\mathbf{U}_A^H \tilde{\mathbf{v}}_{B,m} = \mathbf{0}, \ \mathbf{U}_B^H \tilde{\mathbf{v}}_{A,m} = \mathbf{0}, \ \forall m \in \mathcal{M} \tag{8.23b}$$

$$\mathbf{v}_{A,m} \leftarrow \underset{\mathbf{v}_{A,m}}{\arg\min} \sum_{k=1}^{K} |\Gamma_{k,m} - (\Sigma_A V_A^H)_k^H \mathbf{v}_{A,m} + \lambda_{k,m}|^2$$

$$+ ||\tilde{\mathbf{v}}_{A,m} - \mathbf{U}_A \mathbf{v}_{A,m} + \mathbf{z}_{A,m}||^2, \qquad \forall m \in \mathcal{M} \tag{8.23c}$$

$$\mathbf{v}_{B,m} \leftarrow \underset{\mathbf{v}_{B,m}}{\arg\min} ||\tilde{\mathbf{v}}_{B,m} - \mathbf{v}_{B,m} + \mathbf{z}_{B,m}||^2, \ \forall m \in \mathcal{M} \tag{8.23d}$$

$$\lambda_{k,m} \leftarrow \lambda_{k,m} + \Gamma_{k,m} - (\Sigma_A V_A^H)_k^H \mathbf{v}_{A,m}, \quad \forall k \in \mathcal{K}, \ \forall m \in \mathcal{M} \tag{8.23e}$$

$$\mathbf{z}_{A,m} \leftarrow \mathbf{z}_{A,m} + \tilde{\mathbf{v}}_{A,m} - \mathbf{U}_A \mathbf{v}_{A,m}, \qquad \forall m \in \mathcal{M} \tag{8.23f}$$

$$\mathbf{z}_{B,m} \leftarrow \mathbf{z}_{B,m} + \tilde{\mathbf{v}}_{B,m} - \mathbf{v}_{B,m}, \qquad \forall m \in \mathcal{M} \tag{8.23g}$$

where $\{\{\lambda_{k,m}\}_{k=1}^{K}\}_{m=1}^{M}$, $\{\mathbf{z}_{A,m}\}_{m=1}^{M}$ and $\{\mathbf{z}_{B,m}\}_{m=1}^{M}$ are the scaled dual variables corresponding to the equality constraints in (8.22b), (8.22d), and (8.22e), respectively. $\rho > 0$ is the penalty parameter used in augmented Lagrangian [106]. The optimum updates of the ADMM algorithm in (8.23a-g) are derived except the one in (8.23b) in the previous part.

Now, let us consider the optimization problem in (8.23b). In order to simplify (8.23b), let us assume that $\mathbf{z}_{A,m}$ and $\mathbf{z}_{B,m}$ are initialized such that they lie in the column space of $\mathbf{U}_A$ and $\mathbf{U}_B$, respectively without loss of generality. Assume also that initial value of $\mathbf{v}_{B,m}$ is selected from the column space of $\mathbf{U}_B$ in accordance with the constraints (8.22e-f). In this case, following (8.23d) and (8.23f-g), $\mathbf{z}_{A,m}$ and $\mathbf{z}_{B,m}$ continue to

182

remain in the same subspaces if they are initialized in this way. Under these assumptions, (8.23b) can be expressed as follows,

$$\min_{\{\tilde{\mathbf{v}}_{A,m}, \tilde{\mathbf{v}}_{B,m}\}_{m=1}^{M}} \sum_{m=1}^{M} \left((\tilde{\mathbf{v}}_{A,m} + \tilde{\mathbf{v}}_{B,m})^H (\tilde{\mathbf{v}}_{A,m} + \tilde{\mathbf{v}}_{B,m}) \right.$$
$$\left. + \rho || \tilde{\mathbf{v}}_{A,m} + \tilde{\mathbf{v}}_{B,m} - (\mathbf{U}_A \mathbf{v}_{A,m} - \mathbf{z}_{A,m} + \mathbf{v}_{B,m} - \mathbf{z}_{B,m}) ||^2 \right) \tag{8.24a}$$

$$s.t. \ \sum_{m=1}^{M} |\tilde{v}_{A,m,n} + \tilde{v}_{B,m,n}|^2 \le P_n, \ \forall n \in \mathcal{N} \tag{8.24b}$$

$$|\tilde{v}_{A,m}^{p,r} + \tilde{v}_{B,m}^{p,r}| = |\tilde{v}_{A,m}^{p,1} + \tilde{v}_{B,m}^{p,1}|, \ \forall r \in \mathcal{R} \setminus \{1\}, \ \forall p \in \mathcal{P}, \ \forall m \in \mathcal{M} \tag{8.24c}$$

$$\mathbf{U}_A^H \tilde{\mathbf{v}}_{B,m} = \mathbf{0}, \ \mathbf{U}_B^H \tilde{\mathbf{v}}_{A,m} = \mathbf{0}, \ \forall m \in \mathcal{M} \tag{8.24d}$$

Now, let us define $\tilde{\mathbf{w}}_m \triangleq \tilde{\mathbf{v}}_{A,m} + \tilde{\mathbf{v}}_{B,m}$. If we further define $\tilde{\mathbf{z}}_m \triangleq \mathbf{U}_A \mathbf{v}_{A,m} - \mathbf{z}_{A,m} + \mathbf{v}_{B,m} - \mathbf{z}_{B,m}$ for ease of notation, the objective function in (8.24a) can be expressed as $(1 + \rho) || \tilde{\mathbf{w}}_m - \frac{\rho}{1+\rho} \tilde{\mathbf{z}}_m ||^2 + \frac{\rho}{1+\rho} || \tilde{\mathbf{z}}_m ||^2$. The second term is constant and can be removed. Note that $\tilde{\mathbf{v}}_{A,m}$ and $\tilde{\mathbf{v}}_{B,m}$ lie in the column space of $\mathbf{U}_A$ and $\mathbf{U}_B$, respectively. Hence, they can be expressed in terms of new variables as $\tilde{\mathbf{v}}_{A,m} = \mathbf{U}_A \boldsymbol{v}_{A,m}$ and $\tilde{\mathbf{v}}_{B,m} = \mathbf{U}_B \boldsymbol{v}_{B,m}$. Using these variables, (8.24) can be reformulated as follows,

$$\min_{\{\tilde{\mathbf{w}}_m, \boldsymbol{v}_{A,m}, \boldsymbol{v}_{B,m}\}_{m=1}^{M}} \sum_{m=1}^{M} || \tilde{\mathbf{w}}_m - \frac{\rho}{1+\rho} \tilde{\mathbf{z}}_m ||^2 \tag{8.25a}$$

$$s.t. \ \sum_{m=1}^{M} |\tilde{w}_{m,n}|^2 \le P_n, \ \forall n \in \mathcal{N} \tag{8.25b}$$

$$|\tilde{w}_m^{p,r}| = |\tilde{w}_m^{p,1}|, \ \forall r \in \mathcal{R} \setminus \{1\}, \ \forall p \in \mathcal{P}, \ \forall m \in \mathcal{M} \tag{8.25c}$$

$$\boldsymbol{v}_{A,m} = \mathbf{U}_A^H \tilde{\mathbf{w}}_m, \ \boldsymbol{v}_{B,m} = \mathbf{U}_B^H \tilde{\mathbf{w}}_m, \ \forall m \in \mathcal{M} \tag{8.25d}$$

In the formulation (8.25), (8.25d) does not have any effect on both the objective function and the other constraints in (8.25b-c). Hence, the optimum solution is found by solving (8.25a-c). Note that the problem (8.25a-c) can be decomposed into P subproblems. The pth subproblem is given as follows,

$$\min_{\{\{\tilde{w}_m^{p,r}\}_{r=1}^{R}\}_{m=1}^{M}} \sum_{m=1}^{M} \sum_{r=1}^{R} |\tilde{w}_m^{p,r} - \frac{\rho}{1+\rho} \tilde{z}_m^{p,r}|^2 \tag{8.26a}$$

$$s.t. \ \sum_{m=1}^{M} |\tilde{w}_m^{p,1}|^2 \le P^p \tag{8.26b}$$

$$|\tilde{w}_m^{p,r}| = |\tilde{w}_m^{p,1}|, \ \forall r \in \mathcal{R} \setminus \{1\}, \ \forall m \in \mathcal{M} \tag{8.26c}$$

where P^p is the minimum of power limits among the antennas connected to the pth RF chains of digital beamformer blocks, i.e., $P^p = \min\{P_n\}_{n=(p-1)R+1}^{pR}$. Now, express the optimization variable $\tilde{w}_m^{p,r}$ in terms of its amplitude and phase as $\tilde{w}_m^{p,r} = \beta_m^p e^{j\phi_m^{p,r}}$ where $\beta_m^p = |\tilde{w}_m^{p,r}|$ for $\forall r \in \mathcal{R}$. Note that all the constraints are independent of $\phi_m^{p,r}$, and hence optimum $\phi_m^{p,r}$ is given by $\phi_m^{p,r\star} = \angle \tilde{z}_m^{p,r}$. Using this, the optimization problem in (8.26) can be expressed in terms of $\{\beta_m^p\}_{m=1}^M$ as follows,

$$\min_{\{\beta_m^p\}_{m=1}^M} \sum_{m=1}^M \left(\beta_m^p - \frac{\rho}{1+\rho} \frac{\sum_{r=1}^R |\tilde{z}_m^{p,r}|}{R}\right)^2 \tag{8.27a}$$

$$s.t. \ \sum_{m=1}^M (\beta_m^p)^2 \le P_p. \tag{8.27b}$$

The optimum solution of (8.27) can easily be obtained as

$$\beta_m^{p\star} = \min\left\{\frac{R\sqrt{P^p}}{\sqrt{\sum_{m'=1}^M (\sum_{r=1}^R |\tilde{z}_{m'}^{p,r}|)^2}}, \frac{\rho}{1+\rho}\right\} \times \frac{\sum_{r=1}^R |\tilde{z}_m^{p,r}|}{R} \tag{8.28}$$

Eventually, the optimum update for $\{\tilde{\mathbf{v}}_{A,m}, \tilde{\mathbf{v}}_{B,m}\}_{m=1}^M$ is given as follows,

$$\tilde{w}_m^{p,r} \leftarrow \min\left\{\frac{R\sqrt{P^p}}{\sqrt{\sum_{m'=1}^M (\sum_{l=1}^R |\tilde{z}_{m'}^{p,l}|)^2}}, \frac{\rho}{1+\rho}\right\} \times$$

$$\frac{\sum_{l=1}^R |\tilde{z}_m^{p,l}|}{R} e^{j\angle \tilde{z}_m^{p,r}}, \quad \forall r \in \mathcal{R}, \ \forall p \in \mathcal{P}, \ \forall m \in \mathcal{M} \tag{8.29a}$$

$$\tilde{\mathbf{v}}_{A,m} \leftarrow \mathbf{U}_A \mathbf{U}_A^H \tilde{\mathbf{w}}_m, \ \forall m \in \mathcal{M} \tag{8.29b}$$

$$\tilde{\mathbf{v}}_{B,m} \leftarrow \mathbf{U}_B \mathbf{U}_B^H \tilde{\mathbf{w}}_m, \ \forall m \in \mathcal{M} \tag{8.29c}$$

The steps of the ADMM algorithm for digital beamforming in the previous part are simplified for more memory and computational efficient update equations. Using the same transformations and simplifications, the steps of the ADMM algorithm for hybrid beamforming with phase shifters are outlined as follows.

Algorithm 8.2: ADMM for Hybrid Beamforming with Phase Shifters

---

Initialization: Initialize $\tilde{\mathbf{w}}_m^0 \sim \mathcal{CN}(\mathbf{0}, \mathbf{I}_N)$, $\mathbf{v}_{A,m}^0 = \mathbf{U}_A^H \tilde{\mathbf{w}}_m^0$, $\lambda_{k,m}^0 \leftarrow 0$, $\forall k \in \mathcal{K}$, $\mathbf{u}_m^0 \leftarrow \mathbf{0}$, $\forall m \in \mathcal{M}$. Set the iteration number $i \leftarrow 0$ and the penalty parameter ρ.

Repeat

$$\Gamma_{k,m_k}^{i+1} \leftarrow \begin{cases} \zeta_{k,m_k}^i & \text{if } \phi_k^i(0) \geq 0 \\ \frac{\zeta_{k,m_k}^i}{1-\mu_k^\star} & \text{if } \phi_k^i(0) < 0 \end{cases} \tag{8.30a}$$

$$\Gamma_{k,m'}^{i+1} \leftarrow \begin{cases} \zeta_{k,m'}^i & \text{if } \phi_k^i(0) \geq 0 \\ \frac{\zeta_{k,m'}^i}{1+\gamma_k\mu_k^\star} & \text{if } \phi_k^i(0) < 0 \end{cases}, \quad \forall m' \neq m_k, \tag{8.30b}$$

$$\forall k \in \mathcal{K}$$

$$\tilde{\mathbf{z}}_m^{i+1} \leftarrow \mathbf{U}_A(\mathbf{v}_{A,m}^i - \mathbf{u}_m^i) + \tilde{\mathbf{w}}_m^i - \mathbf{U}_A\mathbf{U}_A^H\tilde{\mathbf{w}}_m^i, \quad \forall m \in \mathcal{M} \tag{8.30c}$$

$$(\tilde{w}_m^{p,r})^{i+1} \leftarrow \min\left\{ \frac{R\sqrt{P^p}}{\sqrt{\sum_{m'=1}^M(\sum_{l=1}^R |(\tilde{z}_{m'}^{p,l})^{i+1}|)^2}}, \frac{\rho}{1+\rho} \right\} \times$$

$$\frac{\sum_{l=1}^R |(\tilde{z}_m^{p,l})^{i+1}|}{R} e^{j\angle(\tilde{z}_m^{p,r})^{i+1}}, \quad \forall r \in \mathcal{R}, \forall p \in \mathcal{P}, \forall m \in \mathcal{M} \tag{8.30d}$$

$$\mathbf{v}_{A,m}^{i+1} \leftarrow \left(\mathbf{I}_L + \Sigma_A^2\right)^{-1}\left(\mathbf{U}_A^H\tilde{\mathbf{w}}_m^{i+1} + \mathbf{u}_m^i\right.$$

$$\left. + \sum_{k=1}^K (\Sigma_A\mathbf{V}_A^H)_k(\Gamma_{k,m}^{i+1} + \lambda_{k,m}^i)\right), \quad \forall m \in \mathcal{M} \tag{8.30e}$$

$$\lambda_{k,m}^{i+1} \leftarrow \lambda_{k,m}^i + \Gamma_{k,m}^{i+1} - (\Sigma_A\mathbf{V}_A^H)_k^H\mathbf{v}_{A,m}^{i+1}, \quad \forall k \in \mathcal{K}, \forall m \in \mathcal{M} \tag{8.30f}$$

$$\mathbf{u}_m^{i+1} \leftarrow \mathbf{u}_m^i + \mathbf{U}_A^H\tilde{\mathbf{w}}_m^{i+1} - \mathbf{v}_{A,m}^{i+1}, \quad \forall m \in \mathcal{M} \tag{8.30g}$$

Set $i \leftarrow i + 1$.

Until stopping criterion is met.

In Algorithm 8.2, $\zeta_{k,m}^i \triangleq (\Sigma_A\mathbf{V}_A^H)_k^H\mathbf{v}_{A,m}^i - \lambda_{k,m}^i$ and $\phi_k^i(\mu) = \frac{|\zeta_{k,m_k}^i|^2}{(1-\mu)^2} -$ $\gamma_k \sum_{m'\neq m_k} \frac{|\zeta_{k,m'}^i|^2}{(1+\gamma_k\mu)^2} - \gamma_k\sigma_k^2$. $\mu_k^\star$ is the unique solution of $\phi_k^i(\mu) = 0$ in $0 < \mu < 1$ in case $\phi_k^i(0) < 0$. Note that $\mu_k^\star$ can easily be found by a one dimensional search or solving a quartic equation.

8.5 Hybrid Beamforming with Vector Modulators

In this part, partially connected hybrid beamformer structure as shown in Fig. 8.2 is considered for multi-group multicasting scenario. This structure is adopted for

the same scenario in [81]. Note that the algorithm in [81] realizes an alternating minimization over two different optimizations problems each of which consists of two iteration layers. In this chapter, we will propose an ADMM algorithm which directly solves the reformulated problem. This will bring us a high computational advantage as shown in the simulations.

The hybrid structure in Fig. 8.2 consists of digital and analog beamformer stages similar to the previous structure. There are P RF chains and each RF chain is connected to R antennas through vector modulators which allows for varying both phase and amplitude of RF signals in a continuous manner. In this system, a digitally weighted sum of multicast symbols, i.e., $\sum_{m=1}^{M} w_m^p s_m$, $\forall p \in \mathcal{P}$, is sent to a separate RF chain. Then, each analog RF signal is split into R vector modulators. The phase and amplitude change of the rth vector modulator following the pth RF chain is denoted by the complex scalar $\chi_{p,r}$, $\forall r \in \mathcal{R}$ and $\forall p \in \mathcal{P}$. In total, there are PR vector modulators and hence PR antennas. The beamforming weight vector for the mth multicast group is
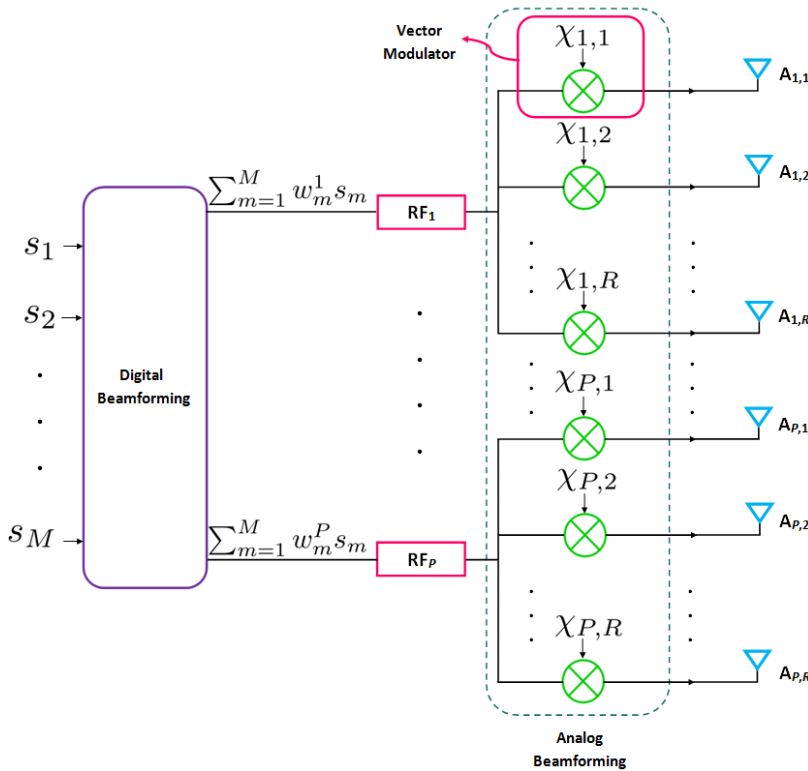

Figure 8.2: Hybrid Structure with Vector Modulators.

$PR \times 1$ complex vector $\mathbf{w}_m = [\ w_m^{1,1}\ w_m^{1,2}\ ...\ w_m^{1,R}\ w_m^{2,1}\ ...\ w_m^{2,R}\ ...\ w_m^{P,1}\ ...\ w_m^{P,R}\ ]^T$ where

$w_m^{p,r} = w_m^p \chi_{p,r}$. Using this, the QoS-aware hybrid beamforming problem with vector modulators can be expressed as follows,

$$\min_{\{\mathbf{w}_m, \{w_m^p\}_{p=1}^P\}_{m=1}^M, \{\{\chi_{p,r}\}_{r=1}^R\}_{p=1}^P} \sum_{m=1}^M \mathbf{w}_m^H \mathbf{w}_m \tag{8.31a}$$

$$s.t. \quad \frac{|\mathbf{h}_k^H \mathbf{w}_{m_k}|^2}{\sum_{m' \neq m_k} |\mathbf{h}_k^H \mathbf{w}_{m'}|^2 + \sigma_k^2} \geq \gamma_k, \quad \forall k \in \mathcal{K} \tag{8.31b}$$

$$\sum_{m=1}^M |w_{m,n}|^2 \leq P_n, \quad \forall n \in \mathcal{N} \tag{8.31c}$$

$$w_m^{p,r} = w_m^p \chi_{p,r}, \quad \forall r \in \mathcal{R}, \ \forall p \in \mathcal{P}, \ \forall m \in \mathcal{M}. \tag{8.31d}$$

As in the previous section, (8.31) can be reformulated appropriately for ADMM algorithm as follows,

$$\min_{\substack{\{\mathbf{v}_{A,m}, \tilde{\mathbf{v}}_{A,m}, \mathbf{v}_{B,m}, \tilde{\mathbf{v}}_{B,m}, \\ \{\Gamma_{k,m}\}_{k=1}^K, \{w_m^p\}_{p=1}^P\}_{m=1}^M, \\ \{\{\chi_{p,r}\}_{r=1}^R\}_{p=1}^P}} \sum_{m=1}^M (\tilde{\mathbf{v}}_{A,m}^H \tilde{\mathbf{v}}_{A,m} + \tilde{\mathbf{v}}_{B,m}^H \tilde{\mathbf{v}}_{B,m}) \tag{8.32a}$$

$$s.t. \quad (8.22\text{b-h}) \tag{8.32b}$$

$$\tilde{v}_{A,m}^{p,r} + \tilde{v}_{B,m}^{p,r} = w_m^p \chi_{p,r}, \quad \forall r \in \mathcal{R}, \ \forall p \in \mathcal{P}, \ \forall m \in \mathcal{M}. \tag{8.32c}$$

The steps of ADMM algorithm for the problem (8.32) are the same as those given in (8.23a-g) except the one in (8.23b) due to the only different constraint in (8.32c). In addition, the variables $\{\{w_m^p\}_{p=1}^P\}_{m=1}^M$ and $\{\{\chi_{p,r}\}_{r=1}^R\}_{p=1}^P$ should be updated in the ADMM framework. The update for $\{\tilde{\mathbf{v}}_{A,m}, \tilde{\mathbf{v}}_{B,m}\}_{m=1}^M$ can be obtained by solving the following problem, i.e.,

$$\min_{\{\tilde{\mathbf{v}}_{A,m}, \tilde{\mathbf{v}}_{B,m}\}_{m=1}^M} \sum_{m=1}^M \left((\tilde{\mathbf{v}}_{A,m} + \tilde{\mathbf{v}}_{B,m})^H (\tilde{\mathbf{v}}_{A,m} + \tilde{\mathbf{v}}_{B,m}) \right.$$
$$\left. + 2\rho \left\| \tilde{\mathbf{v}}_{A,m} + \tilde{\mathbf{v}}_{B,m} - \frac{\mathbf{U}_A \mathbf{v}_{A,m} - \mathbf{z}_{A,m} + \mathbf{v}_{B,m} - \mathbf{z}_{B,m} + \dot{\mathbf{v}}_m - \dot{\mathbf{z}}_m}{2} \right\|^2 \right) \tag{8.33a}$$

$$s.t. \quad \sum_{m=1}^M |\tilde{v}_{A,m,n} + \tilde{v}_{B,m,n}|^2 \leq P_n, \quad \forall n \in \mathcal{N} \tag{8.33b}$$

$$\mathbf{U}_A^H \tilde{\mathbf{v}}_{B,m} = \mathbf{0}, \quad \mathbf{U}_B^H \tilde{\mathbf{v}}_{A,m} = \mathbf{0}, \quad \forall m \in \mathcal{M} \tag{8.33c}$$

where $\dot{\mathbf{v}}_m - \dot{\mathbf{z}}_m$ term is added due to the constraint in (8.32c). Here, the elements of $\dot{\mathbf{v}}_m$ are $w_m^p \chi_{p,r}$ such that $\dot{\mathbf{v}}_m = [\ w_m^1 \chi_{1,1} \ w_m^1 \chi_{1,2} \ ... \ w_m^1 \chi_{1,R} \ w_m^2 \chi_{2,1} \ ... \ w_m^2 \chi_{2,R}$

$\ldots w_m^P \chi_{P,1} \ldots w_m^P \chi_{P,R}$ $]^T$ and $\overset{\bullet}{\mathbf{z}}_m$ is the corresponding scaled dual variable. Using the transformations as in the previous parts, i.e., $\tilde{\mathbf{w}}_m \triangleq \tilde{\mathbf{v}}_{A,m} + \tilde{\mathbf{v}}_{B,m}$, $\tilde{\mathbf{v}}_{A,m} = \mathbf{U}_A \boldsymbol{v}_{A,m}$ and $\tilde{\mathbf{v}}_{B,m} = \mathbf{U}_B \boldsymbol{v}_{B,m}$, (8.33) can be reformulated as follows,

$$\min_{\{\tilde{\mathbf{w}}_m, \boldsymbol{v}_{A,m}, \boldsymbol{v}_{B,m}\}_{m=1}^M} \sum_{m=1}^M ||\tilde{\mathbf{w}}_m - \frac{\rho}{1+2\rho}\tilde{\mathbf{z}}_m||^2 \tag{8.34a}$$

$$s.t. \sum_{m=1}^M |\tilde{w}_{m,n}|^2 \leq P_n, \ \forall n \in \mathcal{N} \tag{8.34b}$$

$$\boldsymbol{v}_{A,m} = \mathbf{U}_A^H \tilde{\mathbf{w}}_m, \quad \boldsymbol{v}_{B,m} = \mathbf{U}_B^H \tilde{\mathbf{w}}_m, \ \forall m \in \mathcal{M} \tag{8.34c}$$

where $\tilde{\mathbf{z}}_m \triangleq \mathbf{U}_A \mathbf{v}_{A,m} - \mathbf{z}_{A,m} + \mathbf{v}_{B,m} - \mathbf{z}_{B,m} + \overset{\bullet}{\mathbf{v}}_m - \overset{\bullet}{\mathbf{z}}_m$. Similar to the previous section, the optimum solution of (8.34) is found by solving (8.34a-b). Defining $\hat{\mathbf{w}}^n \triangleq$ $[\ \tilde{w}_{1,n} \ \tilde{w}_{2,n} \ \ldots \ \tilde{w}_{M,n} \ ]^T$ and $\hat{\mathbf{z}}^n \triangleq [\ \tilde{z}_{1,n} \ \tilde{z}_{2,n} \ \ldots \ \tilde{z}_{M,n} \ ]^T$, $\forall n \in \mathcal{N}$, the optimum update is given as follows,

$$\hat{\mathbf{w}}^n \leftarrow \min\left\{ \frac{\sqrt{P_n}}{||\hat{\mathbf{z}}^n||_2}, \frac{\rho}{1+2\rho} \right\}\hat{\mathbf{z}}^n, \ \forall n \in \mathcal{N} \tag{8.35a}$$

$$\tilde{\mathbf{w}}_m \leftarrow [\ \hat{w}_m^1 \ \hat{w}_m^2 \ \ldots \ \hat{w}_m^N \ ]^T, \ \forall m \in \mathcal{M} \tag{8.35b}$$

$$\tilde{\mathbf{v}}_{A,m} \leftarrow \mathbf{U}_A \mathbf{U}_A^H \tilde{\mathbf{w}}_m, \ \forall m \in \mathcal{M} \tag{8.35c}$$

$$\tilde{\mathbf{v}}_{B,m} \leftarrow \mathbf{U}_B \mathbf{U}_B^H \tilde{\mathbf{w}}_m, \ \forall m \in \mathcal{M} \tag{8.35d}$$

Now, let us consider the update for $\{\{w_m^p\}_{p=1}^P\}_{m=1}^M$ and $\{\{\chi_{p,r}\}_{r=1}^R\}_{p=1}^P$. The optimization problem for this can be expressed as follows,

$$\min_{\{\{w_m^p\}_{p=1}^P\}_{m=1}^M, \{\{\chi_{p,r}\}_{r=1}^R\}_{p=1}^P} \sum_{p=1}^P \sum_{m=1}^M \sum_{r=1}^R \left| w_m^p \chi_{p,r} - (\tilde{v}_{A,m}^{p,r} + \tilde{v}_{B,m}^{p,r} + \overset{\bullet}{\tilde{z}}_m^{p,r}) \right|^2. \tag{8.36}$$

In order to obtain the optimum solution of (8.36), take the derivative of objective function in (8.36) with respect to each variable and equate them to zero. In this case, we obtain the following equations,

$$w_m^p = \frac{\sum_{r'=1}^R \chi_{p,r'}^* \varepsilon_m^{p,r'}}{\sum_{r'=1}^R |\chi_{p,r'}|^2}, \ \forall m \in \mathcal{M}, \ \forall p \in \mathcal{P} \tag{8.37a}$$

$$\chi_{p,r} = \frac{\sum_{m'=1}^M (w_{m'}^p)^* \varepsilon_{m'}^{p,r}}{\sum_{m'=1}^M |w_{m'}^p|^2}, \ \forall r \in \mathcal{R}, \ \forall p \in \mathcal{P} \tag{8.37b}$$

where $\varepsilon_m^{p,r} \triangleq \tilde{v}_{A,m}^{p,r} + \tilde{v}_{B,m}^{p,r} + \overset{\bullet}{\tilde{z}}_m^{p,r}$, $\forall r \in \mathcal{R}$, $\forall p \in \mathcal{P}$, and $\forall m \in \mathcal{M}$ is used for ease of notation. Now, let us express the problem in (8.36) and the necessary conditions in

(8.37) in a more compact way by defining the following vectors and matrix,

$$\chi_p \triangleq \begin{bmatrix} \chi_{p,1} & \chi_{p,2} & \cdots & \chi_{p,R} \end{bmatrix}^T, \ \forall p \in \mathcal{P} \tag{8.38a}$$

$$w_p \triangleq \begin{bmatrix} w_1^p & w_2^p & \cdots & w_M^p \end{bmatrix}^T, \ \forall p \in \mathcal{P} \tag{8.38b}$$

$$E_p \triangleq \begin{bmatrix} \varepsilon_1^{p,1} & \varepsilon_2^{p,1} & \cdots & \varepsilon_M^{p,1} \\ \varepsilon_1^{p,2} & \varepsilon_2^{p,2} & \cdots & \varepsilon_M^{p,2} \\ \vdots & \vdots & & \vdots \\ \varepsilon_1^{p,R} & \varepsilon_2^{p,R} & \cdots & \varepsilon_M^{p,R} \end{bmatrix}, \ \forall p \in \mathcal{P} \tag{8.38c}$$

Using (8.21a-c), the optimization problem in (8.36) can be expressed as follows,

$$\min_{\{\chi_p, w_p\}_{p=1}^P} \sum_{p=1}^P \|\chi_p w_p^T - E_p\|_F^2. \tag{8.39}$$

Note that the Euclidean norm of χ_p can be chosen as unity $\forall p \in \mathcal{P}$ without loss of generality for the optimum solution of (8.39). Under this condition, i.e., $\|\chi_p\|_2 = 1$, $\forall p \in \mathcal{P}$, the necessary conditions for the optimum solution in (8.37a-b) can be expressed as follows,

$$w_p = E_p^T \chi_p^*, \ \forall p \in \mathcal{P} \tag{8.40a}$$

$$\chi_p = \frac{E_p w_p^*}{w_p^H w_p}, \ \forall p \in \mathcal{P} \tag{8.40b}$$

If we plug (8.40a) into (8.40b), we obtain

$$\chi_p = \frac{E_p E_p^H \chi_p}{\chi_p^H E_p E_p^H \chi_p}, \ \forall p \in \mathcal{P}. \tag{8.41}$$

It is seen that χ_p is an eigenvector of $E_p E_p^H$ with eigenvalue $\chi_p^H E_p E_p^H \chi_p$. In order to see which eigenvector with unit norm is the minimizer of objective function in (8.39), insert (8.40a) into the objective function in (8.39), i.e.,

$$\sum_{p=1}^P \|\chi_p \chi_p^H E_p - E_p\|_F^2 = \sum_{p=1}^P \text{Tr}\left((\chi_p \chi_p^H E_p - E_p)^H (\chi_p \chi_p^H E_p - E_p)\right)$$

$$= \sum_{p=1}^P \text{Tr}\left(E_p^H \chi_p \chi_p^H \chi_p \chi_p^H E_p - 2E_p^H \chi_p \chi_p^H E_p + E_p^H E_p\right)$$

$$= \sum_{p=1}^P \text{Tr}\left(-E_p^H \chi_p \chi_p^H E_p + E_p^H E_p\right)$$

$$= \sum_{p=1}^P \left(-\chi_p^H E_p E_p^H \chi_p + \text{Tr}(E_p^H E_p)\right) \tag{8.42}$$

where $\chi_p^H \chi_p = 1, \forall p \in \mathcal{P}$ is used. It is seen that the optimum χ_p maximizes $\chi_p^H E_p E_p^H \chi_p$ by (8.42). Hence, the optimum χ_p is the unit norm eigenvector corresponding to the largest eigenvalue of $E_p E_p^H$. Then, the optimum w_p is obtained by the equation (8.40a). As a final step, the following update is done for the dual variables $\{\dot{\mathbf{z}}_m\}_{m=1}^M$ as follows,

$$\dot{\mathbf{z}}_m \leftarrow \dot{\mathbf{z}}_m + \tilde{\mathbf{w}}_m - \dot{\mathbf{v}}_m, \ \forall m \in \mathcal{M}. \tag{8.43}$$

Overall, the simplified steps of the proposed ADMM algorithm are outlined as follows.

Algorithm 8.3: ADMM for Hybrid Beamforming with Vector Modulators

---

Initialization: Initialize $\tilde{\mathbf{w}}_m^0 \sim \mathcal{CN}(\mathbf{0}, \mathbf{I}_N)$, $(\dot{\mathbf{v}}_m)^0 = \tilde{\mathbf{w}}_m^0$, $\mathbf{v}_{A,m}^0 = \mathbf{U}_A^H \tilde{\mathbf{w}}_m^0$, $\lambda_{k,m}^0 \leftarrow 0$, $\forall k \in \mathcal{K}$, $\mathbf{u}_m^0 \leftarrow \mathbf{0}$, $(\dot{\mathbf{z}}_m)^0 \leftarrow \mathbf{0}$, $\forall m \in \mathcal{M}$. Set the iteration number $i \leftarrow 0$ and the penalty parameter ρ.

Repeat

$$\Gamma^{i+1}_{k,m_k} \leftarrow \begin{cases} \zeta^i_{k,m_k} & \text{if } \phi^i_k(0) \geq 0 \\ \frac{\zeta^i_{k,m_k}}{1-\mu^\star_k} & \text{if } \phi^i_k(0) < 0 \end{cases} \tag{8.44a}$$

$$\Gamma^{i+1}_{k,m'} \leftarrow \begin{cases} \zeta^i_{k,m'} & \text{if } \phi^i_k(0) \geq 0 \\ \frac{\zeta^i_{k,m'}}{1+\gamma_k\mu^\star_k} & \text{if } \phi^i_k(0) < 0 \end{cases}, \quad \forall m' \neq m_k, \tag{8.44b}$$

$\forall k \in \mathcal{K}$

$$\tilde{\mathbf{z}}^{i+1}_m \leftarrow \mathbf{U}_A(\mathbf{v}^i_{A,m} - \mathbf{u}^i_m) + \tilde{\mathbf{w}}^i_m - \mathbf{U}_A\mathbf{U}^H_A\tilde{\mathbf{w}}^i_m + (\mathbf{\dot{v}}_m)^i - (\mathbf{\dot{z}}_m)^i, \quad \forall m \in \mathcal{M} \tag{8.44c}$$

$$(\hat{\mathbf{w}}^n)^{i+1} \leftarrow \min\left\{\frac{\sqrt{P_n}}{||(\hat{\mathbf{z}}^n)^{i+1}||_2}, \frac{\rho}{1+2\rho}\right\}(\hat{\mathbf{z}}^n)^{i+1}, \quad \forall n \in \mathcal{N} \tag{8.44d}$$

$\chi^{i+1}_p \leftarrow$ unit norm eigenvector corresponding to

the largest eigenvalue of $\mathbf{E}^i_p(\mathbf{E}^H_p)^i, \quad \forall p \in \mathcal{P} \tag{8.44e}$

$$\mathbf{w}^{i+1}_p = (\mathbf{E}^T_p)^i(\chi^*_p)^{i+1}, \quad \forall p \in \mathcal{P} \tag{8.44f}$$

$$\mathbf{v}^{i+1}_{A,m} \leftarrow \left(\mathbf{I}_L + \Sigma^2_A\right)^{-1}\left(\mathbf{U}^H_A\tilde{\mathbf{w}}^{i+1}_m + \mathbf{u}^i_m\right.$$

$$\left. + \sum_{k=1}^K (\Sigma_A\mathbf{V}^H_A)_k(\Gamma^{i+1}_{k,m} + \lambda^i_{k,m})\right), \quad \forall m \in \mathcal{M} \tag{8.44g}$$

$$(\mathbf{\dot{z}}_m)^{i+1} \leftarrow (\mathbf{\dot{z}}_m)^i + \tilde{\mathbf{w}}^{i+1}_m - (\mathbf{\dot{v}}_m)^{i+1}, \quad \forall m \in \mathcal{M} \tag{8.44h}$$

$$\lambda^{i+1}_{k,m} \leftarrow \lambda^i_{k,m} + \Gamma^{i+1}_{k,m} - (\Sigma_A\mathbf{V}^H_A)^H_k\mathbf{v}^{i+1}_{A,m}, \quad \forall k \in \mathcal{K}, \forall m \in \mathcal{M} \tag{8.44i}$$

$$\mathbf{u}^{i+1}_m \leftarrow \mathbf{u}^i_m + \mathbf{U}^H_A\tilde{\mathbf{w}}^{i+1}_m - \mathbf{v}^{i+1}_{A,m}, \quad \forall m \in \mathcal{M} \tag{8.44j}$$

Set $i \leftarrow i + 1$.

Until stopping criterion is met.

8.6 Simulation Results

In this section, the performance of the proposed algorithms is compared with the existing benchmarks in [69] and [81]. In the figures, FDB, HB-PS and HB-VM stand for full digital beamforming, hybrid beamforming with phase shifters and hybrid beamforming with vector modulators, respectively. The work in [69] proposes a technique

for full digital beamforming while the one in [81] considers hybrid beamforming with vector modulators.

There are $M = 3$ multicast groups and 8 users in each group, i.e., $K = M \times 8 = 24$ users in total. Per-antenna power limit is taken as $P_n = 1/N$ Watts where N is the number of antennas at the BS. The channel path loss to noise variance ratio for all the users is set as 20 dB. The minimum required SINR is 10 dB for all the users. Two most widely used multipath channel models are considered in accordance with millimeter wave environment [107]. The first model assumes that the scatterers seen by different users are independent. If we assume a uniform linear array (ULA) model at the BS with antenna spacing equal to half of the carrier wavelength, the channel for the kth user is given by

$$\mathbf{h}_k = \sum_{s=1}^{S_k} \alpha_{k,s} [\ 1\ e^{-j\pi \cos(\theta_{k,s})}\ ...\ e^{-j\pi(N-1)cos(\theta_{k,s})}\ ]^T \qquad (8.45)$$

where S_k is the number of scatterers seen by the kth user. $\alpha_{k,s} \sim \mathcal{CN}(0, p_{k,s})$ is the complex gain of the sth path with $\sum_{s=1}^{S_k} p_{k,s} = 1$ [107]. $\theta_{k,s}$ is the angle of arrival of the sth path for the kth user. In the simulations, $p_{k,s}$ for $s = 1, ..., S_k, \forall k \in \mathcal{K}$ is generated randomly from a uniform random variable in [0,1] and normalized such that $\sum_{s=1}^{S_k} p_{k,s} = 1$ is satisfied. Similarly, $\theta_{k,s}$ for $s = 1, ..., S_k, \forall k \in \mathcal{K}$ is generated randomly form a uniform random variable in [0,2π].

The second model we consider is the scatter-sharing multipath channel model where the scatterers seen from all the users are common. Let S be the number of common scatterers. In this case, the channel vector for the kth user can be expressed as

$$\mathbf{h}_k = \sum_{s=1}^{S} \alpha_{k,s} [\ 1\ e^{-j\pi \cos(\theta_s)}\ ...\ e^{-j\pi(N-1)cos(\theta_s)}\ ]^T \qquad (8.46)$$

where $\alpha_{k,s} \sim \mathcal{CN}(0, p_{k,s})$ is the complex gain of the sth path with $\sum_{s=1}^{S_k} p_{k,s} = 1$.

Note that in all the experiments, the number of antennas for all the methods are the same, i.e. $N = PR$ where P is the number of RF chains per multicast stream for HB-PS whereas it is the number of total RF chains for HB-VM. R is the number of phase shifters or vector modulators following each RF chain. Although the number of antennas are the same, the number of RF chains is different for each method. The

number of total RF chains is N, $MP = 3P$, and P for FDB, HB-PS, and HB-VM, respectively.

First, we compare the convergence properties of our proposed algorithms with the benchmarks in [69] and [81]. A single experiment is realized for all the algorithms for $P = 8$ and $R = 10$. We consider independent multipath channel model given in (8.45) with $S_k = 12$, $\forall k \in \mathcal{K}$. Fig. 8.3 shows the transmitted power versus iteration number for the proposed FDB and the one in [69]. The algorithm in [69] consists of both outer and inner iteration loops and Fig. 8.3 denotes the inner loop iteration number for it. For the same experiment, Fig. 8.4 denotes the indicator function for the SINR constraints satisfaction. As shown in Fig. 8.4, the proposed method shows a more stable characteristics in terms of satisfying SINR constraints during iterations. At the 197th and further iterations, all the SINR constraints are satisfied. The transmitted power difference between this iteration and the last iteration is only 0.07 dBW as can be seen from Fig. 8.3. Moreover, there is approximately 12 dB power gain compared to the method in [69] at this iteration. From Fig. 8.3 and 8.4, it seems obvious that the proposed method superior convergence behavior compared to the benchmark in [69]. Note that at the deep points for the method in [69] in Fig. 8.3, the SINR constraints are not satisfied.

Figure 8.3: Transmitted power versus iteration number for FDB, $P = 8$, $R = 10$, and $S_k = 12$, $\forall k \in \mathcal{K}$.

Figure 8.4: Indicator function for the SINR constraints satisfaction for FDB, $P = 8$, $R = 10$, and $S_k = 12$, $\forall k \in \mathcal{K}$.

For the same experiment, the convergence behavior of the proposed HB-PS is shown in Fig. 8.5 and 8.6. Although there are some jumps in the indicator function, the SINR constraints are satisfied for most of the iterations. They are satisfied for the first time at the 510th iteration. At this point, the transmitted power is 0.85 dB more compared to the last iteration. Both Fig. 8.5 and 8.6 show that the proposed algorithm has a nice convergence behavior.

Figure 8.5: Transmitted power versus iteration number for HB-PS, $P = 8$, $R = 10$, and $S_k = 12$, $\forall k \in \mathcal{K}$.
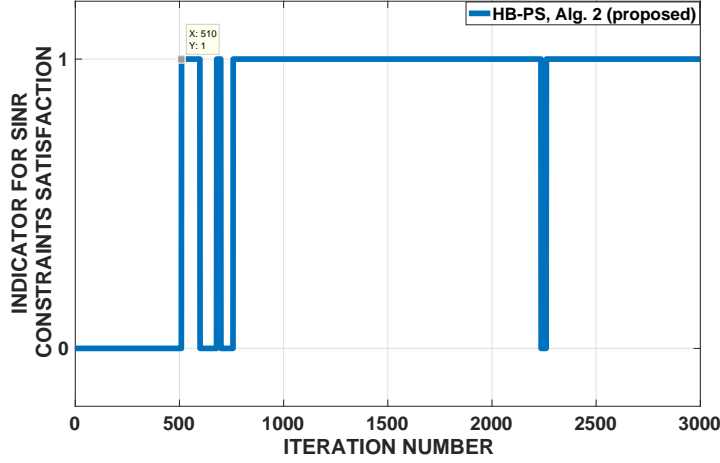
Figure 8.6: Indicator function for the SINR constraints satisfaction for HB-PS, $P = 8$, $R = 10$, and $S_k = 12$, $\forall k \in \mathcal{K}$.

Fig. 8.7 and 8.8 show the transmitted power and indicator function for the SINR constraints in terms of iteration number, respectively. Note that the algorithm in [81] is an alternation minimization over two two-nested loops. Hence, its total number of iterations is relatively large compared to the proposed method. As shown in Fig. 8.7, there is a 1 dBW difference between two methods after convergence. Moreover, the proposed method requires significantly less number of iterations. In a similar manner, the proposed method has a more stable characteristics in satisfying SINR constraints throughout the algorithm as can be seen in Fig. 8.8. Overall, all the figures 8.3-8 show that the proposed algorithms are more advantageous in terms of convergence compared to its existing counterparts.
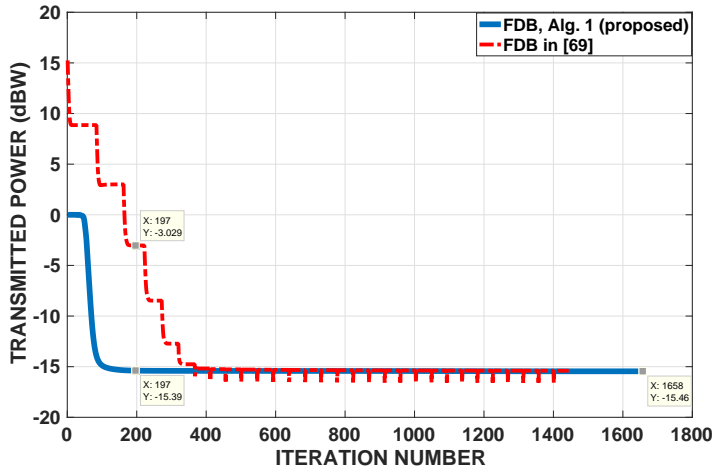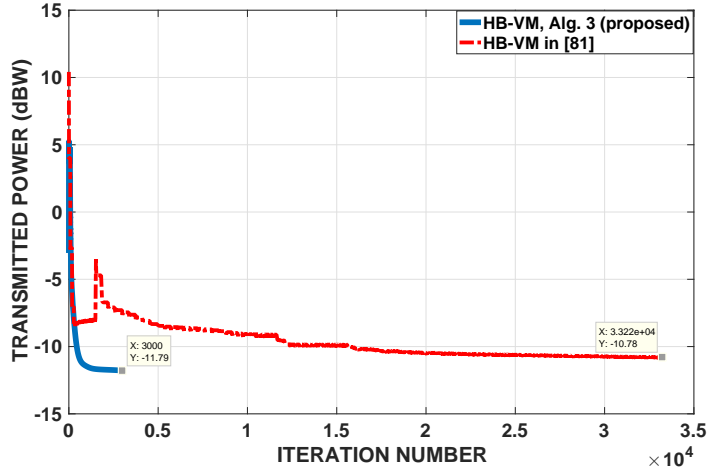
Figure 8.7: Transmitted power versus iteration number for HB-VM, $P = 8$, $R = 10$, and $S_k = 12$, $\forall k \in \mathcal{K}$.
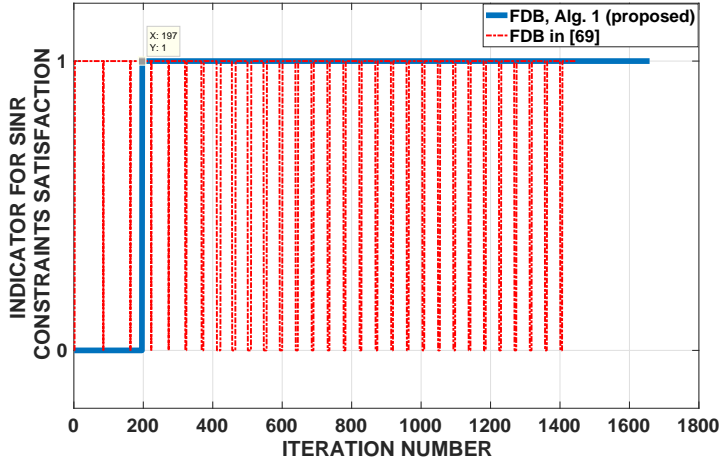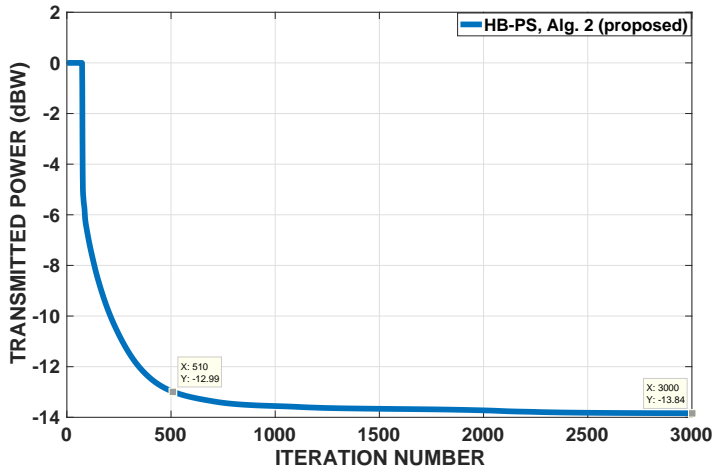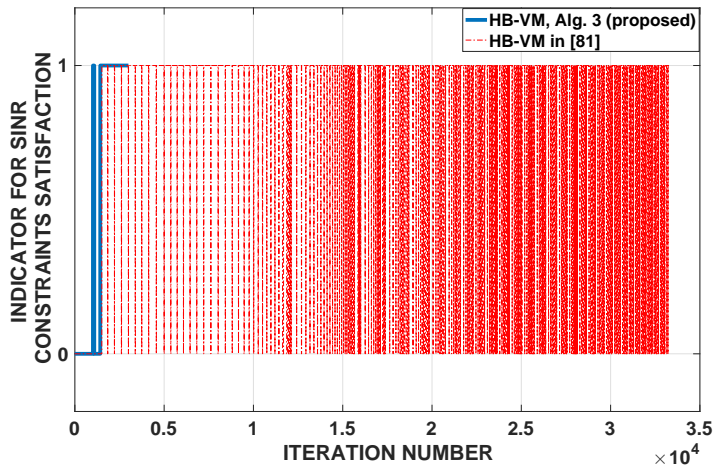

Figure 8.8: Indicator function for the SINR constraints satisfaction for HB-VM, $P = 8$, $R = 10$, and $S_k = 12$, $\forall k \in \mathcal{K}$.

In the following experiments, each point in the figures represent the average of 100 random channel realizations.

In the second experiment, we consider independent multipath channel model given in (8.45) with $S_k = 12$, $\forall k \in \mathcal{K}$. The number of RF chains per each multicast stream for HB-PS and the number of total RF chains for HB-VM are taken as $P = 8$. R is varied from 4 to 12 and all the methods are compared in terms of average

196

transmitted power in Fig. 8.9. As shown in Fig. 8.9, the proposed FDB and the one in [69] perform nearly the same for all the scenarios. The difference between two methods can be observed from Table 8.1 where average run time for each algorithm is presented for each method. The proposed FDB results the same performance with less computational time. When we come back to Fig. 8.9, we see that HB-PS performs worse than FDB as expected since it uses $3P = 24$ RF chains whereas FDB uses $8R$ RF chains. Considering the high loss coming with each RF chain in millimeter wave systems, this performance loss is expected to be overcompensated in a real setup. Furthermore, HB-PS performs better than HB-VM for all the scenarios both in terms of average transmitted power and run time. However, it should be taken into account that HB-PS uses $3P = 24$ RF chains while HB-VM needs $P = 8$ RF chains in total.
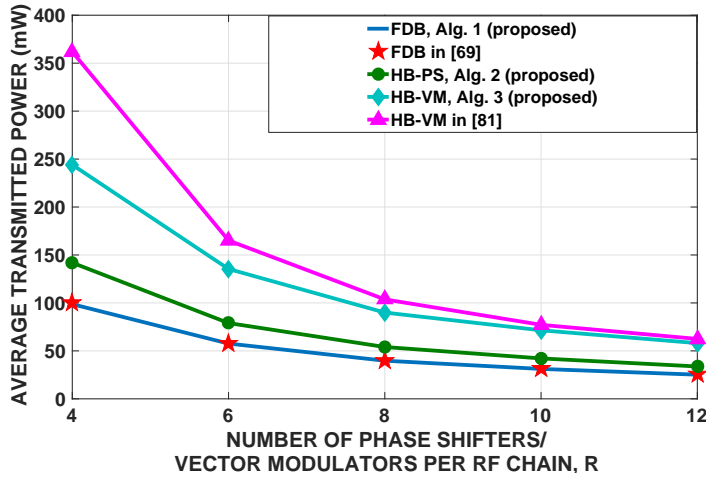
Figure 8.9: Average transmitted power versus number of phase shifters / vector modulators per RF chain, R, for $P = 8$ and $S_k = 12$, $\forall k \in \mathcal{K}$.

The proposed HB-VM results significant computational advantage compared to its counterpart in [81] as can be seen in Table 8.1. Furthermore, Fig. 8.9 shows that it requires also less transmitted power. This double advantage comes from the fact that the proposed method directly tackles the original problem and uses the proposed computationally effective reformulation. On the other hand , the method in [81] adopts a three-layer optimization approach which increases computational burden significantly.

Note that the average transmitted power for all the methods in Fig. 8.9 decreases with

R since number of antennas increases without changing RF chain number. Hence, we can obtain a desired performance by increasing the number of units following each RF chain at the same time using small number of RF chains for a power efficient system.

Table 8.1: Average Run Time (seconds), $P = 8$ and $S_k = 12$, $\forall k \in \mathcal{K}$

	R				
	4	6	8	10	12
FDB, Alg. 1 (proposed)	0.3040	0.4650	0.6822	0.9276	1.2189
FDB in [69]	1.2402	1.1971	1.3483	1.6829	1.8115
HB-PS, Alg. 2 (proposed)	1.9275	2.6339	2.9320	3.3200	3.4757
HB-VM, Alg. 3 (proposed)	2.5306	3.1970	3.4553	3.8923	4.2101
HB-VM in [81]	51.4124	42.8264	50.0095	62.9391	76.1756

Fig. 8.10 and Table 8.2 are for the third experiment where the same independent multipath channel model in (8.45) is considered with $S_k = 12$. The number of phase shifters or vector modulators following each RF chain is set as $R = 10$. In Fig. 8.10 we plot the average transmitted power versus P which is number of total RF chains for HB-VM whereas number of RF chains per each multicast stream for HB-PS. Note that x-axis of Fig. 8.10 is labeled "number of RF chains" for simplicity. Table 8.2 presents the average run time for the same experiment. Similar to the previous experiment, the proposed FDB attains the same performance with less computational complexity thanks to the improved-ADMM algorithm.
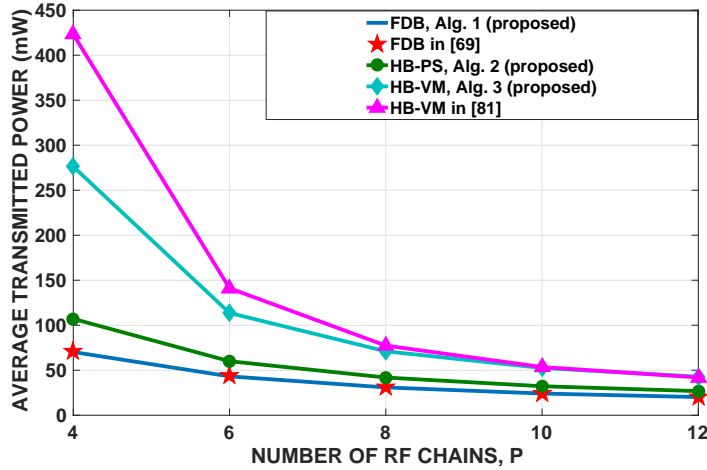
Figure 8.10: Average transmitted power versus number of RF chains, P, for $R = 10$ and $S_k = 12$, $\forall k \in \mathcal{K}$.

In a similar manner, the average transmitted power for HB-PS is more than that of FDB and less than that of HB-VM. Except for $P = 4$ scenario, its computational complexity is less than that of HB-VM. It is an advantageous method and uses simple phase shifters instead of vector modulators. However, it requires M times more RF chain for the same number of antennas. When we observe Table 8.2, we again see the proposed HB-VM method need significantly less run time compared to the one in [81]. In addition to its computational advantage, it performs better in terms of transmitted power especially for smaller P values.

As a final comment to Fig. 8.10, all the methods requires less and less transmitted power as P increases which is an expected result. In fact, both the number of antennas and RF chains increases. The increase in RF chain for hybrid beamforming methods enhances the digital beamforming capability and reduces the transmitted power.

Table 8.2: Average Run Time (seconds), $R = 10$ and $S_k = 12$, $\forall k \in \mathcal{K}$

	P				
	4	6	8	10	12
FDB, Alg. 1 (proposed)	0.4217	0.6757	0.9510	1.2257	1.5083
FDB in [69]	1.2304	1.3535	1.7369	1.9342	2.1072
HB-PS, Alg. 2 (proposed)	2.3327	2.8243	3.2815	3.5152	3.6999
HB-VM, Alg. 3 (proposed)	2.0648	3.3493	3.9612	4.3124	4.5926
HB-VM in [81]	80.9398	46.2869	65.5294	79.6030	95.8791

In the last experiment, we consider the scatterer-sharing multipath channel model in (8.46) with different number of scatterers, S. In Fig. 8.11 and its corresponding run time Table 8.3, S is varied from 16 to 24. S being smaller results the rank of stacked channel $\mathbf{H}$ be smaller. In fact, its rank is at most S. In this case, there is a severe inter-user interference [107] and satisfying QoS-aware constraints becomes more difficult. In this experiment, we set $P = 8$ and $R = 10$. It can be easily seen that transmitted power levels for all the methods is higher compared to the counterpart scenarios in Fig. 8.9 and 8.10. This is due to the fact that the independent scatterer channel model in Fig. 8.9 and 8.10 provides a rich scattering environment.
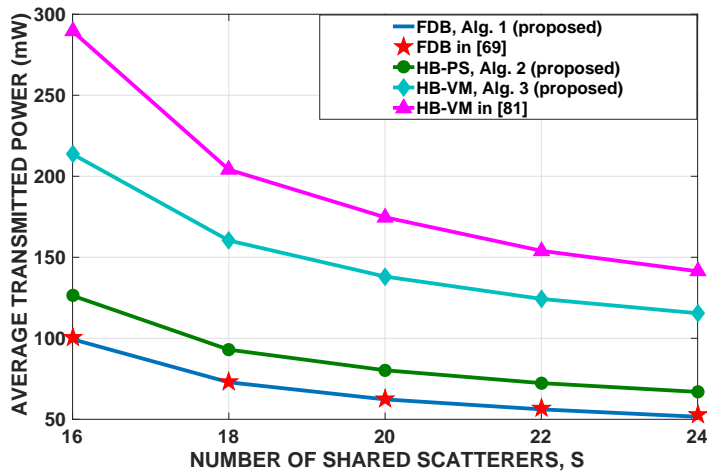

Figure 8.11: Average transmitted power versus number of shared scatterers, S, for $P = 8$ and $R = 10$.

In Fig. 8.11, we see that there is a power difference between the proposed HB-VM and HB-VM in [81] similar to the previous scenarios. Besides that, the proposed methods have significantly less computational complexity as shown in Table 8.3.

As a last comment, we observe that the increase in number of shared-scatterer S results less transmitted power by generating a richer scatterer environment and increasing the rank of stacked channel matrix.

Table 8.3: Average Run Time (seconds), $P = 8$, $R = 10$

	S				
	16	18	20	22	24
FDB, Alg. 1 (proposed)	0.4981	0.6511	0.7555	0.8775	1.0288
FDB in [69]	2.1140	2.1643	2.2089	2.2695	2.3788
HB-PS, Alg. 2 (proposed)	2.2797	2.7534	2.7239	2.9790	3.1008
HB-VM, Alg. 3 (proposed)	3.2435	3.6081	3.8194	3.8645	3.8544
HB-VM in [81]	104.7051	63.9613	55.4497	50.5342	51.7101

8.7 Conclusion

QoS-aware multi-group multicasting problem with per-antenna power constraints is considered. A new reformulation is obtained by using and efficient decomposition of the optimization variables. First, full digital beamformer is considered and the optimum update equations are presented for the ADMM algorithm. After some rearrangements, a memory-efficient implementation of the algorithm is obtained. Then, two different hybrid beamforming structures are investigated by using our effective decomposition method. All the ADMM updates in the beamforming structures are solved optimally and effectively. The first hybrid beamforming system which employs analog phase shifters uses more number of RF chains for a given number of antennas in comparison to the second structure. The second structure uses vector modulators instead of phase shifters. Simulation results show that the first hybrid beamforming system requires significantly less transmission power by taking advantage of the additional RF chains. The proposed full digital beamformer performs

nearly the same as its counterpart benchmark in terms of transmitted power with significantly less computational time. All other proposed algorithms are shown to be computationally more efficient and have better convergence properties compared to the benchmarks in the literature. Furthermore, the proposed hybrid beamformer with vector modulators attains less transmitted power compared to its counterpart for most of the scenarios.

CHAPTER 9

CONCLUSION

This thesis studies a broad range of optimization problems in energy harvesting and multi-user communications area. Several papers are published from these studies and a couple of them are submitted for publication. Each chapter investigates different problems, effective solutions and methods for them in detail. Chapter 2, 3, and 8 consider several design problems in multi-group multicasting context. While Chapter 2 and 3 include simultaneous wireless information and power transfer, Chapter 8 only deals with conventional multi-group multicast beamforming design. In Chapter 2, each user has a power splitting device and energy harvesting constraints are added to the quality of service-aware design problem. Low-cost alternatives to full digital beamforming, namely antenna selection and hybrid beamforming are elaborated and several effective algorithms are proposed. It is observed that the performance of antenna selection degrades compared to the hybrid beamforming as the number of antennas increases. This is due to the fact that hybrid beamforming takes advantage of all the antennas.

In Chapter 3, different from other chapters which consider single-carrier systems, max-min fair based resource allocation for OFDM based multi-group multicasting systems is investigated. An efficient two-stage near-optimum technique is developed using an effectively designed subcarrier allocation algorithm and convex optimization problem solver for power splitting ratios. The minimum signal-to-noise ratio obtained by the proposed method is very close to the optimum solution which is extremely costly in terms of computation.

In Chapter 8, per-antenna power constraints are included to conventional quality-of-service beamformer design problem in order to compare the proposed methods with

the benchmarks in the literature. In this chapter, energy harvesting is not taken into account and full digital beamforming together with hybrid beamforming with phase shifters and vector modulators are considered. Alternating directions method of multipliers which is an efficient first order optimization method is used in order to solve the effectively reformulated problem. In this reformulation, the beamformer weight vectors are decomposed into two subspaces such that the steps of the alternating directions method of multipliers algorithm become computationally efficient compared to its alternatives in the literature. Simulation results show that the proposed algorithms have better convergence properties and less computational time by performing the same or better than the benchmarks in terms of transmitted power.

In Chapter 4, 5, 6, and 7 we consider wireless-powered relaying where a single user exists in the system. Several important scenarios are investigated and the closed-form optimum solutions are derived for most of the problems in these chapters. In Chapter 4, the relay harvests energy from the dedicated energy signal sent from the source and self-energy recycling. The optimization objective is to determine the best transmit relay beamformer which minimizes the transmitted power by the relay's own battery such that signal-to-noise ratio at the destination user is satisfied. This problem is first investigated here and the closed-form optimum solution and feasibility conditions are derived. Simulation results show that improving self-energy recycling loop channel makes the system performance better by decreasing the required power by the relay's own battery.

In Chapter 5, we consider the same scenario in Chapter 4 by employing multiple receive antennas at the relay. This time, signal-to-noise ratio maximization problem is investigated. Two protocols which are self-energy recycling and power splitting based ones are studied and the closed-form optimum solutions are derived for the first time in the literature. Secondly, a new protocol is developed by combining self-energy recycling and power splitting. A near-optimum solution for this protocol is developed. Finally, discrete set of power splitting ratios is considered and the optimum solution for this combinatorial problem is obtained.

Chapter 6 studies the same system in Chapter 4 for two optimization problems, i.e. signal-to-noise ratio maximization and quality of service-aware design problems.

Similar to Chapter 4 and 5, amplify-and-forward relaying protocol is adopted. Differently, the joint source power allocation and relay transmit beamformer design are considered unlike the previous chapters which assume equal power allocation at the source during two phases. The joint optimum solution is derived for signal-to-noise ratio maximization problem while a near-optimum solution is presented for the other one. Simulation results show that inclusion of power allocation to the conventional optimization problem brings about a huge advantage in terms of transmitted power by the relay and signal-to-noise ratio at the user.

Finally, Chapter 7 studies both single and multiple receive antenna relaying for the similar self-energy recycling protocol. Different from Chapter 4, 5, and 6, we adopt decode-and-forward relaying protocol in this chapter. In the literature, a sub-optimum solution exists for the signal-to-noise ratio maximization problem for single receive antenna relay. In this chapter, we derive the optimum solution for both quality of service-aware and signal-to-noise ratio maximization problems. Simulation results show that the proposed method performs better than the sub-optimum one in the literature. In the second part of this chapter, we deal with the same optimization problems for multiple receive antenna relay by taking into the receive beamformer design account. Although a near-optimum solution is found for the joint optimization problems, simulation results verify that the receive beamforming at the multiple antenna relay improves the system performance significantly.

REFERENCES

[1] D. W. K. Ng, E. S. Lo, and R. Schober, "Wireless information and power transfer: Energy efficiency optimization in OFDMA systems," *IEEE Transactions on Wireless Communications*, vol. 12, pp. 6352–6370, December 2013.

[2] R. Zhang and C. K. Ho, "MIMO broadcasting for simultaneous wireless information and power transfer," *IEEE Transactions on Wireless Communications*, vol. 12, pp. 1989–2001, May 2013.

[3] Y. Zeng, B. Clerckx, and R. Zhang, "Communications and signals design for wireless power transmission," *IEEE Transactions on Communications*, vol. 65, pp. 2264–2290, May 2017.

[4] S. Hu, Z. Ding, and Q. Ni, "Beamforming optimisation in energy harvesting cooperative full-duplex networks with self-energy recycling protocol," *IET Communications*, vol. 10, no. 7, pp. 848–853, 2016.

[5] Z. Ding, I. Krikidis, B. Sharif, and H. V. Poor, "Wireless information and power transfer in cooperative networks with spatially random relays," *IEEE Transactions on Wireless Communications*, vol. 13, pp. 4440–4453, Aug 2014.

[6] S. Bi, C. K. Ho, and R. Zhang, "Wireless powered communication: Opportunities and challenges," *IEEE Communications Magazine*, vol. 53, pp. 117–125, April 2015.

[7] X. Lu, P. Wang, D. Niyato, D. I. Kim, and Z. Han, "Wireless networks with RF energy harvesting: A contemporary survey," *IEEE Communications Surveys Tutorials*, vol. 17, pp. 757–789, Secondquarter 2015.

[8] Q. Shi, L. Liu, W. Xu, and R. Zhang, "Joint transmit beamforming and receive power splitting for MISO SWIPT systems," *IEEE Transactions on Wireless Communications*, vol. 13, pp. 3269–3280, June 2014.

[9] X. Chen, C. Yuen, and Z. Zhang, "Wireless energy and information transfer tradeoff for limited-feedback multiantenna systems with energy beamforming," *IEEE Transactions on Vehicular Technology*, vol. 63, pp. 407–412, Jan 2014.

[10] O. T. Demir and T. E. Tuncer, "Antenna selection and hybrid beamforming for simultaneous wireless information and power transfer in multi-group multicasting systems," *IEEE Transactions on Wireless Communications*, vol. 15, pp. 6948–6962, Oct 2016.

[11] L. R. Varshney, "Transporting information and energy simultaneously," in *2008 IEEE International Symposium on Information Theory*, pp. 1612–1616, July 2008.

[12] P. Grover and A. Sahai, "Shannon meets Tesla: Wireless information and power transfer," in *2010 IEEE International Symposium on Information Theory*, pp. 2363–2367, June 2010.

[13] M. R. A. Khandaker and K. Wong, "SWIPT in MISO multicasting systems," *IEEE Wireless Communications Letters*, vol. 3, pp. 277–280, June 2014.

[14] O. T. Demir and T. E. Tuncer, "Multi-group multicast beamforming for simultaneous wireless information and power transfer," in *2015 23rd European Signal Processing Conference (EUSIPCO)*, pp. 1356–1360, Aug 2015.

[15] S. Yin and Z. Qu, "Resource allocation in multiuser OFDM systems with wireless information and power transfer," *IEEE Communications Letters*, vol. 20, pp. 594–597, March 2016.

[16] X. Zhou, R. Zhang, and C. K. Ho, "Wireless information and power transfer in multiuser OFDM systems," *IEEE Transactions on Wireless Communications*, vol. 13, pp. 2282–2294, April 2014.

[17] Y. Liu and X. Wang, "Information and energy cooperation in OFDM relaying: Protocols and optimization," *IEEE Transactions on Vehicular Technology*, vol. 65, pp. 5088–5098, July 2016.

[18] M. Zhang and Y. Liu, "Energy harvesting for physical-layer security in OFDMA networks," *IEEE Transactions on Information Forensics and Security*, vol. 11, pp. 154–162, Jan 2016.

[19] Y. Zeng and R. Zhang, "Full-duplex wireless-powered relay with self-energy recycling," *IEEE Wireless Communications Letters*, vol. 4, pp. 201–204, April 2015.

[20] A. A. Nasir, X. Zhou, S. Durrani, and R. A. Kennedy, "Relaying protocols for wireless energy harvesting and information processing," *IEEE Transactions on Wireless Communications*, vol. 12, pp. 3622–3636, July 2013.

[21] O. T. Demir and T. E. Tuncer, "Optimum QoS-aware beamformer design for full-duplex relay with self-energy recycling," *IEEE Wireless Communications Letters*, vol. 7, pp. 122–125, Feb 2018.

[22] W. Wu, B. Wang, Z. Deng, and H. Zhang, "Secure beamforming for full-duplex wireless powered communication systems with self-energy recycling," *IEEE Wireless Communications Letters*, vol. 6, pp. 146–149, April 2017.

[23] Y. Alsaba, C. Y. Leow, and S. K. A. Rahim, "Full-duplex cooperative non-orthogonal multiple access with beamforming and energy harvesting," *IEEE Access*, vol. 6, pp. 19726–19738, 2018.

[24] N. D. Sidiropoulos, T. N. Davidson, and Z.-Q. Luo, "Transmit beamforming for physical-layer multicasting," *IEEE Transactions on Signal Processing*, vol. 54, pp. 2239–2251, June 2006.

[25] E. Karipidis, N. D. Sidiropoulos, and Z. Luo, "Quality of service and max-min fair transmit beamforming to multiple cochannel multicast groups," *IEEE Transactions on Signal Processing*, vol. 56, pp. 1268–1279, March 2008.

[26] M. Sadeghi, E. Björnson, E. G. Larsson, C. Yuen, and T. L. Marzetta, "Joint unicast and multi-group multicast transmission in massive MIMO systems," *IEEE Transactions on Wireless Communications*, pp. 1–1, 2018.

[27] M. Sadeghi, L. Sanguinetti, and C. Yuen, "Hybrid precoding for multi-group physical layer multicasting," in *European Wireless 2018; 24th European Wireless Conference*, pp. 1–6, May 2018.

[28] M. Sadeghi, L. Sanguinetti, R. Couillet, and C. Yuen, "Reducing the computational complexity of multicasting in large-scale antenna systems," *IEEE Transactions on Wireless Communications*, vol. 16, pp. 2963–2975, May 2017.

[29] M. Sadeghi, E. Björnson, E. G. Larsson, C. Yuen, and T. L. Marzetta, "Max–min fair transmit precoding for multi-group multicasting in massive MIMO," *IEEE Transactions on Wireless Communications*, vol. 17, pp. 1358–1373, Feb 2018.

[30] G. Araniti, M. Condoluci, P. Scopelliti, A. Molinaro, and A. Iera, "Multicasting over emerging 5G networks: Challenges and perspectives," *IEEE Network*, vol. 31, pp. 80–89, March 2017.

[31] J. Montalban, P. Scopelliti, M. Fadda, E. Iradier, C. Desogus, P. Angueira, M. Murroni, and G. Araniti, "Multimedia multicast services in 5G networks: Subgrouping and non-orthogonal multiple access techniques," *IEEE Communications Magazine*, vol. 56, pp. 91–95, March 2018.

[32] Z. Xiang, M. Tao, and X. Wang, "Massive MIMO multicasting in noncooperative cellular networks," *IEEE Journal on Selected Areas in Communications*, vol. 32, pp. 1180–1193, June 2014.

[33] G. Venkatraman, A. Tölli, M. Juntti, and L. Tran, "Multigroup multicast beamformer design for MISO-OFDM with antenna selection," *IEEE Transactions on Signal Processing*, vol. 65, pp. 5832–5847, Nov 2017.

[34] O. Mehanna, K. Huang, B. Gopalakrishnan, A. Konar, and N. D. Sidiropoulos, "Feasible point pursuit and successive approximation of non-convex QCQPs," *IEEE Signal Processing Letters*, vol. 22, pp. 804–808, July 2015.

[35] O. Mehanna, N. D. Sidiropoulos, and G. B. Giannakis, "Joint multicast beamforming and antenna selection," *IEEE Transactions on Signal Processing*, vol. 61, pp. 2660–2674, May 2013.

[36] O. T. Demir and T. E. Tuncer, "Multicast beamforming with antenna selection using exact penalty approach," in *2015 IEEE International Conference on Acoustics, Speech and Signal Processing (ICASSP)*, pp. 2489–2493, April 2015.

[37] S. Y. Park and D. J. Love, "Capacity limits of multiple antenna multicasting using antenna subset selection," *IEEE Transactions on Signal Processing*, vol. 56, pp. 2524–2534, June 2008.

[38] S. Han, C. I, Z. Xu, and C. Rowell, "Large-scale antenna systems with hybrid analog and digital beamforming for millimeter wave 5G," *IEEE Communications Magazine*, vol. 53, pp. 186–194, January 2015.

[39] J. A. Zhang, X. Huang, V. Dyadyuk, and Y. J. Guo, "Massive hybrid antenna array for millimeter-wave cellular communications," *IEEE Wireless Communications*, vol. 22, pp. 79–87, February 2015.

[40] F. Sohrabi and W. Yu, "Hybrid digital and analog beamforming design for large-scale MIMO systems," in *2015 IEEE International Conference on Acoustics, Speech and Signal Processing (ICASSP)*, pp. 2929–2933, April 2015.

[41] G. Wang and G. Ascheid, "Hybrid beamforming under equal gain constraint for maximizing sum rate at 60 GHz," in *2015 IEEE 81st Vehicular Technology Conference (VTC Spring)*, pp. 1–5, May 2015.

[42] F. Sohrabi and W. Yu, "Hybrid beamforming with finite-resolution phase shifters for large-scale MIMO systems," in *2015 IEEE 16th International Workshop on Signal Processing Advances in Wireless Communications (SPAWC)*, pp. 136–140, June 2015.

[43] N. Sharma and A. S. Madhukumar, "Genetic algorithm aided proportional fair resource allocation in multicast OFDM systems," *IEEE Transactions on Broadcasting*, vol. 61, pp. 16–29, March 2015.

[44] M. G. Kibria and L. Shan, "Resource allocation optimization for users with different levels of service in multicarrier systems," *IEEE Signal Processing Letters*, vol. 22, pp. 1869–1873, Nov 2015.

[45] Y. Li, M. Sheng, C. W. Tan, Y. Zhang, Y. Sun, X. Wang, Y. Shi, and J. Li, "Energy-efficient subcarrier assignment and power allocation in OFDMA systems with max-min fairness guarantees," *IEEE Transactions on Communications*, vol. 63, pp. 3183–3195, Sept 2015.

[46] Y. Lee, Y. . Hsieh, and H. . Shieh, "Symbol-based processing with balanced subcarrier performance for MIMO-OFDM systems," *IEEE Communications Letters*, vol. 13, pp. 167–169, March 2009.

[47] J. Leithon, S. Sun, and C. Yuen, "Relay selection algorithms for analog network coding OFDM systems," *IEEE Communications Letters*, vol. 16, pp. 1442–1445, September 2012.

[48] B. Medepally and N. B. Mehta, "Voluntary energy harvesting relays and selection in cooperative wireless networks," *IEEE Transactions on Wireless Communications*, vol. 9, pp. 3543–3553, November 2010.

[49] L. Zhao, X. Wang, and T. Riihonen, "Transmission rate optimization of full-duplex relay systems powered by wireless energy transfer," *IEEE Transactions on Wireless Communications*, vol. 16, pp. 6438–6450, Oct 2017.

[50] Z. Ding and H. V. Poor, "Multi-user SWIPT cooperative networks: Is the max–min criterion still diversity-optimal?," *IEEE Transactions on Wireless Communications*, vol. 15, pp. 553–567, Jan 2016.

[51] I. Krikidis, S. Timotheou, and S. Sasaki, "RF energy transfer for cooperative networks: Data relaying or energy harvesting?," *IEEE Communications Letters*, vol. 16, pp. 1772–1775, November 2012.

[52] D. Wang, R. Zhang, X. Cheng, L. Yang, and C. Chen, "Relay selection in full-duplex energy-harvesting two-way relay networks," *IEEE Transactions on Green Communications and Networking*, vol. 1, pp. 182–191, June 2017.

[53] C. Zhong, H. A. Suraweera, G. Zheng, I. Krikidis, and Z. Zhang, "Wireless information and power transfer with full duplex relaying," *IEEE Transactions on Communications*, vol. 62, pp. 3447–3461, Oct 2014.

[54] M. Mohammadi, B. K. Chalise, H. A. Suraweera, C. Zhong, G. Zheng, and I. Krikidis, "Throughput analysis and optimization of wireless-powered multiple antenna full-duplex relay systems," *IEEE Transactions on Communications*, vol. 64, pp. 1769–1785, April 2016.

212

[55] R. Chen and H. Zhang, "Power efficiency optimisation of wireless-powered full-duplex relay systems," *IET Communications*, vol. 12, no. 5, pp. 603–611, 2018.

[56] D. Wang, R. Zhang, X. Cheng, and L. Yang, "Capacity-enhancing full-duplex relay networks based on power-splitting (PS-)SWIPT," *IEEE Transactions on Vehicular Technology*, vol. 66, pp. 5445–5450, June 2017.

[57] T. Riihonen, L. Zhao, M. Vehkaperä, and X. Wang, "On the feasibility of full-duplex relaying powered by wireless energy transfer," in *2016 IEEE 17th International Workshop on Signal Processing Advances in Wireless Communications (SPAWC)*, pp. 1–5, July 2016.

[58] W. Wang, R. Wang, W. Duan, R. Feng, and G. Zhang, "Optimal transceiver designs for wireless-powered full-duplex two-way relay networks with SWIPT," *IEEE Access*, vol. 5, pp. 22329–22343, 2017.

[59] D. Hwang, S. S. Nam, and J. Yang, "Multi-antenna beamforming techniques in full-duplex and self-energy recycling systems: Opportunities and challenges," *IEEE Communications Magazine*, vol. 55, pp. 160–167, October 2017.

[60] H. Ju and R. Zhang, "Optimal resource allocation in full-duplex wireless-powered communication network," *IEEE Transactions on Communications*, vol. 62, pp. 3528–3540, Oct 2014.

[61] Z. Wang, L. Li, H. Wang, and H. Tian, "Beamforming design in relay-based full-duplex MISO wireless powered communication networks," *IEEE Communications Letters*, vol. 20, pp. 2047–2050, Oct 2016.

[62] D. Hwang, K. C. Hwang, D. I. Kim, and T. Lee, "Self-energy recycling for RF powered multi-antenna relay channels," *IEEE Transactions on Wireless Communications*, vol. 16, pp. 812–824, Feb 2017.

[63] G. A. Ropokis, M. M. Butt, N. Marchetti, and L. A. DaSilva, "Optimal power allocation for energy recycling assisted cooperative communications," in *2017 IEEE Wireless Communications and Networking Conference Workshops (WCNCW)*, pp. 1–6, March 2017.

[64] Y. Su, L. Jiang, and C. He, "Decode-and-forward relaying with full-duplex wireless information and power transfer," *IET Communications*, vol. 11, no. 13, pp. 2110–2115, 2017.

[65] H. Liu, K. J. Kim, K. S. Kwak, and H. V. Poor, "Power splitting-based SWIPT with decode-and-forward full-duplex relaying," *IEEE Transactions on Wireless Communications*, vol. 15, pp. 7561–7577, Nov 2016.

[66] D. Altinel and G. K. Kurt, "Diversity combining for RF energy harvesting," in *2017 IEEE 85th Vehicular Technology Conference (VTC Spring)*, pp. 1–5, June 2017.

[67] R. Vahidnia, A. Anpalagan, and J. Mirzaei, "Diversity combining in bi-directional relay networks with energy harvesting nodes," *IET Communications*, vol. 10, no. 2, pp. 207–211, 2016.

[68] K. Huang and N. D. Sidiropoulos, "Consensus-ADMM for general quadratically constrained quadratic programming," *IEEE Transactions on Signal Processing*, vol. 64, pp. 5297–5310, Oct 2016.

[69] E. Chen and M. Tao, "ADMM-based fast algorithm for multi-group multicast beamforming in large-scale wireless systems," *IEEE Transactions on Communications*, vol. 65, pp. 2685–2698, June 2017.

[70] C. Wang, F. Haider, X. Gao, X. You, Y. Yang, D. Yuan, H. M. Aggoune, H. Haas, S. Fletcher, and E. Hepsaydir, "Cellular architecture and key technologies for 5G wireless communication networks," *IEEE Communications Magazine*, vol. 52, pp. 122–130, February 2014.

[71] K. Xiao, F. Wang, H. Rutagemwa, K. Michel, and B. Rong, "High-performance multicast services in 5G big data network with massive MIMO," in *2017 IEEE International Conference on Communications (ICC)*, pp. 1–6, May 2017.

[72] L. Tran, M. F. Hanif, and M. Juntti, "A conic quadratic programming approach to physical layer multicasting for large-scale antenna arrays," *IEEE Signal Processing Letters*, vol. 21, pp. 114–117, Jan 2014.

[73] D. Christopoulos, S. Chatzinotas, and B. Ottersten, "Multicast multigroup beamforming for per-antenna power constrained large-scale arrays," in *2015 IEEE 16th International Workshop on Signal Processing Advances in Wireless Communications (SPAWC)*, pp. 271–275, June 2015.

[74] D. Christopoulos, S. Chatzinotas, and B. Ottersten, "Weighted fair multicast multigroup beamforming under per-antenna power constraints," *IEEE Transactions on Signal Processing*, vol. 62, pp. 5132–5142, Oct 2014.

[75] X. Shen, L. Chen, Y. Gu, and H. C. So, "Square-root lasso with nonconvex regularization: An ADMM approach," *IEEE Signal Processing Letters*, vol. 23, pp. 934–938, July 2016.

[76] S. Kumar, R. Jain, and K. Rajawat, "Asynchronous optimization over heterogeneous networks via consensus ADMM," *IEEE Transactions on Signal and Information Processing over Networks*, vol. 3, pp. 114–129, March 2017.

[77] M. . Vázquez, A. Konar, L. Blanco, N. D. Sidiropoulos, and A. I. Pérez-Neira, "Non-convex consensus ADMM for satellite precoder design," in *2017 IEEE International Conference on Acoustics, Speech and Signal Processing (ICASSP)*, pp. 6279–6283, March 2017.

[78] Z. Cheng, Z. He, S. Zhang, and J. Li, "Constant modulus waveform design for MIMO radar transmit beampattern," *IEEE Transactions on Signal Processing*, vol. 65, pp. 4912–4923, Sept 2017.

[79] F. He, X. Huang, Y. Liu, and M. Yan, "Fast signal recovery from saturated measurements by linear loss and nonconvex penalties," *IEEE Signal Processing Letters*, vol. 25, pp. 1374–1378, Sept 2018.

[80] J. Wang, H. Xu, B. Zhu, L. Fan, and A. Zhou, "Hybrid beamforming design for mmwave joint unicast and multicast transmission," *IEEE Communications Letters*, pp. 1–1, 2018.

[81] J. Huang, Z. Cheng, E. Chen, and M. Tao, "Low-complexity hybrid analog/digital beamforming for multicast transmission in mmwave systems," in *2017 IEEE International Conference on Communications (ICC)*, pp. 1–6, May 2017.

[82] P. Gui, M. Zhao, Q. Shi, and Q. Wu, "Max-min hybrid precoder design for mmwave multi-group multicasting systems," in *2017 IEEE/CIC International Conference on Communications in China (ICCC)*, pp. 1–5, Oct 2017.

[83] X. Yu, J. Shen, J. Zhang, and K. B. Letaief, "Alternating minimization algorithms for hybrid precoding in millimeter wave MIMO systems," *IEEE Journal of Selected Topics in Signal Processing*, vol. 10, pp. 485–500, April 2016.

[84] F. Sohrabi and W. Yu, "Hybrid digital and analog beamforming design for large-scale antenna arrays," *IEEE Journal of Selected Topics in Signal Processing*, vol. 10, pp. 501–513, April 2016.

[85] O. E. Ayach, S. Rajagopal, S. Abu-Surra, Z. Pi, and R. W. Heath, "Spatially sparse precoding in millimeter wave MIMO systems," *IEEE Transactions on Wireless Communications*, vol. 13, pp. 1499–1513, March 2014.

[86] B. Yang, M. M. Molu, and L. Zhang, "Advanced hybrid beamforming design for MIMO systems," in *2018 IEEE 10th Sensor Array and Multichannel Signal Processing Workshop (SAM)*, pp. 80–83, July 2018.

[87] C. G. Tsinos, S. Maleki, S. Chatzinotas, and B. Ottersten, "On the energy-efficiency of hybrid analog–digital transceivers for single- and multi-carrier large antenna array systems," *IEEE Journal on Selected Areas in Communications*, vol. 35, pp. 1980–1995, Sept 2017.

[88] J. Choi, "Iterative methods for physical-layer multicast beamforming," *IEEE Transactions on Wireless Communications*, vol. 14, pp. 5185–5196, Sept 2015.

[89] X. Gao, L. Dai, S. Han, C. I, and R. W. Heath, "Energy-efficient hybrid analog and digital precoding for mmwave MIMO systems with large antenna arrays," *IEEE Journal on Selected Areas in Communications*, vol. 34, pp. 998–1009, April 2016.

[90] O. T. Demir and T. E. Tuncer, "Hybrid beamforming with two bit RF phase shifters in single group multicasting," in *2016 IEEE International Conference on Acoustics, Speech and Signal Processing (ICASSP)*, pp. 3271–3275, March 2016.

[91] A. d'Aspremont and S. Boyd, "Relaxations and randomized methods for non-convex QCQPs." EE392 Lecture Notes, Stanford Univ., Stanford, CA, USA, 2003.

[92] R. Bosch and M. Trick, "Integer optimization," in *Search Methodologies: Introductory Tutorials in Optimization and Decision Support Techniques* (E. K. Burke and G. Kendall, eds.), pp. 67–92, New York: Springer US, 2014.

[93] T. Antczak, "The exact l_1 penalty function method for constrained nonsmooth invex optimization problems," in *System Modeling and Optimization* (D. Hömberg and F. Tröltzsch, eds.), pp. 461–470, Berlin: Springer, 2013.

[94] O. T. Demir and T. E. Tuncer, "Alternating maximization algorithm for the broadcast beamforming," in *2014 22nd European Signal Processing Conference (EUSIPCO)*, pp. 1915–1919, Sept 2014.

[95] C. L. Byrne, "Alternating minimization as sequential unconstrained minimization: A survey," *Journal of Optimization Theory and Applications*, vol. 156, pp. 554–566, Mar 2013.

[96] M. Grant and S. Boyd, "CVX : Matlab software for disciplined convex programming," 2014.

[97] L. Liang, W. Xu, and X. Dong, "Low-complexity hybrid precoding in massive multiuser MIMO systems," *IEEE Wireless Communications Letters*, vol. 3, pp. 653–656, Dec 2014.

[98] M. S. Lobo, L. Vandenberghe, S. Boyd, and H. Lebret, "Applications of second-order cone programming," *Linear Algebra and its Applications*, vol. 284, no. 1, pp. 193 – 228, 1998. International Linear Algebra Society (ILAS) Symposium on Fast Algorithms for Control, Signals and Image Processing.

[99] W. Pao, Y. Lu, W. Wang, Y. Chang, and Y. Chen, "Improved subcarrier and power allocation schemes for wireless multicast in OFDM systems," in *2013 IEEE 78th Vehicular Technology Conference (VTC Fall)*, pp. 1–5, Sept 2013.

[100] W. Xu, K. Niu, J. Lin, and Z. He, "Resource allocation in multicast OFDM systems: Lower/upper bounds and suboptimal algorithm," *IEEE Communications Letters*, vol. 15, pp. 722–724, July 2011.

[101] R. Neapolitan and K. Naimipour, *Foundations of Algorithms, Fourth Edition*. USA: Jones and Bartlett Publishers, Inc., 4th ed., 2009.

[102] H. . Chen, Y. Li, Y. Jiang, Y. Ma, and B. Vucetic, "Distributed power splitting for SWIPT in relay interference channels using game theory," *IEEE Transactions on Wireless Communications*, vol. 14, pp. 410–420, Jan 2015.

[103] T. Riihonen, S. Werner, and R. Wichman, "Hybrid full-duplex/half-duplex relaying with transmit power adaptation," *IEEE Transactions on Wireless Communications*, vol. 10, pp. 3074–3085, September 2011.

[104] B. Gopalakrishnan and N. D. Sidiropoulos, "High performance adaptive algorithms for single-group multicast beamforming," *IEEE Transactions on Signal Processing*, vol. 63, pp. 4373–4384, Aug 2015.

[105] M. Dai and B. Clerckx, "Hybrid precoding for physical layer multicasting," *IEEE Communications Letters*, vol. 20, pp. 228–231, Feb 2016.

[106] S. Boyd, N. Parikh, E. Chu, B. Peleato, and J. Eckstein, "Distributed optimization and statistical learning via the alternating direction method of multipliers," *Foundations and Trends® in Machine Learning*, vol. 3, no. 1, pp. 1–122, 2011.

[107] J. Li, L. Xiao, X. Xu, and S. Zhou, "Robust and low complexity hybrid beamforming for uplink multiuser mmwave MIMO systems," *IEEE Communications Letters*, vol. 20, pp. 1140–1143, June 2016.

APPENDIX A

PROOFS OF LEMMA 2.2 AND 2.3

A.1 Proof of Lemma 2.2

Consider the following constrained optimization problem given in [93],

$$\min_{\mathbf{x} \in \mathcal{X}} \quad f(\mathbf{x}) \tag{A.1.1a}$$

$$s.t. \quad g_i(\mathbf{x}) \leq 0, \quad i \in \mathcal{I} = \{1, \dots m\} \tag{A.1.1b}$$

$$h_j(\mathbf{x}) = 0, \quad j \in \mathcal{J} = \{1, \dots, s\} \tag{A.1.1c}$$

where $\mathcal{X}$ is a nonempty subset of $\mathbb{R}^n$ and $f : \mathcal{X} \to \mathbb{R}$, $g_i : \mathcal{X} \to \mathbb{R}$, $i \in \mathcal{I}$ and $h_j : \mathcal{X} \to \mathbb{R}$, $j \in \mathcal{J}$ are locally Lipschitz functions on $\mathcal{X}$. Let $\hat{\mathbf{x}}$ be a Karush-Kuhn-Tucker point of (A.1.1) at which the Generalized Karush-Kuhn Tucker conditions are satisfied with Lagrange multipliers $\{\hat{\lambda}_i\}_{i=1}^m$ and $\{\hat{\mu}_j\}_{j=1}^s$ corresponding to $\{g_i(.)\}_{i=1}^m$ and $\{h_j(.)\}_{j=1}^s$. Let $\mathcal{J}^+ = \{j \in \mathcal{J} : \hat{\mu}_j > 0\}$ and $\mathcal{J}^- = \{j \in \mathcal{J} : \hat{\mu}_j < 0\}$. Theorem 6 in [93] states that if f, g_i, $i \in \mathcal{I}$, h_j, $j \in \mathcal{J}^+$ are locally Lipschitz invex and h_j, $j \in \mathcal{J}^-$ are locally Lipschitz incave at $\hat{\mathbf{x}}$ on $\mathcal{X}$ with respect to the same function, then $\hat{\mathbf{x}}$ is also minimizer of the following penalized problem for a sufficiently large c, i.e.,

$$\min_{\mathbf{x} \in \mathcal{X}} \quad f(\mathbf{x}) + c \Big[\sum_{i \in \mathcal{I}} \max\{0, g_i(\mathbf{x})\} + \sum_{j \in \mathcal{J}} |h_j(\mathbf{x})| \Big] \tag{A.1.2}$$

We can express the problem in (2.14) where (2.14d) is replaced by (2.15a-b) in terms of a real vector $\mathbf{x} = [\ \text{Re}(\mathbf{w}_1)^T \ \text{Im}(\mathbf{w}_1)^T \ \dots \ \text{Re}(\mathbf{w}_G)^T \ \text{Im}(\mathbf{w}_G)^T \ \mathbf{b}^T \ \upsilon_1 \ \dots \ \upsilon_N \ \kappa_1 \ \dots \kappa_N \ ]^T$. The problem can be written in form (A.1.1). Let $\mathcal{X} = \{\mathbf{x} : (2.14\text{b-c}), (2.14\text{e-h}), (2.15\text{b})\}$, $f(\mathbf{x}) = \mathbf{x}^T \mathbf{A} \mathbf{x}$ and $h_1(\mathbf{x}) = \mathbf{x}^T \mathbf{B} \mathbf{x} - L$ which is the only constraint except $\mathbf{x} \in \mathcal{X}$. $f(\mathbf{x})$ and $h_1(\mathbf{x})$ correspond to the functions in (2.14a), $\sum_{k=1}^G \mathbf{w}_k^H \mathbf{w}_k$, and (2.15a), $\mathbf{b}^T \mathbf{b} - L$, respectively. Note that both f and h_1 are locally Lipschitz functions on $\mathcal{X}$ since they are quadratic and $\mathbf{x}$ is bounded on $\mathcal{X}$. Since the sign of Lagrange multiplier is not

known, if we can show that f is locally Lipschitz invex function and h_1 is both locally Lipschitz invex and incave function on $\mathcal{X}$ with respect to the same function, then the proof is completed. For this, there should exist a vector-valued function $\eta(\mathbf{x}, \mathbf{u})$ such that the following conditions are satisfied, (please see [93] for details),

$$\mathbf{x}^T \mathbf{A} \mathbf{x} - \mathbf{u}^T \mathbf{A} \mathbf{u} \geq 2\mathbf{u}^T \mathbf{A} \eta(\mathbf{x}, \mathbf{u}), \qquad (A.1.3a)$$

$$\mathbf{x}^T \mathbf{B} \mathbf{x} - \mathbf{u}^T \mathbf{B} \mathbf{u} = 2\mathbf{u}^T \mathbf{B} \eta(\mathbf{x}, \mathbf{u}), \quad \forall \mathbf{x}, \mathbf{u} \in \mathcal{X}. \qquad (A.1.3b)$$

We can choose $\eta(\mathbf{x}, \mathbf{u}) = \frac{1}{2}(-\mathbf{u} + \frac{\mathbf{1_b} \mathbf{x}^T \mathbf{B} \mathbf{x}}{L})$ where $\mathbf{1_b}$ is the vector whose elements corresponding to the indices of $\mathbf{b}$ in $\mathbf{x}$ are 1. Note that $\mathbf{u}^T \mathbf{B} \mathbf{1_b} = L$ by (2.14c), $\mathbf{u}^T \mathbf{A} \mathbf{1_b} = 0$ for any $\mathbf{u} \in \mathcal{X}$ and $\mathbf{x}^T \mathbf{A} \mathbf{x} \geq 0$ for any $\mathbf{x}$. Hence (A.1.3a-b) is satisfied which concludes the proof.

A.2 Proof of Lemma 2.3

Similar to the proof of Lemma 2.2, we can express the problem in (2.22) in terms of a real vector variable $\mathbf{x} = [\ \mathrm{Re}(vec(\mathbf{W}_1))^T \ \mathrm{Im}(vec(\mathbf{W}_1))^T \ ... \ \mathrm{Re}(vec(\mathbf{W}_G))^T$ $\mathrm{Im}(vec(\mathbf{W}_G))^T \ \upsilon_1 \ ... \ \upsilon_N \ \kappa_1 \ ... \kappa_N \ ]^T$ as in the same form (A.1.1). Let $\mathcal{X} = \{\mathbf{x} :$ (2.22b-g)\}. The objective function in (2.22a), $\sum_{k=1}^{G} Tr\{\mathbf{W}_k\}$, and quadratic rank constraints $(Tr\{\mathbf{W}_k\})^2 - Tr\{\mathbf{W}_k^2\} \leq 0$ can be expressed using $f(\mathbf{x}) = \mathbf{c}^T \mathbf{x}$ and $g_k(\mathbf{x}) = \mathbf{x}^T \mathbf{D}_k \mathbf{x}$, $k = 1, ..., G$. If we can show that f and g_k, $k = 1, ..., G$ are locally Lipschitz invex functions on $\mathcal{X}$ with respect to the same vector valued function $\eta(\mathbf{x}, \mathbf{u})$, then the proof is completed [93]. For this, the following conditions should be satisfied,

$$\mathbf{c}^T \mathbf{x} - \mathbf{c}^T \mathbf{u} \geq \mathbf{c}^T \eta(\mathbf{x}, \mathbf{u}), \qquad (A.2.1a)$$

$$\mathbf{x}^T \mathbf{D}_k \mathbf{x} - \mathbf{u}^T \mathbf{D}_k \mathbf{u} \geq 2\mathbf{u}^T \mathbf{D}_k \eta(\mathbf{x}, \mathbf{u}), \quad k = 1, ..., G, \quad \forall \mathbf{x}, \mathbf{u} \in \mathcal{X}. \qquad (A.2.1b)$$

$\eta(\mathbf{x}, \mathbf{u})$ can be simply chosen as $\eta(\mathbf{x}, \mathbf{u}) = -\mathbf{u}$. Since $\mathbf{c}^T \mathbf{x} \geq 0$ and $\mathbf{x}^T \mathbf{D}_k \mathbf{x} \geq 0$, $k = 1, ..., G$, for all $\mathbf{x} \in \mathcal{X}$ by (2.22g) and Theorem 2.2, respectively, (A.2.1a-b) is always satisfied for the given $\eta(\mathbf{x}, \mathbf{u})$. That completes the proof.

APPENDIX B

PROOFS OF LEMMA 5.1, 5.2 AND 5.4

B.1 Proof of Lemma 5.1

We will explore the cases resulting unbounded solution by expressing the relay transmit beamformer vector as $\mathbf{w}_t = \sum_{n=1}^{N_t} \beta_n e^{j\theta_n} \mathbf{u}_n$ where $\beta_n \geq 0$, $n = 1, ..., N_t$ and $\{\mathbf{u}_n\}_{n=1}^{N_t}$ are the orthonormal eigenvectors of the matrix $\mathbf{I}_{N_t} - \eta \mathbf{H}_{rr}^H \mathbf{H}_{rr}$. The problem in (5.8) can be expressed in terms of $\{\beta_n, \theta_n\}_{n=1}^{N_t}$ as follows,

$$\max_{\{\beta_n \geq 0, \theta_n\}_{n=1}^{N_t}} \left| \sum_{n=1}^{N_t} \mathbf{h}_d^H \mathbf{u}_n \beta_n e^{j\theta_n} \right| \tag{B.1.1a}$$

$$s.t. \ \sum_{n=1}^{N_t} \lambda_n \beta_n^2 \leq \gamma, \tag{B.1.1b}$$

where $\{\lambda_n\}_{n=1}^{N_t}$ are the eigenvalues of the matrix $\mathbf{I}_{N_t} - \eta \mathbf{H}_{rr}^H \mathbf{H}_{rr}$ corresponding to the eigenvectors $\{\mathbf{u}_n\}_{n=1}^{N_t}$. In (B.1.1b), $\gamma \triangleq \frac{\eta P_s \|\mathbf{h}_r\|^2 + \eta N_r \sigma_{r,2}^2}{P_s \|\mathbf{h}_r\|^2 + \sigma_{r,1}^2 + \sigma_b^2}$ is defined for ease of notation. Note that (B.1.1b) which is the only constraint of the problem (B.1.1) is independent of the optimization variables $\{\theta_n\}_{n=1}^{N_t}$. Hence, the optimum $\{\theta_n\}_{n=1}^{N_t}$ maximizes the objective function in (B.1.1a). Since β_n is nonnegative $\forall n$, the optimum $\{\theta_n\}_{n=1}^{N_t}$ is given as $\theta_n^\star = \angle -\mathbf{h}_d^H \mathbf{u}_n$, $n = 1, ..., N_t$ which make all the terms in (B.1.1a) aligned in phase. If we insert these optimum values into (B.1.1), we obtain the following optimization problem, i.e.,

$$\max_{\{\beta_n\}_{n=1}^{N_t}} \sum_{n=1}^{N_t} |\mathbf{h}_d^H \mathbf{u}_n| \beta_n \tag{B.1.2a}$$

$$s.t. \ \sum_{n=1}^{N_t} \lambda_n \beta_n^2 \leq \gamma. \tag{B.1.2b}$$

It is easily seen that the optimum $\{\beta_n\}_{n=1}^{N_t}$ should be nonnegative for (B.1.2) since $|\mathbf{h}_d^H \mathbf{u}_n| \geq 0$. Hence, the constraints $\beta_n \geq 0$, $n = 1, ..., N_t$ are not included for simplicity. At this point, consider two cases.

Case 1: At least one of the eigenvalues of the matrix $\mathbf{I}_{N_t} - \eta \mathbf{H}_{rr}^H \mathbf{H}_{rr}$ is zero. Denote the index set of zero eigenvalues by $\mathcal{N}_0$, i.e. $\lambda_n = 0$ for $n \in \mathcal{N}_0$. In this case, $\{\beta_n\}_{n\in\mathcal{N}_0}$ can be chosen infinity without violating (B.1.2b). Furthermore, if at least one of $\{|\mathbf{h}_d^H \mathbf{u}_n|\}_{n\in\mathcal{N}_0}$ is nonzero, then the objective in (B.1.2a) becomes infinity. This will result an unbounded solution.

Case 2: At least one of the eigenvalues of the matrix $\mathbf{I}_{N_t} - \eta \mathbf{H}_{rr}^H \mathbf{H}_{rr}$ is negative. Denote the index set of negative eigenvalues by $\mathcal{N}_-$, i.e. $\lambda_n < 0$ for $n \in \mathcal{N}_-$. In this case, $\beta_n \forall n$ can be made arbitrarily large without violating (B.1.2b). Then the objective in (B.1.2a) becomes infinity. This will result an unbounded solution.

If all the eigenvalues are positive, i.e., $\lambda_n > 0$, $\forall n$, then neither Case 1 nor Case 2 happen and we obtain a bounded problem by (B.1.2b) which completes the proof. ∎

B.2 Proof of Lemma 5.2

First, let us express the problem (5.14) in terms of $\{\beta_n, \theta_n\}_{n=1}^{N_t}$ as follows,

$$\max_{\{\beta_n \geq 0, \theta_n\}_{n=1}^{N_t}} \left| \frac{\widetilde{\mathbf{h}}_d^H \widetilde{\mathbf{h}}_r}{||\widetilde{\mathbf{h}}_r||} \beta_1 e^{j\theta_1} + \frac{\widetilde{\mathbf{h}}_d^H \widetilde{\mathbf{h}}_d - \widetilde{\mathbf{h}}_d^H \mathbf{\Phi}_1 \mathbf{\Phi}_1^H \widetilde{\mathbf{h}}_d}{||\widetilde{\mathbf{h}}_d - \mathbf{\Phi}_1 \mathbf{\Phi}_1^H \widetilde{\mathbf{h}}_d||} \beta_2 e^{j\theta_2} \right| \tag{B.2.1a}$$

$$s.t. \ \gamma_1 \sum_{n=1}^{N_t} \beta_n^2 - 2\eta P_s ||\mathbf{h}_r|| ||\widetilde{\mathbf{h}}_r|| \beta_1 \leq \gamma_2. \tag{B.2.1b}$$

Note that any phase rotation of the function inside the brackets in (B.2.1a) does not affect the optimality. Hence, θ_1 can be chosen as $\theta_1 = 0$ without loss of generality. Under this condition, it can easily be seen that the function in (B.2.1a) is maximized by selecting $\theta_2 = \angle \widetilde{\mathbf{h}}_d^H \widetilde{\mathbf{h}}_r$ for the other variables given. The following upper bound for (B.2.1a) is achieved by aligning phases of both terms inside the brackets with this θ_2, i.e.,

$$\frac{|\widetilde{\mathbf{h}}_d^H \widetilde{\mathbf{h}}_r|}{||\widetilde{\mathbf{h}}_r||} \beta_1^\star + \frac{\widetilde{\mathbf{h}}_d^H \widetilde{\mathbf{h}}_d - \widetilde{\mathbf{h}}_d^H \mathbf{\Phi}_1 \mathbf{\Phi}_1^H \widetilde{\mathbf{h}}_d}{||\widetilde{\mathbf{h}}_d - \mathbf{\Phi}_1 \mathbf{\Phi}_1^H \widetilde{\mathbf{h}}_d||} \beta_2^\star \tag{B.2.2}$$

Note that both terms in (B.2.2) are positive.

Furthermore $\{\beta_n\}_{n=3}^{N_t}$ do not affect the objective function in (B.2.1a). It is obviously seen that for optimum $\widetilde{\mathbf{w}}_t$, $\{\beta_n\}_{n=3}^{N_t}$ should be zero. Suppose that this is not the case for the optimum solution. In this case, $\{\beta_n\}_{n=3}^{N_t}$ can be set to zero and β_1 and β_2 can be increased without violating (B.2.1b). In this case, we obtain an improved objective function which contradicts the optimality of nonzero $\{\beta_n\}_{n=3}^{N_t}$. Hence, the claim of the lemma is true. ∎

B.3 Proof of Lemma 5.4

The quartic function given in (5.55) is equal to the following one by (5.54), i.e.,

$$\widetilde{\delta}_1 D_1 (D_1\widetilde{\beta}_1 - D_2)\widetilde{\beta}_1^3 - \widetilde{\delta}_2\left((D_1\widetilde{\beta}_1 - D2)^2 - D_3\right)^2. \tag{B.3.1}$$

The derivative of (B.3.1) is given by

$$\widetilde{\delta}_1 D_1^2 \widetilde{\beta}_1^3 + 3\widetilde{\delta}_1 D_1 (D_1\widetilde{\beta}_1 - D_2)\widetilde{\beta}_1^2 - 4\widetilde{\delta}_2 D_1\left((D_1\widetilde{\beta}_1 - D2)^2 - D_3\right)(D_1\widetilde{\beta}_1 - D2)$$

$$\tag{B.3.2}$$

Note that the first term in (B.3.2) is obviously positive. The second term is also positive since $(D_1\widetilde{\beta}_1 - D_2) > 0$ which is the term inside the parenthesis in (5.51). If this term would be negative, then β_1 can be increased such that the same ρ is obtained with an improved objective function. Hence, $(D_1\widetilde{\beta}_1 - D_2) > 0$. When it comes to the last term in (B.3.2), it is seen that the term $\left((D_1\widetilde{\beta}_1 - D2)^2 - D_3\right)$ is equal to $\rho - 1$ which is negative. As a result, (B.3.2) is positive in the region $0 \leq \rho < 1$. This proves that the quartic function in (5.55) is monotonically increasing inside the considered interval. ∎

APPENDIX C

PROOFS OF LEMMA 6.2, 6.4 AND 6.5

C.1   Proof of Lemma 6.2

Let us take the derivative of the function $f(x)$ as follows,

$$f'(x) = \frac{2\sigma_r^2(3x^2 + 1)}{(1 - x^2)^3} + \frac{2\sigma_d^2}{||\mathbf{g}||^2} \frac{-f_1''(x)f_1^3(x) + 3f_1^2(x)(f_1'(x))^2}{f_1^6(x)} \tag{C.1.1}$$

Note that in the region of interest, $\tilde{\beta}_1 > 0$, thus $f_1(x) > 0$. Hence, if $f_1''(x) \leq 0$, $f'(x) > 0$ in the region specified by $0 \leq x < 1$ and $\tilde{\beta}_1 > 0$. In order to show that $f_1''(x) \leq 0$, we express the function $f_1(x)$ as $f_1(x) = \sqrt{f_2(x)} - (D_1 x - D_2)$ where $f_2(x) \triangleq \frac{D_4}{d_1 + \frac{\sigma_r^2}{1 - x^2}} - D_3(D_1 x - D_2)^2$. Now, take the first and second derivative of $f_1(x)$ as follows,

$$f_1'(x) = \frac{f_2'(x)}{2\sqrt{f_2(x)}} - D_1 \tag{C.1.2a}$$

$$f_1''(x) = \frac{2f_2''(x)\sqrt{f_2(x)} - \frac{(f_2'(x))^2}{\sqrt{f_2(x)}}}{4f_2(x)} \tag{C.1.2b}$$

225

Let us show that $f_2''(x) < 0$ as follows

$$f_2'(x) = \frac{-D_4 \frac{2\sigma_r^2 x}{(1-x^2)^2}}{\left(d_1 + \frac{\sigma_r^2}{1-x^2}\right)^2} - 2D_1 D_3(D_1 x - D_2) \tag{C.1.3a}$$

$$f_2''(x) = D_4 \frac{-\frac{2\sigma_r^2(3x^2+1)}{(1-x^2)^3}\left(d_1 + \frac{\sigma_r^2}{1-x^2}\right)^2 + \frac{4\sigma_r^4 x^2}{(1-x^2)^4}2\left(d_1 + \frac{\sigma_r^2}{1-x^2}\right)}{\left(d_1 + \frac{\sigma_r^2}{1-x^2}\right)^4} - 2D_1^2 D_3 \tag{C.1.3b}$$

$$f_2''(x) = D_4 \frac{-2\sigma_r^2(3x^2+1)(1-x^2)\left(d_1 + \frac{\sigma_r^2}{1-x^2}\right) + 8\sigma_r^4 x^2}{\left(d_1 + \frac{\sigma_r^2}{1-x^2}\right)^3(1-x^2)^4} - 2D_1^2 D_3 \tag{C.1.3c}$$

$$f_2''(x) = D_4 \frac{-2\sigma_r^2(1-x^2)^2\left(d_1 + \frac{\sigma_r^2}{1-x^2}\right) - 2d_1\sigma_r^2 x^2(1-x^2)}{\left(d_1 + \frac{\sigma_r^2}{1-x^2}\right)^3(1-x^2)^4} - 2D_1^2 D_3 \tag{C.1.3d}$$

As it can be seen from (C.1.3d), $f_2''(x) < 0$ and thus $f_1''(x) < 0$. Hence, $f'(x) > 0$ in the region of interest showing that $f(x)$ is monotonically increasing. ∎

C.2 Proof of Lemma 6.4

Let us take the derivative of the function $g(\tilde{\beta}_1)$ as follows,

$$g'(\tilde{\beta}_1) = \frac{2d_1(d_1 - d_3^2 - d_4^2)}{d_1 - d_4^2} - \frac{2d_1 d_2 d_3}{d_1 - d_4^2}\frac{g_1'(\tilde{\beta}_1)}{\sqrt{g_1(\tilde{\beta}_1)}}$$

$$- \frac{d_1 d_2 d_3}{d_1 - d_4^2}\frac{\tilde{\beta}_1\left(g_1''(\tilde{\beta}_1)\sqrt{g_1(\tilde{\beta}_1)} - \frac{(g_1'(\tilde{\beta}_1))^2}{2\sqrt{g_1(\tilde{\beta}_1)}}\right)}{g_1(\tilde{\beta}_1)} - \frac{d_1 d_2^2}{d_1 - d_4^2}g_1''(\tilde{\beta}_1) \tag{C.2.1a}$$

$$g'(\tilde{\beta}_1) = \frac{2d_1(d_1 - d_3^2 - d_4^2)}{d_1 - d_4^2} - \frac{d_1 d_2 d_3}{d_1 - d_4^2}\frac{2g_1'(\tilde{\beta}_1) + \tilde{\beta}_1 g_1''(\tilde{\beta}_1)}{\sqrt{g_1(\tilde{\beta}_1)}}$$

$$+ \frac{d_1 d_2 d_3}{d_1 - d_4^2}\frac{\tilde{\beta}_1(g_1'(\tilde{\beta}_1))^2}{2(g_1(\tilde{\beta}_1))^{3/2}} - \frac{d_1 d_2^2}{d_1 - d_4^2}g_1''(\tilde{\beta}_1) \tag{C.2.1b}$$

where $g_1'(\tilde{\beta}_1) = \frac{2E_2 E_3 \tilde{\beta}_1}{(E_1 \tilde{\beta}_1^2 - E_3)^2}$ and $g_1''(\tilde{\beta}_1) = \frac{2E_2 E_3(-3E_1 \tilde{\beta}_1^2 - E_3)}{(E_1 \tilde{\beta}_1^2 - E_3)^3}$. We will now show that all the terms in (C.2.1b) are nonnegative. Let us insert (6.62) into (6.50a) and obtain

$$\left(d_1 - d_3^2 - \frac{d_3^2 d_4^2}{d_1 - d_4^2}\right)\tilde{\beta}_1 - \left(d_2 d_3 + \frac{d_2 d_3 d_4^2}{d_1 - d_4^2}\right)x \geq 0 \tag{C.2.2}$$

For $\tilde{\beta}_1 > 0$, it is required that $d_1 - d_3^2 - \frac{d_3^2 d_4^2}{d_1 - d_4^2} \geq 0$ which is equivalent to $d_1 \geq d_3^2 + d_4^2$. Hence, the first term in (C.2.1b) is nonnegative. The second term is also nonnegative,

i.e.,

$$-\left(2g_1'(\tilde{\beta}_1) + \tilde{\beta}_1 g_1''(\tilde{\beta}_1)\right) = -\frac{4E_2 E_3 \tilde{\beta}_1}{(E_1 \tilde{\beta}_1^2 - E_3)^2} - \frac{2E_2 E_3 \tilde{\beta}_1(-3E_1 \tilde{\beta}_1^2 - E_3)}{(E_1 \tilde{\beta}_1^2 - E_3)^3} \quad \text{(C.2.3a)}$$

$$= \frac{2E_2 E_3 \tilde{\beta}_1(E_1 \tilde{\beta}_1^2 + 3E_3)}{(E_1 \tilde{\beta}_1^2 - E_3)^3} > 0 \quad \text{(C.2.3b)}$$

It can easily be seen that other terms are positive. This shows that $g(\tilde{\beta}_1)$ is monotonically increasing in the region specified by $\tilde{\beta}_1 > 0$ and $0 \le x < 1$.

∎

C.3   Proof of Lemma 6.5

Let us take the derivative of the function $h(\tilde{\beta}_1)$ as follows,

$$h'(\tilde{\beta}_1) = \frac{d_2\left(2g_1''(\tilde{\beta}_1)\sqrt{g_1(\tilde{\beta}_1)} - \frac{\left(g_1'(\tilde{\beta}_1)\right)^2}{\sqrt{g_1(\tilde{\beta}_1)}}\right)}{4g_1(\tilde{\beta}_1)} - \frac{d_4}{\sqrt{\frac{P_{max}}{d_1} - \tilde{\beta}_1^2}} - \frac{d_4 \tilde{\beta}_1^2}{\left(\frac{P_{max}}{d_1} - \tilde{\beta}_1^2\right)^{3/2}} \quad \text{(C.3.1)}$$

where $g_1''(\tilde{\beta}_1) = \frac{2E_2 E_3(-3E_1 \tilde{\beta}_1^2 - E_3)}{(E_1 \tilde{\beta}_1^2 - E_3)^3} < 0$ and all the terms above in (C.3.1) are negative in the region specified by $\tilde{\beta}_1 > 0$, $\tilde{\beta}_2 \ge 0$, and $0 \le x = \sqrt{\frac{(E_1 - E_2)\tilde{\beta}_1^2 - E_3}{E_1 \tilde{\beta}_1^2 - E_3}} < 1$. Hence, $h(\tilde{\beta}_1)$ is monotonically decreasing function in the region of interest.   ∎

<div align="center">**CURRICULUM VITAE**</div>

PERSONAL INFORMATION

Surname, Name: Demir, Özlem Tuğfe

Nationality: Turkish (TC)

Date and Place of Birth: 17.02.1990, Ankara

Marital Status: Single

Phone: 0 312 210 4587

Fax: 0 312 210 2304

EDUCATION

Degree	Institution	Year of Graduation
M.S.	Middle East Technical University	2014
B.S.	Middle East Technical University	2012
High School	Ankara Atatürk Anatolian High School	2008

PROFESSIONAL EXPERIENCE

Year	Place	Enrollment
2012-2018	Middle East Technical University	Research Assistant

PUBLICATIONS

- Ö. T. Demir and T. E. Tuncer, "Improved ADMM-based algorithms for multi-group multicasting in large-scale antenna systems with extension to hybrid beamforming ", to be submitted to *Digital Signal Processing.*

- Ö. T. Demir and T. E. Tuncer, "Optimum and near-optimum beamformers for decode-and-forward full-duplex multi-antenna relay with self-energy recycling", submitted to *IEEE Trans. Wirel. Commun.*

- Ö. T. Demir and T. E. Tuncer, "Joint source power allocation and relay beamformer design for wireless-powered relaying with self-energy recycling", to be submitted to *IEEE Trans. Green. Commun. Network.*

- Ö. T. Demir and T. E. Tuncer, "Optimum closed-form beamformers for self-energy recycling full-duplex relay with a new power splitting protocol", to be submitted to *IEEE Trans. Green. Commun. Network.*

- Ö. T. Demir and T. E. Tuncer, "Optimum qos-aware beamformer design for full-duplex relay with self-energy recycling", *IEEE Wirel. Commun. Letters*, vol. 7, no. 1, pp. 122-125, Feb. 2018.

- Ö. T. Demir and T. E. Tuncer, "Max-min fair resource allocation for SWIPT in multi-group multicast OFDM systems", *IEEE Commun. Leters*, vol. 21, no. 11, pp. 2508-2511, Nov. 2017.

- Ö. T. Demir and T. E. Tuncer, "Antenna selection and hybrid beamforming for simultaneous wireless information and power transfer in multi-group multicasting systems", *IEEE Trans. Wirel. Commun.*, vol. 15, no. 10, pp. 6948-6962, Oct. 2016.

- Ö. T. Demir and T. E. Tuncer, "Optimum discrete phase-only multicast beamforming with joint antenna and user selection in cognitive radio networks", *Digital Signal Processing*, vol. 46, pp. 81-96, Nov. 2015.

- Ö. T. Demir and T. E. Tuncer, "Optimum discrete transmit beamformer design", *Digital Signal Processing*, vol. 36, pp. 57-68, Jan. 2015.

International Conference Publications

- Ö. T. Demir and T. E. Tuncer, "A new beamformer design method for multi-group multicasting by enforcing constructive interference" in *26th European Signal Processing Conference (EUSIPCO)*, 2018.

- Ö. T. Demir and T. E. Tuncer, "Improved ADMM-based algorithm for multi-group multicast beamforming in large-scale antenna systems" in *26th European Signal Processing Conference (EUSIPCO)*, 2018.

- Ö. T. Demir and T. E. Tuncer, "SWIPT for max-min fair multi-group multicast beamforming through power splitting", in *Proc. IEEE Wireless Communications and Networking Conference, IEEE WCNC 2017*, 2017.

- Ö. T. Demir and T. E. Tuncer, "Distributed beamforming in relay networks for energy harvesting multi-group multicast systems", in *Proc. IEEE International Conference on Acoustics, Speech and Signal Processing (ICASSP)*, 2016.

- Ö. T. Demir and T. E. Tuncer, "Hybrid beamforming with two bit RF phase shifters in single group multicasting", in *Proc. IEEE International Conference on Acoustics, Speech and Signal Processing (ICASSP)*, 2016.

- Ö. T. Demir and T. E. Tuncer, "Multi-group multicast beamforming for simultaneous wireless information and power transfer", in *Proc. European Signal Processing Conference (EUSIPCO)*, 2015.

- Ö. T. Demir and T. E. Tuncer, "Joint optimization of transmit and relay beamformer for single group multicast transmission", in *Proc. European Signal Processing Conference (EUSIPCO)*, 2015.

- Ö. T. Demir and T. E. Tuncer, "Optimum phase-only discrete broadcast beamforming with antenna and user selection in interference limited cognitive radio networks", in *Proc. IEEE International Conference on Acoustics, Speech and Signal Processing (ICASSP)*, 2015.

- Ö. T. Demir and T. E. Tuncer, "Optimum discrete distributed beamforming for single group multicasting relay networks with relay selection", in *Proc. IEEE International Conference on Acoustics, Speech and Signal Processing (ICASSP)*, 2015.

- Ö. T. Demir and T. E. Tuncer, "Multicast beamforming with antenna selection using exact penalty approach", in *Proc. IEEE International Conference on Acoustics, Speech and Signal Processing (ICASSP)*, 2015.

- Ö. T. Demir and T. E. Tuncer, "Alternating maximization algorithm for the broadcast beamforming", in *Proc. European Signal Processing Conference (EUSIPCO)*, 2014.

- Ö. T. Demir and T. E. Tuncer, "Optimum discrete phase-only transmit beamforming with antenna selection", in *Proc. European Signal Processing Conference (EUSIPCO)*, 2014.

- Ö. T. Demir and T. E. Tuncer, "Optimum discrete single group multicast beamforming", in *Proc. IEEE International Conference on Acoustics, Speech and Signal Processing (ICASSP)*, 2014.

- Ö. T. Demir and T. E. Tuncer, "Optimum design of discrete transmit phase only beamformer", in *Proc. European Signal Processing Conference (EUSIPCO)*, 2013.

National Conference Publications

- Ö. T. Demir and T. E. Tuncer, "Two-bit hybrid beamforming for broadcasting", in *Proc. Signal Processing and Communications Applications Conference (SIU)*, 2016.

- Ö. T. Demir and T. E. Tuncer, "Relay-assisted beamforming for multicast systems with energy harvesting capability", in *Proc. Signal Processing and Communications Applications Conference (SIU)*, 2016.

- Ö. T. Demir and T. E. Tuncer, "Multicast beamforming with antenna selection using alternating maximization", in *Proc. Signal Processing and Communications Applications Conference (SIU)*, 2015.

- Ö. T. Demir and T. E. Tuncer, "Discrete relay beamforming for broadcasting with relay selection", in *Proc. Signal Processing and Communications Applications Conference (SIU)*, 2015.

- Ö. T. Demir and T. E. Tuncer, "Discrete broadcast beamforming with antenna and user selection", in *Proc. Signal Processing and Communications Applications Conference (SIU)*, 2015.

- Ö. T. Demir and T. E. Tuncer, "Iterative rank minimization for broadcast beamforming", in *Proc. Signal Processing and Communications Applications Conference (SIU)*, 2014.

- Ö. T. Demir and T. E. Tuncer, "Optimum discrete max-min style broadcast beamforming design", in *Proc. Signal Processing and Communications Applications Conference (SIU)*, 2014.

- Ö. T. Demir and T. E. Tuncer, "Joint discrete phase-only broadcast beamforming with antenna selection", in *Proc. Signal Processing and Communications Applications Conference (SIU)*, 2014.

- Ö. T. Demir and T. E. Tuncer, "Transmit beamformer design with nonlinear optimization", in *Proc. Signal Processing and Communications Applications Conference (SIU)*, 2013.